

# On the Synthesis of Tetradentate Ligands

## Dissertation

zur Erlangung des akademischen Grades doctor rerum naturalium  
(Dr. rer. nat.)

vorgelegt dem Rat der Chemisch-Geowissenschaftlichen Fakultät der  
Friedrich-Schiller-Universität Jena

von Diplomchemiker Martin Schulz  
geboren am 11.12.1980 in Bad Salzungen

1. Gutachter: Prof. Dr. Matthias Westerhausen, FSU Jena
  2. Gutachter: Prof. Dr. Rainer Beckert, FSU Jena
- Tag der öffentlichen Verteidigung: 16. Dezember 2009

# Contents

<b>List of Abbreviations</b>	<b>4</b>
<b>1 Introduction</b>	<b>6</b>
1.1 Background . . . . .	6
1.2 Preparatory work . . . . .	8
1.3 Aims . . . . .	15
<b>2 Results and Discussion</b>	<b>16</b>
2.1 Ligand design via nitroaldol reaction with pyridine-2-carbaldehyde . . .	16
2.1.1 Overview . . . . .	16
2.1.2 Synthesis and reactivity of 2-nitro-1,3-di(pyridine-2-yl)propane-1,3-diol . . . . .	18
2.1.3 Synthesis of 2-nitro-1,3-di(pyridin-2-yl)propane-1,3-diolato zinc dichloride . . . . .	29
2.1.4 Development of macromolecular catalysts for nitroaldol reactions	32
2.1.5 O-Trialkylsilyl protection of 2-nitroalcohols . . . . .	34
2.1.6 Reduction of the nitro group . . . . .	42
2.1.7 Synthesis of a N-salicylaldimine ligand, its vanadium(v) complex and catalytic activity . . . . .	46
2.2 N-(Pyridine-2-ylmethylidene)amines as ligands and ligand precursors .	57
2.2.1 Synthesis of N-(pyridine-2-ylmethylidene)amines . . . . .	57
2.2.2 Synthesis and structural diversity of 2-pyridylmethylideneamine complexes of zinc(II) chloride . . . . .	58
2.2.3 Synthesis of 1,4-diamino-2,3-di(2-pyridyl)butane and its zinc(II) chloride complex . . . . .	65
2.2.4 Synthesis of a tetraaryl substituted piperazine (ZnCl <sub>2</sub> ) <sub>2</sub> complex with unexpected stereoselectivity . . . . .	75
2.2.5 Miscellaneous reactions . . . . .	81
<b>3 Summary</b>	<b>84</b>
<b>4 Zusammenfassung</b>	<b>87</b>
<b>5 Experimental</b>	<b>91</b>
<b>References</b>	<b>111</b>

A Crystallographic Data	119
Acknowledgment	124
Declaration of Originality	124

## List of Abbreviations

$\delta$ .....	Chemical shift
$\Delta\nu$ .....	Line width
$\epsilon$ .....	Extinction coefficient
$\lambda$ .....	Wavelength
$\tilde{\nu}$ .....	Wave number
a .....	Coupling constant (EPR)
aibn .....	2,2'-Diazo-bis(2-methylpropanenitrile)
bipy .....	2,2'-Bipyridine
Bu .....	Butyl
d .....	Doublet ( $^1\text{H}$ NMR)
dd .....	Doublet of doublets ( $^1\text{H}$ NMR)
ddd .....	Doublet of doublets of doublets ( $^1\text{H}$ NMR)
de .....	Diastereomeric excess
DEI .....	Direct electron impact
DEPT .....	Distortionless enhancement by polarization transfer
dmap .....	N,N-Dimethylpyridine-4-amine
dmf .....	N,N-Dimethylformamide
dmsO .....	Dimethyl sulfoxide
ee .....	Enantiomeric excess
EI .....	Electron impact
EPR .....	Electron paramagnetic resonance
ESI .....	Electron spray ionization
FAB .....	Fast atom bombardment
GC .....	Gas chromatography
HMBC .....	Heteronuclear multiple bond correlation
HSQC .....	Heteronuclear single quantum coherence
IR .....	Infrared spectroscopy
J .....	Coupling constant (NMR)
LMCT .....	Ligand to metal charge transfer
m .....	Mass, multiplet ( $^1\text{H}$ NMR), medium (IR)
Me .....	Methyl
MS .....	Mass spectrometry
nba .....	3-Nitrobenzyl alcohol
NMR .....	Nuclear magnetic resonance
NOE .....	Nuclear Overhauser effect

NOESY .....	Nuclear Overhauser and exchange spectroscopy
p .....	Primary ( <sup>13</sup> C NMR)
Prop .....	Propyl
pyr .....	Pyridyl
q .....	Quartet ( <sup>1</sup> H NMR), quaternary ( <sup>13</sup> C NMR)
quint .....	Quintet ( <sup>1</sup> H NMR)
r.t. ....	Room temperature
s .....	Singlet ( <sup>1</sup> H NMR), secondary ( <sup>13</sup> C NMR)
st .....	Strong (IR)
t .....	Triplet ( <sup>1</sup> H NMR), tertiary ( <sup>13</sup> C NMR)
tbd .....	1,5,7-Triazabicyclo[4.4.0]dec-5-ene
TBDMS .....	<i>Tert</i> -butyldimethylsilyl
thf .....	Tetrahydrofuran
TLC .....	Thin layer chromatography
tmb .....	Trimethoxybenzene
tmeda .....	N,N,N',N'-Tetramethylethylene-1,2-diamine
TMS .....	Trimethylsilyl
TOF .....	Turnover frequency
TON .....	Turnover number
TSA .....	Transition state analogue
w .....	Weak (IR)
w% .....	Weight percent
z .....	Charge

IUPAC Naming was realized using ACD/ChemSketch Freeware, version 11.02, Advanced Chemistry Development, Inc., Toronto, ON, Canada, [www.acdlabs.com](http://www.acdlabs.com), **2008**.

---

# 1 Introduction

## 1.1 Background

The activation of small molecules such as CO<sub>2</sub>, CO, NO, CH<sub>4</sub>, H<sub>2</sub>O and others has been a field of research for decades.<sup>1</sup> And research in this area is of growing interest, since for example small molecules such as H<sub>2</sub>, N<sub>2</sub> and O<sub>2</sub> are an ubiquitous reservoir of chemical energy. But they also serve as synthons for (bio)chemical processes or signaling agents in biological systems. CO<sub>2</sub> for example is used in biological systems as C1 synthon for the production of glucose, malonic acid, oxaloacetate and others. This is accomplished by enzymes such as ribulose-1,5-bis(phosphate)-carboxylase-oxidase (RuBisCO), acetyl-CoA carboxylase or phosphoenolpyruvate carboxykinase. Artificial processes use CO<sub>2</sub> for the carboxylation of phenol or production of organic and inorganic carbonates. NO is an example for a signaling agent in biological systems and its chemistry is of medical importance. Since the early days of chemistry it has been known that metals or metal ions are able to catalyze reactions of these often thermodynamically stable molecules. Thus, researchers were concerned with the coordination behavior of small molecules towards metal centers, the reasons for their activation, the basis of selectivity of metal/small-molecule interactions and the transfer of knowledge for laboratory and industrial or medical use. Activation of small molecules by metal ions or complexes is a process that occurs in every organism. Hence, investigations on biocatalysts help to gain deeper insights into activation mechanisms, while contrariwise, fundamental inorganic, organic and theoretical research can help to understand the enzyme's mode of action. Research in this field is strongly interdigitated and has been forwarded by recent advances in synthetic and theoretical methods as well as spectroscopic techniques. Gathering information of the enzyme's mode of action is approached by mimicking the active center of a metalloenzyme. Since biocatalysts often comprise of huge proteins, their spectroscopic examination is strongly hampered and smaller model compounds are desired. These model complexes are divided into structural mimics and functional mimics. Structural models mimic the coordination site, for instance donor atoms, conformation, bond lengths and angles. They do not necessarily mimic the catalytic function but provide useful comparative data for spectroscopic studies of the natural counterpart. Functional mimics often have little resemblance with the binding sites of its natural analogue but have similar catalytic properties like activity or selectivity. The challenging task when modeling parts of a biocatalyst was summarized by PARKIN: "The construction of accurate synthetic analogues is therefore nontrivial, and considerable attention must be given to ligand

design in order to achieve a coordination environment, which is similar to that enforced by the unique topology of a protein."<sup>2</sup> This challenge was addressed in the collaborative research center "Metal-mediated reactions modeled after nature" (SFB 436) at the university of Jena, where our group was also involved. Parts of these investigations were focused on functional mimics of homo- and heterodinuclear zinc containing metalloenzymes in order to develop catalysts for the activation of small molecules. Natural examples are metallo- $\beta$ -lactamase (Zn(II), Zn(II)), bovine lens leucine amino peptidase (Zn(II), Zn(II)), alkaline phosphatase (Zn(II), Zn(II)), kidney bean purple acid phosphatase (Zn(II), Fe(III)) and DNA polymerase I (Zn(II), Mg(II)).<sup>3,4</sup> Although these enzymes catalyze the cleavage of peptide or phosphate ester bonds or the transfer of nucleotides to DNA, the underlying mechanisms also apply for the activation of small molecules. A selection of published dinuclear zinc enzyme models is given in Figure 1. They comprise phenolate, phthalazine or pyrazolyl linkers as well as cryptands and calix[4]arenes.<sup>4</sup> Their common feature are N and O donor sites, while the two metal centers are bridged via water, hydroxide, carboxylate, or phosphate moieties.

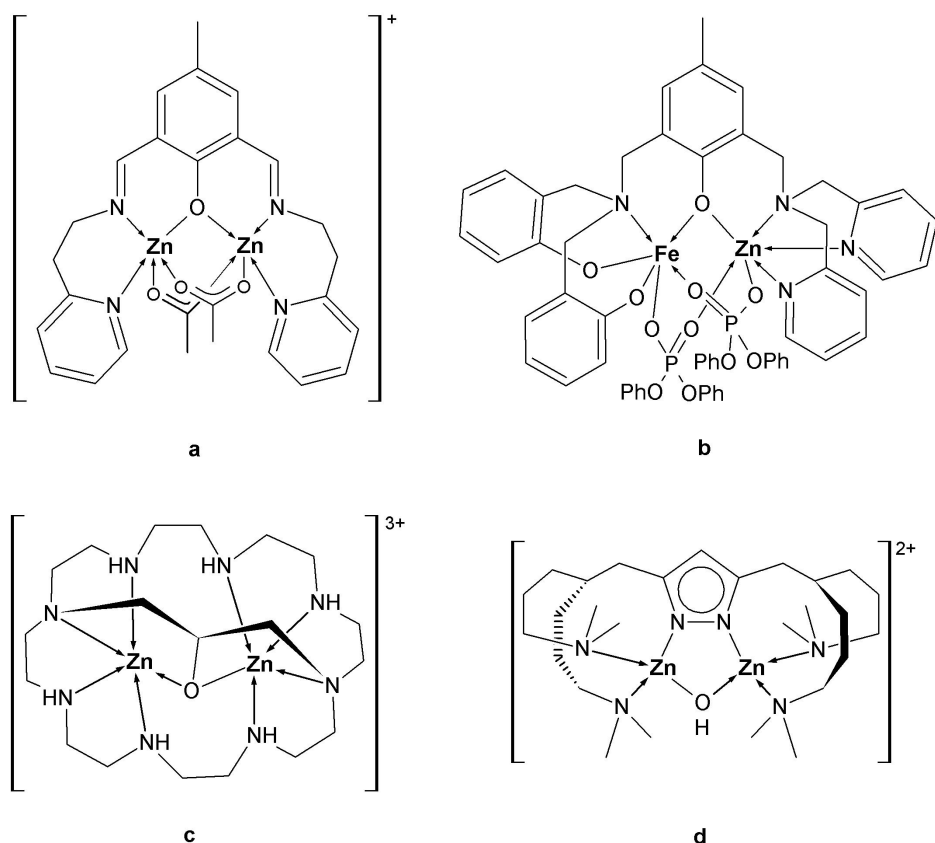


**Figure 1:** Selection of published structural and functional models of dinuclear zinc-containing enzymes: **a**,<sup>5</sup> **b**,<sup>6</sup> **c**,<sup>7</sup> **d**.<sup>8</sup>

Similar coordination environments as given in Figure 1 were applied in artificial



catalysts for CO<sub>2</sub> activation and transfer. COATES and coworkers employed dinuclear  $\beta$ -diiminato zinc complexes for the copolymerization of CO<sub>2</sub> and cyclohexene oxide with TONs up to 478.<sup>9</sup> Their mechanistic investigations revealed dramatic changes in the catalytic activity by subtle changes of ligand modifications. Later NOZAKI and coworkers reported on the asymmetric copolymerization of CO<sub>2</sub> and cyclohexene oxide.<sup>10</sup> They also used dinuclear zinc complexes with a N,O donor set. Comparable to the catalyst applied by COATES, the metal ions are part of a Zn<sub>2</sub>O<sub>2</sub> ring as given in Figure 2. The metal...metal distance in the catalyst applied by COATES is 298 pm, while NOZAKI'S catalyst shows a zinc-zinc distance of 307 pm. Furthermore, NOZAKI reported on cooperative effects that led to asymmetric amplification\*. Cooperative effects were also described for the ring opening reaction of cyclohexene oxide with oligonuclear chrom(III) and cobalt(III) complexes by JACOBSEN et al.<sup>12,13</sup>

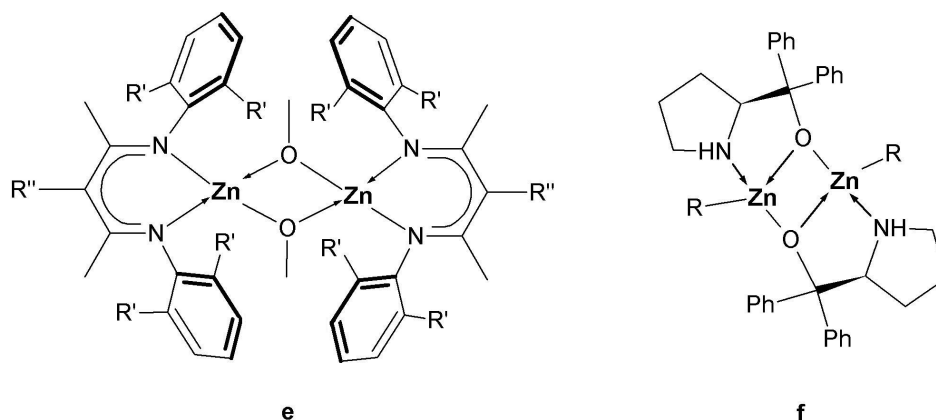


**Figure 2:** Catalysts complexes used by COATES (e) and NOZAKI (f) for activation of CO<sub>2</sub> in a copolymerization reaction.

## 1.2 Preparatory work

In contrast to the above mentioned Zn<sub>2</sub>O<sub>2</sub> motif, four-membered metalla rings with a Zn<sub>2</sub>N<sub>2</sub> motif were reported by VAN KOTEN and coworkers. They examined the reactions between dialkyl zinc compounds with N-substituted 1,4-diaza-1,3-butadienes.<sup>14</sup> Beside N- and C-alkylation reactions they observed the formation of the C-C coupled dimer of [alkylzinc-1,4-diaza-1,3-butadiene] radicals. Detailed investigations revealed an equilibrium between the C-C coupled dimer and the radical species.<sup>15,16</sup> However, the dimer is formed as dinuclear zinc complex with a folded Zn<sub>2</sub>N<sub>2</sub> ring, enabling

\*Asymmetric amplification is a positive non-linear effect. The term means a deviation from the assumed linear correlation of the product's ee with the ee of the chiral auxiliary in an asymmetric reaction. The opposite is denoted asymmetric depletion.<sup>11</sup>

a short metal···metal distance.<sup>17</sup> A similar C-C coupling reaction was reported by WESTERHAUSEN and coworkers with 2-pyridylmethylamines **h**.<sup>18</sup> In the first step 2-pyridylmethylamine **h** is metallated by dialkyl zinc in 1:1 molar ratio. The complexes **i** are dimeric compounds with a planar Zn<sub>2</sub>N<sub>2</sub> ring (Zn···Zn distance is 288 pm). Excess of dialkyl zinc led to an oxidative C-C coupling reaction and precipitation of equimolar amounts of zinc. C-C Coupling was also observed during thermolysis of the (alkyl)(2-pyridylmethylamide) zinc complex **i** at 150 °C. The coupling product **j** was found with a folded Zn<sub>2</sub>N<sub>2</sub> ring (Zn···Zn distance is 272 pm). In contrast to VAN KOTEN'S findings no monomer-dimer equilibrium was observed by WESTERHAUSEN and coworkers, which made the obtained dinuclear zinc complexes **j** an ideal molecule for investigations on cooperative behavior of such closely bound zinc(II) centers. Further investigations showed, that C-C coupling is also possible with tin(II) under elimination of tin metal.<sup>19</sup> However, the redox potential of Mg(II) was not sufficient to mediate the C-C coupling reaction. But the proposed intermediate, a metallated bisamide, could be isolated and crystallized as magnesium(II) complex.<sup>19</sup> This was accomplished with sterically demanding trialkylsilyl groups bound to the exocyclic nitrogen of the 2-pyridylmethylamine moiety. Although these large groups stabilized the Mg(II) complex they had no effect on the zinc-mediated C-C coupling.<sup>20</sup> Interestingly, several byproducts such as bis[methylzinc-2-pyridylmethylamido]-N,N'-bis(methylzinc)-2,3,5,6-tetrakis(2-pyridyl)piperazyl and 1-amino-1,2-dipyridylethene were obtained when unsubstituted 2-pyridylmethylamine was C-C coupled.<sup>20</sup> Furthermore, the pyridyl moiety was found to have a major influence on the C-C coupling mechanism. Substitution of pyridyl by isoelectronic phenyl did not lead to the formation of a C-C coupled product, even in refluxing toluene.<sup>19</sup> Early investigations showed, that in the C-C coupled product the zinc-bound alkyl groups can be exchanged by trialkylsilylphosphanes and arsanes yielding the compounds **m**.<sup>21</sup> Moreover, the reaction of bis(methylzinc) 1,2-bis((trialkylsilyl) amido)-1,2-dipyridylethane **j** with acetamide yielded the demetallated product 1,2-bis((trialkylsilyl)amine)-1,2-dipyridylethane **k**, whereas hydrolysis also cleaved the N-trialkylsilyl bonds under formation of **l**. In this context it is noteworthy, that the C-C coupling proceeds diastereoselectively to the (*R,R*) and (*S,S*) isomers of **j**. Thus, this method represents a diastereoselective ligand preparation pathway. Surprisingly, the reaction with aniline led to the C-N activation at the diaminoethane backbone of **j** and to substitution of N-trialkylsilyl by N-C<sub>6</sub>H<sub>5</sub> (compound **n**).<sup>22</sup>

Beside the C-C coupling pathways described by VAN KOTEN and WESTERHAUSEN also reductive procedures exist, that afforded symmetrically substituted vicinal diamines. These procedures represent ligand preparation pathways without the formation

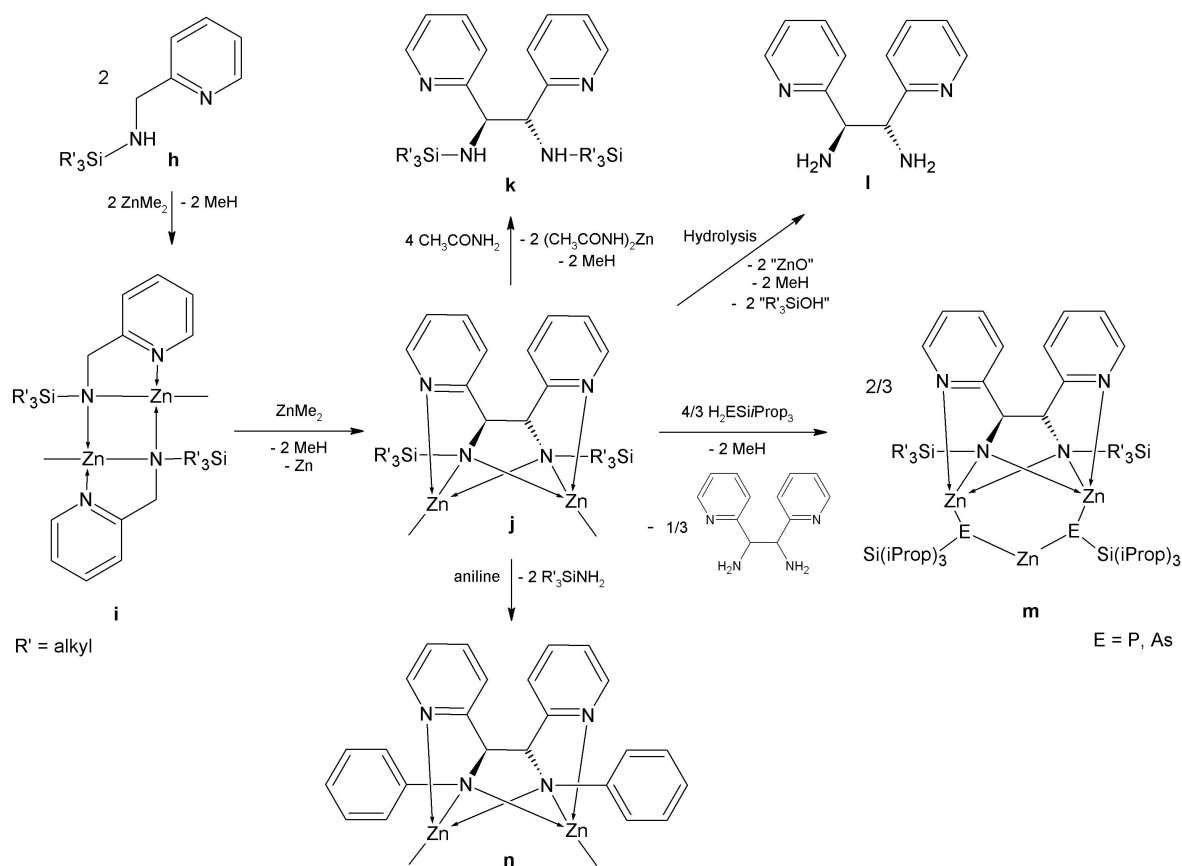


**Figure 3:** Presentation of the oxidative C-C coupling reaction and possible transformations.

of a metal complex. N-Alkyl substituted N-(pyridin-2-ylmethylidene)amines provided the starting compounds, which were coupled via oxidation of metals such as zinc or magnesium in the presence of equimolar amounts of trimethylsilyl chloride (TMSCl) as well as by titanium(III).<sup>23</sup> The latter was generated in situ by magnesium amalgam and the C-C coupling proceeded with moderate to good yields and highly diastereoselectively to the (*R,R*) and (*S,S*) isomers.<sup>24</sup> In contrast, the zinc mediated coupling reaction proceeded nearly quantitatively but with a statistical mixture of the possible diastereomers. However, isomerization of the *meso*-isomers to the respective (*R,R*) and (*S,S*) compounds was accomplished with lithium/isoprene for the diphenyl substituted vicinal diamines but was inapplicable with pyridyl substituents.<sup>25,26</sup> Further methods using  $\text{SmI}_2$ , aluminium or bismuth also afforded vicinal diamines with good to very good yields but with varying diastereoselectivities.<sup>27,28</sup> Products available via the described reductive coupling procedures can be expected to be suitable ligands for homo-dinuclear complexes similar to those obtained by oxidative coupling but without limitation to metal ions used in the coupling reaction.

The couplings described by VAN KOTEN and WESTERHAUSEN afforded complexes

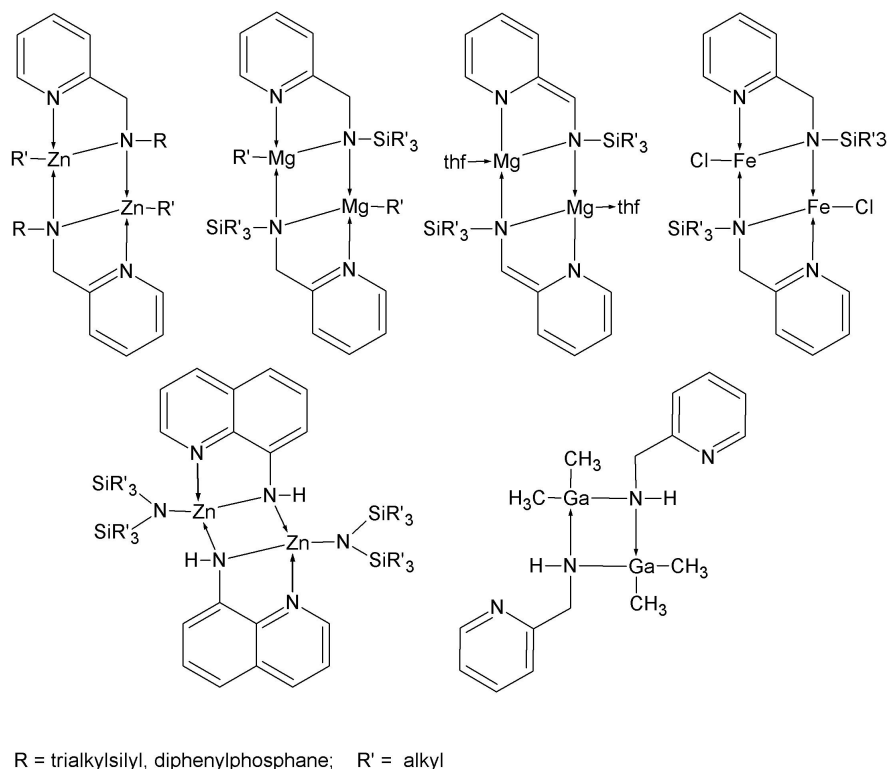


**Figure 4:** Presentation of selected complexes with four-membered  $Zn_2N_2$  rings.

with folded four-membered  $Zn_2N_2$  rings with a N-substituted 2-pyridylmethanamine motif. However, planar four-membered metalla rings were obtained with metal ions other than zinc and N-substituted 2-pyridylmethanamine ligands (see Figure 4). These complexes comprise metal centers such as Li(I), Mg(II), Zn(II), Fe(II), or Ga(III).<sup>19, 29–33</sup> In addition N-phosphanylated 2-pyridylmethanamines were also employed as ligands for dinuclear zinc complexes with a central  $Zn_2N_2$  ring.<sup>34</sup> Alkylation of the methylene moiety with *tert*-butyl is favored against the N-substitution of lithiated 2-pyridylmethanamine and also yielded the dimeric zinc complexes after reaction with dimethyl zinc.<sup>34</sup> Similar complexes of Zn(II) and Ga(III) were obtained with the more rigid 8-aminoquinoline ligand.<sup>35</sup>

1-(Pyridin-2-yl)-N-(pyridin-2-ylmethyl)methanamine **o** represents a very interesting ligand due to an additional donor site. Reaction of this ligand with dimethyl zinc led to formation of the dimeric complex bis[1-((pyridin-2-yl)-N-(pyridin-2-ylmethyl)methanamide) methylzinc] **p** with a planar  $Zn_2N_2$  ring, showing a transannular  $Zn \cdots Zn$  distance of 296 pm (Figure 5). Interestingly, only one zinc-bound methyl group was substituted and the ligand served as didentate chelator.<sup>36</sup> However, thermolysis of the solid complex led to the unexpected formation of gold-shining crystals of zinc bis[1,3-di(2-pyridyl)-2-azapropenide] **q**. This compound consisted of a tridentate 2-

azaallyl ligand backbone, which octahedrally coordinated one Zn(II) center. Reaction at room temperature of 1-(pyridin-2-yl)-N-(pyridin-2-ylmethyl)methanamine **o** with an excess of dimethyl zinc also led to crystallization of the zinc 2-azapropenide complex **q**. Bis(1-((pyridin-2-yl)-N-(pyridin-2-ylmethyl)methanamides) alkyl zinc complexes **p** with a planar Zn<sub>2</sub>N<sub>2</sub> ring also formed with bulky zinc-bound substituents such as the CH(SiMe<sub>3</sub>)<sub>2</sub> group. Also the Lewis basic thf did not lead to monomerization of the dimeric complex. However, exposure to air led to substitution of one 1-(pyridin-2-yl)-N-(pyridin-2-ylmethyl)methanamine ligand against a  $\mu$ -OH moiety. The obtained complex **t** showed a planar four-membered ZnNZnO ring.<sup>37</sup> Recently, the similar complex **u** was reported by ANANTHARAMAN and ELANGO who stabilized a Zn<sub>2</sub>(OH)<sub>2</sub> ring with N-heterocyclic carbenes and sterically demanding trimethylphenolato ligands.<sup>38</sup> Nevertheless, the addition of even small amounts of water to concentrated solutions of bis(1-((pyridin-2-yl)-N-(pyridin-2-ylmethyl)methanamides) alkyl zinc complexes **p** led to often violent decomposition. Detailed mechanistic investigations on the B3LYP/lanl2dz level of theory shed light on the hydrolysis mechanism and the influence of the steric demand of the zinc-bound ligand.<sup>37</sup> Very recently, our group reported the reaction of 1-(pyridin-2-yl)-N-(pyridin-2-ylmethyl)methanamine **o** and dimethyl zinc in the presence of equimolar amounts of *tert*-butylamine.<sup>39</sup> The reaction yielded the heteroleptic dinuclear complex **r** with a bridging *tert*-butylamide moiety with very good yields. Moreover, nearly quantitative exchange of the bridging *tert*-butylamide was possible by addition of methanol, yielding the comparable methoxy bridged complex **s** without affecting the zinc-bound alkyl ligands. This complex was also accessible by reaction of 1-(pyridin-2-yl)-N-(pyridin-2-ylmethyl)methanamine with dimethyl zinc in the presence of methanol. Central parts of both complexes **r** and **s** were four-membered Zn<sub>2</sub>N<sub>2</sub> and ZnNZnO rings, respectively. The Zn<sub>2</sub>N<sub>2</sub> ring was reported to be significantly folded with a transannular Zn···Zn distance of 285 pm. In contrast, the ZnNZnO cycle was found to be nearly planar with a Zn···Zn distance of 291 pm.

Folded and planar zinc-containing rings were prepared by a variety of methods and different transannular Zn···Zn distances were achieved. Investigations on the reactivity of the obtained complexes sometimes led to surprising results such as C-N activation and exchange by aniline. Furthermore, examinations showed that most of these reactions are invariant towards the zinc-bound ligand. However, the 1-(pyridin-2-yl)methanamine moiety played a crucial role during C-C coupling reactions. Attempts to C-C couple 1-(pyridin-2-yl)methanol via zinc mediated oxidative coupling were not successful and led to polymeric zinc complexes.<sup>29</sup> Also C-C coupling attempts of 1-(pyridin-2-yl)ethanamine as well as of benzylamines were unsuccessful. Oxidative coupling reactions were possible with N-trialkylsilyl or N-alkyl moieties, the latter,

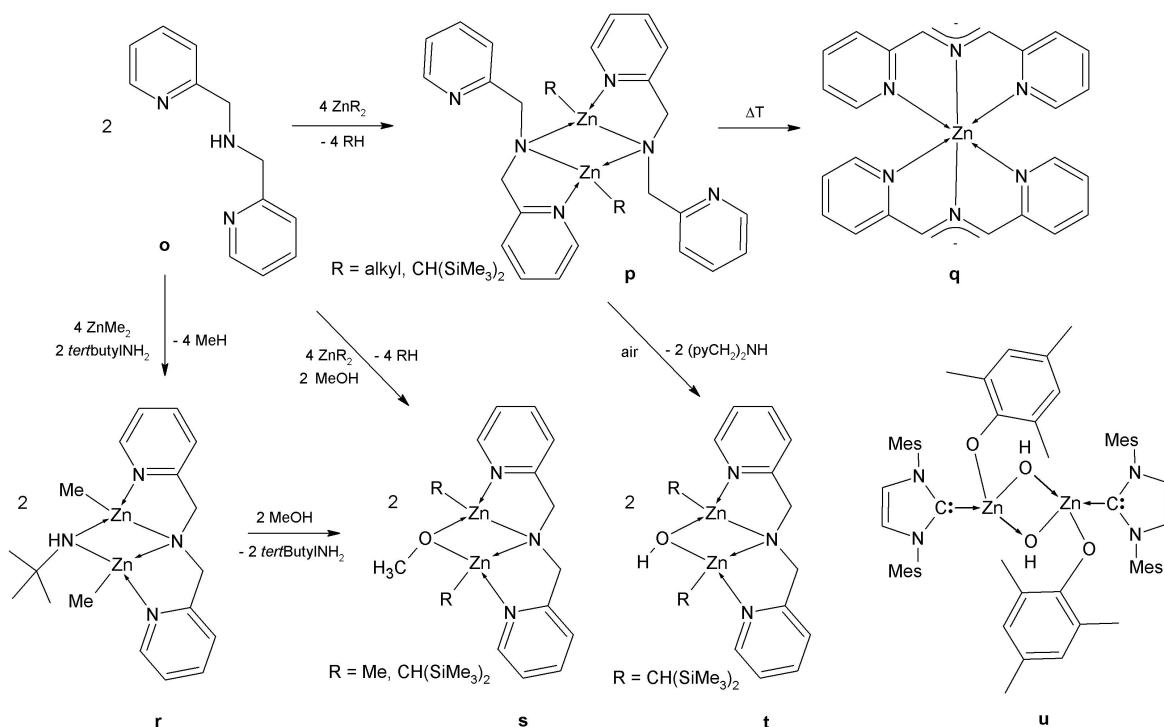


**Figure 5:** Presentation of dinuclear zinc complexes with the 1-(pyridin-2-yl)-N-(pyridin-2-yl-methyl)methanamine ligand reported by WESTERHAUSEN and coworkers and ANANTHARAMAN’S and ELANGO’S dinuclear hydroxyl-bridged complex **u**.

however, was reported to be an equilibrium between the monomer radical complexes and the dimeric complexes. Nevertheless, alkyl substituted ligands are accessible by several reductive coupling pathways. Thus also the nature of the N-bound substituent had a major influence on reactivity. When this substituent is the pyridin-2-ylmethyl moiety, a third coordination site is available and hydroxo, alkoxo and amido bridged dinuclear complexes were described. These complexes may have interesting catalytic properties for the activation of small molecules such as CO<sub>2</sub>. In spite of everything, the above described coupling pathways exclusively led to symmetrically substituted vicinal diamines and their homo-dinuclear complexes. With these systems only nitrogen donor atoms are available since the introduction of oxygen or sulfur donor sites in the ligand backbone is not possible. Furthermore, due to fixation to the 1-(pyridin-2-yl)methanamine moiety also the N-metal-N bite angle is fixed. However, the attractiveness of these systems is the access to folded metalla rings with short metal···metal distances. Planar metalla rings are available as homo- and heteroleptic complexes even with oxygen donor sites (see Figure 2) but have larger metal···metal distances.

To circumvent the drawbacks, new ligand preparation pathways for homo- and heterodinuclear complexes have to be considered. These pathways should allow a modular ligand preparation with different sets of donor atoms and the possibility to alter the coordination environment (bite angle, metal···metal distance, coordination number) and/or the electronic properties of the ligand. Custom tailoring of single ligands seems not to be appropriate since often quick and flexible alterations of the coordination sphere is not possible.

A modular ligand preparation pathway for homo- and hetero-dinuclear complexes was established by ROTH et al. Their procedure allows the formation of unsymmetric ligands via SCHIFF-base reactions starting with 1-hydroxyphenyl-2,6-diformyl compounds. These starting compounds were reacted with different primary amines such as 1-(pyridin-2-yl)methanamine, N-(aminoethyl)-1-(pyridin-2-yl)-N-(pyridin-2-yl-methyl)methanamine, benzoic acid hydrazide or thiosemicarbazide. The challenging task was the separation of symmetric byproducts, which always accompany such reactions. This, however, was hardly possible with standard chromatographic methods on silica or alumina due to the high polarity of the products. The problem was solved by application of size exclusion chromatography opening the way to compartmental unsymmetric "end-off" double SCHIFF-bases.<sup>40</sup> Nitrogen-rich, oxygen-rich and even sulfur containing binding sites were accessible by this method and homo- and hetero-dimetallic complexes of iron(II), nickel(II), copper(II) and zinc(II) were reported.<sup>40–42</sup> Examples are given in Figure 6. Although the ligand preparation pathway introduced by ROTH et al. is simple, versatile and straightforward it is fixed to at least one nitrogen donor due to the employed SCHIFF-bases. Thus, exclusive oxygen or sulfur donor sites are not accessible. Furthermore, the employment of carbonyl carbon atoms as linkers (imine moiety) affords planar metalla rings.

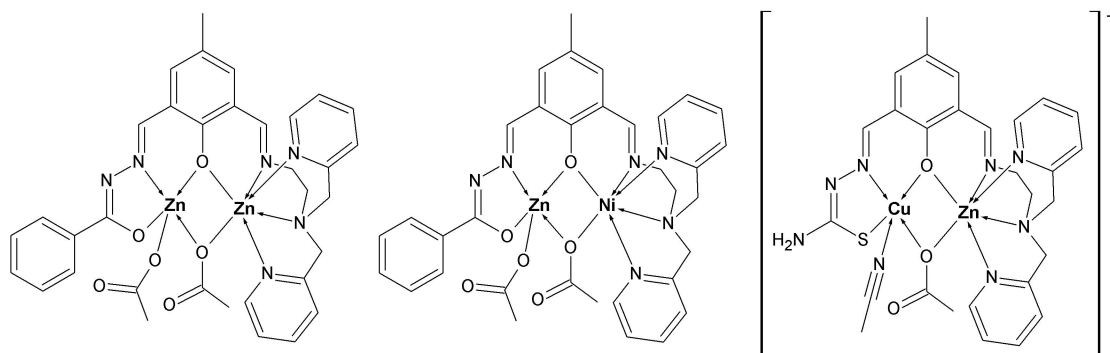


**Figure 6:** Presentation of selected complexes with double "end-off" SCHIFF-base ligands.

### 1.3 Aims

Based on the 1,2-di(pyridin-2-yl)-1,2-diaminoethane motif new ligand preparation pathways ought to be found that gain access to modified ligand backbones and allow the selection of nitrogen and/or oxygen donor atoms. A modular preparation protocol should allow the quick and flexible formation of new ligands. Emphasis was put on the ligand preparation and characterization as well as on its precursor compounds. For this purpose the well established nitroaldol reaction was chosen. Since this type of reaction also possesses an aza-variant the introduction of oxygen and nitrogen donor sites is possible. Firstly, a suitable catalyst ought to be found and the conditions of proligand syntheses should be examined. Furthermore, the nitro group is reported to be interchangeable into a variety of other functional groups, first and foremost to an amino moiety. It was also a goal of the presented work to examine conditions for functional group interchange. Nevertheless, also the synthesis of metal complexes was within the scope of the presented work. The examination of the catalytic activity of prospective custom tailored complexes should serve as a benchmark for the developed pathway. The complexation behavior of prospective ligands should be examined by preparation of their zinc(II) complexes. The use of zinc ions possesses clear advantages, which are the borderline hardness of zinc(II) and thus the coordination to nitrogen oxygen or sulfur donor sites. Furthermore, redox reactions are not to be expected due to the stability of the +2 oxidation state and its diamagnetic nature enables NMR spectroscopic investigations.



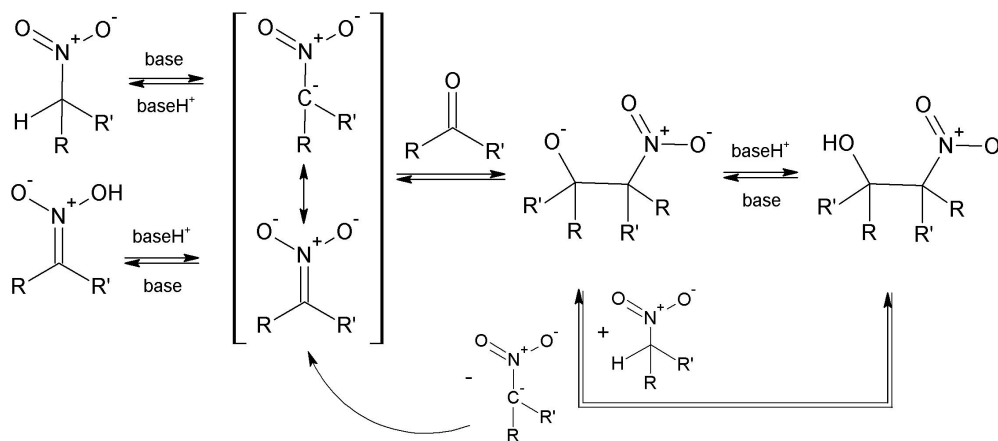
---

## 2 Results and Discussion

### 2.1 Ligand design via nitroaldol reaction with pyridine-2-carbaldehyde

#### 2.1.1 Overview

Nitro compounds are valuable precursors for a wide range of compounds. Aryl-nitro compounds for example have been used for the preparation of azo dyes or explosives for decades. Aliphatic nitro compounds were found to be valuable reagents for the synthesis of complex molecules. The latter is especially due to the ready availability of those compounds. Aliphatic nitro compounds can for example be synthesized by the substitution of alkyl halides or azides by nitrite or the oxidation of oximes.<sup>43</sup> Beyond that, nitronate anions obtained from primary and secondary nitroalkanes are valuable donor synthons and are used in the important nitroaldol reaction. The nitroaldol or HENRY reaction was discovered in 1895 by HENRY and is the base catalyzed addition of an  $\alpha$ -CH acid nitro compound to an aldehyde or ketone.<sup>44</sup> This reaction yields  $\beta$ -nitroalcohols and has emerged to an important carbon-carbon bond formation reaction. It is mechanistically similar to the aldol reaction as depicted in Scheme 1.



**Scheme 1:** Presentation of equilibria and intermediates involved in the nitroaldol reaction.

Firstly, the nitroalkane is deprotonated by the base under formation of a nitronate anion. This anion is, comparable to the enolate generated in an aldol reaction, stabilized by charge delocalization. It attacks the electrophilic carbonyl carbon under formation of an alkoxide, which itself can abstract a proton from the nitroalkane or from baseH<sup>+</sup>. In many cases this reaction is an equilibrium and  $\beta$ -nitroalcohols may undergo retro-HENRY reaction. Further side reactions may be the self-addition

of  $\alpha$ -CH acidic carbonyl compounds or the CANNIZARRO reaction. Moreover, aryl-substituted nitroalcohols were reported to eliminate water under formation of an often not unwanted nitroalkene compound. NEF-reaction<sup>†</sup> may also be an unwanted side reaction.

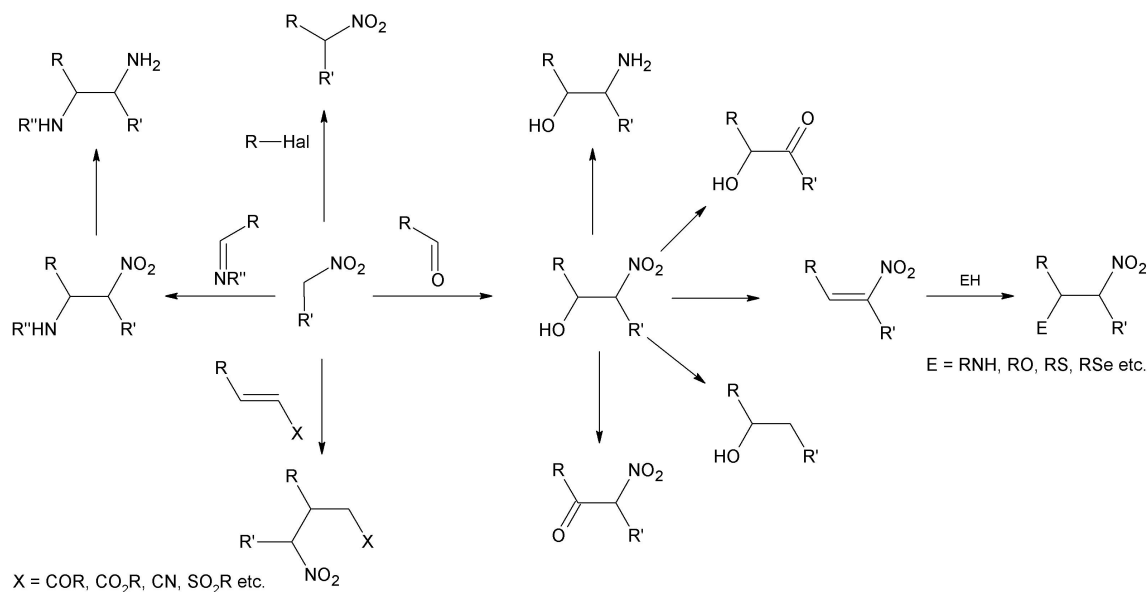
To suppress competitive reactions the conditions, especially the basicity of the medium, have to be carefully chosen. Thus, a great variety of base catalysts were developed, including alkali metal hydroxides, carbonates, bicarbonates, alkoxides, calcium and barium hydroxides as well as magnesium and aluminium ethoxides. Furthermore, polymer supported bases such as anion exchange resins or polymer supported tbd (p-tbd) were successfully applied. Among organic bases are also primary and tertiary amines, ammonium acetate, fluoride and even enzymes have proven to efficiently catalyze the nitroaldol reaction.<sup>45-47</sup>

However, the value of this reaction is not because of the formation of nitroalcohols but is due to a great variety of consecutive products that may be obtained from these compounds. For example, nitroaldol reactions are a valuable tool for the total synthesis of biologically important aminodeoxy sugars. Vicinal amino alcohols, obtained via nitroaldol reaction and subsequent reduction of the nitro group have a broad significance in organic chemistry. Their biological relevance can be seen in the structures of epinephrine (adrenalin) and related mediators. Furthermore, anthracycline antibiotics, such as L-daunosamine, L-ristosamine, L-acosamine and L-vancosamine are biologically important members of the family of amino sugars. Functionalized nitroalkanes were reported to be useful functionalized alkyl anion synthons in the synthesis of natural products via  $\beta$ -nitro alcohols and  $\alpha$ -nitro ketone intermediates.<sup>43,45</sup> Transformations of nitroalcohols comprise the dehydration yielding nitroalkenes, which themselves are valuable reagents as MICHAEL acceptors or dienophiles in DIELS-ALDER reactions. As already mentioned, reduction of the nitro group leads to  $\beta$ -amino alcohols, an important class of compounds. Oxidation of the alcohol moiety affords  $\beta$ -nitro ketones, while  $\beta$ -hydroxy ketones are available by NEF reaction. Also denitration with tributylstannane was described in literature.<sup>45,46</sup> An overview over important transformations is given in Scheme 2. Having the use of the obtained compounds as ligands in mind, the addition of thiols to nitroalkenes is a valuable reaction. Moreover, this reaction was reported to proceed in situ with the carbonyl, nitroalkane, thiol, and triethylamine.<sup>48</sup>

Also the carbonyl analogous imines were reported to be electrophiles for HENRY-type reactions. These additions are also called aza-HENRY or nitro-MANNICH reaction.<sup>49,50</sup> The obtained  $\beta$ -nitroamines often tend to undergo retro-addition and thus

---

<sup>†</sup>The conversion of nitro compounds to carbonyl compounds was reported in 1894 by the chemist JOHN ULRIC NEF.



**Scheme 2:** Overview over reactions of aliphatic nitro compounds.

were converted to the stable vicinal diamines. However, silylated nitronates were found to lead to stable isolable products. The great value of vicinal diamines as ligands or antitumor agents has triggered efforts towards their diastereoselective and enantioselective synthesis. But also the above described  $\beta$ -nitroalcohols were targets for stereoselective syntheses and during the last decade efficient catalysts for both HENRY and aza-HENRY reaction were developed.<sup>51–54</sup>

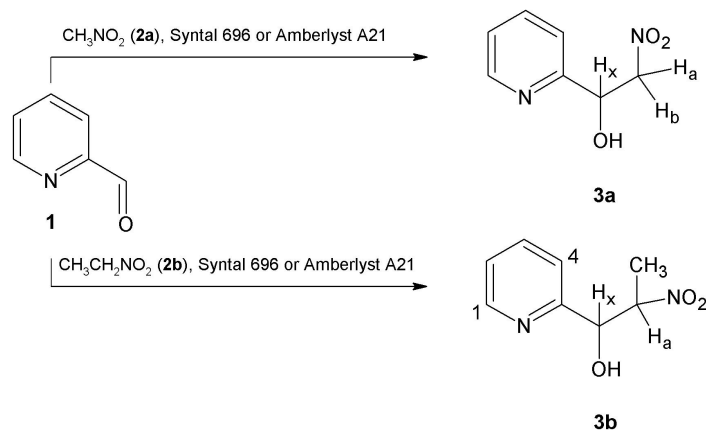
### 2.1.1.2 Synthesis and reactivity of 2-nitro-1,3-di(pyridine-2-yl)propane-1,3-diol

**Introduction** As described above, basic catalysts are necessary for the nitroaldol reaction and a great variety such as organic and inorganic bases, quaternary ammonium salts or enzymes are used to name a few. Despite that, even today the development of new catalysts is a field of extensive research.<sup>47,55</sup> This is due to different sets of conditions such as solubility of the reactants, work-up conditions, presence of other functional groups and ease of nitronate generation. Furthermore, the increasing requirement for stereochemically pure compounds has prompted the development of various asymmetric catalysts.<sup>53</sup> For reaction between nitroalkanes and pyridine-2-carbaldehydes several boundary conditions have to be taken into account. First of all, the selected conditions should be transferable to substituted pyridine-2-carbaldehydes if fine-tuning of the ligand is necessary. Furthermore, the reaction protocol should be as simple as possible, followed by a simple work-up procedure. And of course, side reactions such as dehy-

dration to the nitroalkene or NEF-type reactions should be avoided. That requires a catalyst which reacts under mild conditions and is easy to remove. In addition, the basicity of the catalyst should lie between that of the nitronate and the obtained alcoholate. In this case the catalyst acts as a proton relay and acidic work-up is avoided. For this work two catalyst were selected which meet all criteria. The first is a basic magnesium-aluminium hydroxy carbonate (Syntal 696<sup>®</sup> Südchemie AG, Munich), a white non-toxic powder which exhibits a pH of 9.5 in a suspension in water/ethanol (50 g/l, 20°C according to safety data sheet). This commercially available hydrotalcite was firstly used by HELL and coworkers who described it as a compound, which can easily be handled under aerobic conditions and does not require high-temperature pretreatment or long procedures such as rehydration to be activated.<sup>56</sup> Hydrotalcites consist of brucite-like layer structures. In brucite Mg(OH)<sub>2</sub> the divalent magnesium ions M(II) are octahedrally coordinated by hydroxide ions. But other divalent cations M(II) such as Cu, Zn, Ni, Co or Mn are also possible choices. Partially isomorphous substitution of M(II) by trivalent aluminium ions M(III) (or Fe, Ga, V, Ru, Rh, Y) leads to a positive net charge, which is compensated by additional anions such as carbonate, nitrate or sulfate A<sup>n-</sup>. These anions and crystal water are intercalated in interstitial layers between the brucite-like sheets. The general formula can be written as [M(II)<sub>1-x</sub>M(III)<sub>x</sub>(OH)<sub>2</sub>]<sup>x+</sup> (A<sup>-n</sup><sub>x/n</sub> · Y H<sub>2</sub>O), with x in the range from 0.1-0.33.<sup>57,58</sup> Hydrotalcites, such as anionic clays, are members of an interesting family of materials, which are used as catalysts, catalyst supports, anion exchangers or composite materials.<sup>59-61</sup>

The second solid, Amberlyst A21<sup>®</sup>, which is a weak basic anion exchange resin, was firstly used by BALLINI and coworkers.<sup>62</sup> The spherical beads are a functionalized styrene, divinylbenzene, polyacrylic copolymer with tertiary amine moieties as active sites. Amberlyst A21<sup>®</sup> is non-toxic, cheap, easy to handle and needs no pretreatment. In fact, Amberlyst A21<sup>®</sup> seems to be more active than Syntal 696<sup>®</sup> but has a huge specific pore volume of 0.1 ml/g, which lowers the yields by retaining the reactants. With both catalysts, however, the advantages of heterogeneous catalysis are met.

**Results** The reaction of pyridine-2-carbaldehyde **1** in nitromethane **2a** in the presence of Syntal 696<sup>®</sup> or Amberlyst A21<sup>®</sup> led to the complete conversion of the aldehyde and to the formation of 2-nitro-1-(pyridin-2-yl)ethanol **3a** (Scheme 3).<sup>56,63,64</sup> The catalysts were removed by filtration and reusable nitromethane by distillation. Reduction of the solvent to a fourth of its original volume and storage at -20°C yielded crystals suitable for X-ray analysis.



**Scheme 3:** Nitroaldol reaction of pyridine-2-carbaldehyde **1** with nitromethane **2a** and nitroethane **2b**.

Compound **3a** can be stored at room temperature and aerobic conditions. Although within two weeks the solid became brown, NMR investigations showed no decomposition products. The observed covering seemed to be only a very thin layer, which could not be detected by NMR spectroscopy. Also the filtrate (from crystallization) became violet within hours. However, dehydration reactions to the nitroalkene were not observed, which is in agreement with literature reports.<sup>56,65</sup> Due to the chiral carbon  $\alpha$ -O-CH the adjacent methylene protons are diastereotopic, hence showing an ABX spin system in the proton NMR. The geminal coupling constant is  $^2J(\text{H}_A, \text{H}_B) = 13.2$  Hz, the vicinal coupling constants are  $^3J(\text{H}_A, \text{H}_X) = 4.0$  Hz and  $^3J(\text{H}_B, \text{H}_X) = 8.4$  Hz.

The  $\beta$ -nitroalcohol **3a** crystallized in the chiral space group  $P2_12_12_1$ . However, measurements of the optical rotation revealed the racemic nature of **3a** as expected. With the applied Mo- $K_\alpha$  radiation the determination of the absolute configuration is not possible. Hydrogen bonds between the OH moiety and the pyridyl nitrogen lead to an arrangement of the molecules on a 2-fold screw axis (Figure 8). These interactions are rather strong, since an  $\text{O1}\cdots\text{N1}'$  donor distance of 272 pm is found (" ' " is used to label atoms of adjacent molecules). All bond lengths and angles are within the expected range.<sup>66</sup> The molecular structure of **3a** is depicted in Figure 7, a comparison of bond lengths and angles is given in Table 1.

The reaction between nitroethane **2b** and pyridine-2-carbaldehyde **1** in thf with Syntal 696<sup>®</sup> furnished 2-nitro-1-(pyridin-2-yl)propan-1-ol **3b** with excellent yield and a diastereomeric excess of the *erythro* isomer of  $de = 30\%$ .<sup>56</sup> Reacting pyridine-2-carbaldehyde **1** in a 20-fold molar excess of nitroethane **2b** with Amberlyst A21<sup>®</sup> led to formation of **3b** with 39% yield and a 1:1 molar ratio of the *erythro*- and *threo*-isomers. With the employment of Amberlyst A21<sup>®</sup> under neat conditions the product

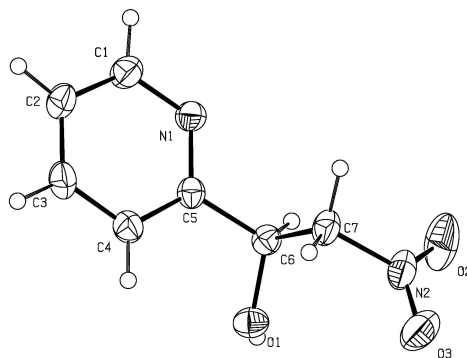


**Figure 7:** Molecular structure and numbering scheme of **3a**. The ellipsoids represent a probability of 40 %, H atoms are drawn with arbitrary radii.

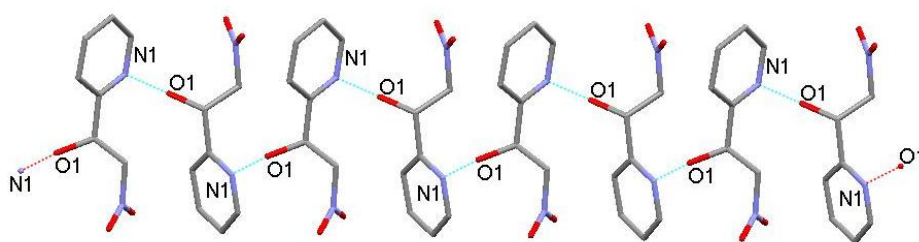


**Figure 8:** Arrangement of **3a** on 2-fold screw axis.

**3b** was obtained with a yield of 79 % and a 9:1 ratio of the *threo*:*erythro* isomers (de = 80 %). Both isomers can be distinguished by the vicinal coupling constants of the  $\alpha$ -O-CH<sub>x</sub> doublet. But since there are three groups capable of forming hydrogen bonds, which would affect the conformation, the simple recognition that  ${}^3J_{anti} > {}^3J_{syn}$  is not necessarily straightforward.<sup>67</sup> Hence, the assignment of NMR data was made according to the method of ROUSH and coworkers, who studied the ABX patterns of a vast number of substituted  $\beta$ -hydroxy ketones.<sup>68</sup> They showed that internal hydrogen bonds affect the conformation to a significant extent. The adoption of ROUSH'S method to the diastereomeric  $\beta$ -nitroalcohol **3b** is illustrated in Figure 9.<sup>68</sup> Consequently, the larger coupling constant can be assigned to the *threo* isomer ( ${}^3J = 7.2$  Hz), while the smaller coupling constant belongs to the *erythro* isomer ( ${}^3J = 4.0$  Hz). If these findings are correct and the internal hydrogen bonds determine the conformation, the proton H<sub>x</sub> of the *erythro* isomer should not exhibit dipole-dipole interactions with the methyl group. In contrast the *threo* isomer's H<sub>x</sub> should, which was shown by selective NOE experiments. Irradiation at the NMR frequencies of H<sub>x</sub> and observation of the NOE signals confirmed the above made assumptions. The results can be summarized as follows: *erythro*:  $\delta$  (H<sub>x</sub>) = 5.39 ppm,  ${}^3J = 4.0$  Hz, no NOE signal at 1.4 ppm; *threo*:  $\delta$  (H<sub>x</sub>) = 5.06 ppm,  ${}^3J = 7.2$  Hz, NOE signal at 1.4 ppm.

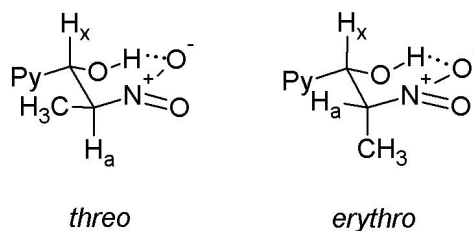


**Figure 9:** Sawhorse projection of the *threo*- and *erythro* isomers of **3b**. Hydrogen bonds between OH and NO<sub>2</sub> determine the conformation and hence the vicinal coupling constant  $^3J(\text{H}_a, \text{H}_x)$ .

Slow evaporation of a chloroformic solution yielded crystals suitable for X-ray analysis in form of the hydrochloride of **3b** (see Figure 10). The molecules in the solid state of **3bHCl** are arranged along a 2-fold screw axis, forming hydrogen bonds between Cl $\cdots$ HN and OH $\cdots$ Cl (Figure 11). Bond lengths and angles are compared in Table 1. Two crystallographically independent molecules are present in the asymmetric unit, both have *threo*-configuration and are distinguished by the letters "A" and "B". They are mutually connected with the chloride ion via hydrogen bonds along the screw axis. Both have slightly different bond lengths and angles within standard deviations. These differences are caused by packing effects, since the arrangement of the molecules in the lattice is controlled by hydrogen bonds. Hydroxyl hydrogen atoms were not refined but the dihedral angles of the H-O1-C6-C(5,7) moieties can be determined by choosing the hydrogen position between the two hydrogen bond forming donor atoms O1 and Cl1. The distance between O1 and Cl1 is approximately 302.5 pm in "A" and 306.4 pm in "B", indicating a weak interaction. As can be seen from the dihedral angles, all three molecules have a nearly syn-planar conformation around O1-C6 (see Table 1).

In the solid states of both  $\beta$ -nitroalcohols **3a** and **3b**, hydrogen bonds between the OH moiety and the pyridyl nitrogen were found and led to an arrangement of the molecules on a 2-fold screw axis. In contrast, NMR investigations in chloroformic solution revealed hydrogen bond interactions between the OH moiety and the nitro group, which determine the conformation. In solution, the pyridyl nitrogen is not or only to a minor extent involved in hydrogen bond interactions. This was shown by selective NOE experiments with **3b**. Irradiation at the NMR frequency of the methyl group resulted in NOE signals for the pyridyl protons H1 and H4 (see Scheme 3). This indicates a free rotation of the pyridyl group and hence no or only minor hydrogen bond interactions.

The proton adjacent to the nitro group of the compounds **3a** and **3b** remains acidic allowing further reactions. The selected reaction pathway contains a second nitroaldol reaction step at this position (Scheme 4). This again was achieved with pyridine-2-

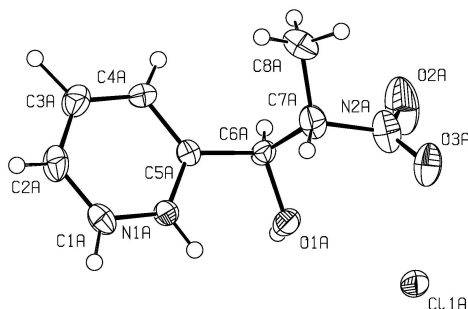


**Figure 10:** Molecular structure and numbering scheme of **3bHCl**. The ellipsoids represent a probability of 40 %, H atoms are drawn with arbitrary radii.

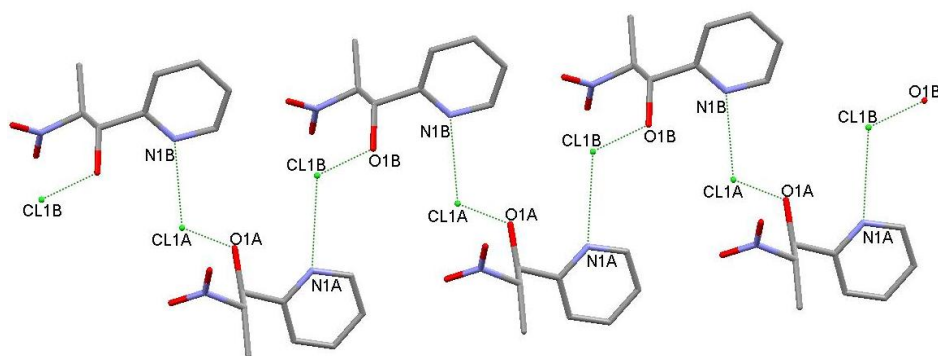


**Figure 11:** Arrangement of **3bHCl** on a 2-fold screw axis.

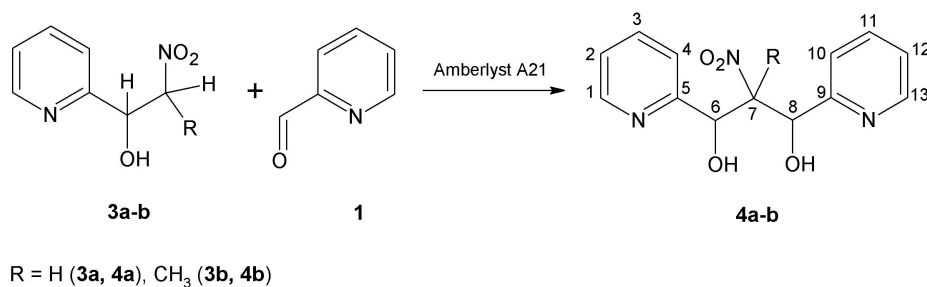
carbaldehyde **1** as the substrate and the conditions for this reaction were examined. The distinct advantage of using the same aldehyde is of course the receipt of a symmetric molecule with a decreased number of possible diastereomers. The reaction was conducted with Amberlyst A21<sup>®</sup> as the catalyst under neat conditions. However, minor formation of the diol **4a** was also found with Syntal 696<sup>®</sup> after several weeks. The nitro compound and pyridine-2-carbaldehyde **1** were reacted in a 1:1 molar ratio. A slight temperature decrease was observed during dissolving the nitro compound **3a** or **3b** in pyridine-2-carbaldehyde. In contrast, the addition of Amberlyst A21<sup>®</sup> led to an increase in temperature up to 60 °C. During the reaction a white precipitate is formed, which can be separated either by washing the products **4a** and **4b** through a porous frit and retaining the catalyst beads (useful for small amounts up to 3 g) or by separation of the dry powder on a sieve with 0.25 mm mesh size. Both products **4a** and **4b** tend to get slightly brownish when stored at room temperature but remain white when stored at -20 °C.

Due to the symmetric substitution of the ligand's backbone, four stereomers are possible. These are two *meso*-isomers and a pair of enantiomers (*R,R*) and (*S,S*). The



**Table 1:** Comparison of selected bond lengths [pm] and angles [ $^{\circ}$ ] of the compounds **3a** and **3b**. Atoms of adjacent molecules are labeled with " ' ". They are used to calculate dihedral angles involving the OH moiety. The OH hydrogen atom is assumed to lie on the connecting line between donor atoms of adjacent molecules

Parameter	<b>3a</b>	<b>3bA</b>	<b>3bB</b>
O1-C6	140.9(2)	140.3(4)	141.1(4)
C6-C7	152.5(2)	154.0(5)	153.6(5)
C5-C6	152.0(2)	150.9(4)	152.4(4)
C6-H6	101.6(17)	91.(3)	98.(4)
C7-N2	149.4(2)	148.6(5)	148.9(5)
O1-C6-C5	111.60(14)	110.8(2)	109.7(2)
C5-C6-C7	108.56(14)	108.9(3)	107.2(2)
N2-C7-C6	108.34(14)	107.0(3)	108.0(3)
N1'...O1-C6-C7	-126.3	—	—
N1'...O1-C6-C5	114.5	—	—
C11...O1-C6-C7	—	147.8	-122.1
C11...O1-C6-C5	—	-93.9	121.0



**Scheme 4:** Nitroaldol reaction of pyridine-2-carbaldehyde **1** with the  $\beta$ -nitroalcohols **3a** and **3b**.

central carbon C7 in the *meso*-isomers is pseudo-asymmetric or pseudo-chiral<sup>‡</sup>. Due to identical absolute configurations of the carbons C6 and C8 of the (*R,R*)- and (*S,S*)-isomers, the central carbon C7 is symmetric. Since the *meso*-isomers are diastereomers, both can be distinguished in the NMR spectra. But having a closer look on either one of the *meso*-isomers, the protons H6 and H8 are enantiotopic. Thus the positions 6 and 8 in each *meso*-compound can't be distinguished but one can distinguish between both *meso*-isomers. This of course is also true for the pyridyl rings. Things are different regarding the pair of enantiomers, which of course can't be distinguished by achiral methods like NMR spectroscopy (in achiral solvents and without shift reagents). But

<sup>‡</sup>The traditional name for a tetrahedrally coordinated carbon atom bonded to four different entities, two and only two of which have the same constitution but opposite chirality sense. The r/s descriptors of pseudo-asymmetric carbon atoms are invariant on reflection in a mirror (i.e. r remains r, and s remains s), but are reversed by the exchange of any two entities (i.e. r becomes s, and s becomes r).<sup>69</sup>

the protons H6 and H8 are diastereotopic, which makes them distinguishable inside each antipode (which themselves are undistinguishable). This again is true for the pyridyl rings. These considerations lead to the expectation of complex NMR patterns. In the following the expected and observed NMR spectra of **4a**, which bears a proton at position 7, will be discussed. According to the above made considerations one would expect one doublet and one triplet signal for each *meso*-isomer. Furthermore, two sets of pyridyl signals should be observed. But no relations should be found between the two expected sets of pyridyl signals along the propyl backbone in the HMBC spectra, since both would belong to different *meso*-isomers. For the pair of enantiomers also two doublets could be expected each for the position 6 and 8 and a doublet of doublets for the position 7. Again one would expect two sets of pyridyl signals but also a relation between those rings via the propyl backbone in the HMBC spectra. In the  $^1\text{H}$  NMR a pseudotriplet and two doublets are found with an intensity ratio of 1:1:1. The intensity ratio proves, that the triplet does not originate from *meso*-isomers, which could accidentally be isochronic and would then have a ratio of 1:1:2 (doublet(*meso a*):doublet(*meso b*):triplet(*meso a + b*)). Moreover, all  $^{13}\text{C}$  NMR signals appear as separate signals and C6 exhibits a cross signal to H8 and vice versa in the HMBC spectrum. This indicates the formation of the (*R,R*)- and (*S,S*)-isomers of **4a**. However, minor signals are also found but are mostly covered by the major ones. Due to an excellent elemental analysis they can be assigned to the *meso*-isomers. From the  $^1\text{H}$  NMR spectrum a diastereomeric excess of  $de = 77\%$  for the (*R,R*)- and (*S,S*)-isomers was calculated. Analysis of the vicinal coupling constants  $^3J$  of the adjacent protons unfolded a value of  $^3J = 6.0$  Hz. This indicates the energetic equality of the possible rotamers in solution, which leads to the observed average value for  $^3J$ . For compound **4a** no isomerization was observed.

The analysis of the NMR spectra of **4b** is more complicated than of **4a**. However, the same considerations made for **4a** concerning the number of stereoisomers and their distinction can be made. But, due to the quaternary carbon C7 the useful vicinal H,H coupling is omitted and NMR signals of the protons at C6 and C8 thus can be expected as singlets. NMR experiments in  $\text{CD}_2\text{Cl}_2$  or  $\text{CD}_3\text{OD}$  showed that most of the proton signals are isochronic or chemical shifts differ only to a very small extent. In the  $^{13}\text{C}$  NMR two sets of signals are observed also with little differences. All  $^{13}\text{C}$  NMR signals could be assigned to  $^1\text{H}$  NMR signals via HSQC spectroscopy but assignment to the absolute position or isomer impossible. Due to the observation of only two sets of signals one could consider the existence of only one set of isomers (the two *meso*-isomers or the (*R,R*)- and (*S,S*)-isomers). HMBC spectra, however, revealed a cross coupling between C6 and C8, which led to the conclusion that (*R,R*)- and (*S,S*)-isomers were present in

solution. But in contrast to compound **4a** isomerization together with decomposition was observed over a period of several hours in solution.  $^1\text{H}$  and  $^{13}\text{C}$  NMR spectra then showed four sets of signals. Distinction between the *meso*-isomers was impossible due to signal overlaps of the respective stereoisomers together with decomposition products. The assignment of NMR data of the (*R,R*)- and (*S,S*)-isomers has been made on the basis of NMR spectra obtained at 273 K.

Both 2-nitro diols **4a** and **4b** decompose very slowly under atmospheric conditions at r.t. Due to two electron withdrawing groups ( $\text{NO}_2$  and  $\text{OH}$ ), retroaldol reaction occurs and the obtained retro-HENRY products may also undergo subsequent reactions. Moreover, pyridine-2-carbaldehyde **1** is always found as a decomposition by-product. Although the color slowly turns to brown the degree of decomposition is small when stored as a solid since only small signals of decomposition products are found in the NMR. However, it was found that decomposition of **4a** and **4b** in solution is the faster the more polar the solvent is. This is an indicator for an ionic decomposition pathway. NMR investigations in  $\text{D}_2\text{O}$  /  $\text{CD}_3\text{OD}$  showed the formation of about 5 % of pyridine-2-carbaldehyde **1** after 4 h. This was also found when triethyl amine or dmap were added. In contrast, no color change could be observed when **4a** was heated for several hours under reflux in hydrous thf. Unfortunately, zinc salts such as zinc chloride or zinc perchlorate were found to catalyze the decomposition. Again decomposition was the faster the more polar the solvent was. For example, when **4a** was reacted with zinc chloride in dmsO the solution turned dark brown within half an hour. A solution in thf under the same conditions slowly turned brown during a period of several hours. Furthermore, during the zinc catalyzed decomposition the presence of water plays a crucial role and complexation had to be conducted under anhydrous conditions.

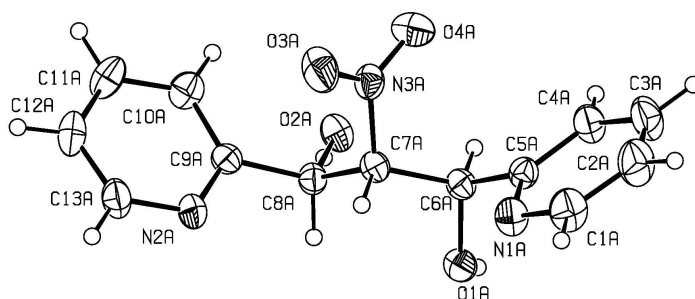


**Figure 12:** Molecular structure and numbering scheme of (*R,R*)/(*S,S*)-**4a**. The ellipsoids represent a probability of 40 %, H atoms are drawn with arbitrary radii. Solvent molecules have been omitted for clarity.

Slow evaporation of ethereal solvents such as diethyl ether or thf yielded crystals suitable for single crystal X-ray diffraction of **4a** and **4b**. The structure of 2-nitro-1,3-dipyridin-2-ylpropane-1,3-diol **4a** was solved in the space group  $\text{P}\bar{1}$  and is affected

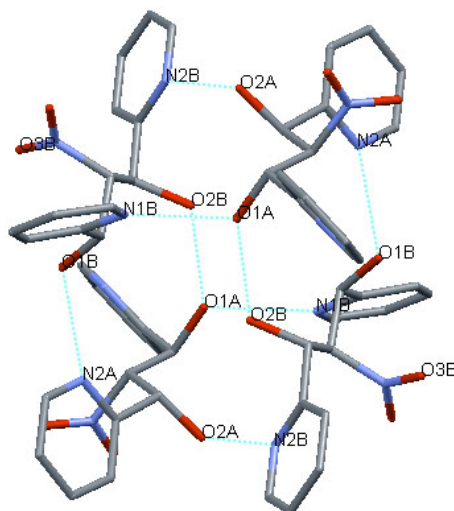


**Figure 13:** Hydrogen bond controlled arrangement of  $(R,R)/(S,S)$ -**4a** in the solid state. H atoms and solvent molecules have been omitted for clarity.

by hydrogen bond interactions between the pyridyl nitrogen atoms and the hydroxyl groups. Four molecules are arranged around the inversion center via hydrogen bonds and form a globular entity, which is depicted in Figure 13. The gaps between those entities contain solvent molecules (thf or diethyl ether). The  $(R,R)$ - and  $(S,S)$ -isomers are found in the solid state and due to inversion symmetry compound **4a** crystallized as racemate. Two crystallographically independent molecules of **4a** are found in the asymmetric unit and are distinguished by the letters "A" and "B" as depicted in Figure 12. The disparity is due to different dihedral angles, which are affected by hydrogen bond interactions. Other angles and bond lengths differ only slightly within standard deviations and are summarized in Table 4 on page 32. However, larger differences of about 3 pm (within standard deviations) are found between the O1-C6 and O2-C8 bond lengths of **4aB**. Also a staggered conformation is found along the O1-C6 (N2A'-O1B-C6B-C5B = 73.7°) bond while an eclipsed conformation is found along O2-C8 (O1B'-O2B-C8B-C9B = -122.3°). Thus the different O-C bond lengths may be due to negative hyperconjugative effects, since the conformation around O1-C6 allows a charge transfer interaction between an O1 lone pair ( $n_{O1}$ ) and the antibonding  $\sigma^*$  orbital of the C6-C5 bond. Within standard deviations a slight elongation of C6-C5 is found with respect to C8-C9 where the conformation precludes this interaction. The negative hyperconjugation effect, however, is considered to be small, since a  $\sigma_{C-C}^*$  orbital is known to be a poor acceptor.

2-Methyl-2-nitro-1,3-dipyridin-2-ylpropane-1,3-diol **4b** crystallized in the monoclinic space group  $P2_1/c$ . Again two crystallographically independent molecules are found in the asymmetric unit, which are distinguished by the characters "A" and "B". They are

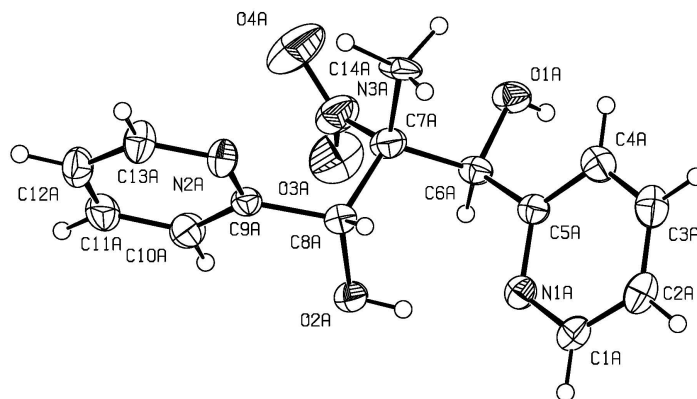


**Figure 14:** Molecular structure and numbering scheme of *meso*-**4b**. The ellipsoids represent a probability of 40 % , H atoms are drawn with arbitrary radii.

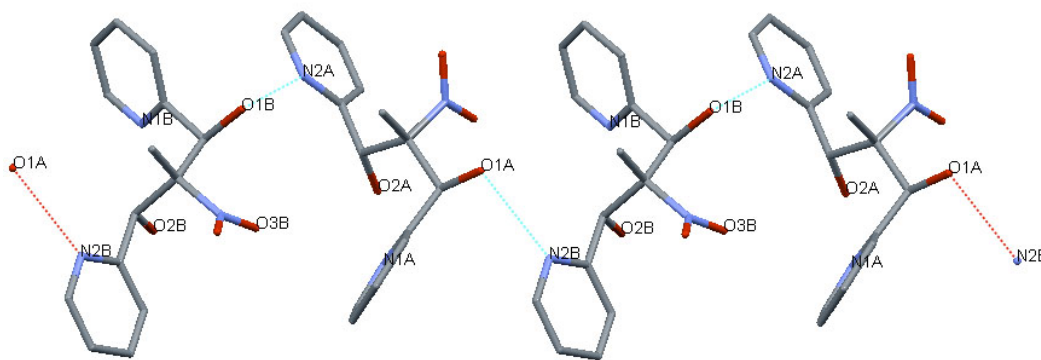


**Figure 15:** Arrangement of *meso*-**4b** on a 2-fold screw axis in the solid state. H atoms have been omitted for clarity.

mutually arranged via hydrogen bond interactions between the pyridyl nitrogen and the hydroxyl groups on a two-fold screw axis (Figure 15). In contrast to the diol **4a**, the *meso*-isomer (*1R,2r,3S*)-**4b** is found in the solid state. Bond lengths and angles are within the expected range and are summarized in Table 4 on page 32.<sup>66</sup>

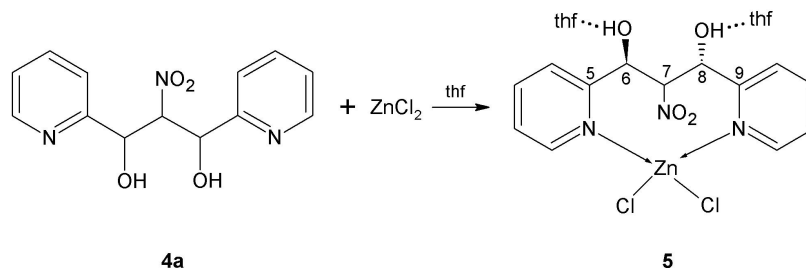
**Concluding remarks** With the applied solid catalysts Syntal 696<sup>®</sup> and Amberlyst A21<sup>®</sup> a modular procedure to 1,3-dipyridin-2-yl-propane-1,3-diols was developed. The first step of the nitroaldol reaction proceeds with very good yields and the procedure involves a simple work-up. Consecutive reactions of the products **3a** and **3b** with pyridine-2-carbaldehyde **1** were not observed under the applied conditions. With the second step the introduction of a different aldehyde such as salicyl aldehyde should be possible. However, pyridine-2-carbaldehyde was chosen to limit the number of possible diastereomers. NMR investigations of the obtained 1,3-dipyridin-2-yl-propane-1,3-diols led to the conclusion that the second step proceeds diastereoselectively. Although, isomerization of 2-methyl-2-nitro-1,3-dipyridin-2-ylpropane-1,3-diol **4b** occurred in so-

**Table 2:** Comparison of selected NMR data (chemical shift,  $\delta$ ) of the compounds **3a**, **3b**, **4a**, **4b** and **5**. As a convention for compound **5**, H6 is assigned to the proton with the smaller vicinal coupling constant  $^3J$ .

Parameter	<b>3a</b>	<b>3b</b>	<b>4a</b>	<b>4b</b>	<b>5</b>
C5	156.6	156.4	160.3	156.4	159.6
C6	70.4	73.3	73.3	74.8	69.7
C7	80.7	86.6	95.5	98.0	97.6
C8	—	—	72.5	74.8	69.6
C9	—	—	160.3	156.4	160.7
(HO1)	(4.30)	(4.59)	(5.91)	(4.90)	(5.92)
(HO2)	—	—	(6.06)	(5.40)	(6.34)
H6	5.45	5.39	5.33	5.32	5.16
H7	4.79, 4.62	4.84	5.61	—	5.09
H8	—	—	5.52	5.32	5.49

lution if this product was redissolved. The crystal structures of the compounds **3a**, **3b**, **4a** and **4b** were found to be governed by hydrogen bond interactions. It is noteworthy, that the asymmetric units of **3b**, **4a** and **4b** consist of two molecules. Crystal structures with  $Z' > 1$  cover approx. 10 % of organic compounds ( $Z'$  is the number of molecules per asymmetric unit).<sup>70,71</sup> Investigations addressing the stability of **4a** and **4b** revealed that decomposition occurs slowly in solution and is faster the more polar the solvent is. Zinc cations were found to promote decomposition. Not surprisingly an ionic decomposition pathway can be assumed, which might also be triggered by negative hyperconjugation ( $n_O/\sigma_{C-C}^*$  interaction).

### 2.1.3 Synthesis of 2-nitro-1,3-di(pyridin-2-yl)propane-1,3-diolato zinc dichloride

**Scheme 5:** Reaction of 2-nitro diol **4a** with zinc chloride and formation of its mononuclear complex **5**.

**Table 3:** Comparison of the Cl-Zn-Cl angle [ $^{\circ}$ ] with the Zn-Cl and Zn-N bond lengths [pm] of presented and selected published compounds of the type  $(L_2)ZnCl_2$ 

Compound	Cl-Zn-Cl	Zn-Cl	Zn-N	Reference
(bipy) $ZnCl_2$	117.1	220.4	205.9	<sup>76</sup>
(4-vinyl-py) $_2ZnCl_2$	118.7	220.9	204.8	<sup>77</sup>
(tmeda) $ZnCl_2$	119.0	221.4	209.2	<sup>78</sup>
<b>5</b>	121.16(2)	221.8	206.4	
(4-acetyl-py) $_2ZnCl_2$	123.6	221.1	205.2	<sup>77</sup>
(4-cyano-py) $_2ZnCl_2$	125.7	221.3	206.5	<sup>77</sup>

A mononuclear zinc chloride complex **5** was obtained when anhydrous zinc chloride was reacted with **4a** in anhydrous thf (Scheme 5). Surprisingly, neither the N,O nor the O,O donor side was occupied by zinc. Instead the metal ion was found to be coordinated by the two pyridyl nitrogen atoms in a distorted tetrahedral environment, forming an eight-membered ring. Two thf molecules are hydrogen bonded to the hydroxyl groups with an average  $O \cdots O$  distance of 268 pm. A comparison of bond lengths and angles between the complex **5** and the ligand **4a** is given in Table 4. The Zn-N bond lengths in **5** are equal and within the expected range but not surprisingly a large N-Zn-N angle of  $115.41(6)^{\circ}$  is found. Bond lengths and angles of the ligand backbone are within the expected range and the complex is found to be the  $(R,R)/(S,S)$ -isomer.<sup>66</sup> However, due to crystallographic inversion symmetry the racemate is found in the solid state.<sup>72</sup> The Cl-Zn-Cl angle is found to be  $121.16(2)^{\circ}$  and is comparable with several complexes of the type  $(L_2)ZnCl_2$ , which are shown in Table 3. Previous investigations of WESTERHAUSEN and coworkers show a linear correlation between the Zn-N bond length and the X-Zn-X angle of tetrahedral complexes of the type  $L_2ZnX_2$  (with L = Lewis base with nitrogen donors and X being any monodentate anionic ligand).<sup>73-75</sup> Short Zn-N bond lengths indicate strong Lewis donor acceptor interactions and as a result small X-Zn-X angles are found. In this context the ligand can be considered as strong, which is also supported by the complex' insensitiveness against hydrolysis. No decomposition could be observed when stored under atmospheric conditions for several days.

The complex was found to be stable in anhydrous thf as indicated by NMR investigations. An analysis of the vicinal coupling constants of the  $O_2NC-H7$  proton revealed, that no major conformational changes or rearrangement reactions took place. In the  $^1H$  as well as in the  $^{13}C$  NMR spectra one set of signals as expected for the  $(R,R)/(S,S)$ -isomer is observed. This, however, indicates that no decomposition occurs during the NMR investigation. Moreover, if rearrangement reactions such as alteration of the coordination sphere took place, which are fast on the NMR time scale, an averaged

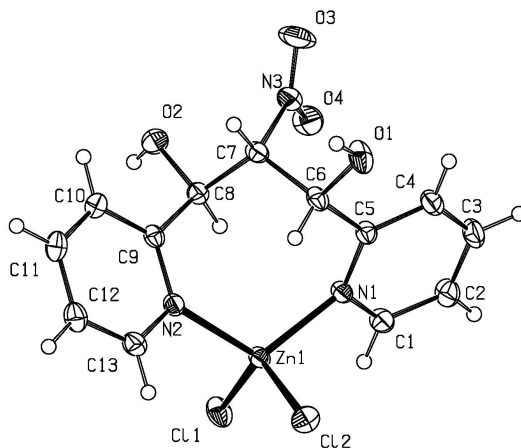


**Figure 16:** Molecular structure and numbering scheme of **5**. The ellipsoids represent a probability of 40 %, H atoms are drawn with arbitrary radii. Solvent molecules have been omitted for clarity.

set of signals would be observed. But such rearrangements would also imply a major change of torsion angles which could be observed by an averaged vicinal coupling constant  ${}^3J(\text{H,H})$  of  $\text{O}_2\text{NC-H7}$  (cf. coupling constants of **4a**, page 25). The observed  ${}^1\text{H}$  NMR signal ( $\delta = 5.09$ ) for  $\text{O}_2\text{NC-H7}$  is a doublet of doublets with  ${}^3J = 1.6$  Hz and  ${}^3J = 10.0$  Hz. Similar coupling constants have been calculated from dihedral angles, obtained by single crystal X-ray analysis of complex **5**. The dihedral angles were determined to be  $\text{H7A-C7-C6-H6A} = 70^\circ$  and  $\text{H7A-C7-C8-H8A} = 173^\circ$  (see Figure 16, H atoms were found by single crystal X-ray analysis). Hypothetical coupling constants were calculated from these angles using an extended KARPLUS equation introduced by HAASNOOT and coworkers.<sup>79</sup> They empirically parameterized the equation, also taking the relative orientations of the non-H-substituents into account, as well as the contributions of the different electronegativities.<sup>§</sup> With this equation two hypothetical coupling constants were calculated:  ${}^3J(\text{H7A,H6A}) = 1.9$  Hz ( $\phi = 70^\circ$ ) and  ${}^3J(\text{H7A,H8A}) = 8.7$  Hz ( $\phi = 173^\circ$ ). These hypothetical coupling constants, calculated from solid state geometry values, are in very good agreement with the observed coupling constants. As a result, one can assume that the conformation of complex **5** in thf solution is similar to the one in the solid state and rearrangement equilibria can be excluded. These findings are supported by the fact that two species of thf were found in the NMR spectra, the NMR solvent residue and hydrogen bridged thf. Deviations between calculated and observed coupling constants, however, arise from errors in molecular structure determination as well as from limitations of the employed equation.

<sup>§</sup> $J(\text{H}, \text{H}) = P_1 \cos^2 \phi + P_2 \cos \phi + P_3 + \sum \Delta \chi_i (P_4 + P_5 \cos^2 (\xi_i \phi + P_6 |\Delta \chi_i|))$ ; with  $P_{1-6}$  empirical parameters ( $P_1 = 13.24$ ,  $P_2 = -0.91$ ,  $P_3 = 0$ ,  $P_4 = 0.53$ ,  $P_5 = -2.41$ ,  $P_6 = 15.5$ ),  $\phi$  torsion or dihedral angle,  $\Delta \chi_i$  electronegativity difference,  $\xi_i = +1$  or  $-1$  to address the relative orientation.



**Table 4:** Comparison of selected bond lengths [pm] and angles [°] of **4a**, **4b** and **5**.

Parameter	<b>5</b>	<b>4aA</b>	<b>4aB</b>	<b>4bA</b>	<b>4bB</b>
Zn-N1	206.74(15)	—	—	—	—
Zn-N2	206.08(15)	—	—	—	—
C6-C5	151.6(3)	151.6(6)	153.8(6)	151.9(4)	152.5(4)
C7-C6	155.3(3)	152.7(6)	152.9(6)	154.9(4)	154.2(4)
C7-C8	153.3(3)	154.2(6)	153.7(6)	156.7(4)	157.2(4)
C8-C9	151.7(2)	152.2(6)	150.4(7)	151.2(4)	150.9(4)
O1-C6	140.6(2)	141.5(5)	138.7(6)	141.6(4)	142.1(4)
O2-C8	140.8(2)	142.1(5)	145.3(6)	141.0(3)	140.8(3)
C9-N2	134.8(2)	134.0(6)	133.9(6)	133.5(4)	134.2(4)
C5-N1	134.6(2)	134.6(6)	132.9(6)	134.3(4)	134.0(4)
O1-H	79.(3)	— <sup>a</sup>	— <sup>a</sup>	74.(4)	82.(5)
O2-H	75.(3)	— <sup>a</sup>	— <sup>a</sup>	87.(4)	89.(5)
C6-C7-C8	115.89(15)	111.9(3)	112.8(4)	112.3(2)	111.0(2)
C7-C8-C9	109.35(15)	112.9(4)	112.2(4)	112.2(2)	112.8(2)
C7-C6-C5	113.28(15)	112.8(4)	110.6(4)	113.0(2)	111.9(2)
C6-C5-N1	116.94(16)	115.8(4)	114.9(4)	114.7(2)	114.8(3)
C8-C9-N2	117.79(15)	115.6(4)	116.8(4)	116.8(2)	117.2(2)
N1-Zn-N2	115.41(6)	—	—	—	—
Cl1-Zn-Cl2	121.16(2)	—	—	—	—
(H)-O1-C6-C7 <sup>b</sup>	63.7	143.3	161.7	162.5	159.5
(H)-O1-C6-C5 <sup>b</sup>	−172.2	−94.2	−73.7	73.0	77.7
(H)-O2-C8-C7 <sup>b</sup>	163.4	161.8	117.5	72.3	80.9
(H)-O2-C8-C9 <sup>b</sup>	−77.7	−72.8	−122.3	−162.7	−154.2

<sup>a</sup> H atoms were not refined.

<sup>b</sup> Dihedral angles were determined using the donor atom of an adjacent molecule instead of H. The hydrogen atom is assumed to lie between the O1 or O2 and the respective donor atom. While the donor⋯donor distance must not be more than 310 pm with a donor-O-C angle between 90° and 120°.

#### 2.1.4 Development of macromolecular catalysts for nitroaldol reactions

**Introduction** In the course of the nitroaldol reaction between nitromethane **2a** and pyridinealdehyde **1** a new stereogenic center is formed at the prostereogenic aldehyde carbon. The above described reactions with Syntal 696<sup>®</sup> or Amberlyst A21<sup>®</sup>, how-

ever, yielded the racemic products. Nevertheless, an enantioselective nitroaldol reaction is preferred and many homogeneous catalysts were developed, which applied perfectly to this purpose.<sup>53,54,80</sup> Enantioselective, heterogeneous catalysis is possible with molecularly imprinted polymeric layers or particles. Molecularly imprinted polymers are used as enzyme or antibody mimics,<sup>81</sup> stationary phases for chromatography<sup>82</sup> or recognition elements in sensor materials.<sup>83–85</sup> They can for example be made of inorganic compounds such as silica derivatives<sup>86,87</sup> or organic polymeric materials like methacrylate derivatives. Molecular imprinting is the template assisted creation of a rigid (crosslinked) polymer matrix, in which the form of the template (size and position of functional groups) is retained after copolymerization. Functionalized monomers or crosslinkers are used to achieve specific intermolecular interactions (e.g. hydrogen bonds) with the template, thus creating a binding pocket after copolymerization of the matrix.<sup>88</sup> After removal of the template, the shape of the imprint and the arrangement of the functional groups are complementary to the structure of the template. For enantioselective reactions the transition state has to be imprinted into the matrix. This implies the development of a template molecule which, matches the transition state (transition state analogue, TSA) and the careful selection of monomers and crosslinkers to obtain a specific binding pocket.<sup>89</sup> However, the development of a suitable template and fine-tuning of the matrix in order to carry out enantioselective nitroaldol reactions was not within the scope of the presented work. But the question, if one could develop a polymeric catalyst that is able to catalyze the nitroaldol reaction and provides a starting point for the development of imprinted polymer catalysts for enantioselective nitroaldol reactions, became apparent during the examination of the nitroaldol reaction with Amberlyst A21<sup>®</sup>.

**Results** As described above the catalytically active site of Amberlyst A21<sup>®</sup> is a dialkyl amino moiety (cf. page 19). Therefore three macromolecular catalysts which contain a diethyl amino group as prospective catalytically active site were examined, in cooperation with SCHULZ and MOHR of the institute of physical chemistry of the Friedrich-Schiller Universität. This moiety is part of the major monomer 2-(diethylamino)ethyl 2-methylprop-2-enoate **1**, which is shown with further monomers and crosslinkers in Table 5. In this table the composition of all three polymers is also given. The selected monomers and crosslinkers are well known and widely used. The compounds were polymerized with 1 mol % aibn by thermal activation at 70 °C in acetonitrile, the obtained solid was grinded in a mortar, washed and dried in vacuo. The nitroaldol reaction was carried out with one to three millimeter sized pieces.

As a result, all three catalysts converted pyridinealdehyde **1** into the nitro alcohol

**Table 5:** Selected monomers and crosslinkers for the preparation of polymer catalysts and their composition in w%.

monomers	catalyst 1	catalyst 2	catalyst 3
2-(diethylamino)ethyl-2-methylprop-2-enoate	50	50	50
methacrylic acid	20	20	20
styrene	-	-	10
crosslinker			
ethylene glycol-bis(methacrylate)	30	-	-
1,4-divinyl benzene	-	30	20

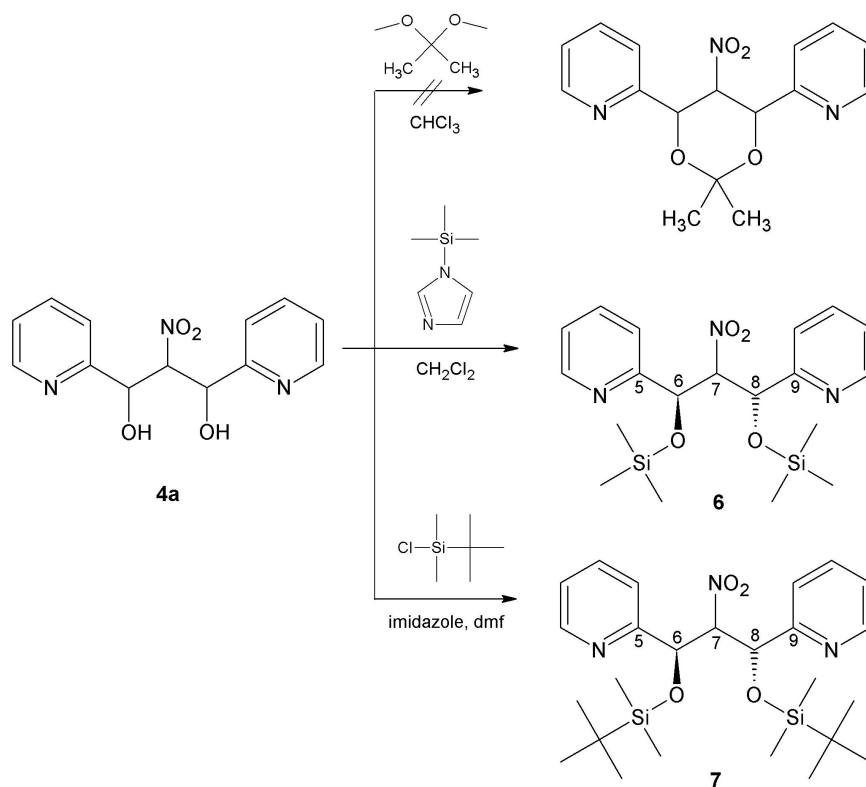
**3a** after 24 hours at room temperature with yields >90 %. The workup procedure comprised filtration of the catalyst and removal of all volatile compounds yielding the product with 95 % purity. Pure product was obtained by reduction of the volume to one fourth and crystallization at -20 °C. The selected diethylamino moiety, embedded in the aforementioned polymeric matrix, can be considered as a suitable catalyst for the nitroaldol reaction.

### 2.1.5 O-Trialkylsilyl protection of 2-nitroalcohols

**Introduction** In section 2.1.2 on page 26 the stability of both dipyridyl-nitro-1,3-diols **4a** and **4b** was discussed. It is obvious, that retro-HENRY reactions occur especially in polar solvents. Decomposition reactions were also a major drawback during attempts to reduce the nitro group, which is described in section 2.1.6. To circumvent decomposition reactions, the deployment of protective groups for the hydroxyl moieties was necessary. Preliminary tests with both  $\beta$ -nitro alcohols **3a** and **3b** in order to react them with N-methyl-pyridylmethylideneamine **15a** by means of an aza-HENRY reaction also showed, that protection of the hydroxyl moiety was necessary.

**Results** 2-Nitro-1,3-dipyridin-2-ylpropane-1,3-diol **4a** was chosen for the development of a protection strategy, due to its higher stability in solution with respect to **4b**. Firstly 2,2-dimethoxypropane **2**, which was widely used for the protection of 1,3-diols, was chosen as protective agent.<sup>90</sup> The aspired ketal was expected to be insensitive against most oxidizing and reducing agents and can be cleaved under acidic conditions. Moreover, diastereoselective cleavage was reported.<sup>90</sup> Compound **4a** was reacted with an excess of 2,2-dimethoxypropane **2** in dilute chloroformic solution employing *p*-toluenesulfonic acid as a catalyst. To shift the equilibrium, the methanol, which was formed during the reaction was removed with molecular sieve 3 Å in a KUMAGAWA extractor.<sup>91</sup> After three hours at reflux the <sup>1</sup>H NMR, <sup>13</sup>C NMR and IR spectra indicated the formation of the respective hemiketal. But unfortunately a four-fold set of signals in the <sup>13</sup>C NMR also indicated isomerization of compound **4a**. 2-Nitro-1,3-dipyridin-2-ylpropane-1,3-diol **4a** could be easily protected with trimethylsilyl imidazole to form 2-nitro-1,3-di(pyridin-2-yl)-1,3-di(trimethylsilyloxy)propane **6** with good yields as a yellowish oil. During the protection no isomerization occurred and the (*R,R*) and (*S,S*) isomers of **6** were received as the main components. Rotation around the C-C bonds of the propyl backbone is hindered at room temperature and two distinct vicinal coupling constants were observed (H6 <sup>3</sup>J = 4.4 Hz, H8 <sup>3</sup>J = 8.0 Hz). The NMR spectra comprise a 2-fold set of signals, which is in agreement with the observations for compound **4a**. Unfortunately, the TMS group turned out to be unstable under the conditions for the functional group interchange described in section 2.1.6. For the subsequent examinations the *tert*-butyl-dimethylsilyl (TBDMS) protective group was deployed, that is also a very common protective group. Its usefulness is due to the ease of protection and cleavage conditions, which do not interfere with other functional groups. Furthermore, the TBDMS group is stable against most oxidizing and reducing agents as well as under basic conditions.<sup>90</sup> The TBDMS-O- moiety is reported to be 10<sup>4</sup> times more stable than the trimethylsilyl-O moiety.<sup>90</sup> Protection of both hydroxyl moieties of **4a** was achieved in a concentrated dmf solution with TBDMSCl and an excess of imidazole.<sup>92</sup> Due to the hydrophobic and sterically demanding alkyl groups, aqueous work-up led to precipitation of almost pure product **7** with very good yields.

The above made considerations concerning the number of possible diastereomers is also valid for compound **7** (see NMR discussion for compound **4a** on page 23). Also two sets of signals are observed in the <sup>1</sup>H NMR as well as in the <sup>13</sup>C NMR spectra. Cross signals between both OCH moieties in the HMBC spectrum, however, revealed the existence of the (*R,R*) and (*S,S*) isomers. In contrast to compound **4a** no signals of the *meso*-isomers were observed for **7** in the NMR spectra because the rotation of the bulky *tert*-butyl-dimethylsilyl groups around C6-C7 and C7-C8 is hindered at room



**Scheme 6:** Protection of 2-nitro-1,3-dipyridin-2-ylpropane-1,3-diol **4a** with 2,2-dimethoxypropane, TMSimidazole and TBDMSCl.

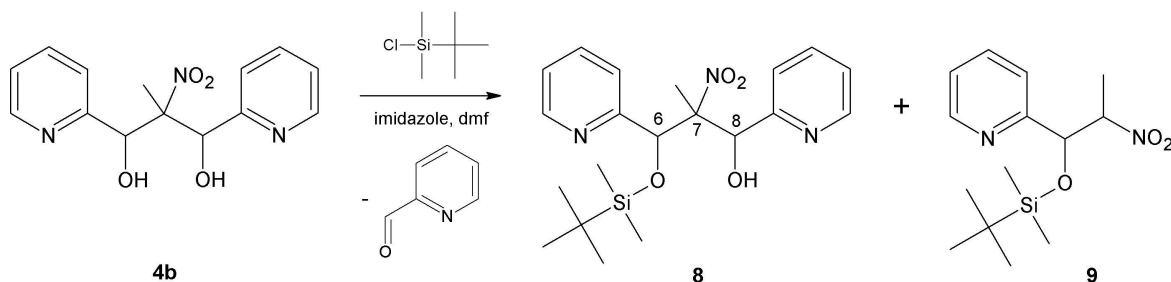
temperature. Therefore, two doublets are observed for H6 as well as H8 with coupling constants of  $^3J = 2.2$  Hz and  $^3J = 9.6$  Hz. For the central H atom a doublet of doublets is observed with  $^3J = 2.0$  Hz and  $^3J = 9.6$  Hz. These findings are in contrast to those of compound **4a** where average vicinal coupling constants were observed ( $^3J = 6.0$  Hz). The rotation around the O-Si bonds is also hindered at room temperature. NMR spectra show distinct signals for all four Si-bound methyl groups, whereas both *tert*-butyl groups appear as two distinct singlets. Table 6 gives an overview over selected chemical shifts of the compounds **4a**, **6**, **7** and **5**. However, no major differences are found between the four compounds in the NMR spectra.

Crystals suitable for single crystal X-ray diffraction were obtained by slow solvent evaporation of a solution of **7** in methanol. The crystal structure of silylether **7** was solved in space group  $P\bar{1}$  and due to crystallographic inversion symmetry it is a racemate. Bond lengths and angles are within the expected range and are compared with other compounds in Table 7. The Si1-O1-C6 angle was found to be  $131.15(13)^\circ$  and Si2-O2-C8 =  $126.39(12)^\circ$ . These large angles are typical for alkylsilyl ethers and hint at  $sp^2$  hybridized oxygen atoms.

**Table 6:** Comparison of selected NMR data (chemical shifts,  $\delta$ ) of the compounds **4a**, **6**, **7** and **5**. As a convention for the compounds **5** and **7**, H6 is assigned to the proton with the smaller vicinal coupling constant  $^3J$ .

Parameter	<b>4a</b>	<b>6</b>	<b>7</b>	<b>5</b>
C5	160.3	159.0	158.6	159.6
C6	73.3	73.8	74.0	69.7
C7	95.5	96.6	96.9	97.6
C8	72.5	73.6	73.2	69.6
C9	160.3	158.8	157.6	160.7
(HO1)	(5.91)	—	—	(5.92)
(HO2)	(6.06)	—	—	(6.34)
H6	5.33	5.16	5.10	5.16
H7	5.61	5.64	5.67	5.09
H8	5.52	5.54	5.55	5.49

The same protecting conditions as used for **4a** were employed to protect **4b**. Aqueous work-up and extraction with pentane afforded 3-(*tert*-butyldimethylsilyloxy)-2-methyl-2-nitro-1,3-di(pyridin-2-yl)propan-1-ol **8** as pentane insoluble precipitate. This product molecule bears only one TBDMS group (Scheme 7).



**Scheme 7:** Protection of 2-methyl-2-nitro-1,3-di(pyridin-2-yl)propane-1,3-diol **4b** with TBDMSCl.

From the organic phase an oily residue was obtained, which was mainly 2-nitro-1-(pyridin-2-yl)-1-(*tert*-butyldimethylsilyloxy)propane **9**. This finding, however, indicates that retroaldol reactions may occur under the applied protection conditions. Due to this fact, the obtained yields of **8** were only 30 % but with sufficient purity. The mono-protected silyl ether **8** exhibits three stereogenic centers and thus eight possible stereoisomers (four different pairs of enantiomers). NMR investigations showed that only one pair of enantiomers was obtained. This is indicated by the observation of a single set of signals, where of course both pyridyl rings are distinguishable. Stereochemical assignment is complicated, due to the loss of the propyl backbone's vicinal proton-proton coupling. Furthermore, rotation around the C-C single bonds is not fully hindered at room temperature (as observed for compound **7**), thus NOE exper-

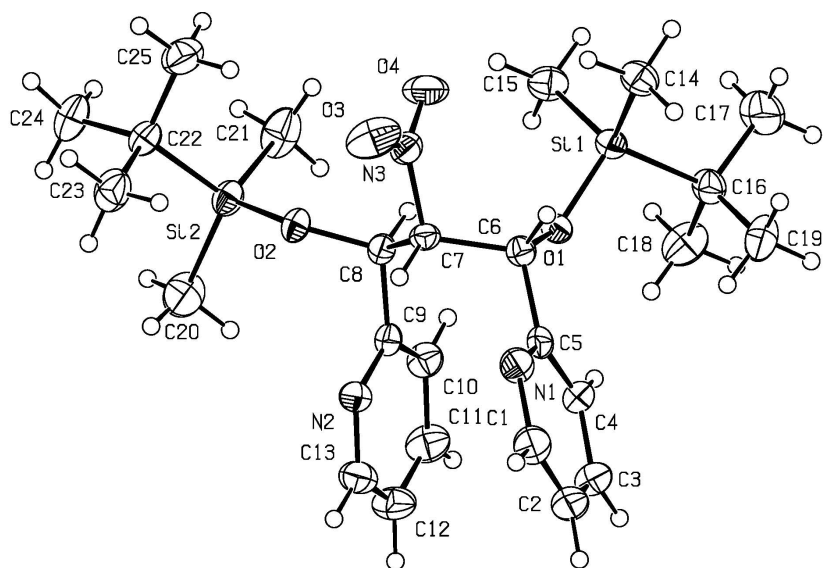


**Figure 17:** Molecular structure and numbering scheme of **7**. The ellipsoids represent a probability of 40 %, H atoms are shown with arbitrary radii.

iments could only give a rough idea of the obtained isomers. Therefore single crystal X-ray diffraction was employed to determine the relative configuration of compound **8**. Suitable crystals were obtained by slow solvent evaporation of a solution of **8** in diethyl ether. The obtained colorless crystals were uniform in shape and represented almost the whole dissolved mass of **8**. X-ray diffraction results revealed a solvent-free lattice, which crystallized in the centrosymmetric space group  $C2/c$ . The hydrogen atoms were located in difference Fourier syntheses and refined isotropically. Thus the relative configuration was determined to be  $6S7S8R$  and  $6R7R8S$ , respectively (numbering according to Scheme 7). This is in agreement with NOE results in solution. It is noteworthy that the conformation in the solid state is affected by an internal hydrogen bond between O1 and N2 (see Figure 18) with a donor...donor distance of 270 pm. Bond lengths and angles are comparable with those of the precursor compound **4b** and are summarized in Table 7. They were found to lie in the expected range.<sup>66</sup>

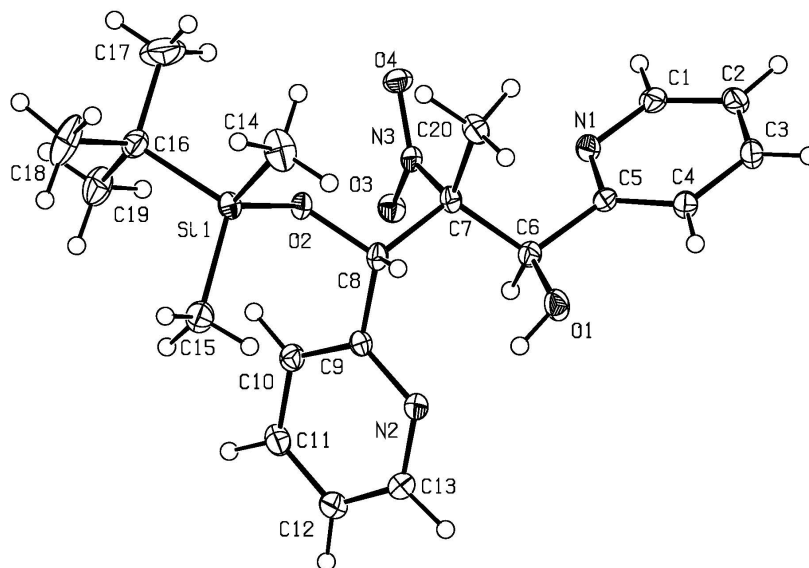


**Figure 18:** Molecular structure and numbering scheme of **8**. The ellipsoids represent a probability of 40 %, H atoms are shown with arbitrary radii.

**Table 7:** Comparison of selected bond lengths [pm] and angles [°] of **4a**, **4b**, **7** and **8**.

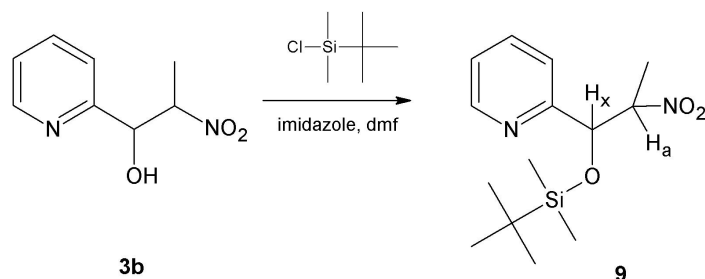
Parameter	<b>4aA</b>	<b>4aB</b>	<b>4bA</b>	<b>4bB</b>	<b>7</b>	<b>8</b>
C6-C5	151.6(6)	153.8(6)	151.9(4)	152.5(4)	151.9(3)	151.4(3)
C7-C6	152.7(6)	152.9(6)	154.9(4)	154.2(4)	154.3(3)	155.3(3)
C7-C8	154.2(6)	153.7(6)	156.7(4)	157.2(4)	151.9(3)	156.6(3)
C8-C9	152.2(6)	150.4(7)	151.2(4)	150.9(4)	151.2(3)	152.1(3)
O1-C6	141.5(5)	138.7(6)	141.6(4)	142.1(4)	141.4(2)	141.8(2)
O2-C8	142.1(5)	145.3(6)	141.0(3)	140.8(3)	142.7(2)	141.6(2)
C9-N2	134.0(6)	133.9(6)	133.5(4)	134.2(4)	133.7(3)	135.0(3)
C5-N1	134.6(6)	132.9(6)	134.3(4)	134.0(4)	134.2(3)	134.4(3)
O1-H	— <sup>a</sup>	— <sup>a</sup>	74.(4)	82.(5)	—	86.(3)
O2-H	— <sup>a</sup>	— <sup>a</sup>	87.(4)	89.(5)	—	—
C6-C7-C8	111.9(3)	112.8(4)	112.3(2)	111.0(2)	114.75(17)	111.89(16)
C7-C8-C9	112.9(4)	112.2(4)	112.2(2)	112.8(2)	110.84(17)	117.08(18)
C7-C6-C5	112.8(4)	110.6(4)	113.0(2)	111.9(2)	109.62(18)	112.88(16)
C6-C5-N1	115.8(4)	114.9(4)	114.7(2)	114.8(3)	113.82(19)	114.85(18)
C8-C9-N2	115.6(4)	116.8(4)	116.8(2)	117.2(2)	115.36(18)	115.13(18)

<sup>a</sup> H atoms have not been refined.

2-Nitro-1-(pyridin-2-yl)propan-1-ol **3b** was chosen as a precursor for subsequent aza-HENRY reactions, due to the fact that it bears only one acidic proton in  $\alpha$ -position



to the nitro group. To protect  $\beta$ -nitro alcohol **3b** with TBDMS, a similar protection protocol as employed for compound **7** was used. Aqueous work-up and extraction with diethyl ether afforded pure 2-nitro-1-(pyridin-2-yl)-1-(*tert*-butyldimethylsilyloxy)propane **9** as a yellowish oil with moderate yield (Scheme 8).



**Scheme 8:** Protection of 2-nitro-1-(pyridin-2-yl)propan-1-ol **3b** with TBDMSCl.

As already described for compound **3b** the formation of two pairs of enantiomers can be expected. These are (*R,S*)/(*S,R*) or *erythro* and (*R,R*)/(*S,S*) or *threo*, respectively. Both pairs were observed by NMR spectroscopy and their relative configuration (*erythro* and *threo*) was determined. Surprisingly, the two isomers were found with a ratio of 1.5:1 *erythro:threo* (de = 20 %). The excess of *erythro*-isomer is in contrast to compound **3b** where an excess of the *threo*-isomer was observed. Due to the protected hydroxyl group, the aforementioned assumptions according to ROUSH (ref.<sup>68</sup>) could not be made (cf. page 21). Fortunately, the bulky TBDMS group hinders rotation around the C6-C7 bond. This is indicated by the valuable observation of two distinct vicinal coupling constants ( $^3J(\text{H}_x, \text{H}_a)$ ) for  $\text{H}_x$ . They appeared to be  $^3J = 2.8$  Hz (*threo*-**9**) and  $^3J = 8.0$  Hz (*erythro*-**9**), respectively. First of all *erythro*-**9** will be discussed. Due to its large vicinal coupling constant an *anti*-configuration of the protons  $\text{H}_x$  and  $\text{H}_a$  can be assumed. Since rotation around the OHC-CNO<sub>2</sub> bond is hindered two configurations of the methyl group relative to the pyridyl ring are possible, that are the *syn*- or the *anti*- configuration. Selective irradiation at the NMR frequency of the methyl group resulted in NOE on  $\text{H}_x$  but none on the pyridyl ring protons. Furthermore, a small NOE was detected on the *tert*-butyl group. When irradiated on the NMR frequency of  $\text{H}_x$ , a NOE on the methyl group but none on  $\text{H}_a$  could be observed. In conclusion, the relative configuration of the methyl group must be *anti* with respect to the pyridyl ring and *syn* with respect to the O-TBDMS group. Discussing *threo*-**9** the same experiments led to different observations. Due to the small vicinal coupling constant the *syn*-configuration of  $\text{H}_x$  with respect to  $\text{H}_a$  can be assumed. Irradiation on the NMR frequency of  $\text{H}_x$  resulted in a strong NOE on  $\text{H}_a$  but only a small one on the methyl group. When the NMR frequency of the methyl group was irradiated a small NOE on the pyridyl ring and on  $\text{H}_x$  could be observed as well as a strong

NOE on the *tert*-butyl group. These findings originate from the two possible positions for the *syn*-configuration of  $H_a$  and  $H_x$  (positive or negative torsion angle<sup>69</sup>) and indicate the *syn*-configuration of the methyl group with respect to O-TBDMS and an *anti*-configuration with respect to the pyridyl ring. The results are depicted in Figure 19.

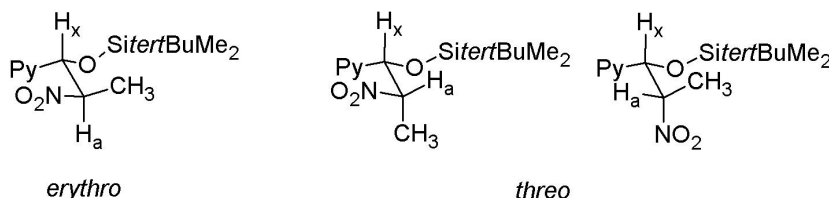


**Figure 19:** Sawhorse projection of the *erythro*- and *threo*-isomers of compound **9**.

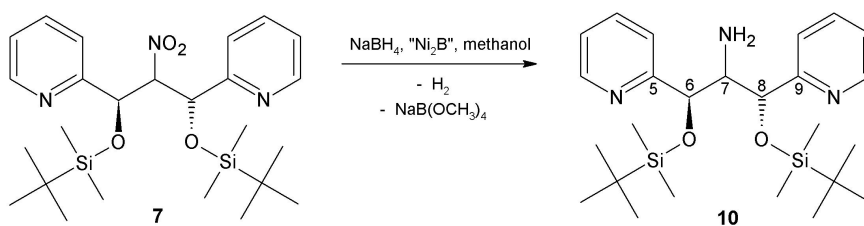
**Concluding remarks** Retro-HENRY reactions of the 2-nitro diols **4a** and **4b** required the development of a protection strategy. This was successfully accomplished for the protection of **4a** with TBDMSCl in dmf. Protection with 2,2-dimethoxypropane failed and the stability of the TMS group was not sufficient. Furthermore, the protection with TBDMS proceeded diastereoselectively and yielded the (*R,R*)/(*S,S*)-isomers with very good yields. Employment of a similar protection protocol to **4b** resulted in a diastereoselective protection of only one hydroxyl group. Under the applied conditions also retro-HENRY reaction took place, which lowered the yields dramatically and led to the formation of **9** as a second product. The relative configuration of **8** could be determined by single crystal X-ray analysis and turned out to be 1*S*, 2*S*, 3*R* and 1*R*, 2*R*, 3*S* respectively. This observation denotes isomerization reactions during the protection procedure. Isomerization in solution and especially in polar solvents has already been described for compound **4b**. It is, nevertheless, remarkable that only one pair of enantiomers out of four was obtained by this reaction. Moreover, the resulted product **8** comprises a NNO donor set and should be applicable as di- or tridentate ligand. 2-Nitro-1-(pyridin-2-yl)propan-1-ol **3b** was protected with TBDMS and the product **9** was received with moderate yields. Rearrangements of the relative configuration took place during the protection. The starting compound **3b** was a 9:1 mixture of the *threo*- and *erythro*-isomers (cf. page 20) but the protected compound was received as a 1.5:1 (*erythro:threo*) mixture of isomers. Isomerization must proceed via a prochiral intermediate. On the one hand deprotonation/protonation of the H-CNO<sub>2</sub> proton with an intermediate nitronate anion is possible. On the other hand a retro-HENRY reaction may occur, which would proceed via a prochiral pyridine-2-carbaldehyde. Yet, with the available experimental data none of the discussed pathways can be preferred.

### 2.1.6 Reduction of the nitro group

**Introduction** A key step in the development of a modular ligand preparation pathway is the interchange of functional groups. In the preceding section the modular design of ligands was achieved via nitroaldol reactions. Thus the reduction of the nitro group to other functionalities first and foremost to the amine was self-evident. A multitude of articles was published on this subject giving rise to resume to find an appropriate reaction pathway but also indicating the specificity of each procedure to a small range of substrates.<sup>93</sup> As a fact, the reduction of aromatic nitro groups is considerably more simple than reduction of aliphatic nitro groups and much work was done to overcome the drawbacks. Especially, reduction in the presence of other (sensitive) functional groups or of unstable nitro compounds was a subject of research.

**Results** Due to the fact that retro-HENRY reaction of **4a** may occur in solution, the selected transformation conditions should comprise low temperature and short reaction times. Thus, several catalytic reactions were selected, which are described in the following. Early examinations were carried out using palladium on carbon as catalyst and hydrogen as the reducing agent in an autoclave reaction. This is an often used reaction in literature to convert both aromatic and aliphatic nitro groups. However, several attempts to reduce **4a** with hydrogen and Pd/C failed and tarry products were obtained. No reaction was observed when ammonium formate was used as reducing agent with catalytic amounts of Pd/C.<sup>94-96</sup> Ammonium formate was made according to literature procedures from ammonium carbonate and formic acid.<sup>97</sup> Decomposition of **4a** occurred when it was reacted with ammonium formate and Pd/C under microwave irradiation in ethanol (100 W, 1 h). Sodium borohydride was reported to efficiently reduce both aromatic and aliphatic nitro compounds in the presence of nickel boride under mild conditions.<sup>98-100</sup> Although nickel boride was made in situ by OSBY and GANEM,<sup>98</sup> preliminary tests with their procedure were not successful. Instead of that the catalyst was prepared separately by reduction of nickel acetate with sodium borohydride in methanol as a black clumpy solid. It can be stored for months under argon atmosphere at room temperature without loss of activity but should not be completely dried. Removal of solvent residues under aerobic conditions led to a marked warming and the formation of grey nickel oxides accompanied by a dramatic loss of activity. The composition of the black catalyst is mostly Ni<sub>2</sub>B, Ni<sub>3</sub>B and traces of NiB, as stated by powder X-ray diffraction analysis. Unfortunately, attempts to reduce **4a** with sodium borohydride and nickel boride led to retro-HENRY reaction. Despite that, distinct degradation products were obtained without formation of tarry residues. The boric

acid ester of picoly alcohol and methanol as well as the crystalline  $\text{Na}^+ \text{B}(\text{OMe})_4^- \cdot \text{H}_2\text{O} \cdot \text{CH}_3\text{OH}$ , were isolated as the main products. The latter has a pronounced tendency to crystallize and was already described by HELLER and HORBAT.<sup>101</sup> To circumvent decomposition, the trialkylsilyl protected compounds **6** and **7** were employed. But also the TMS group was unstable under all of the above described conditions. Also reduction attempts of **6** with sodium borohydride and Pd/C as well as with hydrogen and RANEY nickel were unsuccessful. Reduction of the TBDMS protected compound **7** with Pd/C and ammonium formate under microwave irradiation did not give any reaction. Finally, reduction of compound **7** to the amine was successful with sodium borohydride and nickel boride catalyst (Scheme 9). Quantitative conversion of **7** to 2-amino-1,3-di(pyridin-2-yl)-1,3-di(*tert*-butyldimethylsilyloxy)propane **10** was achieved within 30 minutes. The product is sufficiently pure but contains traces of the catalyst. For that reason no satisfactory elemental analysis could be obtained although the catalyst traces could be depleted by column chromatography (Silica gel, methanol). Distillation of the oil was also not successful and rapid decomposition occurred at 170 °C and  $1.3 \cdot 10^{-2}$  mbar.



**Scheme 9:** Reduction of **7** with sodium borohydride and nickel boride.

Not surprisingly, the NMR signals of C7 and H7 of the propyl backbone are significantly high field shifted ( $^1\text{H} \Delta\delta = 2.2$  ppm,  $^{13}\text{C} \ ^1\text{H} \Delta\delta = 34$  ppm) in comparison with the nitro compound **7** (see Table 8), whereas the other signals of **10** only show slight differences in comparison with **7**. These differences are due to small conformational changes in **10** with respect to **7**. The absolute configuration of the carbons C6 and C8 was retained during reduction yielding the (*R,R*) and (*S,S*) isomers of **10**. Thus, two sets of signals for the pyridyl rings are observed and a cross signal between position 6 and 8 in the HMBC spectrum (cf. NMR discussion of the 2-nitro-1,3-di(pyridin-2-yl)propane-1,3-diols **4a** and **4b** on page 23). In the IR spectrum the asymmetric N-O stretching vibration at  $1554 \text{ cm}^{-1}$  disappeared and a broad band in the range between  $3600\text{-}3200 \text{ cm}^{-1}$  indicates a hydrogen bonded  $\text{NH}_2$  moiety.

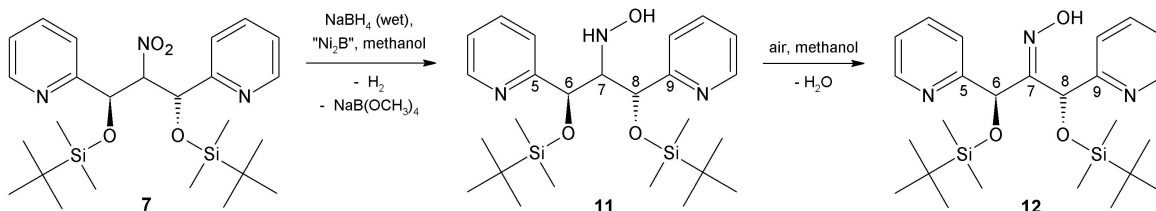
The reduction of an aliphatic nitro group to the amine proceeds via several intermediates. Firstly, the nitro group is converted into the nitroso group, which cannot be isolated in many cases. The tautomeric oxime, however, is often described as reduction

**Table 8:** Comparison of selected NMR data (chemical shifts,  $\delta$ ) of the compounds **7** and **10**. As a convention for the compounds **7** and **10**, H6 is assigned to the proton with the smaller vicinal coupling constant  $^3J$ .

Parameter	<b>7</b>	<b>10</b>
C5	158.6	162.6
C6	74.0	75.4
C7	96.9	62.8
C8	73.2	76.9
C9	157.6	162.1
NH	—	1.50
H6	5.10	5.10
H7	5.67	3.44
H8	5.55	4.72

product. The second often isolable stage is the hydroxylamine moiety. Both "intermediates" were obtained during the reduction of **7** with nickel boride and partially hydrolyzed sodium borohydride as given in Scheme 10. Active sodium borohydride is a fine trickling powder and was used for reduction of **7** to **10**. In contrast, the now applied sodium borohydride consisted of crusty hydrous clots. During the reduction with the partially inactivated sodium borohydride, the starting **7** was completely consumed according to TLC within 30 minutes and converted into the hydroxylamine **11** without the formation of amine **10**. This product then slowly underwent oxidation to the oxime **12**. A mixture of both compounds **11** and **12** could be obtained by slow evaporation of methanol from a water/methanol mixture with the hydroxylamine **11** as the major product after three days as colorless rhombic single crystals. Due to heavy disordering, single crystal X-ray analysis could give no evidence on whether the hydroxylamine was obtained or a solid solution of hydroxylamine and oxime. Three days later nearly pure oxime **12** was obtained from the same solution by further evaporation of methanol. The oxime **12** crystallized in colorless fibrous needles, which were not suitable for single crystal X-ray diffraction. Aerial oxidation of aliphatic hydroxylamines to the corresponding oximes was already described by several other groups.<sup>102</sup> Also heavy metal or pH dependency of hydroxylamine oxidation were described (see ref.<sup>102</sup> and references cited therein). HORIYAMA et al. found that oxidation is faster in methanolic solution than in chloroformic solution.<sup>102</sup> NMR spectra taken immediately after reduction of **7** with partially inactivated sodium borohydride showed nearly no oxime signals. An increase of the oxime's signal intensity was observed, if the solution was allowed to stay for several days. For that reason, one can assume that the nitro compound **7** is directly converted to hydroxylamine **11**, which itself is oxidized by aerial oxygen to oxime **12**. Thus, reduction of **7** to the nitroso compound and sub-

sequent tautomerization can be excluded. It is noteworthy, that attempts to reduce **7** to hydroxylamine **11** with sodium cyanoborohydride or sodium triacetoxyborohydride afforded a mixture of amine **10** and the hydroxylamine **11** according to TLC.



**Scheme 10:** Reduction of **7** with partially inactivated sodium borohydride and nickel boride to the hydroxylamine **11** and subsequent oxidation to the respective oxime **12**.

In the NMR spectrum of the hydroxylamine **11** always signals of the oxime **12** are found. The important signals are listed in Table 8 in comparison with the oxime **12**. As already found for the amine **10**, two sets of pyridyl signals are also found for **11**. Cross coupling along the propyl backbone indicated the formation of the (*R,R*) and (*S,S*) isomers of **11**. Furthermore, the chemical shift of the NH proton is a doublet at  $\delta = 6.42$  in [D<sub>6</sub>]benzene, while the OH proton appeared as a broad singlet at  $\delta = 6.5$  in the same solvent.

**Table 9:** Comparison of selected NMR data (chemical shifts,  $\delta$ ) of the compounds **12** and **11**. As a convention for **11**, H6 is assigned to the proton with the smaller vicinal coupling constant <sup>3</sup>J.

Parameter	<b>12</b>	<b>11</b>
C5	163.1	162.9
C6	77.1	75.4
C7	157.4	72.7
C8	69.4	74.7
C9	162.4	161.7
NH	—	6.42
OH	11.76	6.50
H6	6.09	5.56
H7	—	4.23
H8	6.97	5.50

The oxime **12** was detected in the NMR spectra by the significant down field shift of C7 ( $\delta = 157.4$ ) with respect to the amine **10** ( $\delta = 62.8$ ) or hydroxylamine **11** ( $\delta = 72.7$ ). Furthermore, C7 is a quaternary carbon as indicated by DEPT135 NMR spectroscopy. The neighboring protons H6 and H8 thus appeared as singlets in the <sup>1</sup>H NMR spectrum and are also down field shifted in comparison with **10** or **11**. The

IR spectrum shows O-H vibrations at  $3362\text{ cm}^{-1}$  and  $3191\text{ cm}^{-1}$ , indicating hydrogen bridged species. As reported for oximes, the C=N stretching vibration is weak and is observed at  $1636\text{ cm}^{-1}$ .

**Concluding Remarks** Several attempts to reduce the nitro compound **4a**, such as widely used procedures with hydrogen and palladium on carbon or RANEY-nickel failed and decomposition was observed. The reduction was possible with the TBDMS protected nitro compound **7** using sodium borohydride and nickel boride. The applied procedure proceeds quickly, at slightly elevated temperatures and with quantitative yields. The obtained purity was sufficient for subsequent reactions although a marked amount of catalyst was retained in the oily product. Reduction intermediates were obtained by use of partially inactivated (wet) sodium borohydride. According to NMR spectroscopy and TLC the reduction stopped on the hydroxylamine stage **11**, while its slow oxidation afforded the respective oxime **12**. Both compounds **11** and **12** are of immediate interest as ligands.<sup>103,104</sup> Furthermore, the hydrolysis of oxime **12** may provide an alternative route to the respective ketone beside the direct NEF conversion of the nitro compound **4a**.<sup>105</sup>

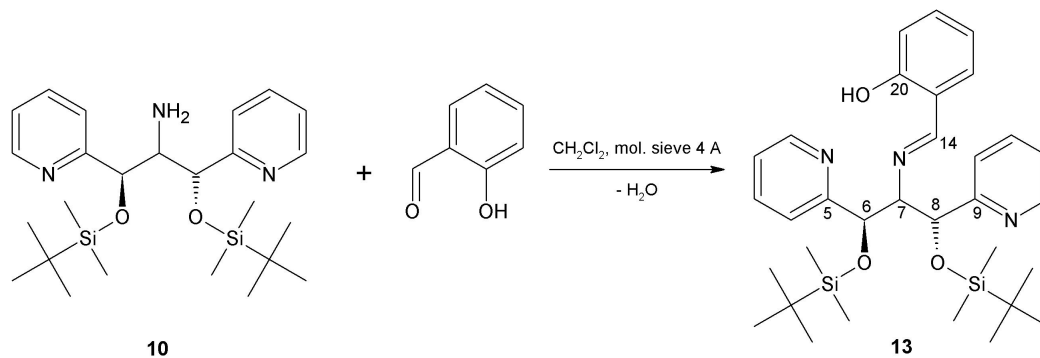
### 2.1.7 Synthesis of a N-salicylaldimine ligand, its vanadium(v) complex and catalytic activity

**Introduction** Haloperoxidases catalyze the two electron oxidation of halides by hydrogen peroxide. Chloro-, bromo-, and iodoperoxidases are known and are further divided into three different classes. Firstly the so-called "metal-free haloperoxidases" are to be named, which were recently described.<sup>106</sup> The other classes contain a prosthetic group and are divided into heme-containing haloperoxidases and vanadium-containing haloperoxidases.<sup>107</sup> Since the discovery of vanadium dependent enzymes especially the practical applications of bromo- and chloroperoxidases for the halogenation of organic substrates have triggered research efforts.<sup>107,108</sup> Structural investigations revealed similarities between several phosphatases and the haloperoxidases.<sup>109,110</sup> The active sites of both contain vanadate covalently bound by histidine and stabilized by an H-bonding network.<sup>111</sup> The vanadium atom is found in a trigonal bipyramidal coordination sphere. Furthermore, also vanadium-containing nitrogenases are known.<sup>110</sup> Heme-dependent haloperoxidases as well as molybdate-containing enzymes<sup>112</sup> are known to catalyze the oxidation of thioethers to sulfoxides.<sup>113</sup> Later the asymmetric catalytic oxidation of sulfides by vanadium-bromoperoxidase and vanadium-chloroperoxidase was reported.<sup>114</sup> Tricoordinated sulfur compounds and especially sulfoxides are among excellent chiral

auxiliaries for asymmetric transformations. The discovery of their usefulness has not only stimulated academic but also applied synthetic interest in industry. Three factors contribute to the success of chiral sulfoxides: (i) the optical stability, which is due to an inversion barrier of  $\Delta H^\ddagger = 35$  to  $42$  kcal/mol and  $\Delta S^\ddagger = -8$  to  $+4$  cal/(mol K) for many sulfoxides, (ii) the efficiency in transferring the chiral information and (iii) the accessibility of both enantiomeric forms.<sup>113</sup>  $C_2$  symmetric sulfoxides were employed as ligands in asymmetric hydrogenation using ruthenium catalysts.<sup>115</sup> Furthermore, enantioselective Diels-Alder reactions with Fe(III) sulfoxide catalysts were described as well as the enantioselective addition of  $\text{Et}_2\text{Zn}$  to benzaldehyde accelerated by chiral sulfoxides. Also palladium-sulfoxide catalyzed allylic substitution was reported.<sup>113</sup> The optical stability and accessibility of both antipodes of many sulfoxides has made them a target of drug research, since racemization in vivo could lead to severe diseases and several policies rule the investigation of both antipodes of optical active drugs. However, over the last decades a plethora of drugs containing a sulfinyl sulfur have been developed. Among them are anticancer drugs like Sulforaphane and Sparsomycin, the potassium channel activator Aprikalim or the gastric proton pump inhibitor Omeprazole to name a few.<sup>113</sup> Not surprisingly, even today the research of many groups is focused on the development of catalysts and pathways for sulfoxidation. Beside metal-mediated sulfoxidation with for instance Ti, V, Mo or Mn also other methods exist, which use chiral oxazaridines or peroxides, antibodies or enzymes. However, a wide tolerance of substrates, high yields and enantiomeric excesses as well as the suppression of subsequent oxidations to sulfones remain major goals. BOLM and coworkers introduced the salicylimine moiety, which proved to be suitable for the formation of vanadium complexes and sulfoxidation reactions.<sup>116</sup> Also the group of PLASS investigates vanadium- and molybdenum-containing enzyme models for several years.<sup>117,118</sup> They also reported on sulfoxidations catalyzed by their complexes, which contained the salicylimine moiety as a central part.<sup>119-121</sup> The following results show the ease of introducing the salicylimine motif into the developed ligand precursor, its complexation behavior towards vanadium and the ability to catalyze sulfoxidation. Sulfoxidation reactions were carried out together with ROBERT DEBEL of the group of PLASS who developed a feasible protocol to obtain quantitative information on the catalytic sulfoxidation.

**Results** The preparation of compound **13** was achieved by reacting the amine **10** with salicylaldehyde in methylene chloride (Scheme 11). The SCHIFF base **13** was obtained as a yellow viscous oil in nearly quantitative yields. It slowly became solid upon standing for several days.





**Scheme 11:** Formation of the SCHIFF base ligand **13** from amine **10** and salicyl aldehyde.

The NMR spectrum of **13** is comparable to that of the 2-nitro-1,3-di(pyridin-2-yl)-1,3-di(*tert*-butyldimethylsilyloxy)propane **7**. Conformational stability in solution is indicated by the vicinal coupling constants of the propyl backbone protons. They appear to be  $^3J = 2.2$  Hz and  $^3J = 9.0$  Hz, respectively. One can assume the existence of the (*R,R*)- and (*S,S*)-isomers in solution. The NMR spectra show two sets of signals for the pyridyl rings and one for the salicylaldimine moiety. Cross signals are found along the propyl backbone between the two heteroaryl rings in the HMBC spectrum (cf. NMR discussion of the 2-nitro-1,3-di(pyridin-2-yl)propane-1,3-diols **4a** and **4b** on page 23). In comparison with nitro-compound **7** and amine **10** two new bands are observed in the IR spectrum. They can be assigned to the exocyclic HC=N moiety ( $1633\text{ cm}^{-1}$ ) and to the ring deformation vibration of the salicyl ring ( $1500\text{ cm}^{-1}$ ). The O-H stretching vibration, however, is found as broad band between  $3100\text{--}2900\text{ cm}^{-1}$  and is overlaid by C-H stretching bands. This is in agreement with other salicylaldimine compounds and indicates hydrogen bonding.

In Figure 20 the UV-Vis spectrum of **13** is shown. The observed bands originate from the salicylaldimine moiety and the wavelength maximum  $\lambda_{257}$  is in excellent agreement with the SCOTT rules. The extinction coefficients of compound **13** were determined to be  $\epsilon_{257} = 1.9 \cdot 10^4\text{ l mol}^{-1}\text{ cm}^{-1}$ ,  $\epsilon_{317} = 4410\text{ l mol}^{-1}\text{ cm}^{-1}$  and  $\epsilon_{410} = 343\text{ l mol}^{-1}\text{ cm}^{-1}$ . However, a shift of 20 nm towards shorter wavelengths of the lowest energy absorption band was observed in the absorption spectra when **13** was deprotonated with a 15-fold molar excess of potassium *tert*-butanolate or tbd.

Greater differences between the neutral form of **13** and its deprotonated form are found in their emission properties. Excitation of **13** in ethanol at 410 nm led to a weak fluorescence with a maximum at 496 nm. The fluorescence quantum yield was not more than  $4 \cdot 10^{-3}$ . When **13** was deprotonated with a 15-fold excess of potassium *tert*-butanolate considerable blue-green fluorescence could be observed with an emission maximum at 496 nm ( $\lambda_{exc} = 385\text{ nm}$ ). The fluorescence quantum yield was determined

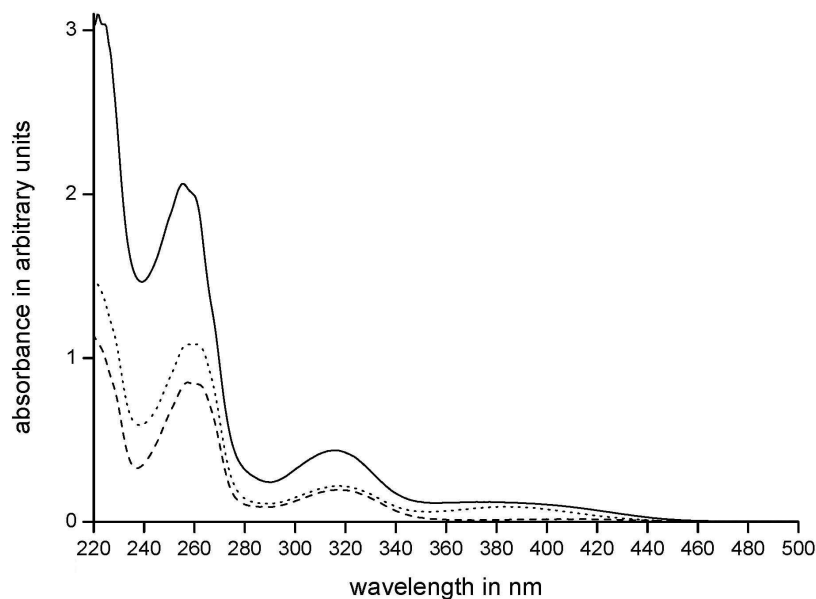


**Figure 20:** UV-Vis absorption spectra of **13** and its deprotonated form in ethanol. Dashed line: compound **13**; Dotted line: compound **13** with excess potassium *tert*-butanolate; Straight line: compound **13** with excess tbd. Differences in the magnitude of absorbance are due to different concentrations. Extinction coefficients of the deprotonated form correspond with that of compound **13**.

to be  $1 \cdot 10^{-1}$ . When **13** was deprotonated with a 15-fold excess of tbd a similar effect was observed. Excitation at 385 nm also led to a blue-green emission with a maximum at 496 nm. However, the calculated fluorescence quantum yield was  $4 \cdot 10^{-2}$ . Figure 21 shows the emission spectra of deprotonated **13**. Comparison of the excitation spectra and the absorption spectra showed, that both are different. Owing to this fact, one must assume the presence of at least two different species in this solutions.

Compound **13** was successfully applied as ligand precursor for vanadium(v) complexation. The SCHIFF base **13** was reacted with vanadyl acetylacetonate ( $\text{VO}(\text{acac})_2$ ) in anhydrous methanol in an argon atmosphere. Stirring under reflux for four hours and over night at room temperature led to a green to yellowish solution. Subsequently, vanadium was oxidized with air under basic conditions, which afforded a deep red solution (see Scheme 12). Slow solvent evaporation of the filtered solution yielded red and orange crystals of **14**. The orange crystals (space group  $\text{Fdd}2$ ) contained solvent molecules, while the red ones were solvent-free. Their IR and  $^{51}\text{V}$  NMR spectra (vide infra) were identical. Both kinds of crystals were suitable for single crystal X-ray diffraction and vanadium was found in the same coordination sphere. But due to the disorder of the solvent molecules, the quality of the orange crystal's structure determination is hampered and the structure of the red, solvent-free product will be discussed. The latter crystallized as racemate in the centrosymmetric space group  $\text{P}2_1/\text{n}$ . The

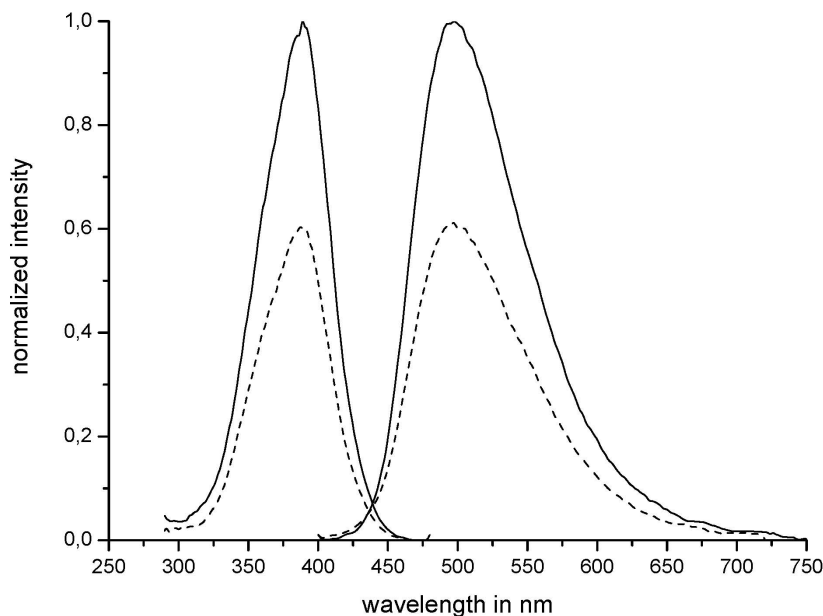
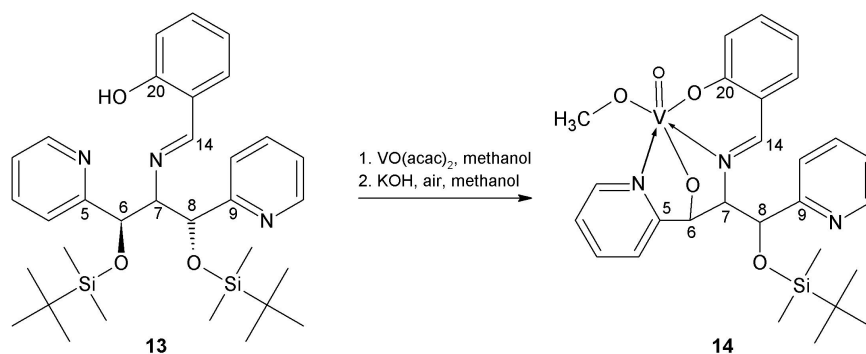


**Figure 21:** Fluorescence ( $\lambda_{max} = 496$  nm) and excitation spectra ( $\lambda_{max} = 385$  nm) of the deprotonated form of **13** in ethanol. Straight line: **13** with excess potassium *tert*-butanolate; Dashed line: compound **13** with excess tbd.

molecular structure is given in Figure 22.



**Scheme 12:** Formation of the vanadium complex **14** with SCHIFF base ligand **13**.

Vanadium is found in a distorted octahedral environment, coordinated by the deprotonated oxygen and the imine nitrogen of the salicylimine moiety, a pyridyl nitrogen and an oxygen from the cleaved O-TBDMS moiety. This oxygen is neighbored to the coordinating pyridyl ring, while the second pyridyl ring is not involved in metal complexation. The other coordination sites are occupied by a terminal oxo ligand, which is *trans* to the pyridyl nitrogen and a terminal methanolate ligand, which is *trans* to the imine nitrogen. The V=O5 bond length in **14** is 160.32(15) pm. This is in the expected range for  $\text{VO}^{3+}$  ions, where V=O bond lengths are found between 155 and 162 pm.<sup>122</sup> Also the V-O1 bond length is observed as expected (188.83(15) pm) but

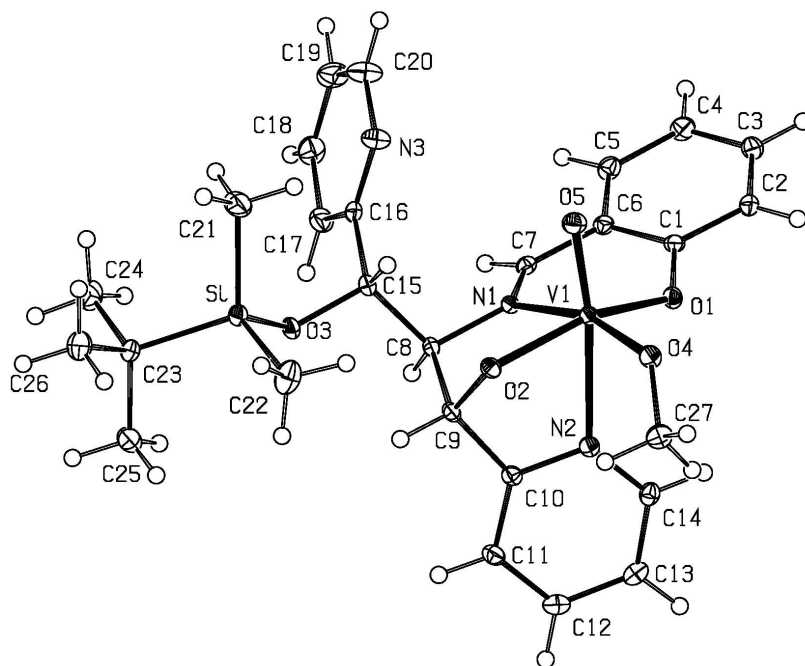


**Figure 22:** Molecular structure and numbering scheme of **14**. The ellipsoids represent a probability of 40 %, H atoms are shown with arbitrary radii.

is found at the range's bottom. V-OAryl bonds are reported between 187 and 196 pm.<sup>122</sup> The V-O2 bond length (190.02(14) pm), however, is markedly elongated and nearly as long as the V-O1 length within standard deviations. This observation may be a result of its *trans* position with respect to the V-O1 bond and the strain induced by the five-membered V1-N1-C8-C9-O2 and V1-O2-C9-C10-N2 rings. The expected range for terminal vanadium-alkoxy bonds is 176 and 186 pm and is very much dependent on the *trans* substituent.<sup>72,122</sup> This can also be seen in comparison with the V-O4 bond length (179.39(15) pm), which is within the expected range. In fact, the methoxy ligand is not subjected to steric strain and little *trans* influence (structural *trans* effect)<sup>123</sup> can be expected from the imine nitrogen N1.<sup>122,124</sup> In turn, the oxo ligand exhibits a strong *trans* influence and thus the V-N2 distance is remarkably long (234.29(18) pm). This influence on bond lengthening is certainly much greater than bond lengthening induced by steric strain. The same effect can be observed in other octahedral complexes of the type O=V(OMe)(quinolin-8-olato-2N,O)<sub>2</sub>.<sup>124,125</sup> In these complexes one quinoline nitrogen is *trans* positioned to the oxo ligand, while the other is in *trans* position to the methoxy ligand. Thus, the V-N bond length of the former is found to be 229 pm<sup>125</sup> and 230 pm,<sup>124</sup> while the latter exhibits a bond length of 218 pm<sup>125</sup> and 221 pm,<sup>124</sup> respectively. Both quinoline ligands coordinate vanadium in five-membered chelate rings. In vanadium complex **14** V-N1 is found to be 213.86(17) pm and thus also elongated but to a smaller extent than V-N2. The bite angles of the

five membered chelate rings are small, as expected (O2-V1-N1 77.24(6)°, O2-V1-N2 74.02(6)), while a slightly larger bite angle is observed for the six-membered chelate ring (O1-V1-N1 83.09(6)°). Bond lengths and angles of the ligand backbone are within the expected range and are comparable with those of compound **7**.

As expected, no O-H vibration is observed in the IR spectrum. But a strong band is observed at 959 cm<sup>-1</sup>, which can be assigned to the V=O vibration. V=O stretching vibrations are typically observed between 910-1040 cm<sup>-1</sup>.<sup>122</sup> Interestingly, the C=N stretching vibration of the imine moiety shows no significant shift (complex **14** 1636 cm<sup>-1</sup>, ligand **13** 1633 cm<sup>-1</sup>). Hence, the C-N bond is not weakened by the coordination, which is in agreement with literature statements.<sup>122</sup> Also a shift of the pyridyl C=N vibration is observed. For the coordinated pyridyl ring a wave number of  $\tilde{\nu} = 1599$  cm<sup>-1</sup> is observed and  $\tilde{\nu} = 1587$  cm<sup>-1</sup> for the non-coordinated pyridyl ring. The latter is consistent with the free ligand **13**. Also the NMR spectra of **14** show significant differences in comparison with the ligand **13**. A comparison of selected chemical shifts is given in Table 10. The carbon of the desilylated O-C6 moiety is down field shifted by 10 ppm. But only slight down field shifts are observed for neighboring carbons C5, C7, C8 and C9, which are due to conformational changes of **14** in comparison with **13**. The same applies for the respective protons. H6 appears as a broad singlet signal and is down field shifted by 1.2 ppm, while H7 and H8 show only slight shifts. The imine moiety's carbon C14, however, is slightly up field shifted (about 2 ppm), while the adjacent proton H14 shows a significant up field shift of 1.4 ppm. The quaternary phenyl carbon C20 is slightly down field shifted by 3 ppm. The other phenyl ring carbon atoms are nearly unaffected and chemical shifts are comparable with the free ligand precursor **13**. Two methanol signals are observed in the <sup>1</sup>H NMR spectrum with a slight down field shift of the coordinated methanolate protons. They appear at 3.34 ppm and are thus only 0.03 ppm higher than the signals of uncoordinated methanol. Only one signal is observed in the <sup>51</sup>V NMR spectrum at  $\delta = -518$ . The value is within the expected range for a penta-coordinated VO<sup>3+</sup> moiety and exhibits a half line width<sup>¶</sup> of  $\Delta\nu = 70$  Hz.<sup>126,127</sup> This is considerably small, since  $\Delta\nu$  may vary between 30-3000 Hz in <sup>51</sup>V NMR spectra.<sup>126</sup> But its explanatory power is not straightforward, since several effects contribute to the line width. Such as the bulkiness and  $\sigma$  donor strength of the ligand, symmetry of the complex, or viscosity of the solution.<sup>126</sup> As a result, conformational rigidity can be assumed due to the observation of one set of distinct signals. Also no alteration of the coordination sphere was observed during NMR measurements. This fact is indicated by the occurrence of only one <sup>51</sup>V signal.

---

<sup>¶</sup> $\Delta\nu$  is the line width of the NMR signal measured at the half of its height in Hertz.

**Table 10:** Comparison of selected NMR data (chemical shifts,  $\delta$ ) of the compounds **13** and **14**. As a convention for compound **13**, H6 is assigned to the proton with the smaller vicinal coupling constant  $^3J$ . For compound **14** H6 is assigned adjacent to the coordinating alcoholate moiety.

Parameter	<b>13</b>	<b>14</b>
C5	162.7	162.5
C6	76.5	87.3
C7	82.1	85.7
C8	75.8	77.6
C9	162.2	161.0
C14	168.9	166.7
C20	161.9	135.1
H14	8.36	6.90
H6	4.88	6.08
H7	4.07	4.04
H8	5.26	5.68

The UV-Vis absorption spectrum was taken in ethanol and is depicted in comparison with the spectrum of **13** in Figure 23. Three major bands can be observed between 220-550 nm. The highest energy band ranges from 220-300 nm and has two distinctive shoulders at its low energy flank ( $\lambda_{max} = 233$  nm,  $\epsilon_{230} = 3 \cdot 10^4$  l mol $^{-1}$  cm $^{-1}$ ). A second broad band appears between 250 nm and 400 nm ( $\lambda_{max} = 330$  nm,  $\epsilon_{330} = 8 \cdot 10^3$  l mol $^{-1}$  cm $^{-1}$ ). The complex's red to orange color originates from the low energy band between 400 nm and 550 nm ( $\lambda_{max} = 460$  nm,  $\epsilon_{460} = 3 \cdot 10^3$  l mol $^{-1}$  cm $^{-1}$ ) and may be attributed to a LMCT transition.<sup>126</sup> However, no fluorescence could be observed in the visible region. This is in contrast to the findings for compound **13**.

Catalytic sulfoxidation was carried out with (methylsulfonyl)benzene **I** as substrate in methylene chloride/methanol (v/v 7:3). Hydrogenperoxide was used as oxidizing agent in 25 % excess with respect to the substrate, while the catalyst systems were employed with 1 Mol% with regard to the substrate. As shown in Scheme 13 the observed products are the (methylsulfonyl)benzene **II**, which is the volitional product and (methylsulfonyl)benzene **III**, which is obtained by oxidation of **II** but is unwanted. Three catalytic systems were tested, that comprise complex **14**, compound **13** with V-O(acac)<sub>2</sub> and compound **13** with MoO<sub>2</sub>(acac)<sub>2</sub>. Product formation was followed by <sup>1</sup>H NMR spectroscopy with 1,3,6-tri(methoxy)benzene (tmb) as an internal standard. NMR samples were prepared by taking 2 ml aliquots from the reaction mixture and subsequent quenching in 5 ml of a 0.1 M aqueous Na<sub>2</sub>SO<sub>3</sub>. All organic compounds were extracted four times with 2 ml methylene chloride each and the solvent was carefully removed in vacuo. Immediately, the <sup>1</sup>H NMR spectra were measured in chloroform.

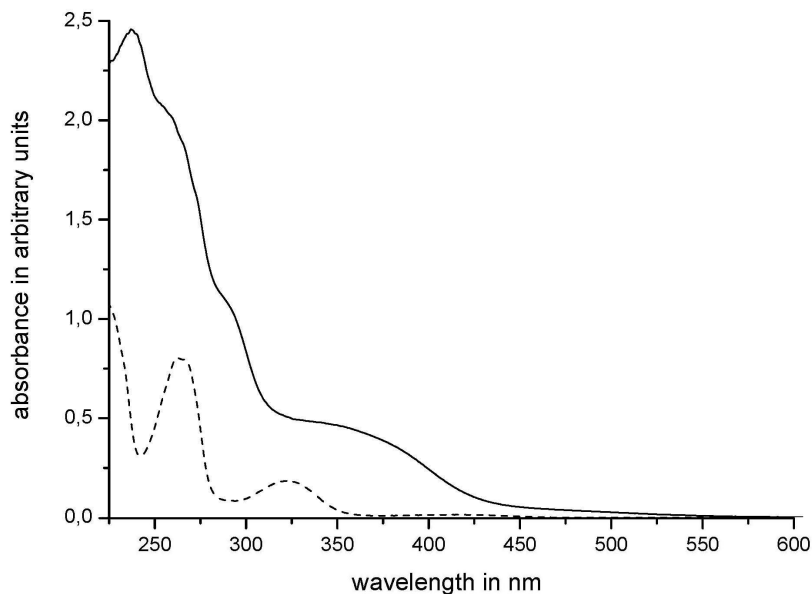
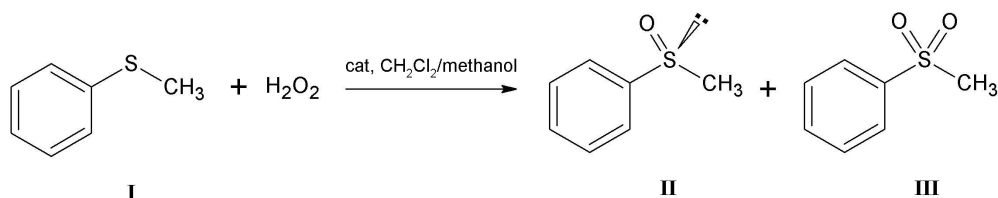


**Figure 23:** UV-Vis absorption spectra taken in ethanol. Straight line: Vanadium complex **14**. Dashed line: SCHIFF base ligand precursor **13**.

To obtain quantitative information on the reaction progress the NMR signals were integrated within defined intervals.



**Scheme 13:** Schematic representation of the catalytic sulfoxidation of (methylsulfanyl)benzene **I**.

The first experiments were carried out with the SCHIFF base ligand **13** and  $\text{MoO}_2(\text{acac})_2$  or  $\text{VO}(\text{acac})_2$ , respectively. The ligand, hydrogen peroxide, tmb and the metal precursor were combined at room temperature and allowed to react for half an hour. Subsequently, the yellow mixture was cooled to 10 °C and (methylsulfanyl)benzene **I** was added, which was also the starting point for time measurement. Figure 24 shows the formation of (methylsulfinyl)benzene **II** versus the reaction time. Both catalytic systems were able to nearly quantitatively convert **I** to **II**. The vanadium based catalyst, however, showed the best starting activity with an initial turnover frequency (TOF)<sup>||</sup> of  $0.041 \text{ s}^{-1}$ . A lower activity was observed for the molybdenum based catalyst system. Its initial turnover frequency was calculated to be  $\text{TOF} = 0.028$

<sup>||</sup> $\text{TOF} = n_{\text{product}} / (n_{\text{catalyst}} \cdot t)$ ; n is the molar amount and t is the time interval.

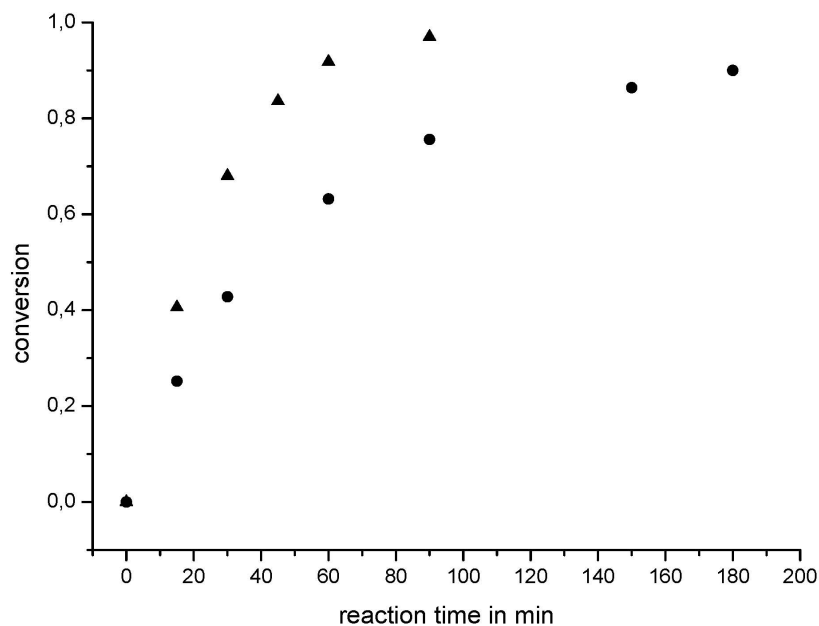


**Figure 24:** Conversion (formation of the sulfoxide **II**) is plotted versus the reaction time. **▲**: Schiff base ligand **13** with vanadyl acetylacetonate (VO(acac)<sub>2</sub>). **●**: Schiff base ligand **13** with molybdenyl acetylacetonate (MoO<sub>2</sub>(acac)<sub>2</sub>).

s<sup>-1</sup>. In both tests only traces of (methylsulfonyl)benzene **III** were found. The results are given in Table 11. It is noteworthy, that a green fluorescence was observed in the reaction mixture when excited with an UV lamp used for thin layer chromatography ( $\lambda_{exc} = 365$  nm).

Vanadium complex **14** was tested as catalyst for sulfoxidation. Again the complex was stirred for half an hour with hydrogen peroxide and tmb at room temperature and time measurement was started after addition of (methylsulfonyl)benzene **I** at 10°C. However, the plot of conversion vs. time also clearly shows a lag phase of almost two hours (Figure 25). During these two hours the initially red solution slowly turned yellow. After the lag phase also a green fluorescence was observed in the reaction mixture when excited at 365 nm. But smaller initial activity was observed when complex **14** was used as catalyst. The initial turnover frequency was calculated to be  $TOF = 5.7 \cdot 10^{-4} \text{ s}^{-1}$  and nearly quantitative conversion of **I** to **II** was observed after 24 hours. But also only little formation of (methylsulfonyl)benzene **III** was determined by NMR spectroscopy. It seems to be likely, that the catalytically active species was formed during the lag phase. The observed color change may hint on the formation of a dioxovanadium compound which are often pale yellow colored.

**Concluding remarks** The amine **10** was successfully converted into compound **13**. This yellow product and its deprotonated form were examined by UV-Vis absorption



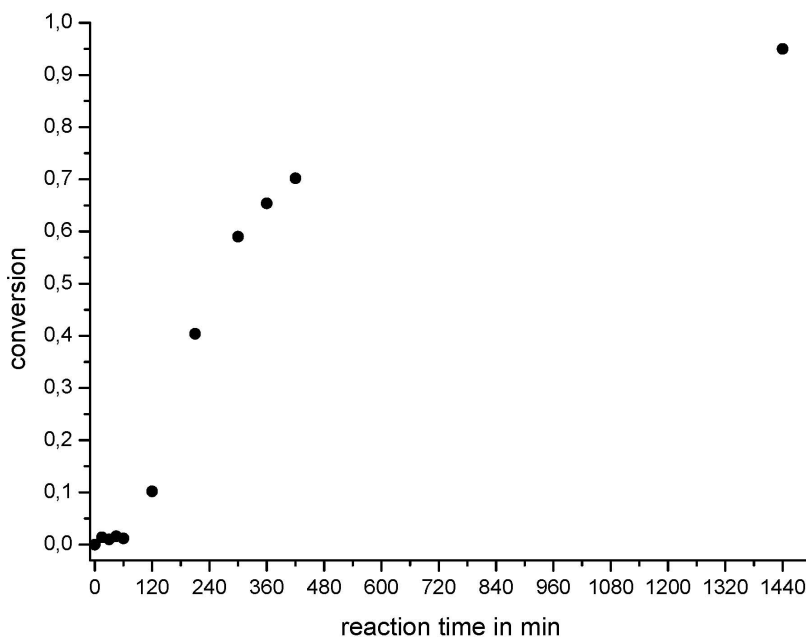


**Figure 25:** Conversion (formation of the sulfoxide **II**) is plotted versus the reaction time. The vanadium complex **14** was used as catalyst.

**Table 11:** Comparison of the catalytic performances of the three tested catalytic systems.

Catalyst	$t_{1/2}$ [min]	TOF <sup>†</sup> [ $s^{-1}$ ]
<b>13</b> + VO(acac) <sub>2</sub>	19	0.041
<b>13</b> + MoO <sub>2</sub> (acac) <sub>2</sub>	40	0.026
<b>14</b>	254	$5.7 \cdot 10^{-4}$ <sup>‡</sup>

<sup>†</sup>TOF =  $n_{product} / (n_{catalyst} \cdot t)$ ; n is the molar amount and t is the time interval. TOF was calculated for the first two time intervals (starting activity).

<sup>‡</sup>TOF was calculated for the first two time intervals after the lag phase.

and emission spectroscopy. In contrast to deprotonated **13**, the protonated form revealed only a weak fluorescence. No visible fluorescence was observed for the vanadium complex **14**. This was of special interest, since a green fluorescence was observed during the catalytic sulfoxidation with either the complex **14** or an in situ generated catalyst from VO(acac)<sub>2</sub> and **13**. This green emission might stem from the catalytic active species or an intermediate. Furthermore, sulfoxidation of (methylsulfanyl)benzene **I** to (methylsulfinyl)benzene **II** was successfully conducted with excellent yields and only little formation (methylsulfonyl)benzene **III** (< 4 %). The best results were obtained with VO(acac)<sub>2</sub> and **13**, with which the reaction was completed in 1.5 hours. Compound **13** could successfully be applied as ligand precursor for vanadium complexation. During the complexation reaction one O-TBDMS moiety is desilylated under formation

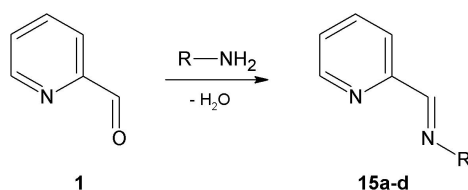
of a tetradentate ligand. The remaining O-TBDMS group mediates the solubility of the complex. Also one pyridyl ring remains uncoordinated with an approximate distance of 450 pm to the metal center. The pyridyl nitrogen may be employed as proton relays during proton transfer reactions but may also participate in hydrogen bonding. It is noteworthy that vanadium complexation occurs stereospecifically.

## 2.2 N-(Pyridine-2-ylmethylidene)amines as ligands and ligand precursors

### 2.2.1 Synthesis of N-(pyridine-2-ylmethylidene)amines

**Introduction** 2-Pyridylmethylideneamines may be considered as the heteroanalogs of carbonyl compounds and can be used as electrophiles for aza-HENRY reactions (or nitro-MANNICH). However, the ease of those reactions and possible consecutive reactions like deamination is very much dependent on the N-bound ligand. For that reason, several well known 2-pyridylmethylideneamines were synthesized by a straightforward procedure. Moreover, they are not only precursors for aza-HENRY reactions but serve also as starting materials for reductive C-C coupling reactions.<sup>23,25,28</sup> Such coupling reactions can be understood as the aza-analogs of pinacol couplings and lead to symmetrically substituted vicinal diamines, which themselves are valuable ligands and are within the scope of our ongoing research.<sup>22</sup> Reactions using 2-pyridylmethylideneamines as the starting material are described in the following section. Their ligation behavior towards zinc chloride, some aza-HENRY reactions as well as C-C coupling reactions will be presented.

**Results** Methyl (Me),<sup>128</sup> phenyl (Ph), benzyl (Bz), and allyl<sup>129</sup> were applied as N-bound substituents and the corresponding 2-pyridylmethylideneamines **15a**, **15b**, **15c**, **15d** were prepared by simple reactions of the respective amine with pyridine-2-carbaldehyde **1**. The products were obtained in good to excellent yields (see Scheme 14).



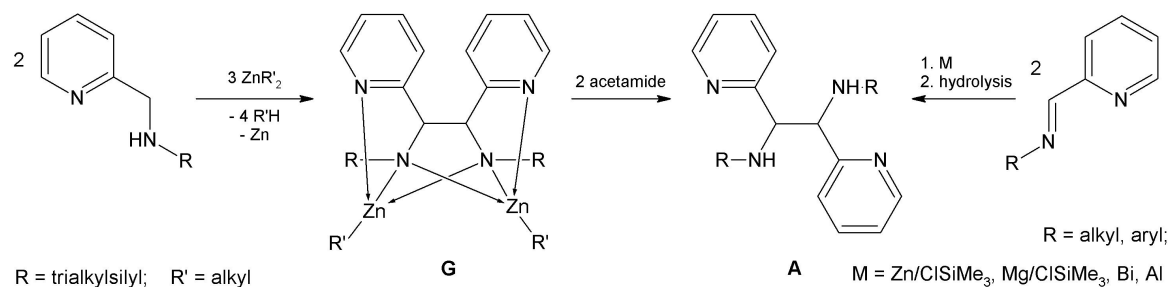
R = methyl **15a**, phenyl **15b**, benzyl **15c**, allyl **15d**

**Scheme 14:** Formation 2-pyridylmethylideneamines **15a**, **15b**, **15c** and **15d**.

If compound **15a** is allowed to stay for a few weeks at room temperature as well as at  $-20\text{ }^{\circ}\text{C}$  the formation of a white crystalline precipitate can be observed. This compound was correctly identified by VASYLYEV et al. as the trimerization product of **15a**, 1,3,5-trimethyl-2,4,6-tris(2-pyridyl)hexahydro-s-triazine **15a<sub>3</sub>**.<sup>130</sup> The trimere **15a<sub>3</sub>** can also be used as starting material. Upon heating, complete monomerization occurs in solution within a few seconds. However, the trimer **15a<sub>3</sub>** cannot only be obtained by slow crystallization. Stirring of a solution of **15a** in diethyl ether with catalytic amounts of *p*-toluenesulfonic acid afforded **15a<sub>3</sub>** with moderate yields and excellent purity. The molecular structure of **15a<sub>3</sub>** is discussed in section 2.2.3 on page 67.

### 2.2.2 Synthesis and structural diversity of 2-pyridylmethylideneamine complexes of zinc(II) chloride

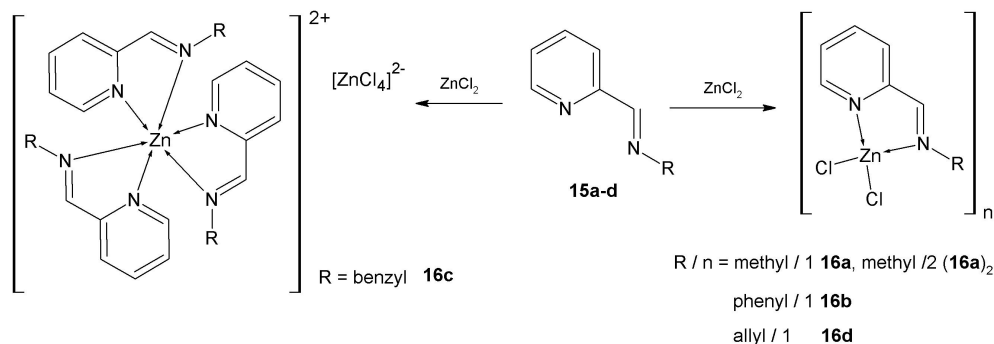
**Introduction** Bis(alkylzinc) substituted derivatives **G** (Scheme 15) of tetradentate azaligands are accessible via an oxidative C–C coupling reaction of 2-pyridylmethylamines with excess of dialkylzinc at elevated temperatures.<sup>18,19</sup> Similar dinuclear zinc complexes with the N,N'-di(*tert*-butyl)-1,2-di(2-pyridyl)-1,2-diamidoethane ligand were prepared by VAN KOTEN and coworkers.<sup>14,15,17,131</sup> Protonation of these complexes with acetamide yields N,N'-substituted 1,2-dipyridyl-1,2-diaminoethanes **A**,<sup>22</sup> which are also accessible via a reductive coupling of 2-pyridylmethylideneamines **15a**.<sup>23,25,28</sup>



**Scheme 15:** Oxidative C–C coupling reaction and protolysis of the thus formed zinc complex (left pathway) and reductive C–C coupling (right pathway).

The 2-pyridylmethylideneamines **15a**, **15b**, **15c**, **15d** (azomethines) are easily accessible by straight-forward procedures and therefore represent convenient starting materials for the synthesis of these ligands as well as for aza-HENRY reactions. Despite the availability of these imines, there exist only very few zinc(II) chloride complexes of these ligands (**16a**,<sup>128</sup> **16b**<sup>132</sup>) which were, however, not characterized by X-ray structure analysis (Scheme 16). In order to investigate the reductive coupling of these imines in the boundary of a zinc(II) ion, we were interested in the coordination behav-

ior of these imines. The applied azomethines **15a**, **15b**, **15c**, **15d** are wellknown and in some cases even commercially available [R = methyl (Me),<sup>128</sup> phenyl (Ph), benzyl (Bz), allyl<sup>129</sup>]. The results presented in this section were published in *Inorg. Chim. Acta* **2009**, *362*, 4706-4712 (Publication 7).



**Scheme 16:** Reaction scheme for the formation of the zinc complexes **16a–16d**.

**Results** Zinc atoms favor tetrahedral environments, however, depending on the bulkiness of the ligands coordination numbers between two and six can be realized. In fact tetrahedral, square pyramidal and octahedral coordination spheres are observed depending solely on the N2-bound substituent. The crystalline state of complex **16a** (see Figure 26 and 27) contains dimeric and monomeric complexes at the same time in a 1:1 ratio ("A" and "B" distinguish between the mono- and dinuclear complex, in molecule B "a" is used for equivalent atoms generated by symmetry transformation (-x+1, -y+1, -z+2)).

In the dimer the zinc atom is in a square pyramidal environment with the basis formed by the azomethine moiety and two bridging chloro ligands whereas another chloro ligand occupies the apical position. The monomeric zinc complex contains a distorted tetrahedrally coordinated zinc atom. For N2 a nearly planar surrounding was found in both species (angle sums 359.9°) and due to the small bites of the ligands narrow N1-Zn-N2 angles (80.66(9)° in the monomer and 77.33(9)° in the dimer) are observed. Regarding the Zn-Cl bond lengths in both species significant differences are found. The smaller coordination number of the zinc atom leads to shorter Zn-Cl bonds. Furthermore the Zn-Cl distance of the terminal chloro ligand in the dimer lies within the expected range<sup>72</sup> (224.04(8) pm) whereas two significantly different Zn-Cl distances are observed for the  $\mu$ -chloro ligands (239.85(7) and 250.99(9) pm). Selected bond lengths and angles are summarized in Table 12.

Fragments of the dimer of **16a** were detected in a FAB mass spectrum such as the [(**16a**)<sub>2</sub>-Cl]<sup>+</sup> ion at m/z = 477 with a low intensity. Comparison of the experimental

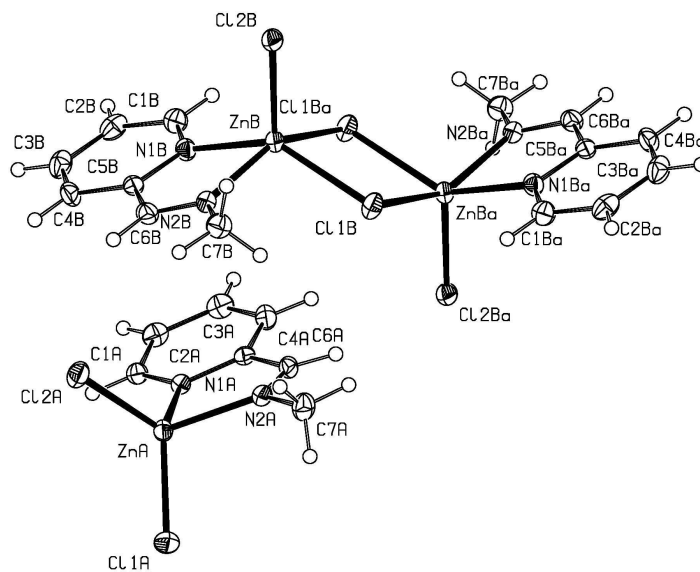


**Figure 26:** Molecular structure and numbering scheme of **16a**. The ellipsoids represent a probability of 40 %, H atoms are shown with arbitrary radii. The letter "a" is used for equivalent atoms generated by symmetry transformation ( $-x+1, -y+1, -z+2$ ).

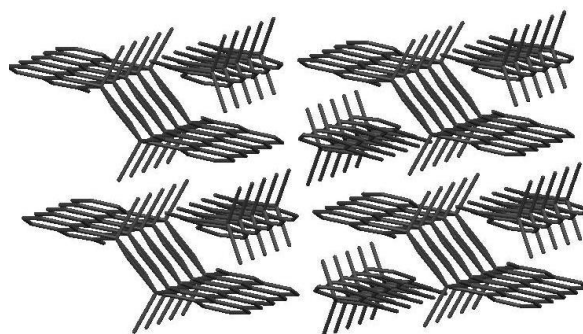


**Figure 27:** Part of the crystal structure of **16a** showing the packing of the mono- and dinuclear molecules in the solid state.

isotopic pattern with the calculated one confirmed this interpretation (Figure 28). Despite these results which show that monomeric and dimeric **16a** are present in the solid and the gaseous phase, only one set of signals was observed in solution by NMR spectroscopy. Either the influence of the aggregation on the chemical shift of the ligand's atoms is too small for discrimination between the two coordination spheres or the monomer/dimer equilibrium is fast on the NMR time scale.

Replacement of the methyl group by a phenyl substituent leads to the monomeric zinc complex **16b** with a distorted tetrahedral environment of the zinc atom (see Figure 29). Due to the small bite of the ligand the N1-Zn-N2 angle shows a value of only  $80.8(3)^\circ$ . The Zn-N and Zn-Cl bond lengths lie in characteristic regions.<sup>72</sup> N2 exhibits a planar environment with an angle sum of  $360.0^\circ$ . Both aryl rings are arranged coplanarly.

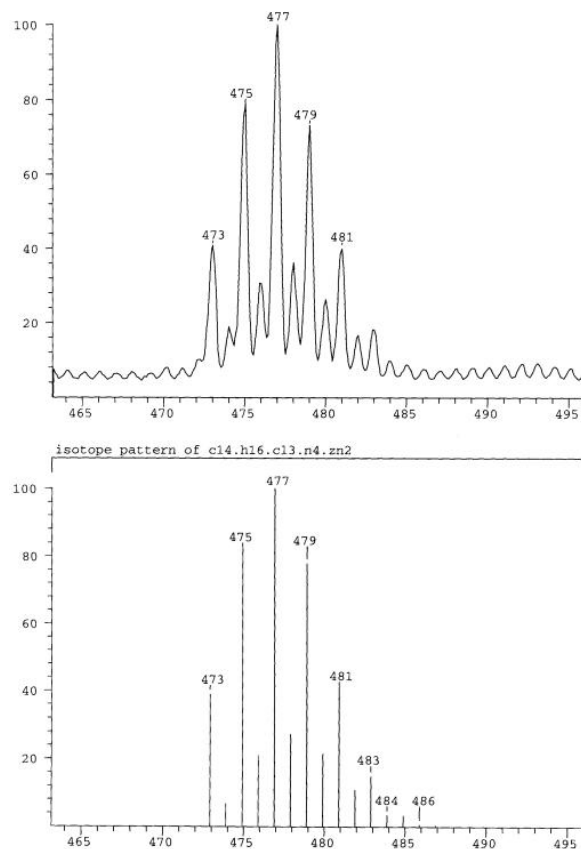


**Figure 28:** Comparison of the fragment  $[(\mathbf{16a})_2\text{-Cl}]^+$  with the calculated isotopic pattern. The upper spectrum shows the experimental data while the lower represents the calculated values. The spectra show  $m/z$  in relation to relative intensities [%].

A different structure is realized in the case of  $R = \text{benzyl}$  (**16c**). In this dinuclear zinc complex, which crystallizes in the space group  $P2_1/n$ , an ion pair is observed. In the cation the zinc atom is in a distorted octahedral coordination sphere, the counter anion being the well-known  $[\text{ZnCl}_4]^{2-}$  anion (Figure 30, the three ligands of the cation are distinguished by the letters "A", "B", and "C"). Due to the crystallographic inversion symmetry a racemate of the  $\Lambda$ - and  $\Delta$ -isomers is found in the solid state. In the gaps between the ions two host methanol molecules per asymmetric unit of **16c** are intercalated as also found in the elemental analysis. The small N1-Zn-N2 angle (averaged  $76.47^\circ$ ) leads to distortion from octahedral geometry. Again, N2 is in a planar environment with an angle sum of  $359.9^\circ$ . The coordination number of the metal ion strongly influences the Zn-N bond lengths. The Zn-N distances of the cation with a six-coordinate zinc atom are larger than those in the complexes with tetrahedrally or square pyramidally coordinated metal atoms (see Table 12). Furthermore, the planes of the phenyl ring (e.g. ligand B) are roughly coplanar to the N1-C5-C6-N2-Zn plane of the neighbor ligand (e.g. of ligand C) with an average distance of approx. 335 pm. This rather small distance (comparable to the distance of the layers in graphite)

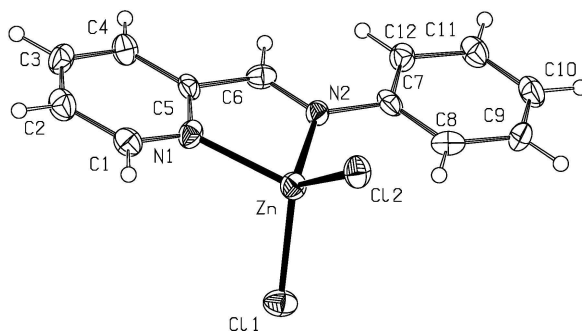


**Figure 29:** Molecular structure and numbering scheme of **16b**. The ellipsoids represent a probability of 40 %; H atoms are shown with arbitrary radii.

allows a  $\pi$ - $\pi$  interaction between the N1-C5-C6-N2 moieties and the phenyl rings thus allowing and stabilizing the large coordination number of the zinc atom.

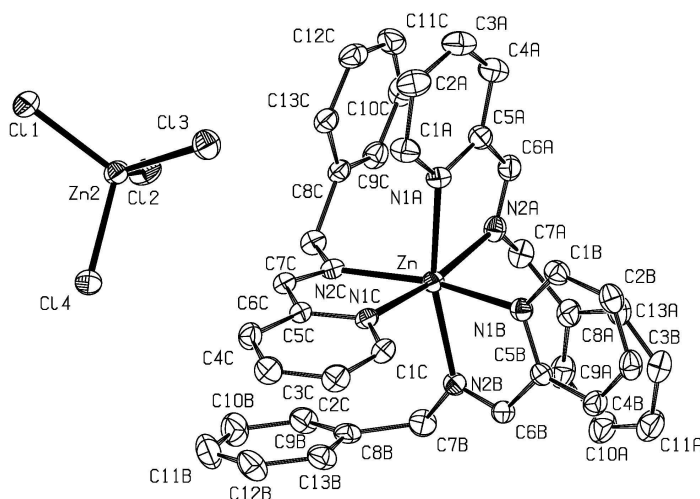


**Figure 30:** Molecular structure and numbering scheme of **16c**. The ellipsoids represent a probability of 40 %; H atoms and methanol solvent molecules have been omitted for clarity.

Reduction of the ability to form  $\pi$ -stacking structures leads to conventional structures with tetra-coordinate zinc atoms as found for the derivative with R = allyl (**16d**) (Figure 31). As expected, the small bite of the ligand again leads to a narrow N1-Zn-N2 angle of  $80.99(6)^\circ$  which also is the reason for the distorted geometry. The atom N2 exhibits a planar environment with an angle sum of  $359.4^\circ$ . In addition, the Zn-Cl and Zn-N as well as the C-C bond lengths lie well within expected ranges<sup>72</sup> and are comparable with those of the tetrahedral complexes **16a** and **16c**.

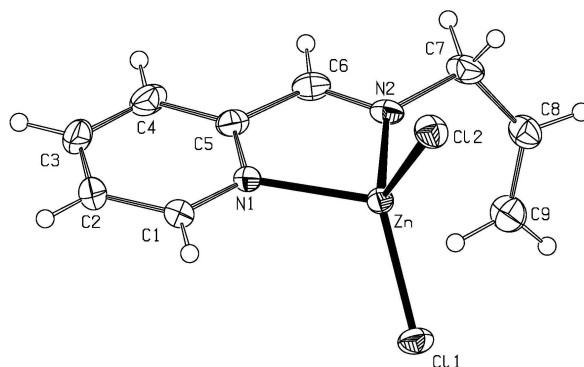


**Figure 31:** Molecular structure and numbering scheme of **16d**. The ellipsoids represent a probability of 40 %, H atoms are shown with arbitrary radii.

**Table 12:** Comparison of selected bond lengths [pm] and angles [°].

Parameter	<b>16aA</b>	<b>16aB</b>	<b>16b</b>	<b>16c</b>	<b>16d</b>
Zn-N1	206.2(2)	212.6(2)	206.3(8)	220.4 <sup>a</sup>	206.73(14)
Zn-N2	206.1(2)	214.2(3)	208.5(8)	216.8 <sup>a</sup>	206.46(14)
Zn-Cl1 (terminal)	220.98(8)	—	222.6(3)	225.28(10)	220.56(4)
Zn-Cl2 (terminal)	221.23(8)	224.04(8)	220.0(3)	228.83(9)	222.13(5)
Zn-Cl3 (terminal)	—	—	—	227.12(10)	—
Zn-Cl4 (terminal)	—	—	—	228.79(9)	—
Zn-Cl1 (bridging)	—	239.85(7)	—	—	—
Zn-Cl1a (bridging)	—	250.99(9)	—	—	—
N2-C6	127.5(4)	128.0(4)	125.5(12)	127.6 <sup>a</sup>	126.9(2)
N2-C7	146.6(4)	146.5(4)	145.1(12)	146.7 <sup>a</sup>	146.7(2)
C6-C5	147.4(4)	147.4(4)	149.0(13)	147.7 <sup>a</sup>	146.9(3)
N1-Zn-N2	80.66(9)	77.33(9)	80.8(3)	76.47 <sup>a</sup>	80.99(6)
Cl-Zn-Cl (tetrahedral)	115.06(3)	—	115.90(18)	—	115.190(18)

<sup>a</sup> Average values

**Concluding remarks** 2-Pyridylmethylideneamines are not only suitable synthons in reductive C–C coupling reactions for the synthesis of 1,2-dipyridyl-1,2-diaminoethanes but also show an interesting coordination behavior. N-Organyl-pyridylmethylideneamines L stabilize coordination numbers of four, five and six at the zinc atom thus showing a strong influence of the nature of the organyl group on the coordination number. Methyl, phenyl, and allyl substituents lead to complexes of the type [(L)ZnCl<sub>2</sub>] with tetra-coordinate zinc atoms. For N-methyl-pyridylmethylideneamines also a dimeric complex of the type [(L)(Cl)Zn(μ-Cl)<sub>2</sub>Zn(Cl)(L)] is observed



**Table 13:** Comparison of the Cl–Zn–Cl angle [°] with the Zn–Cl and Zn–N bond lengths [pm] of presented and selected published compounds of the type (L<sub>2</sub>)ZnCl<sub>2</sub>.

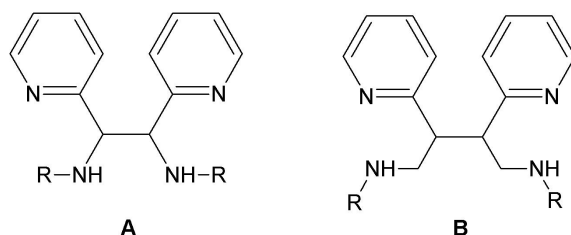
Compound	Cl–Zn–Cl	Zn–Cl	Zn–N	Reference
(H <sub>2</sub> N(CH <sub>2</sub> ) <sub>3</sub> NMe <sub>2</sub> )ZnCl <sub>2</sub>	112.6	223.4	203.6	133
(Py–CH=N–Me)ZnCl <sub>2</sub>	115.1	221.1	206.2	
(Py–CH=N–Allyl)ZnCl <sub>2</sub>	115.2	221.3	206.6	
(Py–CH <sub>2</sub> –N=CMe <sub>2</sub> )ZnCl <sub>2</sub>	115.5	220.5	205.2	75
(Py–CH=N–Ph)ZnCl <sub>2</sub>	115.9	221.3	207.4	
(bpy)ZnCl <sub>2</sub>	117.1	220.4	205.9	76
(Py–CH <sub>2</sub> –N=CPh <sub>2</sub> )ZnCl <sub>2</sub>	117.4	221.3	205.5	134
(tmeda)ZnCl <sub>2</sub>	119.0	221.4	209.2	78

in the crystalline state. The Zn<sub>2</sub>Cl<sub>2</sub> ring shows significantly different Zn–Cl distances which suggest the formation of a loose dimer. However, even in the gaseous phase, fragments stemming from the dimer are found. Zinc complexes with N-benzylpyridylmethylideneamine ligands are stabilized by  $\pi$ -stacking of the aryl groups allowing a coordination number of six for the metal atom. This behavior leads to the formation of the dinuclear ion pair of the type [(L)<sub>3</sub>Zn]<sup>2+</sup> [ZnCl<sub>4</sub>]<sup>2-</sup>. The significantly different molecular structures are solely a consequence of the nature of the N-bound group. In addition the Cl–Zn–Cl angle in complexes with tetra-coordinate metal atoms strongly depends on the Zn–N distances to the neutral aza-coligands. Very weak Lewis bases lead to large X–Zn–X angles whereas strong donor ligands form complexes with a nearly tetrahedral environment of the zinc atom. Investigations on 2-pyridylmethylamine complexes of the zinc(II) halides already showed that ZnCl<sub>2</sub> forms a 1:1 adduct of the type [(L)ZnX<sub>2</sub>] whereas the bromide and iodide yield ion pairs of the type [(L)<sub>2</sub>ZnX]<sup>+</sup> X<sup>-</sup> with penta-coordinate zinc atoms. A comparison of the mononuclear 2-pyridylmethylideneamine complexes of ZnCl<sub>2</sub> **15a**, **15b** and **15d** with e.g. (bpy)ZnCl<sub>2</sub>, (tmeda)ZnCl<sub>2</sub> and (1-amino-3-dimethylaminopropane)zinc(II) chloride shows comparable structural parameters (Table 13). Not only that the donor strength of the amine proved to be of importance but also the steric strain induced by the ligands as well as coligands. This correlation is not only valid for the halides but in general for all compounds of the type [(L<sub>2</sub>)ZnX<sub>2</sub>] with X being halide or pseudo-halide ([1,2-(bis-cinnamaldimino)-phenylZn(CN)<sub>2</sub>]: X–Zn–X = 113.6°; Zn–X = 200.5 pm; Zn–N = 205.0 pm ref.<sup>135</sup> [(H<sub>2</sub>N(CH<sub>2</sub>)<sub>2</sub>NEt<sub>2</sub>)Zn(NCS)<sub>2</sub>]: X–Zn–X = 111.9°; Zn–X = 192.9 pm; Zn–N = 204.8 pm ref.<sup>136</sup>), or alkyl groups. If the donor base is very weakly bound at the zinc atom (most commonly induced by intramolecular steric strain) the coordination number of the zinc atom is reduced to three and multidentate coligands can act as monodentate ones. Correlations between the X–Zn–X angle and the Zn–N

bond lengths have been published previously.<sup>73,75,134</sup> Bond angles and lengths presented in Table 13 also support these findings.<sup>75,134</sup> However, deviations can result from steric strain.

### 2.2.3 Synthesis of 1,4-diamino-2,3-di(2-pyridyl)butane and its zinc(II) chloride complex

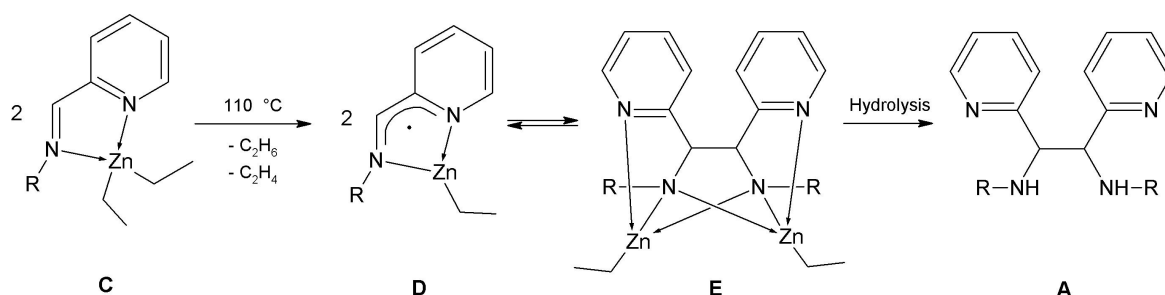
**Introduction** Vicinal diamines represent widely used bidentate Lewis bases. In order to enhance the denticity, 2-pyridyl groups can be bound to these diaminoethanes giving e.g. 1,2-dipyridyl-1,2-diaminoethane **A** (Scheme 1). In contrast to these widely used ligands, 1,4-diamino-2,3-di(2-pyridyl)butane **B** with a larger bite ( $N \cdots N$  distance) are unknown as of yet. Several reaction routes can be employed for the synthesis of the 1,2-dipyridyl-1,2-diaminoethane derivatives **A**. Unsubstituted 1,2-dipyridyl-1,2-diaminoethane **A** ( $R = H$ ) has been shown to be available in good yield from a [3.3]-sigmatropic rearrangement of a diimine with subsequent hydrolysis.<sup>137,138</sup>



**Scheme 17:** Tetradentate amino bases **A** and **B**.

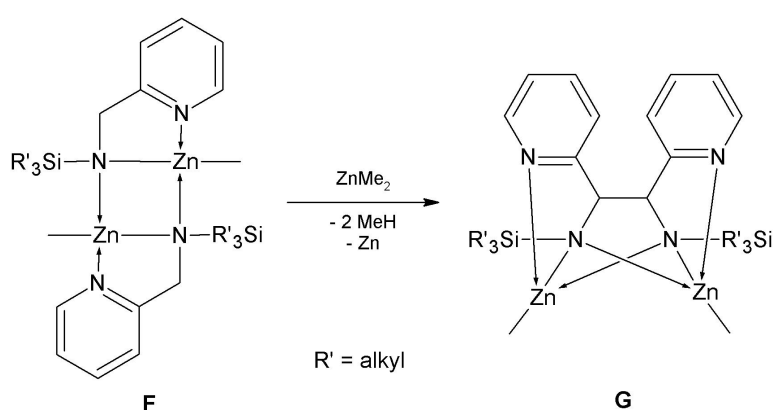
Another pathway started from N-(2-pyridylmethylidene)-alkylamines which were coupled via irradiation with a medium-pressure mercury lamp and treated with  $\text{NaHCO}_3$  yielding 1,2-di(alkylamino)-1,2-di(2-pyridyl)ethanes **A** ( $R = n\text{Hex}, c\text{Pr}, c\text{Hex}, \text{Ph}_2\text{CH}$ ).<sup>139</sup> The reductive coupling of imines with aluminium or bismuth in methanol in the presence of  $\text{KOH}$  also gave vicinal diamines.<sup>28</sup> A variant of this reaction employed a mixture of zinc and chloro-trimethylsilane as reducing agents and allowed the synthesis of **A** ( $R = \text{Me}$ ),<sup>23</sup> whereas lithium is not a suitable reducing reagent if pyridyl groups are present in the molecules.<sup>25</sup> Low-valent titanium species, produced from  $\text{TiCl}_4$  and magnesium amalgam, were also able to reductively couple N-(2-pyridylmethylidene)-methylamine.<sup>24</sup> Treatment of N-(2-pyridylmethylidene)-1-phenylethylamine with methyllithium gave mainly the addition product, but derivative **A** ( $R = \text{CH}(\text{Me})\text{Ph}$ ) was obtained as a byproduct.<sup>140</sup> The reductive coupling with metal-containing reagents often led to the formation of metal complexes with the deprotonated 1,2-diamino-1,2-di-(2-pyridyl)ethanes **A**. The reaction of N-(2-pyridylmethylidene-

dene)-*tert*-butylamine with "gallium(I) iodide" yielded [bis(diiodo gallium(III)) 1,2-di-(*tert*-butylamido)-1,2-di(2-pyridyl)ethane].<sup>141</sup>



**Scheme 18:** Formation of the radical **D** and C-C coupling equilibrium. Subsequent hydrolysis led to the tetradentate ligand **A**.

A coupling of imines could also be promoted by SmI<sub>2</sub> and Lewis acids allowing an efficient stereoselective synthesis of C<sub>2</sub>-symmetric 1,2-diamines.<sup>27</sup> A metal-mediated reductive coupling of N-(2-pyridylmethylidene)-alkylamines with Ru<sub>3</sub>(CO)<sub>12</sub> yielded the ruthenium complex of 1,2-di(alkylamido)-1,2-di(2-pyridyl)ethane (R = *i*Pr, *t*Bu, *c*Hex).<sup>142,143</sup> At elevated temperatures the complex N-(2-pyridylmethylidene)-*tert*-butylaminediethylzinc **C** liberated ethane and ethene giving [bis(ethylzinc) 1,2-di-(*tert*-butylamido)-1,2-di(2-pyridyl)ethane] **E**,<sup>17,131</sup> which showed an equilibrium with its monomer **D** via C–C bond cleavage, as shown in Scheme 18.<sup>14</sup> This interesting monomer-dimer equilibrium, which involves C–C bond cleavage and C–C bond formation was studied in detail thereafter.<sup>15,16</sup> Hydrolytic work-up procedures led to the formation of 1,2-di(*tert*-butylamino)-1,2-di(2-pyridyl)ethane **A** (R = *tert*-butyl).<sup>14</sup>



**Scheme 19:** Oxidative C-C coupling reaction of trialkylsilyl-substituted amide **F**.

The oxidative C–C coupling of 2-pyridylmethylamine also led to the formation of various byproducts.<sup>20</sup> Protection of the amino functionalities by trialkylsilyl groups led to a quantitative formation of C–C coupled [di(methylzinc) 1,2-di(2-pyridyl)-1,2-bis(tri-

alkylsilylamido)ethane] **G**, as shown in Scheme 19.<sup>18,19</sup> Protolysis of this zinc complex with acetamide gave 1,2-di(2-pyridyl)-1,2-bis(trialkylsilylamino)ethanes **A** ( $R = \text{SiR}'_3$ ) in good yields, whereas hydrolysis also cleaved the N-Si bonds.<sup>22</sup> A variant of this method resembled the oxidative C–C coupling of dilithium(2-pyridylmethanidyl)(*tert*-butyldimethylsilyl)amide with white phosphorus yielding [dilithium 1,2-di(2-pyridyl)-1,2-bis(trialkylsilylamido)ethane] and  $\text{Li}_3\text{P}_7$ .<sup>144</sup> An additional methylene group hinders the oxidative C–C coupling reaction; thus 2-pyridylethylamine only formed a zinc complex during the zincation reaction, however, precipitation of zinc metal and a C–C coupling reaction did not occur.<sup>145</sup> In [di(methylzinc)1,2-di(2-pyridyl)-1,2-bis(trialkylsilylamido)ethanes] **G**<sup>19,22</sup> as well as in the corresponding ruthenium complexes<sup>142,143</sup> the metal atoms show very close contacts or metal-metal bonds, respectively. In order to investigate the influence of the small  $\text{Zn} \cdots \text{Zn}$  distance on the reactivity of these complexes, we intended to prepare 1,4-diamino-2,3-di(2-pyridyl)butanes **B** with a larger bite ( $\text{N} \cdots \text{N}$  distance). The following section presents the synthesis of this tetradentate Lewis base 1,4-diamino-2,3-di(2-pyridyl)butane **B** ( $R = \text{H}$ ) and the formation of a zinc(II) chloride complex. These investigations were conducted in cooperation with TOBIAS KLOUBERT, who prepared the compounds **19** and **18**. The results presented in this section were published in *Z. Naturforsch., B: Chem. Sci.*, **2009**, *64b*, 784-792 (Publication 6).

**Results** Due to the failure of the above mentioned metal mediated oxidative C-C coupling reaction a novel procedure had to be developed for the synthesis of 1,4-diamino-2,3-di(2-pyridyl)butane **18**. Therefore, N-(2-pyridylmethylidene)-methylamine **15a** was used as starting material, which was firstly reported by BUSCH and BAILAR.<sup>146</sup> BÄHR and DÖGE isolated the compound and observed the formation of a crystalline solid in pure N-(2-pyridylmethylidene)-methylamine upon standing for several months.<sup>128</sup> VASYLYEV et al. recognized the formation of 1,3,5-trimethyl-2,4,6-tris(2-pyridyl)hexahydro-s-triazine, **15a<sub>3</sub>**, on the basis of IR, UV/Vis, Raman, and NMR spectroscopic investigations.<sup>130</sup> They also pointed out that monomerization of this triazine occurs in solution and is catalyzed by acids. Even though several triazines have already been structurally characterized (e. g. 2,4,6-trimethyl-1,3,5-triazine,<sup>147</sup> 2,4,6-tris(2-pyridyl)-1,3,5-triazine,<sup>148</sup> and N-alkylated 2,4,6-tris(2-pyridyl)-1,3,5-triazine<sup>149</sup>), we also determined the crystal structure of 1,3,5-trimethyl-2,4,6-tris(2-pyridyl)hexahydro-s-triazine, **15a<sub>3</sub>**. Molecular structure and numbering scheme of **15a<sub>3</sub>** (trimeric N-(2-pyridylmethylidene)-methylamine **15a**) are shown in Figure 32. The central triazine ring of the  $C_3$ -symmetric molecule is found in a chair conformation with all pyridyl and methyl groups in equatorial positions which is in agreement with the proposed struc-

ture of VASYLYEV et al.<sup>130</sup> All N-C-N (average value 109.2°) and C-N-C (average value 110.3°) bond angles as well as C-N bond lengths (average C-N 147.0 pm) of the inner cycle are in the expected ranges.

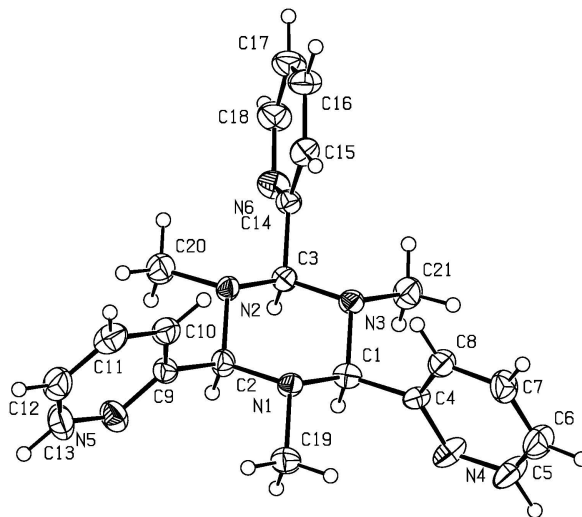
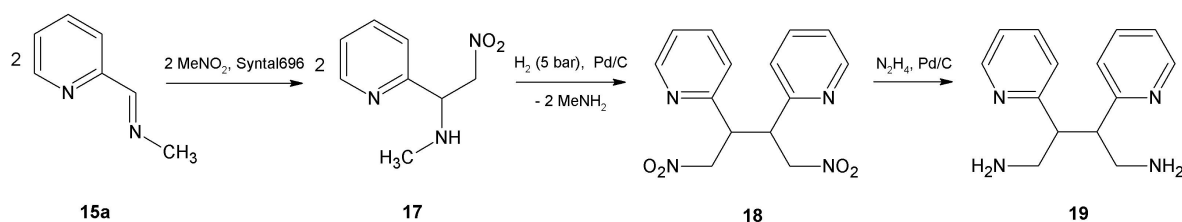


**Figure 32:** Molecular structure and numbering scheme of 1,3,5-trimethyl-2,4,6-tris(2-pyridyl)hexahydro-s-triazine **15a<sub>3</sub>** (displacement ellipsoids at the 40 % probability level, H atoms are drawn with arbitrary radii). Selected bond lengths (pm): N1-C1 147.5(5), N1-C2 145.8(5), N1-C19 148.2(5), N2-C2 147.1(5), N2-C3 147.5(5), N2-C20 147.0(5), N3-C1 146.3(5), N3-C3 147.5(5), N3-C21 147.0(5), C1-C4 152.2(5), C2-C9 151.0(5), C3-C14 151.3(5).

Nitromethane was added to freshly distilled monomeric N-(2-pyridylmethylidene)-methylamine **15a** in the presence of Syntal 696<sup>®</sup> (see section 2.1.2 on page 19) yielding 1-methylamino-1-(2-pyridyl)-2-nitroethane **17** according to Scheme 20 in a HENRY-type reaction. This compound was formed nearly quantitatively as an orange oil which decomposed slowly to a dark brown waxy residue. Air-contact accelerated this decomposition reaction whereas dilution slowed this process down. Therefore, **17** was stored at -78 °C as a methanol solution. The carbon atom which is substituted by 2-pyridyl and methylamino groups is chiral and therefore, the hydrogen atoms of the neighboring methylene moiety are diastereotopic leading to an ABX-type spectrum. The geminal  $^2J(\text{H}_A, \text{H}_B)$  coupling constant shows a value of 12.4 Hz, the vicinal coupling constants are  $^3J(\text{H}_A, \text{H}_X) = 5.2$  Hz and  $^3J(\text{H}_B, \text{H}_X) = 8.6$  Hz with chemical shifts of  $\delta(\text{H}_A) = 4.26$ ,  $\delta(\text{H}_B) = 4.39$ , and  $\delta(\text{H}_X) = 4.10$ .

In an EPR experiment with **17** organic radical species were detected at  $g = 2.0032$ . The EPR spectrum is shown in Figure 33. The shape of the signal suggests that two organic radicals are present. Therefore, the simulation can only give rough clues regarding the hyperfine coupling constants. Best results for the major radical were obtained with  $a(\text{N}) = 9$  G and  $a(\text{H}) = 4.5$  G. The proposed radical is formed via a



**Scheme 20:** Presentation of the reaction procedure for the formation of **18**.

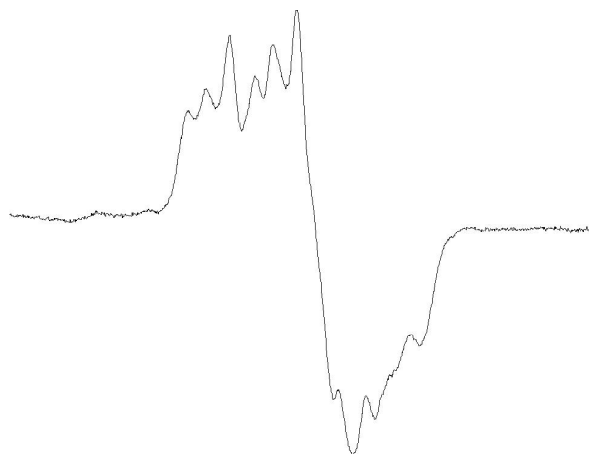
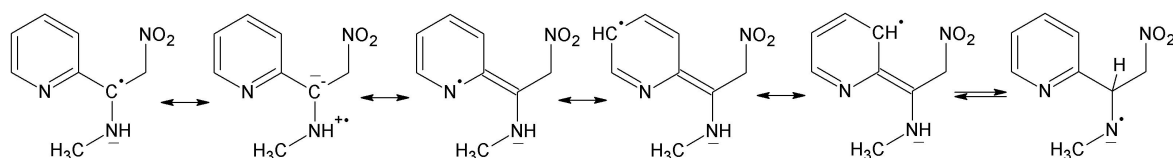


**Figure 33:** EPR signal of the 1-methylamino-1-(2-pyridyl)-2-nitroethyl radical generated from **17** in benzene at 25 °C (see Scheme 21).

hydrogen abstraction from **17** and is shown in Scheme 21 with its mesomeric forms and one tautomeric isomer. The presence of this radical is in agreement with the fact that **17** slowly decomposes in solution at low temperatures. However, decomposition is significantly accelerated in the presence of air and after isolation of **17** as an oily substance. The C-C coupling of **17** was performed with a Pd/C catalyst system in methanol and under a hydrogen pressure of 5 bar leading to the formation of 1,4-diamino-2,3-di(2-pyridyl)butane **18** in rather poor yield.



**Scheme 21:** Mesomeric and tautomeric forms of the 1-methylamino-1-(2-pyridyl)-2-nitroethyl radical produced by hydrogen abstraction from **17**.

The major reason for a yield of approximately 12 % might be that the nitro groups were also attacked under these reaction conditions. Nevertheless, this compound could be isolated with ease by cooling the reaction mixture to -20 °C and therefore, the rather poor yield seems to be acceptable. The major product was *meso*-1,4-diamino-2,3-di-

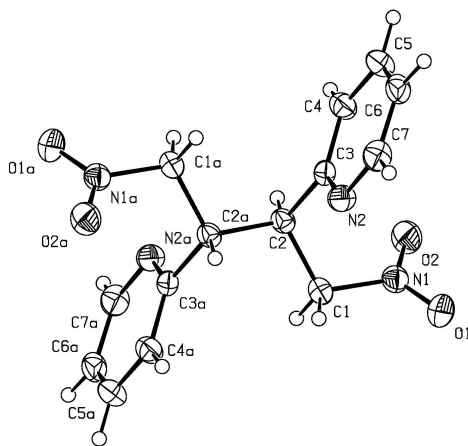


**Figure 34:** Molecular structure and numbering scheme of centrosymmetric 1,4-dinitro-2,3-di(2-pyridyl)butane *meso*-**18** (symmetry-related atoms (-x, -y+1, -z+1) are marked with the letter a; displacement ellipsoids at the 40 % probability level, H atoms are drawn with arbitrary radii). Selected bond lengths (pm): N1-O1 122.4(3), N1-O2 122.5(3), N1-C1 149.8(3), N2-C3 134.1(3), N2-C7 134.1(3), C1-C2 153.5(3), C2-C3 150.9(3), C2-C2A 155.4(5), C3-C4 138.4(4), C4-C5 138.1(4), C5-C6 138.0(4), C6-C7 137.6(4).

(2-pyridyl)butane *meso*-**18** whereas only traces of the (*R,R*)- and (*S,S*)-enantiomers were isolated. Therefore, the NMR data refers to the *meso* isomer. Compound **18** crystallizes either as the *meso* form *meso*-**18** or as the (*R,R*)- and (*S,S*)-enantiomers. The *meso*-isomer exhibits crystallographic inversion symmetry and is displayed in Figure 34. Molecular structure and numbering scheme of the (*R,R*)-enantiomer of **18** are shown in Figure 35. The structural parameters of these isomers are very much alike and are discussed together.

The central C-C bond is the longest bond in the molecule due to the rather high degree of substitution and due to repulsive electrostatic forces between two carbon atoms of identical charge. The nitro groups contain N atoms in a planar environment with N-C bond lengths of 149.3(2) pm for the (*R,R*)-isomer and of 149.8(3) pm for the *meso* form.

The nitro functionalities of **18** were converted into amino groups with hydrazine hydrate in the presence of a Pd/C catalyst system.<sup>150</sup> Tetradentate *meso*-1,4-diamino-2,3-di(2-pyridyl)butane **19** was isolated from this reduction reaction with a yield of 76 %. During reduction of the volume of the reaction mixture in vacuum, **19** precipitated as a colorless microcrystalline powder. Recrystallization of **19** from an aqueous solution afforded the colorless hydrate **19** · 2 H<sub>2</sub>O. Molecular structure and numbering scheme of **19** · 2 H<sub>2</sub>O as the *meso*- isomer are shown in Figure 36. The water molecules show hydrogen bridges to the amino groups and neighboring water molecules. This bonding pattern leads to a corrugated layer structure, as shown in Figure 37. The rather large O···O and O···N contacts suggest that only weak hydrogen bridges are formed. This

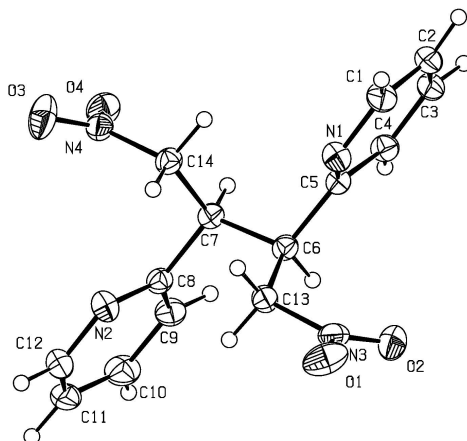


**Figure 35:** Molecular structure and numbering scheme of non-centrosymmetric 1,4-dinitro-2,3-di(2-pyridyl)butane (*R,R*)- and (*S,S*)-**18** (displacement ellipsoids at the 40 % probability level, H atoms are drawn with arbitrary radii). Selected bond lengths (pm): N1-C1 134.2(2), N1-C5 134.0(2), N2-C8 134.0(2), N2-C12 134.8(2), N3-C13 149.4(2), N3-O1 122.2(2), N3-O2 122.0(2), N4-O3 121.5(2), N4-O4 122.4(2), C1-C2 137.8(2), C2-C3 137.8(3), C3-C4 138.1(2), C4-C5 139.2(2), C5-C6 151.7(2), C6-C7 151.7(2), C6-C13 152.2(2), C7-C8 152.5(2), C7-C14 152.8(2), C8-C9 138.5(2), C9-C10 138.1(3), C10-C11 137.3(3), C11-C12 137.5(3).

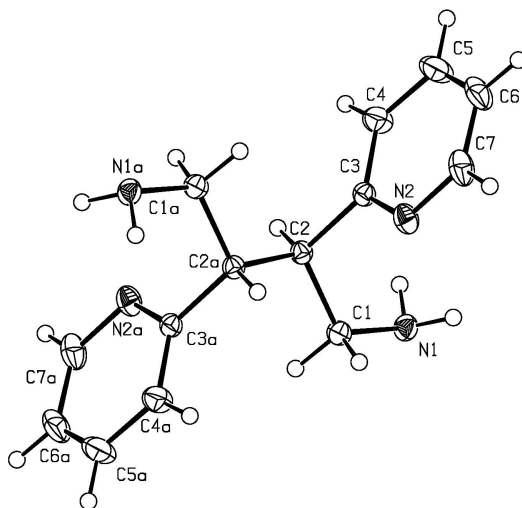


**Figure 36:** Molecular structure and numbering scheme of centrosymmetric 1,4-diamino-2,3-di(2-pyridyl)butane hydrate, *meso*-**19** · 2 H<sub>2</sub>O (symmetry-related atoms (-x+2, -y+1, -z+1) are marked with the letter a; displacement ellipsoids at the 40 % probability level, H atoms are drawn with arbitrary radii and water molecules have been omitted). Selected bond lengths (pm): N1-C1 146.6(2), N2-C3 134.0(2), N2-C7 134.1(2), C1-C2 153.6(2), C2-C3 151.2(2), C2-C2A 155.6(2), C3-C4 138.5(2), C4-C5 138.5(2), C5-C6 136.8(3), C6-C7 137.6(3).



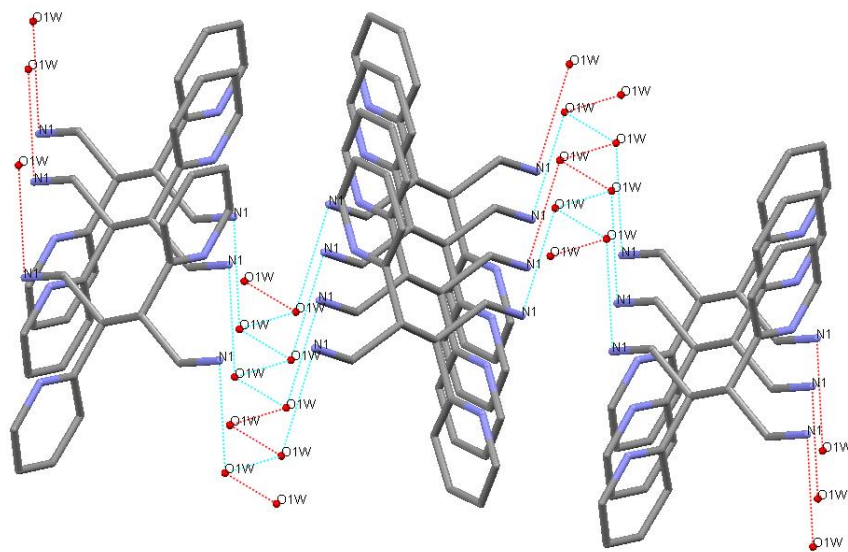


**Figure 37:** Packing of *meso*-**19** · 2 H<sub>2</sub>O in the crystalline state showing the hydrogen bonds and part of the resulting corrugated layer structure.

fact is in agreement with the observation that the anhydrous amine could be distilled at 13 mbar and 30 °C. The N-C bond lengths of these amino groups exhibit values of 146.6(2) pm.

In order to compare the coordination behavior of **19** with that of related ligands in already known complexes, *meso*-1,4-diamino-2,3-di(2-pyridyl)butane **19** was added to zinc(II) chloride in a thf solution. Dinuclear [*meso*-1,4-diamino-2,3-di(2-pyridyl)butane bis(dichlorozinc)] **20** formed quantitatively as a colorless crystalline solid, as shown in Scheme 22. In this complex the zinc atoms are in distorted tetrahedral environments. In contrast to our findings, UHLIG and MAASER suggested a polymeric structure of [2-(aminoethyl)pyridine dichlorozinc] where the two nitrogen bases of the ligand are bound to different zinc atoms.<sup>151</sup> However, later investigations on closely related substituted amines showed that these Lewis bases act as chelating ligands.<sup>152,153</sup> A crystal structure determination by X-ray diffraction of [6-(2-(dimethylamino)-phenyl)-2,2-bipyridine zinc dichloride] showed a penta-coordinate zinc atom with Zn-N bond lengths of 214.2 and 230.8 pm to the pyridyl and the amino groups, respectively, and Zn-Cl distances of 224.5 and 230.7 pm.<sup>154</sup>

Molecular structure and numbering scheme of the dinuclear complex **20** are displayed in Figure 38. The coordination of the zinc cation at the amino group (substitution of water by zinc(II) chloride) leads to a slight elongation of the N1-C1 bond. The Zn-N bonds to the amino and to the pyridyl groups are similar within standard deviations. Due to steric hindrance the Zn-Cl1 bond is slightly shorter than the Zn-Cl2

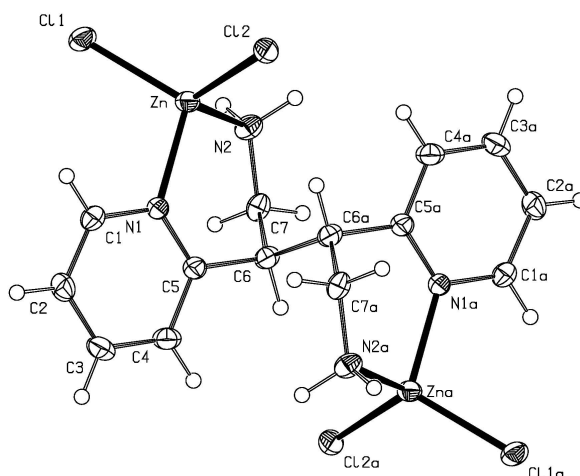
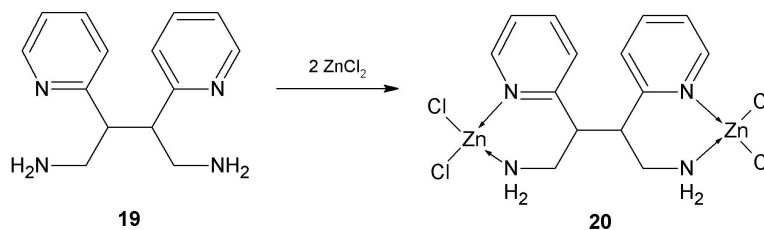


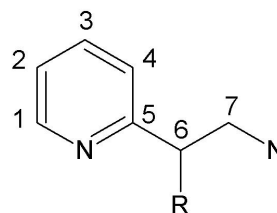
**Figure 38:** Molecular structure and numbering scheme of the centrosymmetric zinc(II) chloride complex **20** of **19** hydrate (symmetry-related atoms (-x+1, -y+1, -z+1) are marked with the letter a; displacement ellipsoids at the 40 % probability level. Hydrogen atoms are drawn with arbitrary radii. Selected bond lengths (pm): Zn-N1 205.4(3), Zn-N2 204.9(4), Zn-Cl1 222.3(1), Zn-Cl2 223.9(1), N1-C1 134.7(5), N1-C5 135.0(5), N2-C7 148.5(5), C1-C2 137.5(5), C2-C3 137.3(6), C3-C4 137.3(6), C4-C5 138.6(5), C5-C6 152.1(5), C6-C6A 153.0(7), C6-C7 153.6(5).



**Scheme 22:** Formation of the dinuclear zinc complex **20**.

**Table 14:** Comparison of selected NMR parameters (chemical shifts in ppm). The numbering scheme is given below.

	17	18	19	20
$\delta$ (H6)	4.09	4.12	3.19	3.55
$\delta$ (H7a)	4.26	4.66	2.31	2.74
$\delta$ (H7b)	4.39	5.04	2.65	2.99
$\delta$ (NH <sub>2</sub> )	—	—	1.98	4.10
$\delta$ (C6)	63.1	46.5	44.6	42.8
$\delta$ (C7)	78.8	76.4	52.5	47.9



bond. However, both values lie well within the characteristic region.<sup>72</sup> The coordination sphere of the zinc atoms in this complex is rather similar to that in (bpy)ZnCl<sub>2</sub> (bpy = 2,2'-bipyridine)<sup>76</sup> and therefore, the tetradentate ligand can be considered as a strong chelate base.<sup>76</sup> In complexes of the type (L)<sub>2</sub>ZnX<sub>2</sub> (L = Lewis base with a nitrogen donor, X = any monovalent anion) with a tetra-coordinate zinc atom, a linear correlation between the X-Zn-X angle and the average Zn-N distance was found.<sup>74,75</sup> Thus, strong nitrogen donors with short Zn-N bond lengths lead to small X-Zn-X angles and vice versa. In (1-amino-3-dimethylaminopropane) zinc dichloride an average Zn-N distance of 203.6 pm and a Cl-Zn-Cl angle of 112.55(3)° were observed.<sup>133</sup> In (tmeda)ZnCl<sub>2</sub> larger Zn-N bonds of 209.2 pm allow a larger Cl-Zn-Cl bond angle of 119.00(2)°.<sup>78,155</sup> Selected NMR data of **17** to **20** are summarized in Table 14. The <sup>1</sup>H as well as the <sup>13</sup>C NMR parameters of the pyridyl group show only a very small dependency of the substitution pattern at the alkyl group. Therefore, only the values of the C6 and C7 units are compared in Table 14. The nitro group leads to deshielded methylene moieties in **17** and **18** whereas amino substitution leads to chemical shifts of approximately  $\delta = 50$  for C7. The hydrogen atoms at C7 are diastereotopic due to the chirality of neighboring C6. A high field shift of approximately 2 ppm is observed when the nitro group is reduced to the amino functionality.

**Concluding remarks** Oxidative C-C coupling of 2-pyridylmethylamines can be performed quantitatively with organozinc or tin(II) compounds with precipitation of metal. Another access route to 1,2-dipyridyl-1,2-diaminoethane is the reductive coupling of 2-pyridylmethylidene amines. For 2,3-dipyridyl-1,4-diaminobutane no comparable reaction routes were available. The addition of nitromethane to N-methyl-2-pyridylmethylideneamine gives 1-methylamino-1-(2-pyridyl)-2-nitroethane **17** with a good yield. In a hydrogen atmosphere methylamine can be eliminated, and C-C coupling is achieved with a rather poor yield due to side-reactions, leading to the formation of 1,4-dinitro-2,3-di(2-pyridyl)butane **18**. The conversion of the nitro functionalities into amino groups is achieved with hydrazine hydrate giving 1,4-diamino-2,3-di(2-pyridyl)butane **19**. Due to the presence of two chiral carbon atoms in 2- and 3-position in the backbone of **18** and **19** the formation of diastereomers and enantiomers is observed. 1,2-Dipyridyl-1,2-diaminoethane easily isomerizes during metalation with dialkylzinc. Therefore, zincation of *meso*- and (*R,R*)/(*S,S*)-1,2-dipyridyl-1,2-diaminoethane yields bis(alkylzinc) (*R,R*)/(*S,S*)-1,2-dipyridyl-1,2-diamidoethane regardless of the employed isomer. First reactivity studies of 1,4-diamino-2,3-di(2-pyridyl)butane **19** show that isomerization occurs far less readily. The zinc(II) chloride adduct, [*meso*-1,4-diamino-2,3-di(2-pyridyl)butane bis(dichlorozinc)] **20**, is formed quantitatively from *meso*-**19**.

Due to the longer butane chain, ligand **19** shows an enhanced flexibility compared to 1,2-dipyridyl-1,2-diaminoethane with its short backbone.

### 2.2.4 Synthesis of a tetraaryl substituted piperazine ( $\text{ZnCl}_2$ )<sub>2</sub> complex with unexpected stereoselectivity

**Introduction** Semistabilized 2-azaallyl anions are used as ligands for metal complexation. They are usually made by deprotonation of imines but also other methods such as desilylation exist.<sup>156</sup> Subsequent reaction of these 1,3 dipoles with alkenes afford five-ring heterocycles and represent an important synthetic route.<sup>157</sup> But also six-ring heterocycles (piperazine derivatives) were described in literature, which in some cases were made accidentally by dimerization of metalla-2-azaallylic compounds. The first example was reported by TREPANIER and WANG who reacted 1-(pyridin-2-yl)-N-(pyridin-2-ylmethyl)methanamine **o** with  $\text{Al}(\text{CH}_3)_3$ .<sup>158</sup> They found the (2,3,5,6-tetra(2-pyridyl)piperazyl)tetramethyl dialuminium complex **H** as minor product. Similar complexes were described by some of us several years ago.<sup>20,159</sup> The bis[methylzink-2-pyridylmethylamido]-N,N'-bis(methylzink)-2,3,5,6-tetrakis(2-pyridyl)piperazyl **J** was found as a side product of the C-C coupling of 2-picolyamine with dimethyl zinc.<sup>20</sup> Recently, CARIOU and coworkers reported on the C-C coupling of phenoxy(benzimidazolyl)imine titanium, zirconium and hafnium complexes **K**.<sup>160</sup> The common feature of the mentioned complexes is a dinuclear tetrasubstituted piperazyl ligand, the latter, however, being the first example with two different substituents at the piperazyl ring. It is worth mentioning, that CARIOU and coworkers solely found the 2,6-bis(benzimidazolyl)-3,5-bis(phenoxy)piperazyl isomer as given in Scheme 39.

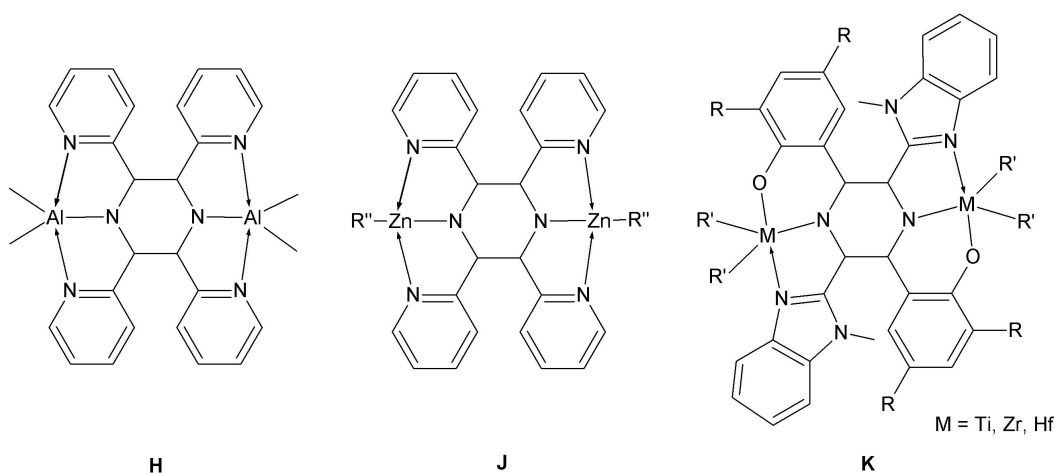
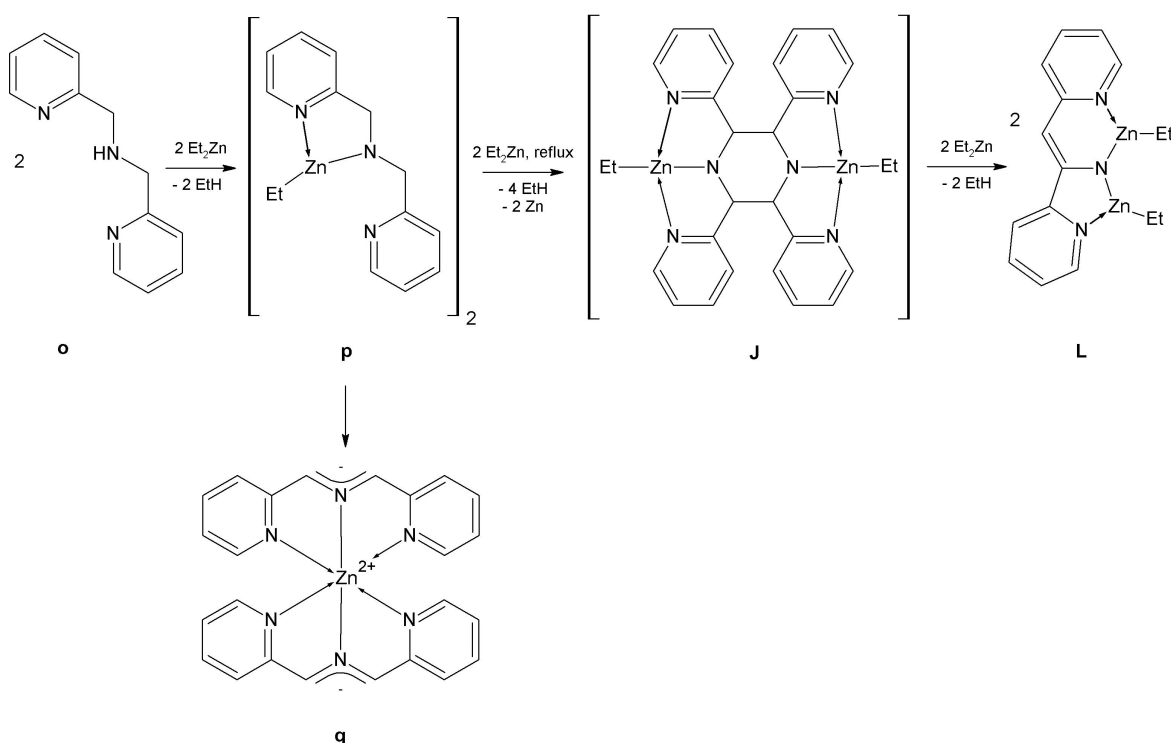


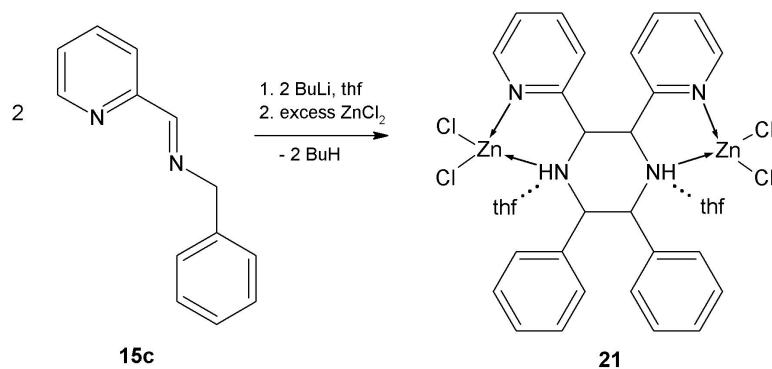
**Figure 39:** Presentation of published piperazyl complexes.

N,N'-Bis(alkylzinc)-2,3,5,6-tetrakis(2-pyridyl)piperazyl **J** played a key role during the formation of bis(alkylzinc)imido-1,2-di(2-pyridyl)ethene **L** by the reaction of 1-(pyridin-2-yl)-N-(pyridin-2-ylmethyl)methanamine **o** with diethyl zinc.<sup>159</sup> The piperazyl ring was formed by an oxidative C-C coupling under precipitation of zinc in refluxing toluene. In contrast, stirring of N-(ethylzinc)-1-(pyridin-2-yl)-N-(pyridin-2-ylmethyl)methanamide **J** at room temperature led to the formation of a gold-shining 2-azaallyl zinc complex, zinc bis[1,3-di(2-pyridyl)-2-azapropenide] **q**.<sup>159,161</sup> N-Benzylpyridylmethylideneamine **15c** represents a precursor for a semistabilized asymmetric substituted 2-azaallyl anion. The coordination behavior of the neutral ligand **15c** towards zinc chloride was already described in section 2.2.2.



**Scheme 23:** Reaction of 1-(pyridin-2-yl)-N-(pyridin-2-ylmethyl)methanamine **o** with diethyl zinc and subsequent formation of either zinc bis[1,3-di(2-pyridyl)-2-azapropenide] **q** or bis(alkylzinc)imido-1,2-di(2-pyridyl)ethene **L** in dependency on the reaction conditions.

**Results** N-Benzylpyridylmethylideneamine **15c** was deprotonated with  $n\text{-BuLi}$  at  $-78\text{ }^\circ\text{C}$  in anhydrous thf. Immediately, upon addition of base the colorless solution turned deep violet. After stirring for 90 minutes an excess of anhydrous zinc chloride was added and the mixture was allowed to warm to room temperature. After stirring over night **21** was obtained as colorless precipitate from a blueish solution. Crystals suitable for single crystal X-ray diffraction were obtained at the glass wall of the vessel. Comparison of the X-ray powder diffraction pattern of the bulk material and the sim-



**Scheme 24:** Reaction of N-benzyl-pyridylmethylideneamine **15c** with butyl lithium and zinc chloride and the isolated product **21**.

ulated powder spectrum of the single crystals revealed their congruence. The product was obtained in 48 % isolated yield as thf adduct. Interestingly, more than a three-fold excess of anhydrous zinc chloride was necessary in order to obtain **21**. The best results were achieved with a five-fold excess.

The C-C coupled product [2,3-diphenyl-5,6-di(pyridin-2-yl)piperazino bis(dichloro zinc)] **21** is depicted in Scheme 24. It is noteworthy, that complex **21** was obtained with a neutral ligand. The product can be considered as the dinuclear zinc chloride complex of a N-benzyl-pyridylmethylideneamine dimer. It crystallized in the chiral space group  $P2_1$  as a homodinuclear complex with two zinc ions in a distorted tetrahedral environment (see Figure 40). The central piperazine ring is found in chair configuration with the aryl rings in the equatorial positions. Hence the carbon bound hydrogen atoms are found in the axial positions. This is in agreement with the tetraaryl substituted piperazine complexes described in ref.<sup>20,158,160</sup>. In contrast, the nitrogen bound protons are found in the equatorial positions and are connected via hydrogen bridges with cocrystallized thf molecules. The average donor...donor distance is 283 pm. Existence of NH protons was also proven by IR spectroscopy, revealing a broadened band at  $3400 \text{ cm}^{-1}$ . All bond lengths and angles are within the expected range.<sup>66,72</sup> Nevertheless, the Zn-N bond lengths are slightly larger than those observed for other tetrahedrally coordinated zinc chloride complexes in the present work. They are found to be Zn1-N1 207.4(4), Zn1-N2 210.7(4), Zn2-N3 208.4(4) and Zn2-N4 213.0(4). These findings can be explained with sterical strain induced by connection of three rings (two 5-membered metalla rings and one piperazine ring). With one piperazine nitrogen and one pyridyl nitrogen atom the zinc forms a five-membered ring with small bite angles (N1-Zn1-N2  $80.10(15)^\circ$ , N3-Zn2-N4  $80.41(16)^\circ$ ). The Cl-Zn-Cl angles are found to be Cl1-Zn1-Cl2  $120.81(7)^\circ$  and Cl3-Zn-Cl4  $118.12(6)^\circ$  and are in very good agreement with the linear correlation between the Zn-N bond length and the Cl-Zn-Cl angle in complexes with

tetrahedrally coordinated zinc.<sup>73–75</sup>

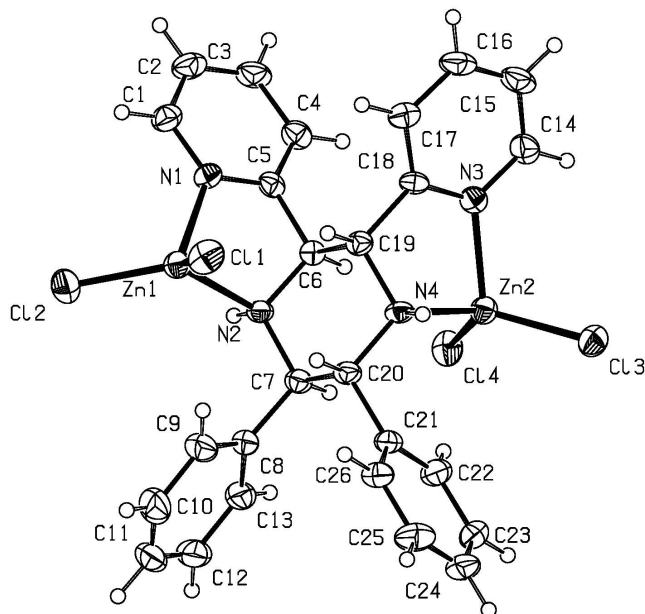
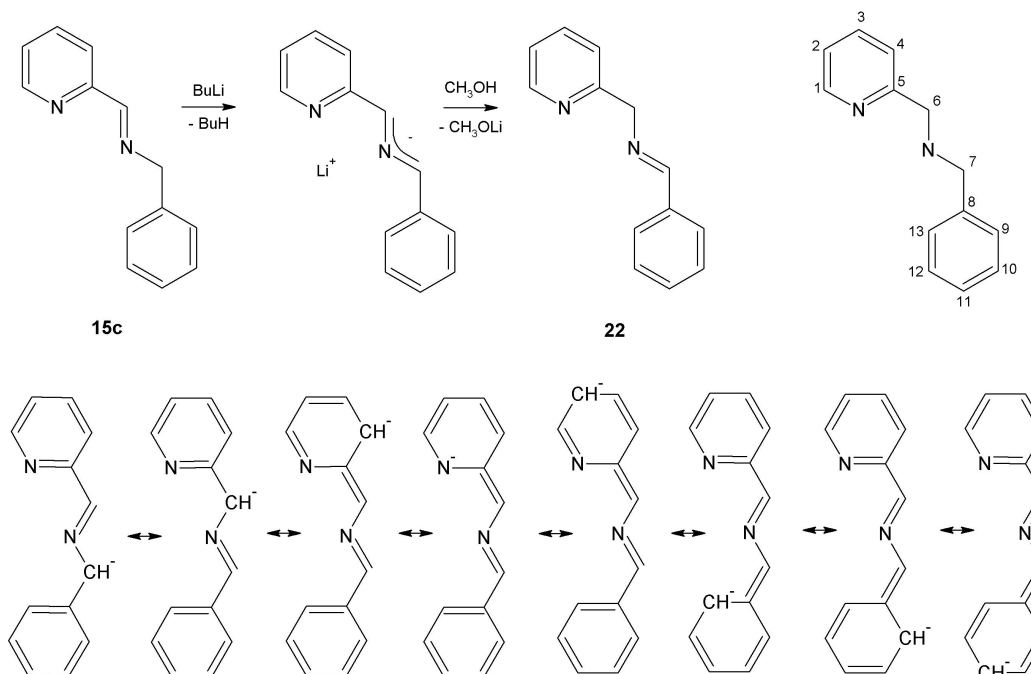


**Figure 40:** Molecular structure and numbering scheme of **21**. The ellipsoids represent a probability of 40 %, H atoms are shown with arbitrary radii. Thf molecules have been omitted for clarity. Selected bond lengths (pm) and angles ( $^{\circ}$ ): Zn1-N1 207.4(4), Zn1-N2 210.7(4), Zn2-N3 208.4(4), Zn2-N4 213.0(4), C6-C19 153.6(7), C7-C20 151.1(7), C6-N2 147.9(6), C7-N2 149.6(6), C19-N4 149.3(6), C20-N3 149.9(6), N1-Zn1-N2 80.10(15), N3-Zn2-N4 80.41(16), C11-Zn1-Cl2 120.81(7), C13-Zn2-Cl4 118.12(6).

One set of signals is found by NMR spectroscopy and is in agreement with the solid state structure. The molecule **21** possesses a  $C_2$  rotational axis, thus the protons adjacent to the pyridyl rings are homotopic as well as the protons adjacent to the phenyl rings. Furthermore, the chemical shifts of both sets of protons are nearly equal and thus they are found as a broadened singlet. Two thf molecules remain bonded after drying in vacuo for several hours at elevated temperatures. This finding was supported by NMR spectroscopy and elemental analysis. Interestingly enough, only the pair of enantiomers given in Scheme 24 was isolated and NMR spectra of the supernatant solution gave no hint on the existence of other isomers. Several NMR experiments were conducted in order to get insights into the underlying coupling mechanism. The imine **15c** was deprotonated by *n*-butyl lithium in  $[D_8]thf$  at  $-78^{\circ}C$  under argon atmosphere (see Scheme 25). Subsequently, NMR spectra were taken at this temperature allowing the conclusion that **15c** was completely deprotonated to form the 2-azaallyl anion. The solution was allowed to warm to room temperature in order to take two-dimensional NMR spectra. For technical reasons the spectrometer used for two-dimensional NMR spectroscopy could not be cooled to  $-78^{\circ}C$ . Nevertheless, only small a temperature dependency of the NMR signals was observed and assignment was made on the basis

of DEPT135, HSQC, H,H COSY and HMBC spectra. The results are summarized in Table 15. In comparison with neutral **15c** the 2-azaallyl anion obtained by deprotonation of **15c** shows a delocalized negative charge, which led to a highfield shift of the respective  $^{13}\text{C}$  NMR signal. This shielding is observed along the whole molecule and is in very good agreement with the mesomeric forms given in Scheme 25. Taking the differences of the chemical shifts of **15c** and the 2-azaallyl anion as an indicator for electron density distribution, one can conclude that most of the charge is localized on the pyridyl side of the 2-azaallylic system. This is also supported by the fact, that careful reprotonation of the 2-azaallyl anion with anhydrous methanol under argon atmosphere led to formation of N-(phenylmethylidene)-1-(pyridin-2-yl)methanamine **22** (see Scheme 25). This was also found by KONAKAHARA and coworkers.<sup>162</sup>



**Scheme 25:** Deprotonation of imine **15c** and formation of the 2-azaallylic system. The mesomeric forms of 2-azaallyl anion show the possible charge distribution. Protonation of the lithium 2-azaallyl complex led to formation of **22**. Furthermore, the numbering scheme is given.

Although **15c** is completely deprotonated in the first step, the product **21** was received with a neutral ligand. Several experiments were carried out to address the origin of the protons. The cleavage was excluded since no cleavage products were found by NMR spectroscopy and GC analysis. Due to the fact that the yield is nearly 50 % one can assume that protons originate from a second deprotonation of the starting compound **15c**. This is supported by the observation of an air sensitive supernatant solution after precipitation of complex **21**. However, NMR investigations of the super-



**Table 15:** Comparison of  $^{13}\text{C}$  NMR data (chemical shift,  $\delta$ ) of **15c**, 2-azaallyl anion and **22**.

Pos.	<b>15c</b> (197K)	2 - <i>azaallyl</i> (197K)	2 - <i>azaallyl</i> (300K)	<b>22</b> (300K)
1	150.3	148.2	148.0	149.7
2	125.9	106.6	106.4	122.3
3	137.3	134.6	134.4	137.6
4	121.2	115.9	116.0	122.5
5	155.5	158.7	159.0	160.8
6	163.7	111.3	111.4	67.3
7	65.2	125.0	123.9	163.1
8	140.2	141.8	142.4	136.7
9, 13	128.8	123.6	122.4	128.8
10, 12	129.1	128.8	128.6	128.9
11	127.6	121.1	121.4	131.2

nant solution as well as addition of methyl iodide as anion scavenger did not lead to identifiable or isolable compounds. CARIOU and coworkers proposed an ionic coupling mechanism for the titanium complex and a radical coupling pathway for the zirconium and hafnium complexes (see **K** in Figure 39).<sup>160</sup> Due to the solely formation of the 2,3-diphenyl-5,6-di(pyridin-2-yl)piperazine complex an ionic coupling pathway seems to be unlikely. As described above the negative charge is mainly located on the pyridyl-side of the 2-azaallyl anion, thus the formation of a 2,5-diphenyl-3,6-di(pyridin-2-yl)piperazine complex would be expected via an ionic mechanism. Although experimental data is not sufficient yet, the observed stereoselectivity of **21** may be explained with a radical mechanism.

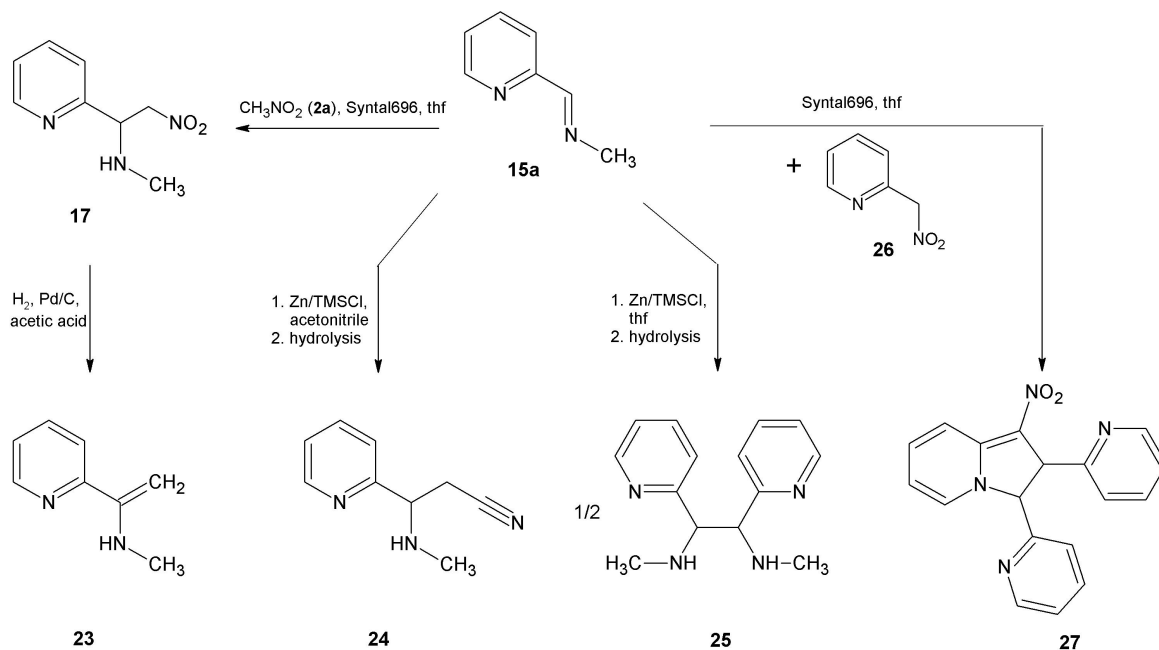
**Concluding remarks** N-Benzyl-pyridylmethylideneamine **15c** was reacted with n-butyl lithium and zinc chloride under anhydrous conditions to form the dinuclear complex **21**. The reaction proceeded stereoselectively with moderate yields and **21** was obtained with 2,3-diphenyl-5,6-di(pyridin-2-yl)piperazine as neutral ligand. But the question of the origin of the N-bound protons remains unanswered. NMR investigations and protolysis experiments shed light on the charge distribution in the 2-azaallyl lithium complex. But several questions such as the necessity of an excess of zinc chloride and its role during the reaction as well as the reasons for the observed stereoselectivity remain future tasks.

### 2.2.5 Miscellaneous reactions

**Introduction** N-Methyl-pyridylmethylideneamine **15a** provides a readily accessible precursor compound for carbon-carbon bond formation reactions (cf. section 2.2.1). As mentioned in the introduction (cf. page 9) this SCHIFF-base was used for reductive C-C coupling to symmetrical vicinal diamines. In section 2.2.3 the aza-HENRY of **15a** with nitromethane **2a** was described and the conversion of the obtained  $\beta$ -nitroamine **17**. The complexation behavior of imine **15a** towards zinc chloride was described in section 2.2.2. In the following several reactions starting with N-methyl-pyridylmethylideneamine **15a** will be described, which did not lead to the expected product but furnished interesting new compounds.

**Results** In section 2.2.3 the  $\beta$ -nitroamine **17** was C-C coupled using hydrogen and catalytic amounts of Pd/C in methanol. In an effort to reduce the nitro group of **17**, this compound was reacted in acetic acid with hydrogen and with Pd/C (10 %) as catalyst. Extraction of the black reaction mixture with methylene chloride afforded N-methyl-1-(pyridin-2-yl)ethenamine **23** as a yellow oil with 90 % purity (Scheme 26). However, **23** was found to be reactive but could be stored for several weeks at -20 °C. Thus, purification methods, such as distillation or column chromatography failed. Product **23** was characterized by one and two dimensional NMR spectroscopy as well as mass spectrometry.

ALEXAKIS and coworkers published a procedure for the zinc mediated reductive C-C coupling of N-methyl-phenylmethylideneamine and subsequent isomerization of the *meso*-form to the (*R,R*) and (*S,S*) isomers.<sup>26</sup> We were interested in the C-C coupling of N-methyl-pyridylmethylideneamine **15a** via this procedure, which was also published by them.<sup>23,24</sup> They reported the best results when the reaction was carried out in acetonitrile. In contrast to their findings we reproducibly obtained 3-(methylamino)-3-(pyridin-2-yl)propanenitrile **24** with an isolated yield of 20 % as given in Scheme 26. This compound may be regarded as the addition product of **15a** and acetonitrile. It was extracted according to the published procedure from the hydrolyzed black reaction mixture as the main product together with the C-C coupling product **25**. The latter was received with a similar procedure in thf as also reported by ALEXAKIS and will be addressed later on.<sup>23</sup> Compound **24** is a yellow to green liquid and was characterized by NMR and IR spectroscopies as well as by mass spectrometry. Similar to the  $\beta$ -nitroalcohol **3a**, the proton NMR spectrum of the ethane backbone protons shows an ABX pattern. The geminal coupling constant was observed to be  $^2J(\text{H,H}) = 4.0$  Hz and the vicinal coupling constant was found to be  $^3J(\text{H,H}) = 6.8$  Hz. The existence of



**Scheme 26:** Reactions starting with N-methyl-pyridylmethylideneamine **15a** and their products.

the nitrile moiety was indicated by the  $^{13}\text{C}$  NMR signal of  $\delta = 118.5$  and confirmed by IR spectroscopy ( $\tilde{\nu}(\text{CN}) = 2247 \text{ cm}^{-1}$ ).

The C-C coupling product **25** was received as reported from the reaction in thf. As reported by ALEXAKIS and coworkers both, the *d,l*- and the *meso*-form distill together. However, after several days the *meso*-form crystallized from the distilled oil and was for the first time characterized by single crystal X-ray diffraction. *Meso*-**25** crystallized in the centrosymmetric space group  $\text{P}2_1/c$  and the molecule was found on an inversion center. The ethane backbone's carbon-carbon bond length was found to be 154.1(2) pm, which is comparable with the central C-C bond length found for *meso*-**19** (155.6(2) pm, see page 71) Bond lengths and angles were found within the expected range.<sup>66</sup>

A nitroaldol reaction between compound **15a** and 2-(nitromethyl)pyridine **26** (vide infra) with Syntal 696<sup>®</sup> in anhydrous thf afforded yellow crystals of compound **27** as a byproduct. This 1-nitro-2,3-di-2-pyridyl-2,3-dihydroindolizine was, however, the only isolable product from the brown reaction mixture and was characterized by  $^1\text{H}$  and  $^{13}\text{C}$  NMR spectroscopy as well as by single crystal X-ray diffraction. The molecular structure of **27** is given in Figure 42. Of the four possible stereoisomers only the *anti*-isomers were found in the solid state. The 2-pyridyl rings of adjacent molecules are arranged coplanarily with an approximate intermolecular distance of 370 pm. With regard to the bond length, the nitro group was found in conjugation with the strained five-membered ring and the six-membered part of the indolizine moiety.<sup>66</sup> Compound

**27** was published in *Acta Crystallogr., Sect. E: Struct. Rep. Online*, **2009**, *65*, o957 (Publication 4).

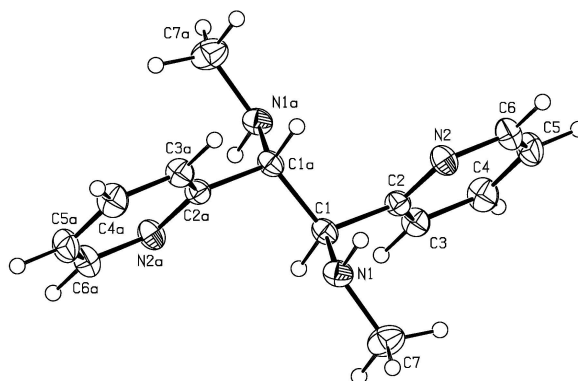


**Figure 41:** Molecular structure and numbering scheme of *meso*-**25** (symmetry-related atoms (-x, -y+1, -z+2) are marked with the letter a). The ellipsoids represent a probability of 40 %, H atoms are shown with arbitrary radii. Selected bond lengths (pm): C1-C1A 154.1(2), C1-N1 146.05(14), C1-C2 152.05(15), N1-C7 145.51(18).

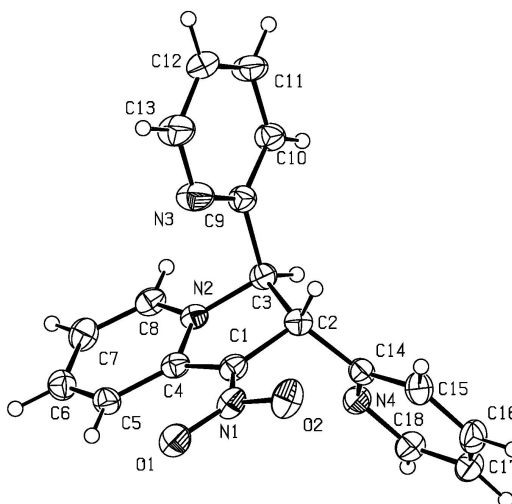


**Figure 42:** Molecular structure and numbering scheme of **27**. The ellipsoids represent a probability of 40 %, H atoms are shown with arbitrary radii. Selected bond lengths (pm): C2-C3 154.5(3), C1-N1 134.2(3), C1-C4 141.0(3), N2-C3 148.7(3).

2-(Nitromethyl)pyridine **26** was prepared according to a literature procedure from 2-methylpyridine (picoline) and n-propylnitrate with sodium amide in liquid ammonia.<sup>163,164</sup> N-propylnitrate was obtained by esterification of n-propylalcohol and nitric acid.<sup>165</sup> Distillation afforded a yellow oil with a yield of 31 %, which was characterized by NMR spectroscopy as well as by mass spectrometry. This compound slowly turned dark at room temperature and thus was stored at -20 °C where it became solid. Attempts to obtain compound **26** by the reaction of 2-(chloromethyl)pyridine with sodium nitrite or silver nitrite were not successful.

### 3 Summary

For the development of a modular ligand preparation pathway the well established nitroaldol reaction was chosen. From the wide variety of published catalysts, two solids were selected, that are cheap, non-toxic and could be employed without elaborate pre-treatment: Syntal 696<sup>®</sup> and Amberlyst A21<sup>®</sup>. Due to their intermediate basicity aqueous work-up can be avoided and catalyst removal was achieved by simple filtration. Pyridine-2-carbaldehyde **1** was chosen as the first building block and reacted with nitromethane **2a** and nitroethane **2b**. Both reactions proceeded with very good yields and the products **3a** and **3b** were obtained by crystallization or precipitation with excellent purity. Side reactions such as the elimination of water under formation of nitroalkenes were not observed in solution. Moreover, neither a second nitroaldol reaction was observed under the applied conditions. This allows the consecutive synthesis of asymmetric substituted ligands. The diastereoselectivity of the reaction of pyridine-2-carbaldehyde **1** with nitroethane **2b** was of interest. In contrast to a published diastereomeric excess of de = 30 % for *erythro-3b*, a diastereomeric excess of de = 80 % was obtained for *threo-3b*. For the first time the solid state structure of the  $\beta$ -nitroalcohols **3a** and **3b** was examined. The arrangement of the molecules in the solid state is strongly affected by hydrogen bond interactions. However, these interactions also account for the observation of two independent molecules in the asymmetric unit. As a third building block also pyridine-2-carbaldehyde **1** was chosen to limit the number of possible stereoisomers. The 2-nitro diols **4a** and **4b** were accessible with moderate to good yields but with excellent purity and a simple work-up procedure. As found by NMR investigations the reaction proceeded diastereoselectively under the applied conditions. Compound **4a** was found with a diastereomeric excess of de = 77 % for the (*R,R*)- and (*S,S*)-isomers. Although the (*R,R*)- and (*S,S*)-isomers of compound **4b** were isolated, isomerization occurred in solution accompanied by retro-HENRY reaction. Both compounds **4a** and **4b** were found to undergo retro-HENRY reaction in polar solvents and also in the presence of zinc salts and water. Nevertheless, a zinc complex of **4a** was obtained in anhydrous thf. Surprisingly, only the pyridyl nitrogen atoms were occupied as donor sites, with zinc(II) in distorted tetrahedral environment. Hydrogen bonds between the hydroxyl moiety and thf were found in the solid state and can also be assumed in thf solution according to NMR spectra. Additionally, complex **5** was stable under atmospheric conditions for several days. Due to the tendency of the prepared 2-nitro diols **4a** and **4b** to undergo retro-HENRY reaction in polar solvents the employment of suitable protecting groups was necessary. Furthermore, several attempts to reduce the nitro group under formation of the respective 2-amino diols were

also unsuccessful and emphasized this proposition. The *tert*-butyldimethylsilyl moiety was found to be a suitable protecting group. Protection was also successfully achieved with trimethylsilylimidazole but the TMS group was not stable under the conditions of nitro group reduction. However, reaction of 2-nitro diol **4a** was conducted with very good yields and the product **7** could be obtained with excellent purity. NMR investigations revealed the only formation of the (*R,R*)- and (*S,S*)-isomers. The same protection protocol was applied for 2-nitro diol **4b** and led to formation of its mono-TBDMS substituted derivative **8**. Both, single crystal X-ray diffraction and NMR spectroscopy results of compound **8** revealed the highly stereoselective formation of the *6S7S8R* and *6R7R8S* isomers. Furthermore, TBDMS protected **3b** was found as a second product **9**, giving evidence that retro-HENRY takes place under the applied protection conditions. Compound **9** was also obtained by reaction of **3b** with TBDMSCl but with an altered *erythro:threo* ratio, with respect to **3b**. This clearly indicates stereoselective HENRY reaction equilibria under the protection conditions. Interestingly enough, differences in solubility of the mono- and disilylprotected diols were found. The diTBDMS protected diol **7** is soluble in nearly every solvent except water and dmso, whereas the monoTBDMS protected **8** was precipitated in pentane. Reduction of the nitro group was considered a key step in the presented work, since it leads to the valuable amino moiety, which is prone for further substitutions, as well as to hydroxylamine or oxime groups. This was achieved by nickel boride catalyzed reduction with sodium borohydride of **7** to the amine **10** with excellent yields and under mild conditions. According to NMR investigations the relative configuration was not changed and compound **10** may be considered as a substitute ligand for 1-(pyridin-2-yl)-N-(pyridin-2-ylmethyl)methanamine **o**. Reduction of **7** with partially hydrolyzed sodium borohydride exclusively led to the formation of the respective hydroxylamine **11**, which underwent aerial oxidation to the oxime **12** in methanol. Attempts to reduce **7** to the hydroxylamine **11** with sodium cyanoborohydride or sodium triacetoxyborohydride led to a mixture of **11** and **10**. Nonetheless, the receipt of oxime **12** is highly desirable, since its hydrolysis would lead to the respective ketone. Moreover, both compounds **11** and **12** also represent prospective ligands and the development of a selective reduction procedure remains a future task. As mentioned above the amino group of **10** is readily available for substitution. In order to test the ease of ligand preparation, it was reacted with salicyl aldehyde. This is a common motif for the complexation of vanadium cations and was used for several years in the group of PLASS for the preparation of haloperoxidase models. Compound **13** was obtained with nearly quantitative yields and excellent purity. Its UV-Vis absorption and emission properties were examined as well as those of its deprotonated derivative. Reaction of proligand **13** with vanadyl

acetylacetonate and subsequent aerial oxidation afforded the vanadium(v) complex **14**. Interestingly, in the course of the complexation reaction one TBDMS group was cleaved and the resulting alcoholate moiety served as donor site. This fact is also useful for the preparation of other complexes, since the deprotection step may be skipped. Together with ROBERT DEBEL from the group of PLASS, complex **14** and compound **13** with either vanadyl acetylacetonate or molybdenyl acetylacetonate were tested as catalyst for sulfoxidation with hydrogenperoxide. All catalytic systems led to nearly quantitative conversion of the (methylsulfanyl)benzene **I** but showed significant differences concerning their activity. Nevertheless, since the preparation of compound **13** and of complex **14** proceeded stereoselectively to only one pair of enantiomers, their separation and subsequent enantioselective sulfoxidation is imaginable. The vanadium complex **14** is also interesting from an other point of view. It possesses an uncoordinated pyridyl nitrogen with an approximate distance of 450 pm to the metal center. This nitrogen could serve as proton relay or donor for hydrogen bonds. Both interactions were found to be essential in enzyme catalyses.<sup>166</sup> Furthermore, the remaining TBDMS group mediates the solubility in nonpolar solvents.

The second part of the the presented work was concerned with preparation, characterization and reactions of the carbonyl analogue SCHIFF-bases **15a**, **15b**, **15c** and **15d**. They were intended to serve as building blocks for aza-HENRY reactions but sometimes furnished unexpected new compounds. Examination of their coordination behavior towards zinc chloride revealed interesting differences in dependency on the N-bound substituent. In most cases zinc(II) was found in a distorted tetrahedral environment. However, with methyl as N-bound substituent also penta-coordinated zinc(II) cocrystallized with the tetrahedral zinc complex **16a**. The N-benzyl ligand led to formation of octahedrally coordinated zinc(II) with a tetrachloro zincate counterion (**16c**). Aza-HENRY reaction of the N-methyl substituted SCHIFF-base **15a** afforded  $\beta$ -nitroamine **17**. The existence of radical species of **17** was proven by EPR spectroscopy. Its coupling product **18** was obtained in an autoclave reaction with hydrogen and in the presence of palladium on carbon in methanol but with poor yields. Reduction of the nitro groups with hydrazine hydrate afforded the respective diamine **19**. The dinuclear zinc chloride complex **20** was obtained by reaction of **19** with zinc chloride. This work was conducted in cooperation with TOBIAS KLOUBERT. An interesting reaction was discovered when the N-benzyl substituted SCHIFF-base **15c** was deprotonated with n-butyl lithium. The formed 2-azaallyl anion dimerized in the presence of zinc chloride. The received product **21** was found as the dinuclear zinc complex of a tetraaryl substituted piperazine derivative with unexpected stereoselectivity. Charge distribution within the 2-azaallyl moiety was examined by NMR spectroscopy and gave first hints on a possi-

ble mechanism. Several unexpected reactions were observed with SCHIFF-base **15a** as starting compound. As mentioned the nitroaldol reaction with nitromethane afforded  $\beta$ -nitroamine **17**. While **17** was C-C coupled in methanol with hydrogen and Pd/C, similar conditions in acetic acid afforded N-methyl-1-(pyridin-2-yl)ethenamine **23**. C-C coupling attempts according to published procedures in acetonitrile led to addition of acetonitrile to **15a** and formation of 3-(methylamino)-3-(pyridin-2-yl)propanenitrile **24**. Reaction of **15a** with 2-(nitromethyl)pyridine **26** and Syntal 696<sup>®</sup>, furnished 1-nitro-2,3-di-2-pyridyl-2,3-dihydroindolizine **27** as a crystalline byproduct.

## 4 Zusammenfassung

Für die Entwicklung von modularen Reaktionswegen zur Darstellung neuer Liganden, wurde die gut erforschte Nitroaldolreaktion gewählt. Aus der Vielzahl der bereits publizierten Katalysatoren für diese Reaktion, wurden zwei Festkörper ausgesucht. Diese sind billig, nicht toxisch und können ohne aufwendige Vorbehandlung eingesetzt werden. Aufgrund ihrer mittleren Basenstärke wirken sie als Protonenrelais und eine wässrige Aufarbeitung konnte vermieden werden. Weiterhin gelang die Abtrennung der Katalysatoren durch einfache Filtration. Als erster Baustein wurde Pyridin-2-carbaldehyd **1** gewählt und mit Nitromethan **2a** und Nitroethan **2b** zur Reaktion gebracht. Beide Reaktionen verliefen mit hohen Ausbeuten zu den Produkten **3a** und **3b**, welche durch Kristallisation oder Fällung mit hoher Reinheit erhalten wurden. Nebenreaktionen, wie beispielsweise die Eliminierung von Wasser unter Bildung von Nitroalkenen wurde in Lösung nicht beobachtet. Weiterhin wurde, unter den gewählten Bedingungen, keine zweite Nitroaldolreaktion beobachtet. Dies gestattet den konsekutiven Aufbau von asymmetrisch substituierten Liganden. Die Diastereoselektivität der Reaktion zwischen Pyridin-2-carbaldehyd **1** und Nitroethan **2b** stand ebenfalls im Mittelpunkt des Interesses. Im Gegensatz zu veröffentlichten Diastereomerenüberschüssen von  $de = 30\%$  für *erythro*-**3b**, wurden mit einer modifizierten Methode ein Überschuss des *threo* Isomeren von **3b** von  $de = 80\%$  erreicht. In der vorliegenden Arbeit wurden zum ersten Mal die Festkörperstrukturen der  $\beta$ -Nitroalkohole **3a** und **3b** untersucht. Die Anordnung der Moleküle im Festkörper wird maßgeblich durch die Ausbildung von Wasserstoffbrücken bestimmt. Dies führt auch dazu, dass bei einigen Verbindungen zwei kristallographisch unabhängige Moleküle in der asymmetrischen Einheit gefunden werden. Als dritter Baustein wurde ebenfalls Pyridin-2-carbaldehyd **1** eingesetzt um zunächst die Zahl der möglichen Stereoisomeren einzugrenzen. Aus den Reaktionen erhielt man die 2-Nitrodiole **4a** und **4b** in mittleren bis guten Ausbeuten, jedoch mit hoher Reinheit. Weiterhin zeichnet sich die Reaktion durch eine einfache Aufar-



beitung aus. Mittels NMR-Untersuchungen konnte gezeigt werden, dass die Reaktion zu **4a** mit einem Diastereomerenüberschuss von  $de = 77\%$  für die (*R,R*)- und (*S,S*)-Isomeren verläuft. Verbindung **4b** wird ebenfalls mit einem deutlichen Überschuss der (*R,R*)- und (*S,S*)-Isomeren erhalten, isomerisiert jedoch in Lösung begleitet von Retro-HENRYreaktionen. Diese Rückreaktion wurde bei beiden Verbindungen **4a** und **4b** vor allem in polaren Lösungsmitteln beobachtet und insbesondere in der Gegenwart von Zinksalzen und Wasser. Trotzdem gelang die Darstellung eines Zinkchloridkomplexes mit **4a** in wasserfreiem THF. Die Einkristallstrukturanalyse des Komplexes **5** zeigte überraschenderweise, dass Zink jeweils von den Pyridylstickstoffatomen koordiniert wird. Die Hydroxygruppen beteiligen sich nicht an der Koordination sondern gehen Wasserstoffbrückenbindungen mit THF ein, was auch in Lösung beobachtet wurde. Zink(II) wurde hierbei in einer verzerrt tetraedrischen Koordination gefunden und der Komplex war einige Tage unter atmosphärischen Bedingungen stabil. Aufgrund der Neigung der 2-Nitrodiole **4a** und **4b** Retro-HENRYreaktion einzugehen, war der Einsatz von Schutzgruppen notwendig. Weiterhin schlugen mehrere Versuche fehl, die Nitrogruppe, unter Erhalt der entsprechenden 2-Aminodiole, zu reduzieren und unterstrich nochmals die Notwendigkeit Schutzgruppen einzuführen. Die *tert*-Butyldimethylsilylgruppe erwies sich hierbei als geeignet. Zwar gelang ebenfalls die einfache Einführung der Trimethylsilylschutzgruppe, so war diese jedoch unter den Bedingungen der Nitrogruppenreduktion nicht stabil. Verbindung **4a** konnte mit guten Ausbeuten und sehr hoher Reinheit mit TBDMS geschützt werden und man erhielt **7** ausschließlich als (*R,R*)- und (*S,S*)-Isomer. Wendete man die gleichen Bedingungen auf **4b** an, so wurde lediglich das mono-TBDMS-substituierte Produkt **8** erhalten. Kombinierte NMR- und Einkristallstrukturanalysen zeigten jedoch, dass auch diese Reaktion mit hoher Stereoselektivität unter Bildung der *6S7S8R*- und *6R7R8S*-Isomere verläuft. Weiterhin wurde TBDMS-geschütztes **3b** gefunden, was Retro-HENRYreaktionen unter den gewählten Bedingungen beweist. Diese Verbindung **9** wurde außerdem durch die Umsetzung von **3b** mit TBDMSCl dargestellt. Dabei verändert sich auch hier das *erythro:threo* Verhältnis im Vergleich mit **3b**. Dies zeigt ebenfalls Gleichgewichte an, wie sie für HENRYreaktionen beschrieben sind. Interessanterweise zeigten die mono- und diTBDMS-geschützten 2-Nitrodiole unterschiedliche Löslichkeiten. Während das zweifach geschützte Produkt **7** sich in fast allen Lösemitteln außer Wasser und DMSO löst, kann die monosubstituierte Verbindung **9** in Pentan gefällt werden. Ein Schlüsselschritt in dieser Arbeit war die Reduktion der Nitrogruppe zur synthetisch wertvollen Aminofunktion, kann diese doch als Ausgangspunkt für weitere Substitutionen dienen. Weiterhin sind das Hydroxylamin und Oxim durch Reduktion erhältlich. Die Reduktion von **7** mittels Natriumborhydrid zu **10**, wurde Nickelborid katalysiert mit ho-

hen Ausbeuten und unter milden Bedingungen erreicht. Gemäß den Ergebnissen der NMR-Untersuchungen wurde die relative Konfiguration nicht verändert. Verbindung **10** könnte als Ersatz für 1-(Pyridin-2-yl)-N-(pyridin-2-ylmethyl)methanamin **o** dienen. Reduktion von **7** mit teilweise hydrolysiertem Natriumborhydrid führte ausschließlich zur Bildung des Hydroxylamins **11**, welches durch Luftsauerstoff teilweise zum Oxim **12** oxidiert wurde. Jedoch wurden bei Versuchen, das Hydroxylamin durch Reduktion mit Natriumcyanoborhydrid oder Natriumtriacetoxyborhydrid zu erhalten, lediglich Mischungen aus Hydroxylamin **11** und Amin **10** nachgewiesen. Nichtsdestoweniger ist die Bildung des Oxims **12** sehr erwünscht, da durch dessen Hydrolyse auch das entsprechende Keton zugänglich wäre. Zusätzlich könnten beide Verbindungen **11** und **12** auch als Liganden dienen, so dass die Entwicklung selektiver Reduktionsschritte eine zukünftige Aufgabe bleibt. Um die Flexibilität der Ligandendarstellung zu testen, wurde die Aminogruppe in **10** mit Salicylaldehyd umgesetzt. Diese Gruppierung ist ein verbreitetes Strukturmotiv für die Komplexierung von Vanadiumkationen und wird seit langem auch von der Gruppe um PLASS zur Darstellung von Haloperoxidase-modellverbindungen eingesetzt. Die durch Umsetzung mit Salicylaldehyd erhaltene Verbindung **13** wurde nahezu quantitativ und mit hoher Reinheit erhalten. Ihre UV-Vis-Absorptions- und Emissionseigenschaften wurden untersucht, sowie die ihres deprotonierten Derivats. Die Reaktion des Proliganden **13** mit Vanadylacetylacetonat führte, nach Oxidation mit Luftsauerstoff, zum Vanadium(v)-komplex **14**. Interessanterweise wird im Zuge der Komplexbildung eine TBDMSgruppe abgespalten und das erhaltene Alkoholat diente als Donoratom. Dieser Umstand ist auch für mögliche weitere Komplexbildungen mit anderen Metallen wichtig, da auf diese Weise ein Entschützungs-schritt übersprungen werden kann. In Zusammenarbeit mit ROBERT DEBEL aus der Arbeitsgruppe um PLASS wurden der Komplex **14**, sowie **13** mit Vanadylacetylacetonat oder Molybdänylacetylacetonat auf ihre Eignung als Katalysatorsystem in der Sulfoxidation mit Wasserstoffperoxid getestet. Alle Katalysatorsysteme führten zu nahezu quantitativem Umsatz von (Methylsulfanyl)benzen **I**, zeigten jedoch deutliche Unterschiede in ihrer Aktivität. Da die Darstellung der Verbindung **13** und **14** hoch stereoselektiv zum jeweiligen Enantiomerenpaar verlief, ist deren Trennung und der Einsatz in einer enantiolektiven Sulfoxidation vorstellbar. Der Vanadiumkomplex **14** ist auch noch aus einem anderen Gesichtspunkt interessant. So besitzt er eine unkoordinierte Pyridylgruppe mit einem Abstand von 450 pm zum Metallzentrum. Der Stickstoff kann nun als Protonenrelais oder Vermittler von Wasserstoffbrückenbindungen dienen, Wechselwirkungen also, die auch in Enzymen eine wichtige Rolle spielen.<sup>166</sup> Die verbliebene TBDMSgruppe ihrerseits, vermittelt die Löslichkeit des Komplexes, insbesondere auch in unpolaren Solventien.

Der zweite Teil der vorliegenden Arbeit beschäftigte sich mit der Darstellung, Charakterisierung und den Reaktionen der carbonylanalogen SCHIFFbasen **15a-d**. Diese waren als Bausteine für die Aza-HENRYreaktion gedacht und führten zum Teil zu überraschenden neuen Verbindungen. Die Untersuchung ihres Koordinationsverhaltens gegenüber Zinkchlorid deckte interessante Unterschiede in Abhängigkeit vom N-gebundenen Substituenten auf. So findet man zwar in den meisten Fällen tetraedrisch koordinierte Zinkzentren, im Falle der N-methyl Verbindung **15a** kokristallisieren ein tetraedrischer und ein quadratisch-pyramidaler Komplex **16a**. Die N-benzyl Verbindung **15c**, führte gar zur Bildung eines oktaedrischen Komplexes **16c** mit Tetrachlorozinkat als Gegenion. Die Aza-HENRYreaktion der N-methyl substituierten SCHIFF-base **15a** ergab das  $\beta$ -Nitroamin **17**. In einer Lösung von **17** konnten überdies Radikalspezies mittels EPR-Spektroskopie nachgewiesen werden. Die Reaktion mit Wasserstoff in methanolischer Lösung und Pd/C im Autoklaven, führte zur C-C Kopplung und Bildung des Dinitrobutans **18**, jedoch mit schlechten Ausbeuten. Das entsprechende Diamin **19** wurde durch Reduktion mit Hydrazinhydrat erhalten. Dessen Umsetzung mit Zinkchlorid führte zum zweikernigen Zinkkomplex **20**. Diese Arbeiten wurden in Kooperation mit TOBIAS KLOUBERT durchgeführt. Eine sehr interessante Reaktion wurde beim Umsatz der N-benzyl substituierten SCHIFF-Base **15c** mit Butyllithium entdeckt. Das gebildete 2-Azaallylanion geht in Gegenwart eines Zinkchloridüberschusses eine Dimerisierung ein. Das erhaltene Produkt **21** ist der dinukleare Zinkchloridkomplex eines tetraaryl-substituierten Piperazinderivates mit unerwarteter Stereoselektivität. Die Ladungsverteilung innerhalb des 2-Azaallylanions wurde mittels NMR-Spektroskopie untersucht und ergab erste Hinweise auf einen möglichen Mechanismus. Einige unerwartete Reaktionen wurden bei Umsetzungen mit dem Imin **15a** beobachtet. Wie bereits erwähnt führt dessen Nitroaldolreaktion mit Nitromethan zum entsprechenden  $\beta$ -Nitroamin **17**, welches in Methanol zum Dinitrobutan **18** gekoppelt wurde. Verwendete man in einer ähnlichen Reaktion von **17** mit Wasserstoff, Pd/C und verdünnter Essigsäure als Lösungsmittel, so wurde N-Methyl-1-(pyridin-2-yl)ethenamin **23** erhalten. Reproduktion einer literaturbekannten C-C Kopplung von **15a** in Acetonitril führte nicht zum Kopplungsprodukt, sondern zur Addition von Acetonitril und Erhalt von 3-(Methylamino)-3-(pyridin-2-yl)propionitril **24**. Die Reaktion von Imin **15a** mit 2-(Nitromethyl)pyridin **26** and Syntal 696<sup>®</sup> wiederum, ergab das 1-Nitro-2,3-di-2-pyridyl-2,3-dihydroindolizin **27** als kristallines Nebenprodukt.

## 5 Experimental

**General remarks** All manipulations were carried out in an argon atmosphere using standard Schlenk techniques. The solvents were dried according to common procedures and distilled under argon. The  $^1\text{H}$  and  $^{13}\text{C}^1\text{H}$  NMR spectra were obtained on a Bruker AC 200 MHz and AC 400 MHz spectrometer. Assignment of NMR data was made on the basis of  $^1\text{H}$ ,  $^{13}\text{C}^1\text{H}$ , DEPT135, HSQC, HMBC, H,H COSY, NOESY and selective NOE experiments. Mass spectra were obtained on a Finnigan MAT SSQ 710 and Finnigan MAZ95XL system. Peaks in the mass spectra were assigned by comparison of the observed isotopic patterns with the calculated ones. IR measurements were carried out using a Perkin-Elmer System 2000 FTIR. The IR spectra were taken as Nujol mulls between KBr windows, as KBr pellets or neat between KBr windows. Melting and decomposition points were measured with a Reichert-Jung apparatus type 302102 and are uncorrected. Absorption spectra were recorded on Perkin-Elmer UV-Vis Lambda 16 spectrometer in a 10 mm quartz cuvette at room temperature. Fluorescence spectra were recorded on a Perkin-Elmer LS 50B in a 10 mm quartz cuvette at room temperature ( $25\pm 1$  °C). Fluorescence quantum yields were determined using quinine sulfate in 0.1 N  $\text{H}_2\text{SO}_4$  solution. Süd-Chemie AG (Munich, Germany) put the hydrotalcite Syntal 696<sup>®</sup> (aluminum magnesium hydroxy carbonate, 20.8%  $\text{Al}_2\text{O}_3$ , 33.8% MgO) to our disposal. The compounds **15a-15d** were prepared according to literature procedures.<sup>24, 167</sup>

### Nickel boride

Nickel boride was prepared according to the procedure published by SELTZMAN and BERRANG (ref.<sup>100</sup>). Nickel acetate tetrahydrate (6.00 g, 24.1 mmol) was solved in 75 ml of water in a 400 ml beaker (!) and cooled to 0 °C. Over a period of 30 minutes solid sodium borohydride (3.00 g, 72.3 mmol) was added under stirring, while the temperature was not allowed to exceed 10 °C. The mixture immediately turned black after addition of sodium borohydride under intense frothing. After addition of sodium borohydride the mixture was allowed to stir for one hour at 0 °C and then was collected on a G4 SCHLENK-frit. The black precipitate was washed three times with 10 ml of methanol each and kept under argon atmosphere. Solvent removal to dryness should be avoided due to the product's sensitivity towards oxidation. The exact composition is unknown but the product can be approximated  $\text{Ni}_2\text{B}$ .<sup>168</sup>

### Protocol for the catalytic sulfoxidation

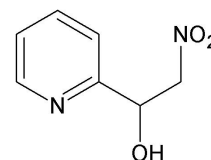
Hydrogen peroxide (6.25 mmol, 0.594 ml of 30 % aqueous solution), trimethoxybenzene (841 mg, 5.00 mmol) and the catalyst (0.05 mmol) were solved in a freshly prepared solution of 50 ml of methylene chloride/methanol (v/v 7:3) and stirred for 30 minutes at room temperature. Subsequently, the mixture was cooled to 10 °C and this temperature was maintained by a cryostat. Time measurement was started immediately after addition of (methylsulfanyl)benzene

**I** (621 mg, 5.00 mmol). For reaction monitoring 2 ml aliquots were taken from the reaction mixture and immediately quenched with 5 ml of a 0.1 M aqueous  $\text{Na}_2\text{SO}_3$ . The organic compounds were extracted four times with 2 ml of methylene chloride each and the solvent was carefully removed in vacuo. Subsequently, NMR spectra were taken in  $\text{CDCl}_3$ . For the quantitative analysis of the obtained proton NMR spectra the aromatic signal of the tmb were set to  $\delta = 6.100$ . As a reference for calculating the molar amounts of the reaction products, the aromatic signals of tmb were integrated between 6.250-5.950 ppm. The obtained peak area was set to 3.00 as an equivalent for three protons. Integration of the aliphatic protons of (methylsulfinyl)benzene **II** was made between 2.400-2.570 ppm (three protons), while the aromatic protons were integrated between 7.000-7.400 ppm (five protons). The aliphatic signals of (methylsulfonyl)benzene **III** were integrated between 2.645-2.815 ppm.

### 2-Nitro-1-(pyridin-2-yl)ethanol (**3a**)

Procedure A: Syntal 696<sup>®</sup> was dried for one hour at 80 °C and 1 mbar.

Pyridine-2-carbaldehyde **1** (8.61 g, 0.08 mol) was solved in nitromethane **2a** (97.66 g, 1.6 mol) and 1.00 of g Syntal 696<sup>®</sup> was added and the mixture was stirred for five hours at room temperature. Subsequently,



the catalyst was removed by filtration and the filtrate was concentrated

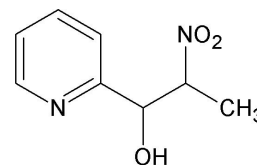
to 15 ml on a rotatory evaporator and then left for crystallization at 5 °C over night. The crystalline product was separated from the violet solution by filtration and washed twice with small amounts of cold diethyl ether. A second crop may be obtained by further reduction of the mother liquor's volume and cooling to -20 °C. The product was dried in vacuo ( $8 \cdot 10^{-3}$  mbar) at room temperature yielding 13.31 g of colorless **3a**.

Procedure B: 15 g of Amberlyst A21<sup>®</sup> was added to a solution of pyridine-2-carbaldehyde **1** (8.61 g, 0.08 mol) in nitromethane **2a** (97.66 g, 1.6 mol). The mixture was stirred for two hours at room temperature. Subsequently, the catalyst beads were removed by filtration and the filtrate was concentrated to 15 ml on a rotatory evaporator and then left for crystallization at 5 °C over night. The crystalline product was separated from the violet solution by filtration and washed twice with small amounts of cold diethyl ether. A second crop may be obtained by further reduction of the mother liquor's volume and cooling to -20 °C. The product was dried in vacuo ( $8 \cdot 10^{-3}$  mbar) at room temperature yielding 12.86 g of colorless **3a**.

Product **3a** was stored in an argon atmosphere at -20 °C. The excess of nitromethane **2a** could be reobtained by distillation and was used for further reactions. Yield: 99 %. m.p.: 70°C. <sup>1</sup>H NMR ( $\text{CDCl}_3$ ):  $\delta = 8.53$  (d,  $J = 4.4$  Hz, 1H, Pyr1), 7.72-7.77 (m, 1H, Pyr3), 7.44 (d,  $J = 7.6$  Hz, 1H, Pyr4), 7.28-7.24 (m, 1H, Pyr2), 5.45 (dd,  $J = 3.6$  Hz,  $J = 8.4$  Hz, 1H, H6), 4.76 (dd,  $J = 13.2$  Hz,  $J = 4.0$  Hz, 1H, H7a), 4.62 (dd,  $J = 13.2$  Hz,  $J = 8.4$  Hz, 1H, H7b), 4.3 (s, br, OH). <sup>13</sup>C NMR ( $\text{CDCl}_3$ ):  $\delta = 148.9$  (t, Pyr1), 137.4 (t, Pyr3), 120.9 (t, Pyr4), 123.6 (t, Pyr2), 156.6 (q, Pyr5), 70.4 (t, C6), 80.7 (s, C7). IR (KBr,  $\text{cm}^{-1}$ ):  $\tilde{\nu} = 3078$  st (OH), 2842 st, 2736 st, 1600 st (C=N), 1576 st (C=C), 1542 st (N-O), 1478 st, 1440 st, 1415 st, 1378 st, 1333 st, 1291 m, 1263 w, 1224 m, 1200 st, 1154 m, 1113 st, 1079 st, 1039

st, 1009 st, 970 w, 962 m, 906 m, 859 w, 785 st, 756 st, 725 m, 643 st, 614 st, 523 st, 464 w. MS (EI):  $m/z$  (%) = 169 (42)  $[M+1]^+$ , 121 (92)  $[M-NO_2]^+$ , 108 (100), 93 (99), 78 (98), 65 (26), 51 (57), 39 (28), 27 (25).  $C_7H_8N_2O_3$  (168.15): calc. C 50.00, H 4.80, N 16.66; found C 50.04, H 4.72, N 16.69.

**2-Nitro-1-(pyridin-2-yl)propan-1-ol (3b)** Pyridine-2-carbaldehyde **1** (11.78 g, 0.11 mol) was solved in nitroethane **2b** (8.26 g, 0.11 mol) and 18 g of AmberlystA21<sup>®</sup> were added. The temperature of the mixture rose to 63 °C within five minutes, while the catalyst's surface colored reddish. After vigorous stirring for one hour the mixture became solid and was suspended in 10 ml of methylene

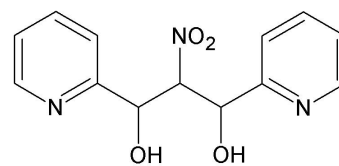


chloride. This suspension was stirred over night at room temperature. Subsequently, all solid products were solved in methylene chloride and separated from the catalyst by filtration. The filtrate was reduced on a rotatory evaporator to a fourth of its original volume and left at -20 °C for precipitation. The obtained solid was washed twice with small amounts of methylene chloride and dried in vacuo ( $8 \cdot 10^{-3}$  mbar) at room temperature yielding 30.00 g of the white to greenish product **3b**. Product **3b** was stored in an argon atmosphere at -20 °C. Crystals suitable for single crystal X-ray diffraction were obtained by slow solvent evaporation of a chloroformic solution of **3b** as hydrochloride **3bHCl**. Yield: 79%. m.p.: 61 °C. *threo*-2-nitro-1-(pyridin-2-yl)propan-1-ol  $^1H$  NMR ( $CDCl_3$ ):  $\delta$  = 8.56-8.54 (m, 1H, Pyr1), 7.77-7.72 (m, 1H, Pyr3), 7.34 (d,  $J$  = 7.6 Hz, 1H, Pyr4), 7.31-7.26 (m, 1H, Pyr2), 5.06 (d,  $J$  = 7.2 Hz, 1H, H6), 4.90 (quint,  $J$  = 6.8 Hz, 1H, H7), 1.42 (d,  $J$  = 6.8 Hz, 3H,  $CH_3$ ), 4.59 (s, br, OH).  $^{13}C$  NMR ( $CDCl_3$ ):  $\delta$  = 148.7 (t, Pyr1), 137.5 (t, Pyr3), 122.2 (t, Pyr4), 123.8 (t, Pyr2), 156.5 (q, Pyr5), 74.6 (t, C6), 87.4 (t, C7), 15.4 (p,  $CH_3$ ).

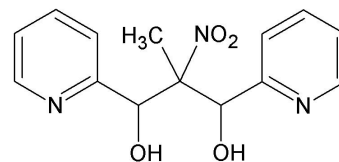
*erythro*-2-nitro-1-(pyridin-2-yl)propan-1-ol  $^1H$  NMR ( $CDCl_3$ ):  $\delta$  = 8.56-8.54 (m, 1H, Pyr1), 7.77-7.72 (m, 1H, Pyr3), 7.38 (d,  $J$  = 8.0 Hz, 1H, Pyr4), 7.31-7.26 (m, 1H, Pyr2), 5.39 (d,  $J$  = 4.0 Hz, 1H, H6), 4.86-4.81 (m, 1H, H7), 1.40 (d,  $J$  = 6.4 Hz, 3H,  $CH_3$ ), 4.59 (s, br, OH).  $^{13}C$  NMR ( $CDCl_3$ ):  $\delta$  = 148.5 (t, Pyr1), 137.4 (t, Pyr3), 121.1 (t, Pyr4), 123.5 (t, Pyr2), 156.4 (q, Pyr5), 73.3 (t, C6), 86.6 (t, C7), 12.2 (p,  $CH_3$ ). IR (KBr,  $cm^{-1}$ ):  $\tilde{\nu}$  = 3108 st (OH), 2946 m, 2909 m, 2842 m, 1598 st (C=N), 1573 m (C=C), 1552 st (N-O), 1547 st (N-O), 1440 st, 1388 st, 1368 st, 1332 m, 1310 m, 1286 m, 1268 m, 1250 m, 1213 m, 1150 m, 1136 m, 1117 w, 1086 w, 1075 m, 1054 m, 1007 st, 997 st, 910 w, 902 w, 892 w, 873 w, 863 w, 794 m, 771 st, 756 m, 704 w, 670 w, 656 w, 632 m, 625 m, 552 w, 537 w, 509 w. MS (EI):  $m/z$  (%) = 183 (36)  $[M+1]^+$ , 136 (100)  $[M-NO_2]^+$ , 118 (89), 108 (82), 78 (45), 52 (26), 39 (8), 27 (12).  $C_8H_{10}N_2O_3$  (182.18): calc. C 52.74, H 5.53, N 15.38; found C 52.64, H 5.65, N 15.24.

***rac*-2-Nitro-1,3-di(pyridin-2-yl)propane-1,3-diol (4a)**

Nitroalcohol **3a** (13.00 g, 0.08 mol) was solved in pyridine-2-carbaldehyde **1** (8.61 g, 0.08 mol) and 13.40 g of Amberlyst A21<sup>®</sup> were added, while the internal temperature markedly increased. After stirring for one hour, 20 ml of methylene chloride were added and the obtained suspension was stirred over night at room temperature. Subsequently, the solids were removed by filtration and carefully dried without vacuo. Separation of the catalyst beads from product **4a** was achieved with a 0.25 mm mesh size sieve. The obtained white powder was washed twice with small amounts of methylene chloride and dried in vacuo ( $8 \cdot 10^{-3}$  mbar) at room temperature yielding 15.86 g of **4a**. Product **4a** was stored in an argon atmosphere at -20 °C. Crystals suitable for single crystals X-ray analysis were obtained by slow solvent evaporation of diethyl ether or thf solutions. Separation of small amounts of **4a** from the catalyst was achieved by transferring the suspension to a porous frit via PASTEUR pipette. Yield: 72 %; m.p. 118 °C (dec.). <sup>1</sup>H NMR (CD<sub>3</sub>OD):  $\delta$  = 8.41 (d, J = 4.8 Hz, 1H, Pyr1), 8.35 (d, J = 4.8 Hz, 1H, Pyr13), 7.70 (ddd, J = 1.6 Hz, J = 7.6 Hz, 1H Pyr11), 7.64 (ddd, J = 1.6 Hz, J = 8.0 Hz, 1H, Pyr3), 7.49 (d, J = 7.6 Hz, 1H, Pyr10), 7.34 (d, J = 8.0 Hz, 1H, Pyr4), 7.19 (m, 1H, Pyr2), 7.19 (m, 1H, Pyr12), 5.61 (t, J = 6.0 Hz, 1H, H7), 5.52 (d, J = 6.0 Hz, 1H, H8), 5.33 (d, J = 5.6 Hz, 1H, H6), 6.07 (s, br, OH), 5.91 (s, br, OH). <sup>13</sup>C NMR (CD<sub>3</sub>OD):  $\delta$  = 149.8 (t, Pyr1), 149.6 (t, Pyr13), 138.3(t, Pyr11), 138.2(t, Pyr3), 123.4 (t, Pyr10), 123.2 (t, Pyr4), 124.3 (t, Pyr2), 124.1 (t, Pyr12), 160.3 (q, Pyr5), 160.2 (q, Pyr9), 95.5 (t, C7), 72.5 (t, C8), 73.3 (t, C6). IR (KBr, cm<sup>-1</sup>):  $\tilde{\nu}$  = 3114 st br (OH), 2846 st (CH), 1597 st, 1574 st, 1541 st (N-O), 1476 st, 1440 st, 1367 st, 1309 m, 1277 m, 1261 m, 1216 m, 1155 m, 1008 st, 975 w, 903 w, 845 m, 812 m, 787 st, 765 st, 694 m, 622 st, 593 m, 566 st, 532 m, 482 w. MS (DEI):  $m/z$  (%) = 275 (76) [M]<sup>-</sup>, 229 (16) [M-NO<sub>2</sub>]<sup>+</sup>, C=N (211) [57]<sup>+</sup>, 149 (13), 134 (15), 122 (33), 108 (42), 106 (28), 93 (20), 78 (100), 65 (7), 50 (67). C<sub>13</sub>H<sub>13</sub>N<sub>3</sub>O<sub>4</sub> (275.26): calc. C 56.72, H 4.76, N 15.15; found C 56.50, H 4.75, N 15.27.

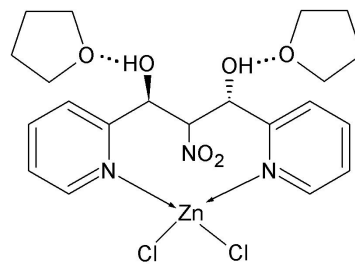
***rac*-2-Methyl-2-nitro-1,3-di(pyridin-2-yl)propane-1,3-diol (4b)**

Nitroalcohol **3b** (12.00 g, 0.07 mol) was solved in pyridine-2-carbaldehyde **1** (7.10 g, 0.07 mol) and 9.50 g of Amberlyst A21<sup>®</sup> were added, while the internal temperature markedly increased. Stirring over night afforded a white solid, which was suspended in diethyl ether and stirred for additional three hours at room temperature. Subsequently, the solids were removed by filtration and carefully dried without vacuo. The ethereal filtrate was reduced to half of its original volume and left at -20 °C, while further product precipitated. Separation of the catalyst beads was achieved with a 0.25 mm mesh size sieve. The combined products were washed twice with small amounts of diethyl ether and dried in vacuo ( $8 \cdot 10^{-3}$  mbar) at room temperature yielding 9.92 g of product **4b**. Product **4b** was stored in an argon atmosphere at -20 °C. Crystals suitable for single crystal X-ray diffraction were obtained by slow solvent



evaporation of solution of **4b** in diethyl ether. Separation of small amounts of **4b** from the catalyst was achieved by transferring the suspension to a porous frit via PASTEUR pipette. Yield: 49 %; m.p. 112 °C. <sup>1</sup>H NMR (CD<sub>2</sub>Cl<sub>2</sub>): δ = 8.60-8.45 (m, 2H, Pyr1, Pyr13), 7.80-7.72 (m, 2H, Pyr3, Pyr11), 7.44 7.52 (d, J = 8.0 d, 7.6 Hz, 2H, Pyr2, Pyr10), 7.39-7.28 (m, 2H, Pyr2, Pyr12), 5.32 (s, 2H, H6, H8), 1.40 (s, 3H, CH<sub>3</sub>). <sup>13</sup>C NMR (CD<sub>2</sub>Cl<sub>2</sub>): δ = 148.7 and 148.2 (t, Pyr1 Pyr13), 137.5 and 137.4 (t, Pyr3, Pyr11), 123.9 and 123.7 (t, Pyr2, Pyr10), 122.7 and 122.4 (t, Pyr2, Pyr12), 98.2 (q, C7), 74.9 and 74.7 (t, C6, C8), 14.4 (p, CH<sub>3</sub>), 156.5 and 156.3 (q, Pyr5 Pyr9). IR (Nujol, cm<sup>-1</sup>):  $\tilde{\nu}$  = 3137 m, br (OH), 1597 m (C=N), 1547 w, 1539 st (N-O), 1344 m, 1315 m, 1250 w, 1232 w, 1151 w, 1116 m, 1065 st, 1002 m, 968 w, 953 w, 933 w, 857 w, 845 w, 759 m, 739 m, 724 m, 688 w, 650 w, 626 w, 607 w, 576 w, 565 w, 550 w, 538 w, 498 w. MS (FAB in nba): *m/z* (%) = 290 (80) [M+1]<sup>+</sup>, 243 (25) [M-NO<sub>2</sub>]<sup>+</sup>, 225 (18), 183 (84), 136 (96), 118 (55), 108 (80), 79 (100), 52 (48), 27 (10). C<sub>14</sub>H<sub>15</sub>N<sub>3</sub>O<sub>4</sub> (289.27): calc. C 58.06, H 5.23, N 14.53; found C 58.13, H 5.19, N 14.71.

[*rac*-2-Nitro-1,3-di(pyridin-2-yl)propane-1,3-diol di-chloro zinc]·2 thf (**5**) Compound **4a** (150 mg, 0.5 mmol) and anhydrous zinc chloride (126 mg, 0.9 mmol) were solved in 3 ml of anhydrous thf in an argon atmosphere. The yellowish solution was stirred over night at room temperature and then left for crystallization at -20°C for several weeks. The formed crystals were separated by filtration and carefully washed with cold anhydrous thf, yielding 91 mg of complex

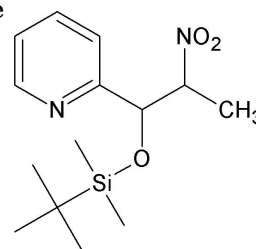


**5**. The complex was stable for several days under atmospheric conditions. Yield: 30 %. 95 °C (loss of THF), 112 °C (dec.). <sup>1</sup>H NMR ([D<sub>8</sub>]thf): δ = 9.01 (d, J = 4.8 Hz, 1H, Pyr13), 8.96 (d, J = 4.8 Hz, 1H, Pyr1), 8.21 (t, J = 7.6 Hz, 1H, Pyr11), 8.07 (t, J = 7.6 Hz, 1H, Pyr3), 8.13 (d, J = 8.0 Hz, 1H, Pyr10), 7.70-7.67 (m, 1H, Pyr12), 7.66-7.63 (m, 1H, Pyr2), 7.76 (d, J = 8.0 Hz, 1H, Pyr4), 5.16 (s, 1H, H6), 5.09 (dd, J = 10.0 Hz, J = 1.6 Hz, 1H, H7), 5.49 (dd, J = 9.6 Hz, J = 2.4 Hz, 1H, H8), 5.92 (s, br, HO-C6), 6.34 (s, br, HO-C8), 3.60 (m, 4H, thf), 1.77 (m, 4H, thf). <sup>13</sup>C NMR ([D<sub>8</sub>]thf): δ = 148.7 (t, Pyr13), 148.6 (t, Pyr1), 140.7 (t, Pyr11), 139.9 (t, Pyr3), 123.6 (t, Pyr10), 124.7 (t, Pyr12), 124.5 (t, Pyr2), 123.5 (t, Pyr4), 160.7 (q, Pyr9), 159.6 (q, Pyr5), 69.7 (t, C6), 97.6 (t, C7), 69.6 (t, C8), 67.0 (s, thf), 25.2 (s, thf). IR (KBr, cm<sup>-1</sup>):  $\tilde{\nu}$  = 3210 m, br (OH), 3055 m, 1606 st (C=N), 1573 m (C=C), 1556 st (N-O), 1482 m, 1327 m, 1275 w, 1226 w, 1126 w, 1131 w, 1107 w, 1085 m, 1025 st, 919 w, 881 m, 846 m, 787 m, 771 st, 758 m, 741 m, 722 w, 701 w, 677 w, 645 m, 613 m, 574 w, 562 m, 519 w, 495 w. MS (FAB in nba): *m/z* (%) = 374 (26) [M-Cl]<sup>+</sup>, 338 (16) [M-2Cl-H]<sup>+</sup>, 276 (100) [M-ZnCl<sub>2</sub>+H]<sup>+</sup>, 242 (11), 229 (18), 211 (50). C<sub>21</sub>H<sub>29</sub>Cl<sub>2</sub>N<sub>3</sub>O<sub>6</sub> (555.79): calc. C 45.57, H 5.26, N 7.56; found C 45.38, H 5.10, N 7.65.



**2-nitro-1-(pyridin-2-yl)-1-(tert-butyltrimethylsilyloxy)propane**

(9) *Tert*-butyl-dimethylsilylchloride (5.99 g, 40 mmol) was suspended in 8 ml of dmf and cooled in an ice bath. Subsequently, solid imidazole (4.85 g, 71 mmol) was carefully added and the mixture was stirred for 15 minutes. A freshly prepared solution of nitroalcohol



**3b** in 10 ml of dmf was added and the greenish solution was stirred

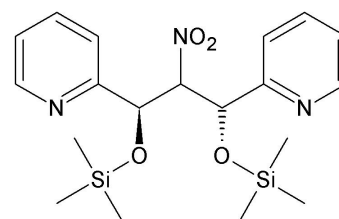
for 20 hours at room temperature, while the color slowly turned to yellow. Subsequently, dmf was removed in vacuo (40 °C,  $8 \cdot 10^{-3}$  mbar). The obtained hygroscopic precipitate was stirred in 50 ml water for two hours, while an oil segregated from the aqueous solution. The oil was extracted three times with 10 ml of diethyl ether each and the phases were separated. Drying of the organic phase over sodium sulfate and removal of the solvent in vacuo afforded product **9** as a yellowish oil with high purity. Yield: 59 %.

*threo*-2-nitro-1-(pyridin-2-yl)-1-(*tert*-butyltrimethylsilyloxy)propane  $^1\text{H}$  NMR ( $\text{CDCl}_3$ ):  $\delta$  = 8.52 (m, 1H, Pyr1), 7.73-7.768 (m, 1H, Pyr3), 7.19-7.16 (m, 1H, Pyr2), 7.46 (d,  $J$  = 8.0 Hz, 1H, Pyr4), 4.96-4.94 (m, 1H, H7), 5.54 (d,  $J$  = 2.8 Hz, 1H, H6), 1.24 (d,  $J$  = 6.8 Hz, 3H,  $\text{CH}_3$ ), 0.77 (s, 9H, *tert*-butyl), -0.02 (s, 3H,  $\text{SiCH}_3$ ), -0.26 (s, 3H,  $\text{SiCH}_3$ ).  $^{13}\text{C}$  NMR ( $\text{CDCl}_3$ ):  $\delta$  = 159.5 (q, Pyr5), 149.0 (t, Pyr1), 136.7 (t, Pyr3), 122.8 (t, Pyr2), 120.7 (t, Pyr4), 86.4 (t, C7), 76.5 (t, C6), 15.7 (p,  $\text{CH}_3$ ), 18.0 (q, *tert*-butyl), 25.7 (p, *tert*-butyl), -5.7 (p,  $\text{SiCH}_3$ ), -4.9 (p,  $\text{SiCH}_3$ ).

*erythro*-2-nitro-1-(pyridin-2-yl)-1-(*tert*-butyltrimethylsilyloxy)propane  $^1\text{H}$  NMR ( $\text{CDCl}_3$ ):  $\delta$  = 8.52 (m, 1H, Pyr1), 7.73-7.768 (m, 1H, Pyr3), 7.24-7.21 (m, 1H, Pyr2), 7.42 (d,  $J$  = 7.6 Hz, 1H, Pyr4), 4.84-4.76 (m, 1H, H7), 5.07 (d,  $J$  = 8.0 Hz, 1H, H6), 1.28 (d,  $J$  = 6.8 Hz, 3H,  $\text{CH}_3$ ), 0.88 (s, 9H, *tert*-butyl), -0.01 (s, 3H,  $\text{SiCH}_3$ ), -0.13 (s, 3H,  $\text{SiCH}_3$ ).  $^{13}\text{C}$  NMR ( $\text{CDCl}_3$ ):  $\delta$  = 158.9 (q, Pyr5), 148.9 (t, Pyr1), 137.0 (t, Pyr3), 123.4 (t, Pyr2), 121.8 (t, Pyr4), 88.5 (t, C7), 78.0 (t, C6), 10.5 (p,  $\text{CH}_3$ ), 17.9 (q, *tert*-butyl), 25.4 (p, *tert*-butyl), -5.7 (p,  $\text{SiCH}_3$ ), -4.9 (p,  $\text{SiCH}_3$ ). IR (neat,  $\text{cm}^{-1}$ ):  $\tilde{\nu}$  = 3057 w, 2956 st, 2931 st, 2895 m, 2859 st, 1681 w, 1590 st (C=N), 1554 st (N-O), 1472 st, 1437 st, 1390 st, 1362 st, 1330 w, 1293 w, 1255 st, 1214 w, 1186 w, 1150 st, 1102 st, 1086 st, 1063 st, 1043 m, 1025 st, 1006 m, 995 m, 939 w, 925 w, 901 w, 870 st, 838 st, 817 m, 838 st, 780 st, 751 st, 671 m, 629 m, 606 m, 576 w, 553 w, 504 w. MS (DEI):  $m/z(\%)$  = 297 (14)  $[\text{M}+1]^+$ , 281 (4)  $[\text{M}-\text{CH}_3]^+$ , 250 (12)  $[\text{M}-\text{NO}_2]^+$ , 239 (100)  $[\text{M}-\text{tert-butyl}]^+$ , 222 (40), 208 (19), 192 (34), 182 (72), 178 (50), 165 (13), 132 (23), 118 (21), 104 (15), 75 (29), 57 (9).  $\text{C}_{14}\text{H}_{24}\text{N}_2\text{O}_3\text{Si}$  (296.44): calc. C 56.72, H 8.16, N 9.45; found C 56.39, H 8.16, N 9.69.

***rac*-2-Nitro-1,3-di(pyridin-2-yl)-1,3-di(trimethylsilyloxy)propane (6)**

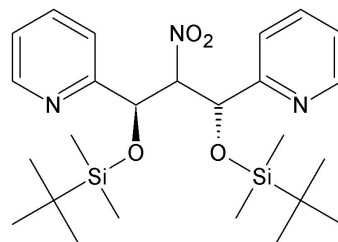
Compound **4a** (3.00 g, 11 mmol) was suspended in 50 ml of anhydrous methylene chloride under argon atmosphere. The mixture was cooled to 0 °C and trimethylsilyl imidazole (3.06 g, 22 mmol) was added via syringe. Within one minute a clear yellow solution was obtained, which was stirred for 1 hour at 0 °C. Subsequently,



the solution was extracted five times with 20 ml of saturated aqueous  $\text{NH}_4\text{Cl}$  each until the pH of the aqueous phase was 6-7. After separation of the organic phase and drying over sodium sulfate, the solvent was removed in vacuo, yielding 3.55 g of a yellowish oil. The oily product **6** was used without further purification. Yield: 77 %.  $^1\text{H}$  NMR ( $\text{CD}_2\text{Cl}_2$ ):  $\delta = 8.39\text{-}8.38$  (m, 1H, Pyr13), 8.47-8.46 (m, 1H, Pyr1), 7.57 (ddd,  $J = 7.6$  3.2 Hz, 1H, Pyr11), 7.45 (ddd,  $J = 8.0$ ,  $J = 2.0$  Hz, 1H, Pyr3), 7.30 (d,  $J = 7.6$  Hz, 1H, Pyr10), 7.12-7.06 (m, 1H, Pyr12), 7.12-7.06 (m, 1H, Pyr2), 7.03 (d,  $J = 7.6$  Hz, 1H, Pyr4), 5.64 (dd,  $J = 8.0$ ,  $J = 4.4$  Hz, 1H, H7), 5.54 (d,  $J = 8.0$  Hz, 1H, H8), 5.16 (d,  $J = 4.4$  Hz, 1H, H6), 0.00 (s, 9H, TMS), -0.04 (s, 9H, TMS).  $^{13}\text{C}$  NMR ( $\text{CD}_2\text{Cl}_2$ ):  $\delta = 149.5$  (t, Pyr13), 149.0 (t, Pyr1), 136.6 (t, Pyr11), 136.5 (t, Pyr3), 123.6 (t, Pyr10), 123.4 (t, Pyr12), 122.9 (t, Pyr2), 121.0 (t, Pyr4), 96.6 (t, C7), 73.6 (t, C8), 73.8 (t, C6), -0.57 (p, TMS), 159.0 (q, Pyr5), 158.8 (q, Pyr9). IR (neat,  $\text{cm}^{-1}$ ):  $\tilde{\nu} = 3058$  m, 3013 m, 2958 st, 2901 m, 1591 st (C=N), 1573 st (C-C), 1557 st (N-O), 1471 st, 1437 st, 1410 m, 1377 st, 1289 m, 1254 st, 1130 st, 1112 st, 1082 st, 1046 st, 996 st, 971 m, 939 m, 853 st, 751 st, 690 m, 655 w, 606 m, 543 st. MS (DEI):  $m/z(\%) = 420$  (6)  $[\text{M}+1]^+$ , 373 (33)  $[\text{M}-\text{NO}_2]^+$ , 283 (81), 180 (85), 73 (100).

***rac*-2-Nitro-1,3-di(pyridin-2-yl)-1,3-di(*tert*-butyldimethylsilyloxy)propane (**7**)**

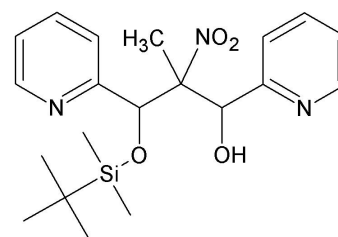
*Tert*-butyl-dimethylsilylchloride (24.40 g, 0.16 mol) was suspended in 28 ml of dmf and cooled in an ice bath. Subsequently, solid imidazole (20.00 g, 0.29 mol) was carefully added and the mixture was stirred for 15 minutes. To the mixture, a suspension of compound **4a** (15.50 g, 0.056 mol) in 30 ml of dmf was added. The brownish solution was stirred for 28 hours at room temperature, while a white solid precipitated. The precipitate was separated by filtration and then stirred for two hours in 80 ml of water yielding a fluffy white solid, which again was filtered off. The dmf filtrate was concentrated at 40 °C and  $1 \cdot 10^{-2}$  mbar until a solid precipitated (one third of the original volume). This suspension was stirred for two hours in 100 ml of water and the obtained fluffy precipitate was collected by filtration. The combined solid products were thoroughly washed with water and dried in vacuo, yielding 23.10 g of the colorless crystalline product **7**. Product **7** was pure and stored under atmospheric conditions at room temperature. Crystals suitable for single crystal X-ray diffraction were obtained by slow solvent evaporation of a methanolic solution. Yield: 82 %. m.p.: 84 °C.  $^1\text{H}$  NMR ( $\text{CDCl}_3$ ):  $\delta = 8.42$  (d,  $J = 4.4$  Hz, 1H, Pyr13), 8.50 (d,  $J = 4.4$  Hz, 1H, Pyr1), 7.54 (t,  $J = 7.6$  Hz, 1H, Pyr11), 7.38 (t,  $J = 7.6$  Hz, 1H, Pyr3), 7.30 (d,  $J = 8.0$  Hz, 1H, Pyr10), 7.12-7.09 (m, 1H, Pyr12), 7.06-7.03 (m, 1H, Pyr2), 6.95 (d,  $J = 8.0$  Hz, 1H, Pyr4), 5.10 (d,  $J = 2.2$  Hz, 1H, H6), 5.67 (dd,  $J = 9.6$  Hz,  $J = 2.0$  Hz, 1H, H7), 5.55 (d,  $J = 9.6$  Hz, H1, H8), 0.92 (s, 9H, *tert*-butyl a), 0.67 (s, 9H, *tert*-butyl b), -0.00 (s, 3H,  $\text{CH}_3$  a), -0.05 (s, 3H,  $\text{CH}_3$  b), -0.23 (s, 3H,  $\text{CH}_3$  b), -0.35 (s, 3H,  $\text{CH}_3$  a).  $^{13}\text{C}$  NMR ( $\text{CDCl}_3$ ):  $\delta = 148.8$  (t, Pyr13), 148.0 (t, Pyr1), 136.6 (t, Pyr11), 136.4 (t, Pyr3), 124.1 (t, Pyr10), 123.3 (t, Pyr12), 122.3 (t, Pyr2), 120.9 (t, Pyr4), 157.6 (q, Pyr9), 158.6 (q, Pyr5), 74.0 (t, C6), 96.8 (t, C7), 73.2 (t, C8), 25.7



(p, *tert*-butyl a), 25.4 (p, *tert*-butyl b), 18.1 (q, *tert*-butyl a), 17.9 (q, *tert*-butyl a), -5.5 (p, CH<sub>3</sub> a), -5.6 (p, CH<sub>3</sub> b), -5.2 (p, CH<sub>3</sub> b), -5.0 (p, CH<sub>3</sub> a). IR (KBr, cm<sup>-1</sup>):  $\tilde{\nu}$  = 3053 w, 3007 w, 2957 st, 2929 st, 2886 m, 2856 st, 1590 st (C=N), 1573 m (C=C), 1554 st (N-O), 1472 st, 1435 m, 1397 m, 1360 m, 1338 m, 1317 m, 1291 w, 1261 st, 1225 w, 1214 w, 1186 w, 1136 st, 1096 st, 1083 st, 1046 m, 1006 m, 996 m, 972 st, 939 m, 900 m, 872 st, 838 st, 803 m, 779 st, 746 st, 711 w, 677 m, 645 w, 629 w, 617 w, 606 m, 569 w, 540 m, 500 w. MS (DEI):  $m/z$  (%) = 504 (9) [M]<sup>+</sup>, 457 (7) [M-NO<sub>2</sub>]<sup>+</sup>, 446 (46) [M-*tert*-butyl]<sup>+</sup>, 399 (33) [M-2*tert*-butyl]<sup>+</sup>, 339 (20), 325 (23), 222 (100), 194 (22), 182 (35), 178 (51), 165 (69), 73 (92), 57 (25), 41 (10). C<sub>25</sub>H<sub>41</sub>N<sub>3</sub>O<sub>4</sub>Si<sub>2</sub> (503.78): calc. C 59.60, H 8.20, N 8.34; found C 59.76, H 8.27, N 8.24.

**3-(*Tert*-butyldimethylsilyloxy)-2-methyl-2-nitro-1,3-di-**  
**(pyridin-2-yl)propan-1-ol (8)**

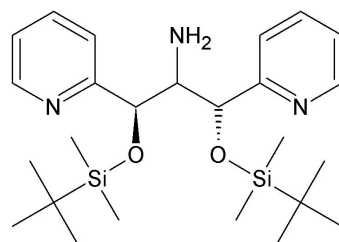
*Tert*-butyl-dimethylsilylchloride (755 mg, 5.0 mmol) was suspended in 0.8 ml of dmf and cooled in an ice bath. Subsequently, solid imidazole (588 mg, 8.7 mmol) was carefully added and the mixture was stirred for 15 minutes. To this mixture, a freshly prepared suspension of compound **4b** (500 mg, 1.7 mmol) in 1 ml of dmf was added. The brownish suspension was stirred



for 28 h at room temperature. Subsequently, the solvent was removed in vacuo at 40 °C and 1·10<sup>-2</sup> mbar. The obtained oily residue was stirred in 5 ml of water for two hours. The aqueous phase was removed with a pipette and the oily residue was stirred in 5 ml of pentane yielding a white precipitate. The precipitate was collected on a filter and dried in vacuo yielding 200 mg of product **8**. Product **8** is stable under atmospheric conditions at room temperature. Crystals suitable for single crystal X-ray diffraction were obtained by slow solvent evaporation of a solution of **8** in diethyl ether. Yield: 30 %. m.p.: 108 °C. <sup>1</sup>H NMR (CDCl<sub>3</sub>):  $\delta$  = 8.49-8.46 (m, 2H, Pyr1 Pyr13), 7.83 (t, J = 7.2 Hz, 1H, Pyr3), 7.70 (t, J = 7.2 Hz, 1H, Pyr11), 7.57 (d, J = 7.6 Hz, 1H, Pyr4), 7.34-7.32 (m, 1H, Pyr2), 7.19-7.17 (m, 1H, Pyr12), 7.46 (d, J = 8.4 Hz, 1H, Pyr10), 5.20 (s, 1H, H6), 5.12 (s, 1H, H8), 5.00 (s, broad, OH) 1.45 (s, 3H, CH<sub>3</sub>), 0.08 (s, 3H, SiCH<sub>3</sub>), -0.35 (s, 3H, SiCH<sub>3</sub>), 0.89 (s, 9H, *tert*-Bu). <sup>13</sup>C NMR (CDCl<sub>3</sub>):  $\delta$  = 159.2 (q, Pyr5), 157.6 (q, Pyr9), 146.8 (t, Pyr1), 148.0 (t, Pyr13), 137.5 (t, Pyr3), 137.5 (t, Pyr11), 124.0 (t, Pyr4), 123.7 (t, Pyr2), 122.8 (t, Pyr12), 121.8 (t, Pyr10), 97.3 (q, C7), 78.2 (t, C6), 74.0 (t, C8), 16.0 (p, CH<sub>3</sub>), -5.2 (p, SiCH<sub>3</sub>), -4.5 (p, SiCH<sub>3</sub>), 17.9 (q, *tert*-butyl), 25.5 (p, *tert*-butyl). IR (KBr, cm<sup>-1</sup>):  $\tilde{\nu}$  = 3200-2600 m broad (OH), 3148 m, 1597 m (C=N), 1590 st (C=N), 1573 m (C=C), 1543 st (N-O), 1407 m, 1312 m, 1293 m, 1269 m, 1252 m, 1214 w, 1186 w, 1155 w, 1114 st, 1084 st, 1069 st, 1004 m, 996 m, 950 w, 938 w, 925 w, 899 w, 863 st, 832 st, 795 st, 776 st, 757 st, 723 m, 684 m, 647 w, 627 w, 617 w, 576 w, 547 m, 530 m, 486 w. MS (DEI):  $m/z$ (%) = 404 (100) [M]<sup>+</sup>, 357 (8) [M-NO<sub>2</sub>]<sup>+</sup>, 346 (28) [M-*tert*-butyl]<sup>+</sup>, 299 (27), 250 (40), 225 (25), 192 (61), 182 (21), 165 (18), 118 (14), 78 (17), 73 (19), 57 (6). C<sub>20</sub>H<sub>29</sub>N<sub>3</sub>O<sub>4</sub>Si (403.55): calcd. C 59.53, H 7.24, N 10.41; found C 59.76, H 7.42, N 10.15.

***rac*-2-Amino-1,3-di(pyridin-2-yl)-1,3-di(*tert*-butyldi-**

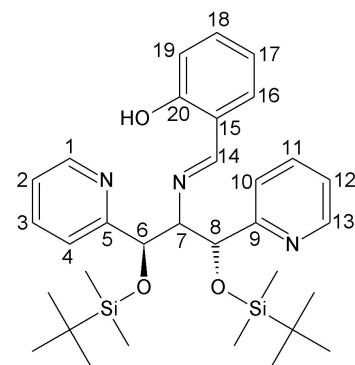
**methylsilyloxy)propane (10)** 1 g of nickel boride was suspended in 40 ml of anhydrous methanol and kept for five minutes in an ultrasound bath. To the black suspension a solution of **7** (2.80 g, 5.6 mmol) in 10 ml of anhydrous methanol was added. The mixture was warmed to 40 °C and sodium borohydride (ca. 2.8 g, 74 mmol) was carefully



added keeping the internal temperature at 65 °C until TLC (silica, diethylether) indicated the total consumption of **7** (ca. 30 minutes). The mixture was allowed to cool to room temperature and was carefully filtered over celite (2 cm height). After removal of the solvent in vacuo the residue was stirred in 20 ml of pentane for 15 minutes. To this mixture 10 ml of water were added and additionally stirred for 10 minutes. Now the phases were separated and the organic phase was dried over sodium sulfate. After removal of pentane in vacuo 2.39 g of an colorless oil were received. The oily product **10** was stable under atmospheric conditions at room temperature. Yield: 90 %. 180 °C ( $9 \cdot 10^{-3}$  mbar) dec..  $^1\text{H}$  NMR ( $\text{CDCl}_3$ ):  $\delta = 8.50$  (m, 2H, Pyr1, Pyr13), 7.62-7.54 (m, 2H, Pyr3,Pyr11), 7.44 (d,  $J = 7.8$  Hz, 1H, Pyr4), 7.38 (d,  $J = 8.0$  Hz, 1H, Pyr10), 7.12-7.06 (m, 2H, Pyr2), 5.10 (d,  $J = 5.2$  Hz, 1H, H6), 4.72 (d,  $J = 5.6$  Hz, 1H, H8), 3.44 (m, 1H, H7), 0.86 (s, 9H, *tert*-butyl), 0.85 (s, 9H, *tert*-butyl), 0.30 (s, 3H,  $\text{SiCH}_3$ ), -0.04 (s, 3H,  $\text{SiCH}_3$ ), -0.28 (s, 3H,  $\text{SiCH}_3$ ), -0.35 (s, 3H,  $\text{SiCH}_3$ ), 1.50 (s broad, 2H, NH).  $^{13}\text{C}$  NMR ( $\text{CDCl}_3$ ):  $\delta = 148.8$  and 148.3 (t, Pyr1, Pyr13), 135.9 (t, Pyr3), 135.6 (t, Pyr11), 122.6 (t, Pyr4), 122.4 (t, Pyr10), 122.0 (t, Pyr2, Pyr12), 162.6 (q, Pyr5), 162.1 (q, Pyr9), 75.4 (t, C6), 76.9 (t, C8), 62.8 (t, C7), 25.9 (p, *tert*-butyl), 25.6 (p, *tert*-butyl), 18.2 (q, *tert*-butyl), 18.1 (q, *tert*-butyl), -3.6 (p,  $\text{SiCH}_3$ ), -4.5 (p,  $\text{SiCH}_3$ ), -4.7 (p,  $\text{SiCH}_3$ ), -4.9 (p,  $\text{SiCH}_3$ ). IR (neat,  $\text{cm}^{-1}$ ):  $\tilde{\nu} = 3391$  st, broad (NH), 3067 m, 3012 m, 2928 st, 2894 st, 2856 st, 2739 w, 2710 w, 1650 m, 1591 st (C=N), 1572 st (C=C), 1471 st, 1435 st, 1407 st, 1389 st, 1254 st, 1216 m, 1075 st, 1005 st, 938 st, 837 st, 777 st, 673 st, 619 m, 597 st, 575 m, 535 m. MS (FAB in nba):  $m/z(\%) = 496$  (49)  $[\text{M}+\text{Na}]^+$ , 474 (63)  $[\text{M}+1]^+$ , 416 (11)  $[\text{M}-\text{tert-butyl}]^+$ , 399 (19), 342 (26), 325 (25), 267 (20), 261 (19), 251 (100), 235 (61), 223 (62), 208 (38).  $\text{C}_{25}\text{H}_{43}\text{N}_3\text{O}_2\text{Si}_2$  (473.78).

***rac*-((2,2,3,3,9,9,10,10-Octamethyl-5,7-di(pyridin-2-yl)-4,8-dioxa-3,9-disilaundecan-6-ylimino)methyl)phenol**

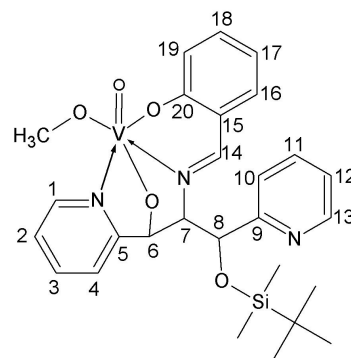
**(13)** Amino compound **10** (1.50 g, 32 mmol) and salicyl aldehyde (0.39 g, 32 mmol) were solved in 40 ml of methylene chloride and molecular sieve 4A was added. The solution was refluxed for one hour until TLC (silica, diethyl ether) indicated the total consumption of **10**. Subsequently the solution was filtered over celite and the solvent was removed in vacuo, yielding a yellow viscous oil. The oil was dried in vacuo for several hours affording the solid product **13** with high purity. Yield: 98 %. m.p.: 84 °C.  $^1\text{H}$  NMR ( $\text{CD}_3\text{OD}$ ):  $\delta = 8.38$  (s,



1H, HC=N), 8.47 (d,  $J = 4.4$  Hz, 1H, Pyr13), 8.50 (d,  $J = 4.4$  Hz, 1H, Pyr1), 7.75 (ddd,  $J = 7.6$  1.6 Hz, 1H, Pyr11), 7.63-7.59 (m, 1H, Pyr3), 7.31-7.26 (m, 3H, Ph12, Ph16, Ph18), 7.60 (d,  $J = 7.6$  1.6 Hz, 1H, Pyr10), 7.21-7.18 (m, 2H, Pyr2, Pyr4), 6.84 (t,  $J = 7.6$  Hz, 1H, Ph17), 6.80 (d,  $J = 8.0$  Hz, 1H, Ph19), 4.07 (dd,  $J = 8.0$  Hz,  $J = 2.8$  Hz, 1H, H7), 4.88 (d,  $J = 2.8$  Hz, 1H, H6), 5.26 (d,  $J = 8.0$  Hz, 1H, H8), 0.87 (s, 9H, *tert*-butyl), 0.64 (s, 9H, *tert*-butyl), -0.12 (s, 3H, SiCH<sub>3</sub>), -0.20 (s, 3H, SiCH<sub>3</sub>), -0.28 (s, 3H, SiCH<sub>3</sub>), -0.32 (s, 3H, SiCH<sub>3</sub>), 12.7 (s broad, H, OH in CDCl<sub>3</sub>). <sup>13</sup>C NMR (CD<sub>3</sub>OD):  $\delta = 168.9$  (t, HC=N), 162.7 (q, Pyr5), 162.2 (q, Pyr9), 150.0 (t, Pyr13), 149.1 (t, Pyr1), 138.1 (t, Pyr11), 137.7 (t, Pyr3), 133.7 and 132.9 (t, Ph16, Ph18), 124.5 (t, Pyr12), 125.9 (t, Pyr10), 123.6 and 123.5 (t, Pyr2, Pyr4), 120.1 (q, Ph15), 119.6 (t, Ph17), 117.8 (t, Ph19), 82.1 (t, C7), 76.5 (t, C6), 75.8 (t, C8), 26.3 (t, *tert*-butyl), 26.2 (t, *tert*-butyl), 19.0 (q, *tert*-butyl), 18.8 (q, *tert*-butyl), -4.6 (p, SiCH<sub>3</sub>), -4.65 (p, SiCH<sub>3</sub>), -4.7 (p, SiCH<sub>3</sub>), -4.8 (p, SiCH<sub>3</sub>). IR (Nujol, cm<sup>-1</sup>):  $\tilde{\nu} = 3100$ -2900 m (OH), 3073 w, 2728 w, 2668 w, 1633 st (C=N exocyc.), 1615 m, 1587 st (C=N endocyc.), 1571 m (C=C), 1500 m, 1316 m, 1282 st, 1251 st, 1212 w, 1149 m, 1110 st, 1075 st, 1044 w, 1005 m, 988 m, 966 m, 939 w, 891 m, 845 st, 837 st, 776 st, 761 m, 750 st, 738 w, 669 w, 641 w, 624 w, 609 w, 577 w, 545 w. MS (DEI):  $m/z$ (%) = 577 (32) [M]<sup>+</sup>, 562 (6), 520 (41) [M-*tert*-butyl]<sup>+</sup>, 355 (61), 223 (100), 178 (12), 165 (17), 73 (26), 28 (20). UV-Vis (ethanol, l mol<sup>-1</sup> cm<sup>-1</sup>):  $\epsilon$  ( $\lambda_{max}$ ) = 1.9·10<sup>3</sup> (257 nm), 4410 (317 nm), 343 (410 nm). C<sub>32</sub>H<sub>47</sub>N<sub>3</sub>O<sub>3</sub>Si<sub>2</sub> (577.90): calcd. C 66.51, H 8.20, N 7.27; found C 66.34, H 8.35, N 6.98.

**[(2-((1-(*Tert*-butyldimethylsilyloxy)-3-hydroxo-1,3-di-**

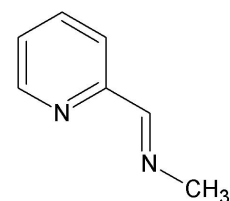
**(pyridin-2-yl)propan-2-ylimino)methyl)phenolato)**  
**(methanolato)oxovanadium(V)] (14)** Proligand **13** (200 mg, 0.35 mmol) and vanadyl acetylacetonate (92 mg, 0.35 mmol) were solved in 12 ml of anhydrous methanol under argon atmosphere. The green to yellow mixture was refluxed for four hours and stirred over night at room temperature. Subsequently, a solution of potassium hydroxide (20 mg, 35 mmol) in 5 ml of methanol was added and the mixture was vigorously stirred over night at room temperature in an open vessel. Upon aerial oxidation the solution slowly colored red. Thereafter, the red solution was filtered and left for crystallization. Crystals suitable for single crystal X-ray diffraction were obtained by slow solvent evaporation. The crystallized complex **14** was found to be stable under atmospheric conditions at room temperature. Yield: 70 %. m.p.: 130 °C (dec.).<sup>1</sup>H NMR (CD<sub>3</sub>OD):  $\delta = 6.90$  (s, 1H, HC=N), 8.58 (d,  $J = 4.4$  Hz, 1H, Pyr13), 8.26 (d,  $J = 4.8$  Hz, 1H, Pyr1), 7.83 (ddd,  $J = 7.6$  Hz,  $J = 1.2$  Hz, 1H, Pyr3), 7.76 (ddd,  $J = 7.6$ ,  $J = 1.6$  Hz, 1H, Pyr11), 7.42-7.35 (m, 3H, Pyr12, Pyr10, Ph18), 6.57 (dd,  $J = 7.6$  Hz,  $J = 1.6$  Hz, 1H, Ph16), 7.27-7.24 (m, 1H, Pyr2), 7.52 (d,  $J = 8.0$  Hz, 1H, Pyr4), 6.64 (t,  $J = 7.2$  Hz, 1H, Ph17), 6.86 (d,  $J = 8.4$  Hz, 1H, Ph19), 6.08 (s broad, 1H, H6), 4.04 (d,  $J = 8.8$  Hz, 1H, H7), 5.68 (d,  $J = 8.8$  Hz, 1H, H8), 0.96 (s, 9H, *tert*-butyl), 0 (25,  $J = s$  Hz, H, SiCH<sub>3</sub>), -0.04 (s, 3H, SiCH<sub>3</sub>), 3.34 (s, 3H, OCH<sub>3</sub>). <sup>13</sup>C NMR (CD<sub>3</sub>OD):  $\delta = 166.7$  (t, HC=N), 162.5 (q, Pyr5),



166.7 (t, HC=N), 162.5 (q, Pyr5),

161.0 (q, Pyr9), 150.4 (t, Pyr13), 148.3 (t, Pyr1), 139.7 (t, Pyr3), 138.6 (t, Pyr11), 136.7 (t, Ph18), 165.5 (q, Ph20), 133.6 (t, Ph16), 125.9 (t, Pyr12), 125.1 (t, Pyr10), 124.6 (t, Pyr2), 121.8 (q, Ph15), 120.9 (t, Pyr4), 119.7 (t, Ph17), 119.1 (t, Ph19), 87.3 (t, C6), 85.7 (t, C7), 77.6 (t, C8), 26.3 (p, *tert*-butyl), 19.2 (q, *tert*-butyl), 3 (-4.7, SiCH<sub>3</sub>), -4.4 (p, SiCH<sub>3</sub>), 49.0 (p, OCH<sub>3</sub>). <sup>51</sup>V NMR (CDCl<sub>3</sub>):  $\delta = -518$ . IR (Nujol, cm<sup>-1</sup>):  $\tilde{\nu} = 2725$  w, 1636 st (C=N exocyc), 1599 st (C=N endocyc), 1587 m (C=N endocyc), 1568 m (C=C), 1552 m (C=C), 1420 m, 1338 m, 1323 m, 1297 st, 1282 st, 1250 st, 1219 m, 1153 st, 1125 m, 1076 st, 1055 st, 1015 m, 1003 m, 991 m, 971 m, 959 st (V=O), p 939 (m), 890 m, 862 st, 846 st, 813 m, 797 m, 777 m, 764 st, 743 st, 722 m, 670 w, 646 w, 639 w, 624 st, 607 st, 596 st, 579 m, 554 m, 534 st, 511 m, 467 m. MS (DEI):  $m/z(\%) = 559 (< 1) [M]^+$ , 543 (2) [M-CH<sub>3</sub>]<sup>+</sup>, 527 (40), 502 (55) [M-*tert*-butyl]<sup>+</sup>, 452 (74), 420 (100), 395 (35), 364 (53), 320 (24), 306 (40), 290 (78), 166 (25), 73 (79), 32 (26). UV-Vis (ethanol, l mol<sup>-1</sup> cm<sup>-1</sup>):  $\epsilon (\lambda_{max}) = 3 \cdot 10^4$  (230 nm),  $8 \cdot 10^3$  (330 nm),  $3 \cdot 10^3$  (460 nm). C<sub>27</sub>H<sub>34</sub>N<sub>3</sub>O<sub>5</sub>SiV (559.60): calcd. = C 57.95, H 6.12, N 7.51; found = C 57.76, H 5.91, N 7.32.

**N-Methyl-pyridylmethylideneamine (15a)** Pyridine-2-carbaldehyde (10.71 g, 0.10 mol) was dissolved in 10.0 ml of a 40% aqueous methylamine solution (0.13 mol methylamine) at 0 °C. After stirring for 1 h the mixture was extracted four times with 20 ml of methylene chloride each. The combined extracts were dried over anhydrous magnesium sulfate. Subsequently, the solvent was removed in vacuo and the obtained dark yellow oil was purified by vacuum distillation



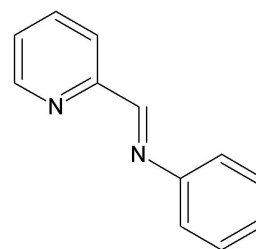
(53 °C at 1 mbar) giving 9.61 g of a pale yellow liquid. Yield: 83%. <sup>1</sup>H NMR (D<sub>2</sub>O):  $\delta = 8.34$ -8.30 (m, 1H, Pyr1), 8.05-8.03 (m, 1H, HC=N), 7.69 (ddd, 1H, J = 1.8 Hz, J = 7.6 Hz, Pyr3), 7.56-7.51 (m, 1H, Pyr4), 7.27 (dddd, 1H, J = 1.2 Hz, J = 7.4 Hz, Pyr2), 3.28 (d, 3H, 1.6 Hz, CH<sub>3</sub>). <sup>13</sup>C NMR (D<sub>2</sub>O):  $\delta = 163.1$  (t, C=N), 151.8 (q, Pyr5), 148.3 (t, Pyr1), 137.7 (t, Pyr3), 125.4 (t, Pyr2), 121.1 (t, Pyr4), 46.1 (p, CH<sub>3</sub>). IR (KBr, cm<sup>-1</sup>):  $\tilde{\nu} = 3054$  w, 3008 w, 2944 m, 2884 m, 2862 2773 w, 1652 st (C=N), 1586 st, 1567 st, 1470 st, 1454 m, 1437 st, 1401 w, 1347 m, 1291 w, 1221 w, 1147 w, 1124 w, 1044 w, 1006 m, 989 st, 969 w, 947 w, 862 w, 773 st, 742 m, 661 w, 617 m, 510 m. MS (EI):  $m/z (\%) = 153$  (17), 149 (7), 136 (16), 120 (25) [M]<sup>+</sup>, 119 (100), 105 (21), 92 (39), 78 (11), 77 (54), 52 (18), 51 (27), 39 (10), 28 (20). C<sub>7</sub>H<sub>8</sub>N<sub>2</sub> (120.15): calc. C 69.97, H 6.71, N 23.32; found: C 69.75, H 6.76, N 23.28.

#### General procedure for the preparation of N-organyl-pyridylmethylideneamines 15b-15d

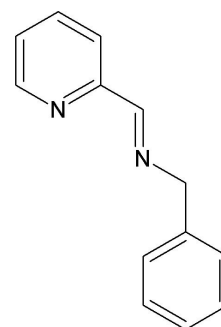
The amine (0.04 mol) was dissolved in 10 ml of methylene chloride and cooled to 0 °C. pyridine-2-carbaldehyde (4.28 g, 0.04 mol) was added dropwise and the mixture was stirred for three hours at 0 °C. The solvent was removed in vacuo and the resulting products were purified by distillation.

**N-Phenyl-pyridylmethylideneamine (15b)**

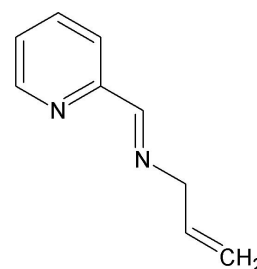
Yellow viscous oil (112 °C at  $5 \cdot 10^{-3}$  mbar, solid beneath r.t.). Yield: 85%.  $^1\text{H}$  NMR ( $\text{CD}_2\text{Cl}_2$ ):  $\delta$  = 8.70 (d, 1H,  $J$  = 4.4 Hz, Pyr1), 8.60 (s, 1H, C=N), 8.22 (d, 1H,  $J$  = 8.0 Hz, Pyr4), 7.83 (ddd, 1H,  $J$  = 1.2 Hz,  $J$  = 7.6 Hz, Pyr3), 7.45–7.41 (m, 2H, m-PhH), 7.38 (dddd, 1H,  $J$  = 1.2 Hz,  $J$  = 7.6 Hz, Pyr2), 7.30–7.27 (m, 3H, o,p-PhH).  $^{13}\text{C}$  NMR ( $\text{CD}_2\text{Cl}_2$ ):  $\delta$  = 161.4 (t, C=N), 155.2 (q, Pyr5), 151.5 (q, PhC), 150.0 (t, Pyr1), 136.9 (t, Pyr3), 129.6 (t, m-PhC), 127.0 (t, p-PhC), 125.5 (t, Pyr2), 121.7 (t, Pyr4), 121.4 (t, o-PhC). IR (KBr,  $\text{cm}^{-1}$ ):  $\tilde{\nu}$  = 3409 w, 3053 m, 3015 m, 2906 w, 2893 w, 1623 st (C=N), 1579 st, 1563 st, 1487 st, 1466 st, 1451 m, 1433 st, 1347 m, 1197 m, 1147 m, 1074 m, 1045 m, 991 st, 980 m, 912 m, 877 m, 782 st, 740 st, 689 st, 665 m, 619 m, 552 m, 539 st. MS (DEI):  $m/z$  (%) = 211 (2), 182 (100)  $[\text{M}]^+$ , 180 (53), 156 (14), 154 (11), 129 (3), 127 (7), 105 (28), 104 (32), 91 (23), 79 (24), 78 (28), 77 (81), 76 (28), 64 (3), 51 (28), 50 (19), 38 (8), 26 (15).  $\text{C}_{12}\text{H}_{10}\text{N}_2$  (182.221): calc. C 79.10, H 5.53, N 15.37; found: C 79.10, H 5.61, N, 15.33.

**N-Benzyl-pyridylmethylideneamine (15c)**

Pale yellow oil (121 °C at  $7 \cdot 10^{-3}$  mbar, solid beneath r.t.). Yield: 94%.  $^1\text{H}$  NMR ( $\text{CD}_2\text{Cl}_2$ ):  $\delta$  = 8.66 (d, 1H,  $J$  = 4.4 Hz, Pyr1), 8.53 (s, 1H, HC=N), 8.09 (d, 1H,  $J$  = 8.0 Hz, Pyr4), 7.75 (ddd, 1H,  $J$  = 1.6 Hz,  $J$  = 7.6 Hz, Pyr3), 7.40–7.38 (m, 4H, o,m-PhH), 7.33–7.30 (m, 2H, Pyr2/p-PhH), 4.88 (s, 2H,  $\text{CH}_2$ ).  $^{13}\text{C}$  NMR ( $\text{CD}_2\text{Cl}_2$ ):  $\delta$  = 163.3 (t, C=N), 155.2 (q, Pyr5), 149.7 (t, Pyr1), 139.6 (q, PhC), 136.7 (t, Pyr3), 128.8 (t, m-PhC), 128.5 (t, o-PhC), 127.4 (t, p-PhC), 125.1 (t, Pyr2), 121.2 (t, Pyr4), 65.2 (s,  $\text{CH}_2$ ). IR (KBr,  $\text{cm}^{-1}$ ):  $\tilde{\nu}$  = 3275 w, 3058 m, 3028 m, 2880 m, 1647 st (C=N), 1586 st, 1567 st, 1495 m, 1467 st, 1451 st, 1434 st, 1378 m, 1335 m, 1225 w, 1144 w, 1077 w, 1043 m, 1028 m, 991 m, 861 w, 770 st, 737 st, 698 st, 616 m, 501 m. MS (DEI):  $m/z$  (%) = 196 (65)  $[\text{M}]^+$ , 180 (98), 168 (29), 119 (91), 91 (100), 65 (64), 51 (34), 39 (18), 28 (6).  $\text{C}_{13}\text{H}_{12}\text{N}_2$  (196.248): calc. C 79.29, H 6.16, N 14.27; found: C 79.29, H 6.18, N 14.40.

**N-Allyl-pyridylmethylideneamine (15d)**

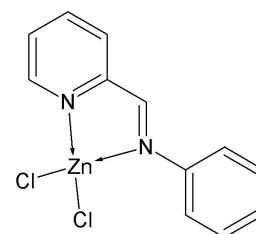
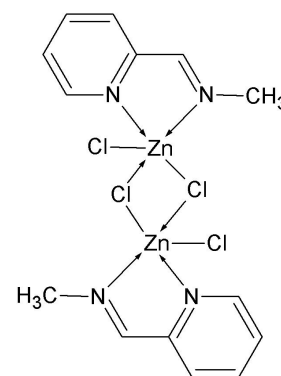
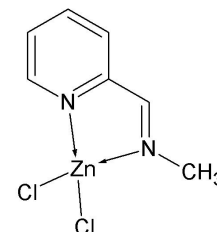
Additionally anhydrous  $\text{Na}_2\text{SO}_4$  was added to the reaction mixture and removed after completion of the reaction. Yellow liquid (112 °C at  $5 \cdot 10^{-3}$  mbar), Yield: 65%.  $^1\text{H}$  NMR ( $\text{CD}_2\text{Cl}_2$ ):  $\delta$  = 8.61 (d, 1H,  $J$  = 4.4 Hz, Pyr1), 8.37 (s, 1H, HC=N), 8.03 (d, 1H,  $J$  = 8.0 Hz, Pyr4), 7.74 (ddd, 1H,  $J$  = 1.6 Hz,  $J$  = 7.6 Hz, Pyr3), 7.33–7.30 (m, 1H, Pyr2), 6.13–6.03 (m, 1H, HC=C), 5.32–5.14 (m, 2H, C=CH<sub>2</sub>), 4.30–4.28 (m, 2H, CH<sub>2</sub>);  $^{13}\text{C}$  NMR ( $\text{CD}_2\text{Cl}_2$ ):  $\delta$  = 163.3 (t, C=N), 155.2 (q, Pyr5), 149.7 (t, Pyr1), 136.7 (t, Pyr3), 136.2 (t, HC=C), 125.0 (t, Pyr2), 121.1 (t, Pyr4), 116.2 (s, C=CH<sub>2</sub>), 63.6 (s, CH<sub>2</sub>). IR (KBr,  $\text{cm}^{-1}$ ):  $\tilde{\nu}$  = 3055 m, 3012 m, 2982 w, 2884 m,



2821 m, 1650 st (C=N), 1586 st, 1567 st, 1468 st, 1436 st, 1418 w, 1356 w, 1314 m, 1291 w, 1226 w, 1146 w, 1106 w, 1087 w, 1044 m, 1023 m, 992 st, 920 st, 853w, 773 st, 742 m, 665 w, 632 w, 614 m, 560 w, 505 w; MS (EI):  $m/z$  (%) = 147 (100)  $[M+1]^+$  130 (94), 118 (10), 92 (6), 78 (8), 39 (15), 27 (14).  $C_9H_{10}N_2$  (146.189): calc. C 73.94, H 6.89, N 19.16; found: C 74.13, H 6.74, N 19.35.

[(N-Methyl-pyridylmethylideneamino)ZnCl<sub>2</sub>]<sub>n</sub> (**16a**) (n = 1, 2) Anhydrous zinc(II) chloride (0.68 g, 5.0 mmol) was dissolved in 5 ml of anhydrous thf. The solution was cooled to 0 °C and the solution of **15a** (0.60 g, 5.0 mmol) in 2 ml of anhydrous thf was added dropwise, while immediately a colorless precipitate was formed. The suspension was diluted with additional 15 ml of anhydrous thf and stirred for half an hour. Subsequently, the colorless precipitate was filtered off, washed with anhydrous thf and dried in vacuo, yielding 1.12 g of **16a**. Colorless needles, suitable for single crystal X-ray diffraction were obtained by cooling a saturated solution of **16a** in acetone (r.t.) to 5 °C. Yield: 87 %. m.p. 201 °C (dec.). <sup>1</sup>H NMR (CD<sub>3</sub>OD): δ = 8.71 (br, 2H, Pyr1, HC=N), 8.28 (t, J = 7.6 Hz, 1H, Pyr3), 8.04 (d, J = 6.8 Hz, 1H, Pyr4), 7.83 (t, J = 4.8 Hz, 1H, Pyr2), 3.49 (s, 3H, CH<sub>3</sub>); <sup>13</sup>C NMR CD<sub>3</sub>OD): δ = 163.8 (t, C=N), 150.25 (t, Pyr1), 148.3 (q, Pyr5), 142.6 (t, Pyr3), 129.9 (t, Pyr2), 129.0 (t, Pyr4), 45.1 (p, CH<sub>3</sub>). IR (Nujol, cm<sup>-1</sup>):  $\tilde{\nu}$  = 3104 w, 3076 w, 3032 m, 1651 m, 1600 st, 1570 w, 1480 m, 1446 st, 1312 st, 1273 w, 1223 m, 1161 m, 1099 w, 1055 w, 1029 m, 1022 st, 975 m, 960 m, 873 w, 774 st, 746 w, 722 w, 668 w, 643 w, 508 m. MS (DEI):  $m/z$  (%) = 221 (44)  $[M-Cl]^+$ , 119 (100), 105 (9), 92 (26), 78 (14), 65 (3), 51 (10), 42 (19), 28 (5); MS (FAB):  $m/z$  (%) = 477  $[2M-Cl]^+$  (1), 339  $[2M-ZnCl_3]^+$  (22), 221  $[M-Cl]^+$  (100).  $C_7H_8Cl_2N_2Zn$  (256.45) calc. C 32.78, H 3.14, N 10.92; found C 33.17, H 3.29, N 10.72.

[(N-Phenyl-pyridylmethylideneamino)ZnCl<sub>2</sub>] (**16b**) Anhydrous zinc(II) chloride (0.30 g, 2.2 mmol) was dissolved in 2 ml of anhydrous methanol and then a solution of **15b** (0.40 g, 2.2 mmol) in 3 ml of anhydrous methanol was added. The mixture was heated under reflux for 5 min while a yellowish solid precipitated. After stirring for an additional hour the precipitate was collected, washed with anhydrous methanol and dried in vacuo, yielding 0.58 g of yellowish **16b**. Crystals, suitable for single crystal X-ray diffraction studies, were obtained by cooling a saturated solution in methanol (r.t.) to 5 °C. Yield: 83 %. m.p. 300 °C (dec.). <sup>1</sup>H NMR ([D<sub>6</sub>]dmsO): δ = 8.89 (d, J = 4.0 Hz, 1H, Pyr1), 8.68 (s, 1H, HC=N), 8.12 (t, J = 7.6 Hz, 1H, Pyr3), 8.07 (d, J = 7.6 Hz, 1H, Pyr4), 7.72 (t, J = 6.4 Hz, 1H, Pyr2), 7.39–7.36 (m, 2H, m-PhH), 7.29–7.26 (m, 3H, o,p-PhH). <sup>13</sup>C NMR

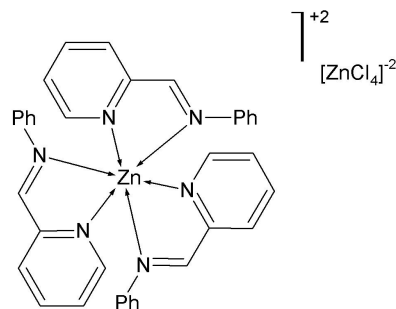




([D<sub>6</sub>]dmsO):  $\delta$  = 159.9 (t, C=N), 150.3 (q, Pyr5), 149.7 (t, Pyr1), 148.4 (q, PhC), 139.2 (t, Pyr3), 129.1 (t, m-PhC), 127.3 (t, Pyr2, p-PhC), 124.9 (t, Pyr4), 121.4 (t, o-PhC). IR (Nujol, cm<sup>-1</sup>):  $\tilde{\nu}$  = 3115 w, 3092 w, 3003 w, 1594 (C=N), 1563 w, 1493 m, 1303 w, 1280 w, 1236 w, 1154 w, 1111 m, 959 w, 971 w, 916 m, 779 st, 741 m, 683 m, 650 m, 567 w, 535 m. MS (Micro-ESI in methanol): m/z (%) = 315 (100) [M-Cl+CH<sub>3</sub>OH]<sup>+</sup>, 281 (69) [M-Cl]<sup>+</sup>, 263 (13) [M-2Cl+OH]<sup>+</sup>, 247 (18) [M-2Cl+H]<sup>+</sup>, 181 (24). C<sub>12</sub>H<sub>10</sub>Cl<sub>2</sub>N<sub>2</sub>Zn (318.52) calc. C 45.25, H 3.16, N 8.80; found C 45.25, H 3.13, N, 8.75.

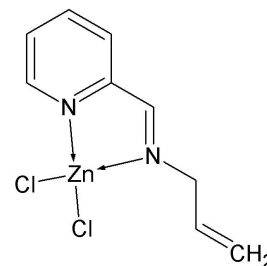
**[(N-Benzyl-pyridylmethylideneamino)<sub>3</sub>Zn(II)][ZnCl<sub>4</sub>]·2CH<sub>3</sub>OH**

(**16c**) Anhydrous zinc (II) chloride (0.20 g, 1.5 mmol) was dissolved in 1 ml of anhydrous methanol and a solution of **15c** (0.43 g, 2.2 mmol) in 2 ml of methanol was added. The mixture was heated under reflux for five minutes and then stirred for one hour at r.t. while a colorless precipitate formed. The solid was collected, washed with anhydrous methanol and dried in vacuo, yielding 0.54 g of **16c**. Crystals suitable for single crystal X-ray diffraction



studies were obtained by cooling a saturated solution (r.t.) in methanol to 5 °C. The product crystallized with two equivalents of methanol. Yield: 80%. m.p. 140 °C (dec.). <sup>1</sup>H NMR ([D<sub>6</sub>]dmsO):  $\delta$  = 8.69 (d, J = 4.0 Hz, 1H, Pyr1), 8.56 (s, 1H, HC=N), 8.07 (t, J = 7.2 Hz, 1H, Pyr3), 7.91 (d, J = 7.6 Hz, 1H, Pyr4), 7.65 (t, J = 5.6 Hz, 1H, Pyr2), 7.23 (s, 3H, m,p-PhH), 7.06 (s, 2H, o-PhH), 4.52 (s, 2H, CH<sub>2</sub>), 4.10 (q, J = 5.2 Hz, 1H, methanol), 3.16 (d, J = 5.2 Hz, 3H, methanol); <sup>13</sup>C NMR ([D<sub>6</sub>]dmsO):  $\delta$  = 162.1 (t, HC=N), 149.8 (q, Pyr5), 149.2 (t, Pyr1), 139.2 (t, Pyr3), 137.0 (q, PhC), 128.3 (t, m-PhC), 128.1 (t, o-PhC), 127.2 (t, p-PhC), 127.0 (t, Pyr2), 124.7 (t, Pyr4), 61.6 (s, CH<sub>2</sub>), 48.6 (p, methanol). IR (Nujol, cm<sup>-1</sup>):  $\tilde{\nu}$  = 3508 m, 3454 m, 3064 m, 3026 m, 1645 st (C=N), 1594 st, 1568 w, 1496 m, 1480 m, 1305 st, 1267 w, 1228 m, 1204 w, 1183 w, 1157 m, 1104 m, 1050 m, 1015 m, 987 w, 954 w, 920 w, 881 w, 812 w, 785 m, 770 m, 751 st, 705 st, 675 w, 638 m, 606 w, 512 w, 500 m. MS (positive Micro-ESI in methanol): m/z (%) = 713 (25), 491 (100) [ZnL<sub>2</sub>Cl]<sup>+</sup>, 327 (21), 294 (10) [ZnLCl]<sup>+</sup>, 228.5 (96) [ZnL<sub>2</sub>]<sup>2+</sup>; MS (negative Micro-ESI in methanol): m/z (%) = 171 (100) [ZnCl<sub>3</sub>]<sup>-</sup>. C<sub>41</sub>H<sub>44</sub>Cl<sub>4</sub>N<sub>6</sub>O<sub>2</sub>Zn<sub>2</sub> (925.42) calc. C 53.21, H 4.79, N 9.08; found C 52.46, H 4.88, N 9.02.

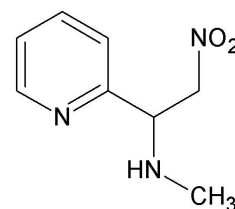
**[(N-Allyl-pyridylmethylideneamino)ZnCl<sub>2</sub>] (16d)** Anhydrous zinc(II) chloride (0.26 g, 1.9 mmol) was dissolved in 2 ml of anhydrous methanol and a solution of **15d** (0.28 g, 1.9 mmol) in 3 ml of anhydrous methanol was added. The mixture was heated under reflux for five minutes and then stirred for one hour at r.t. Subsequently the solvent was removed in vacuo and the resulting colorless foam was stirred in 10 ml of anhydrous diethyl ether. The obtained solid was collected, washed with diethyl ether and dried in vacuo,



yielding 0.47 g of **16d**. Crystals suitable for single crystal X-ray diffraction studies were obtained by cooling a saturated solution in methanol (r.t.) to 5 °C. Yield: 90 %. m.p. 180 °C (dec.). <sup>1</sup>H NMR ([D<sub>6</sub>]dmsO): δ = 8.76 (b, 1H, Pyr1), 8.62 (s, 1H, HC=N), 8.23 (t, J = 7.6 Hz, 1H, Pyr3), 8.05 (d, J = 7.6 Hz, 1H, Pyr4), 7.82-7.76 (m, 1H, Pyr2), 5.80 (m, br, 1H, HC=C), 5.06-5.01 (m, 2H, C=CH<sub>2</sub>), 4.18 (d, J = 5.6 Hz, 2H, CH<sub>2</sub>); <sup>13</sup>C NMR ([D<sub>6</sub>]dmsO): δ = 161.7 (t, C=N), 149.2 (t, Pyr1), 148.3 (q, Pyr5), 140.3 (t, Pyr3), 133.9 (t, HC=C), 127.9 (t, Pyr2), 126.2 (t, Pyr4), 117.9 (s, C=CH<sub>2</sub>), 59.5 (s, CH<sub>2</sub>). IR (Nujol, cm<sup>-1</sup>):  $\tilde{\nu}$  = 3079 m; 1650 m, 1645 m, 1598 st, 1569 m, 1477 m, 1343 w, 1302 st, 1276 w, 1224 m, 1156 m, 1117 m, 1101 m, 1045 m, 1024 m, 995 m, 973 w, 929 st, 866 w, 791 st, 648 m, 561 m, 505 m. MS (DEI): m/z (%) = 247 (15) [M-Cl]<sup>+</sup>, 150 (81), 137 (100), 125 (52), 101 (88), 82 (60), 68 (24), 51 (50), 39 (62). C<sub>9</sub>H<sub>10</sub>Cl<sub>2</sub>N<sub>2</sub>Zn (282.48) calc. C 38.26, H 3.57, N 9.92; found C 38.46, H 3.63, N 10.04.

**1-Methylamino-1-(2-pyridyl)-2-nitroethane (17)** N-Methyl-

(2-pyridyl)methylimine (32.0 g, 266 mmol) and 6 g of Syntal 696<sup>®</sup> were suspended in 208 ml of nitromethane and stirred at 15 °C for 5 h. Then the catalyst was removed by filtration. Under reduced



pressure, all volatile materials were removed, and 35.5 g of an orange

oil (200 mmol) remained. Yield: 74 % <sup>1</sup>H NMR ([D<sub>6</sub>]benzene): δ

= 8.30 (d, <sup>3</sup>J(H1,H5) = 4.4 Hz, 1H, Pyr1), 7.01 (ddd, <sup>3</sup>J(H3,H4,2)

= 7.9 Hz, <sup>4</sup>J(H3,H1) = 1.6 Hz, 1H, Pyr3), 6.76 (d, <sup>3</sup>J(H4,H3) = 7.9 Hz, 1H, Pyr4), 6.59

(ddd, <sup>3</sup>J(H2,H3) = 7.6 Hz, <sup>3</sup>J(H2,H1) = 4.4 Hz, <sup>4</sup>J(H2,H4) = 0.8 Hz, 1H, Pyr2), 4.39 (m,

<sup>2</sup>J(H7b,H7a) = 12.4 Hz, <sup>3</sup>J(H7b,H6) = 8.6 Hz, 1H, H7b), 4.26 (m, <sup>2</sup>J(H7a,H7b) = 12.4 Hz,

<sup>J</sup>(H7a,H6) = 5.2 Hz, 1H, H7a), 4.09 (m, <sup>3</sup>J(H6,H7a) = 5.2 Hz, <sup>3</sup>J(H6,H7b) = 8.6 Hz, 1H,

H6), 1.96 (s, 3H, CH<sub>3</sub>); 1.72 (br, s, 1H, NH). <sup>13</sup>C NMR ([D<sub>6</sub>]benzene): δ = 158.4 (Pyr5),

149.8 (Pyr1), 136.2 (Pyr3), 122.7 (Pyr4,2), 78.8 (C7), 63.1 (C6), 33.6 (CH<sub>3</sub>).

**1,4-Dinitro-2,3-di(2-pyridyl)butane (18)** 1-methylamino-1-

(2-pyridyl)-2-nitroethane **17** (6 g, 33.1 mmol) was stirred in an

autoclave with 100 mg palladium catalyst in 45 ml of methanol at

5 bar hydrogen pressure at -5 °C for 24 h. Thereafter, the nearly in-

soluble product **18** was separated without warming of the reaction

mixture and washed twice with cold methanol. Separation from the

catalyst was performed via extraction of **18** with dichloromethane.

After removal of all volatile materials under vacuum, 600 mg of

a white powder (2 mmol) remained. Yield: 12 %. m. p.: 182

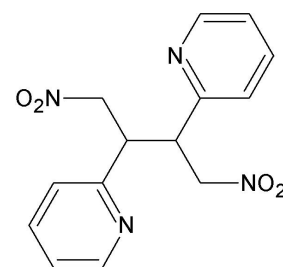
°C (dec.). <sup>1</sup>H NMR ([D<sub>6</sub>]dmsO): δ = 8.52 (d, <sup>3</sup>J(H1,H2) = 4.8 Hz, <sup>4</sup>J(H1,H3) = 1.7 Hz,

1H, Pyr1), 7.74 (ddd, <sup>3</sup>J(H3,H4,2) = 7.6 Hz, <sup>4</sup>J(H3,H1) = 1.7 Hz, 1H, Pyr3), 7.29 (m, 2H,

Pyr4/2), 5.04 (m, 1H, H7a), 4.66 (pdd, 1H, H7b), 4.12 (m, 1H, H6). <sup>13</sup>C NMR ([D<sub>6</sub>]dmsO):

δ = 156.6 (Pyr5), 149.3 (Pyr1), 137.0 (Pyr3), 124.4 (Pyr4), 122.9 (Pyr2), 76.4 (C7), 46.5

(C6). IR (KBr, cm<sup>-1</sup>):  $\tilde{\nu}$  = 3441 m/br, 3090 w, 3063 w, 3017 m, 2910 w, 1592 s, 1570 m,

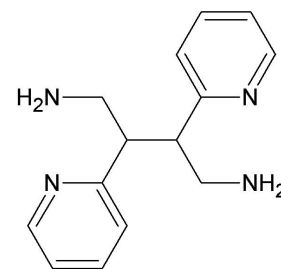


1538 vs, 1474 s, 1440 m, 1425 s, 1380 s, 1337 w, 1295 m, 1256 w, 1209 m, 1148 w, 1092 w, 1051 m, 1001 m, 977 w, 913 w, 810 s, 782 m, 756 s, 629 vw, 619 m, 592 m, 539 m, 483 w, 407 w. MS (EI):  $m/z$  (%) = 303 (19)  $[M+H]^+$ , 256 (100)  $[M-NO_2,-H]^+$ , 209 (73)  $[M-2NO_2,-2H]^+$ , 194 (23)  $[209-CH_3]^+$ .  $C_{14}H_{14}N_4O_4$  (302.29): calcd. C 55.63, H 4.67, N 18.53; found C 55.48, H 4.62, N 18.61.

**1,4-Diamino-2,3-di(2-pyridyl)butane (19)**

1,4-Dinitro-2,3-di(2-pyridyl)butane **18** (351 mg, 1.45 mmol) and 300 mg of Pd/C catalyst were suspended in 70 ml of anhydrous ethanol and heated under reflux. Hydrazine-hydrate (8 ml) was added dropwise; thereafter the solution was boiled for additional 10 h. Then the catalyst was removed. The solution was concentrated until a precipitate formed. Storage at  $-20\text{ }^\circ\text{C}$  led to the precipitation of **19**. Yield: 76 %.

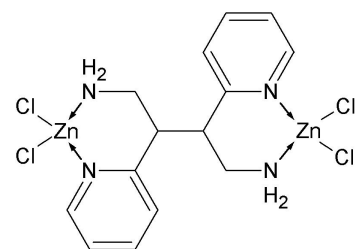
m. p.:  $106\text{ }^\circ\text{C}$ .  $^1\text{H}$  NMR ( $[D_6]$ dmsO):  $\delta$  = 8.58 (dd,  $^3J(\text{H1},\text{H2})$  = 4.9 Hz,  $^4J(\text{H1},\text{H3})$  = 1.2 Hz, 1H, Pyr1), 7.71 (ddd,  $^3J(\text{H3},\text{H4},2)$  = 7.4 Hz,  $^4J(\text{H3},\text{H1})$  = 1.2 Hz, 1H, Pyr3), 7.29 (d,  $^3J(\text{H4},\text{H3})$  = 7.6 Hz, 1H, Pyr4), 7.23 (ddd,  $^3J(\text{H2},\text{H3})$  = 7.4 Hz,  $^3J(\text{H2},\text{H1})$  = 4.9 Hz,  $^4J(\text{H2},\text{H4})$  = 1.2 Hz, 1H, Pyr2), 3.19 (m, 1H, H6), 2.65 (m, 1H, H7a), 2.31 (m, 1H, H7b), 1.98 (s, 2H,  $\text{NH}_2$ ).  $^{13}\text{C}$  NMR ( $[D_6]$ dmsO):  $\delta$  = 162.2 (Pyr5), 149.3 (Pyr1), 136.0 (Pyr3), 124.6 (Pyr4), 121.5 (Pyr2), 52.5 (C6), 44.6 (C7). IR (KBr,  $\text{cm}^{-1}$ ):  $\tilde{\nu}$  = 3448 vw, 3344 s, 3271 s, 3191 w, 3081 m, 3057 m, 3012 s, 2985 w, 2933 vs, 2919 vs, 2860 s, 2296 vw, 1970 w, 1590 vs, 1567 vs, 1474 vs, 1434 vs, 1356 m, 1334 w, 1292 m, 1250 w, 1227 m, 1146 s, 1085 s, 1053 m, 997 vs, 984 vs, 920 vw, 888 vs, 799 vs, 774 m, 757 m, 634 m, 613 m, 548 w, 487 w, 440 w, 407 m. MS (EI):  $m/z$  (%) = 243 (7)  $[M]^+$ , 183 (100)  $[M-2\cdot\text{CH}_2\text{NH}_2]^+$ , 122 (51)  $[M-\text{PyrC}_2\text{H}_3\text{NH}_2]^+$ , 121 (48)  $[122-\text{H}]^+$ , 105 (22)  $[121-\text{NH}_2]^+$ , 30 (9)  $[\text{CH}_2\text{NH}_2]^+$ .  $C_{14}H_{18}N_4$  (242.33): calcd. C 69.39, H 7.49, N 23.12; found C 69.16, H 6.96, N 22.90.



**[meso-1,4-Diamino-2,3-di(2-pyridyl)butanebis(dichloro-zinc)] (20)**

72 mg of 1,4-diamino-2,3-di(2-pyridyl)butane **19** (0.298 mmol) was dissolved in 2 ml of thf and dropped into a solution of 82 mg (0.60 mmol) of  $\text{ZnCl}_2$  in 5 ml of thf. A colorless precipitate formed and was washed twice with thf, yielding 150 mg (291 mmol). Yield: 98 %.

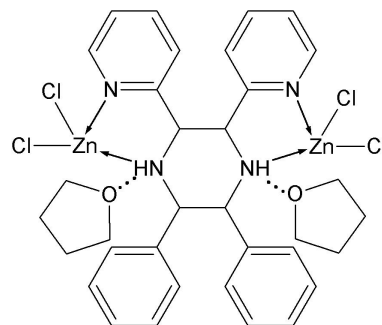
Dec. above  $280\text{ }^\circ\text{C}$  without melting.  $^1\text{H}$  NMR ( $[D_6]$ dmsO):  $\delta$  = 8.47 (dd,  $^3J(\text{H1},\text{H2})$  = 5.1 Hz,  $^4J(\text{H1},\text{H2})$  = 1.5 Hz, 1H, Pyr1), 7.80 (ddd,  $^3J(\text{H3},\text{H4},2)$  = 7.7 Hz,  $^4J(\text{H3},\text{H1})$  = 1.5 Hz, 1H, Pyr3), 7.34 (ddd,  $^3J(\text{H2},\text{H3})$  = 7.62 Hz,  $^3J(\text{H2},\text{H1})$  = 5.1 Hz,  $^4J(\text{H2},\text{H4})$  = 1.8 Hz, 1H, Pyr2), 7.23 (d,  $^3J(\text{H4},\text{H3})$  = 7.8 Hz, 1H, Pyr4), 3.55 (m, 1H, H6), 2.99 (m, 1H, H7a), 2.74 (m, 1H, H7b), 4.1 (s, 2H,  $\text{NH}_2$ ).  $^{13}\text{C}$  NMR ( $[D_6]$ dmsO):  $\delta$  = 161.2 (Pyr5), 148.5 (Pyr1), 138.6 (Pyr3), 122.8 (Pyr2), 124.9 (Pyr4), 42.8 (C6), 47.9 (C7). IR (KBr,  $\text{cm}^{-1}$ ):  $\tilde{\nu}$  = 3450 m, 3314 vs, 3258 vs, 3144 w, 3062 vw, 3032 vw, 2930 s, 2887 m, 1609 vs, 1586 vs, 1571 vs, 1482 vs, 1457 vw, 1442 vs, 1386 m, 1359 w,



1323 s, 1288 m, 1267 m, 1243 w, 1197 w, 1160 m, 1124 vs, 1103 m, 1064 m, 1049 m, 1030 m, 958 s, 911 w, 789 s, 772 s, 669 m, 648 s, 578 w, 561 s, 523 m, 429 vw, 418 w. MS (EI):  $m/z$  (%) = 243 (6) [L]<sup>+</sup>, 195 (100) [L-CH<sub>2</sub>NH<sub>2</sub>,NH<sub>4</sub>]<sup>+</sup>, 183 (81) [L-2-CH<sub>2</sub>NH<sub>2</sub>]<sup>+</sup>, 121 (49) [L-PyrC<sub>2</sub>H<sub>3</sub>NH<sub>2</sub>,H]<sup>+</sup>, 106 (29) [121-NH<sub>2</sub>]<sup>+</sup>. C<sub>14</sub>H<sub>18</sub>N<sub>4</sub>Cl<sub>4</sub>Zn<sub>2</sub> (514.94): calcd. C 32.65, H 3.52, N 10.88; found C 32.70, H 3.55, N 9.97.

**[2,3-Diphenyl-5,6-di(pyridin-2-yl)piperazino bis(dichloro zinc)] (21)**

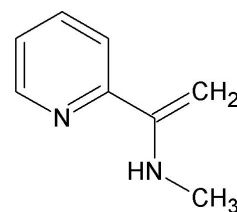
431 mg of N-Benzyl-pyridylmethylideneamine (2.2 mmol) were solved in 10 ml of anhydrous thf under inert conditions and cooled to -78 °C (dry ice/isopropanol). Subsequently, 1.37 ml of a 1.6 M solution of n-butyl lithium in hexane (2.2 mmol) were added dropwise via syringe. The solution immediately turned violet and was stirred for 1.5 hours at -78 °C. Then 1.5 g of zinc chloride (11 mmol) were added as a solid and the solution was allowed to warm to r.t.. Stirring over night afforded



a colorless precipitate, which was filtered and washed with anhydrous thf, yielding 428 mg (0.53 mmol). Yield: 48 %. m.p.: >350°C. <sup>1</sup>H NMR ([D<sub>6</sub>]dmsO): δ = 8.45 (d, J = 4.4 Hz, 2H, Pyr1), 7.72 (ddd, J = 7.6 Hz, J = 1.6 Hz, 2H, Pyr3), 7.37 (m, 4H, *o*-Ph), 7.16 (m, 6H, *m*-Ph, Pyr2), 7.14-7.08 (m, 2H, *p*-Ph), 7.37 (m, 2H, Pyr4), 4.63 (s broad, 4H, CH), 7.0 (s broad, 2H, NH), 3.58-3.55 (m, 8H, thf), 1.77-1.69 (m, 8H, thf). <sup>13</sup>C NMR ([D<sub>6</sub>]dmsO): δ = 157.9 (q, Pyr5), 148.2 (t, Pyr1), 139.5 (q, PhC), 138.0 (t, Pyr3), 128.5 (t, *o*-Ph), 128.0 (t, *m*-Ph, Pyr2), 127.5 (t, *p*-Ph), 123.7 (t, Pyr4), 64.8 (t, CH), 67.0 (s, thf), 25.1 (s, thf). IR (Nujol, anhydrous cond., cm<sup>-1</sup>):  $\tilde{\nu}$  = 3400 w broad (NH), 1609 st (C=N), 1574 m (C=C), 1505 m (C=C), 1482 st, 1331 m, 1274 m, 1158 m, t 1072 (m), 1047 st, 1026 st, 937 m, 885 m, 796 m, 769 st, 705 st, 647 w, 531 m. MS (FAB in nba):  $m/z$ (%) = 629 (<1) [M-2thf-Cl]<sup>+</sup>, 610 (<1), 491 (100) [M-2thf-Zn-3Cl]<sup>+</sup>, 393 (25), 255 (20), 209 (23). C<sub>24</sub>H<sub>40</sub>Cl<sub>4</sub>N<sub>4</sub>O<sub>2</sub>Zn<sub>2</sub> (809.34): calcd. C 50.46, H 4.98, N 6.92; found C 49.11, H 4.71, N 6.61.

**N-Methyl-1-(pyridin-2-yl)ethenamine (23)**

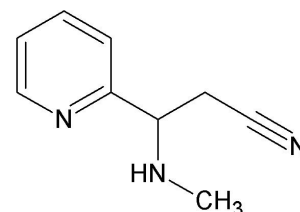
Nitroamine **17** was freshly prepared according to the above described procedure from imine **15a** (5.60 g, 47 mmol) and nitromethane **2a** (48.00 g, 786 mmol) with 1.2 g of Syntal 696®. The obtained orange oil was immediately solved in 120 ml of 10 % aqueous acetic acid and transferred into an autoclave. After addition of Pd/C 10 % (250 mg) the mixture was stirred in a hydrogen atmosphere (6 bar) for 12 hours at room temperature. Subsequently, the catalyst was removed by filtration and the dark brown mixture was neutralized with saturated aqueous sodium carbonate. The solution was now extracted seven times with 10 ml of methylene chloride each and the organic phase was separated and dried over sodium sulfate. Removal of the solvent in vacuo afforded product **23**. The product could be stored for several weeks at -20 °C. It is noteworthy, that no isolable products were



obtained when other amounts of catalyst or acetic acid concentrations were employed. Yield: 55 %.  $^1\text{H}$  NMR ( $\text{CD}_2\text{Cl}_2$ ):  $\delta$  = 8.61 (d,  $J$  = 4.4 Hz, 1H, Pyr1), 7.75 (ddd,  $J$  = 1.6 Hz,  $J$  = 7.6 Hz, 1H, Pyr3), 7.31-7.28 (m, 1H, Pyr2), 7.43 (d,  $J$  = 7.6 Hz, 1H, Pyr4), 5.80 (d,  $J$  = 0.6 Hz, 1H, HC=), 5.56 (d,  $J$  = 0.6 Hz, 1H, HC=), 3.19 (s, 3H,  $\text{CH}_3$ ).  $^{13}\text{C}$  NMR ( $\text{CD}_2\text{Cl}_2$ ):  $\delta$  = 153.4 (q, Pyr5), 149.9 (t, Pyr1), 147.8 (q, C6), 137.2 (t, Pyr3), 124.0 (t, Pyr2), 122.1 (t, Pyr4), 110.5 (s,  $\text{H}_2\text{C=}$ ), 33.17 (p,  $\text{CH}_3$ ). MS (EI):  $m/z(\%)$  = 267 (36)  $[\text{2M-1}]^+$ , 163 (70), 134 (61)  $[\text{M}]^+$ , 133 (89), 119 (100), 106 (63), 92 (25), 78 (38), 65 (13), 51 (15).

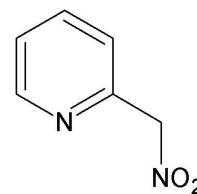
### 3-(Methylamino)-3-(pyridin-2-yl)propanenitrile (**24**)

Zinc dust (1.34 g, 21 mmol) was suspended in 10 ml of anhydrous acetonitrile in an argon atmosphere and 0.16 ml of 1,2-dibromethane were added dropwise, while the evolution of gas could be observed. The mixture was refluxed for one minute and then allowed to cool to room temperature. Subsequently, 0.34 ml of trimethylsilylchloride were added dropwise (gas evolution) and the mixture was stirred for 45 minutes. Compound **15a** (2.46 g, 21 mmol) was



solved in 10 ml of anhydrous acetonitrile and added to the suspension, maintaining the temperature below 35 °C. Under vigorous stirring, trimethylsilylchloride (3.34 g, 31 mmol) was added dropwise at a rate that maintains the temperature below 35 °C (30 minutes). Thereafter the mixture was additionally stirred for two hours. Subsequently, the reaction mixture was cooled to 0 °C and cautiously hydrolyzed under vigorous stirring with  $\text{NH}_4\text{Cl}/\text{NH}_3$  (prepared from 140 ml of saturated  $\text{NH}_4\text{Cl}$  and 60 ml of concentrated aqueous ammonia). The excess zinc was removed by filtration and the organic phase was then separated. The aqueous phase was extracted twice with 30 ml diethyl ether and 30 ml methylene chloride and the combined organic phases were dried over sodium sulfate. Removal of the solvents in vacuo afforded a brown to green oil, which was purified by distillation yielding product **24** as green to yellow oil. Compound **24** slowly hydrolyzes to the corresponding carbonic acid when stored under atmospheric conditions. Yield: 20 %. b.p.: 95 °C ( $1.2 \cdot 10^{-2}$  mbar).  $^1\text{H}$  NMR ( $\text{CD}_2\text{Cl}_2$ ):  $\delta$  = 8.59 (d,  $J$  = 4.4 Hz, 1H, Pyr1), 7.73-7.69 (m, 1H, Pyr3), 7.25-7.22 (m, 1H, Pyr2), 7.34 (d,  $J$  = 8.0 Hz, 1H, Pyr4), 3.90 (t,  $J$  = 6.8 Hz, 1H, CH), 2.28 (dd,  $J$  = 6.8 Hz,  $J$  = 4.0 Hz, 2H,  $\text{CH}_2$ ), 2.32 (s, 3H,  $\text{CH}_3$ ), 1.93 (s broad, H, NH).  $^{13}\text{C}$  NMR ( $\text{CD}_2\text{Cl}_2$ ):  $\delta$  = 159.8 (q, Pyr5), 150.1 (t, Pyr1), 136.9 (t, Pyr3), 123.3 (t, Pyr2), 122.7 (t, Pyr4), 118.5 (q, CN), 62.0 (t, CH), 24.6 (s,  $\text{CH}_2$ ), 34.2 (p,  $\text{CH}_3$ ). IR (neat,  $\text{cm}^{-1}$ ):  $\tilde{\nu}$  = 3323 m broad (NH), 3053 w, 3009 w, 2940 m, 2855 m, 2799 m, 2247 m (CN), 1590 st (C=N), 1571 m (C=C), 1473 st, 1451 m, 1435 st, 1342 w, 1293 w, 1149 w, 1132 w, 1112 m, 1049 w, 997 m, 951 w, 871 w, 783 m, 752 st, 624 w, 592 w, 566 w. MS (EI):  $m/z(\%)$  = 162 (9)  $[\text{M}+1]^+$ , 132 (70), 121 (100), 104 (7), 94 (37), 78 (22), 51 (11), 42 (19), 28 (18).

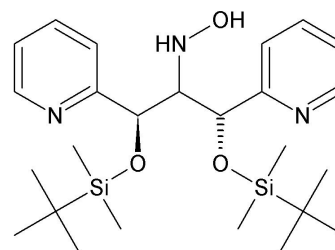
**2-(Nitromethyl)pyridine (26)** Preparation of n-propylnitrate: Concentrated nitric acid (65 %, 21.00 g, 218 mmol), urea (2.50 g) and n-propylalcohol (13.00 g, 218 mmol) were mixed in a distillation apparatus. The mixture was heated up to 95 °C under distillation of n-propylnitrate. This procedure was repeated by adding the above given mixture of nitric acid and n-propylalcohol to the hot reaction mixture until enough product was distilled. The distillate was washed with water and the n-propylnitrate was obtained as colorless oil with a higher density than water. N-propylnitrate was purified by distillation. Preparation of 2-(nitromethyl)pyridine: Sodium amide (7.00 g) were added in a 500 ml SCHLENK tube and cooled with dry ice/isopropanol. In this vessel gaseous ammonia was condensed until the liquid ammonia had a volume of 230 ml. The temperature was maintained between -40 °C and -35 °C, however, the sodium amide was not totally solved under this conditions. Subsequently, 2-methylpyridine (6.50 g, 69 mmol) was added via syringe and the mixture was stirred for 10 minutes. The color changed to red upon addition of 2-methylpyridine. Thereafter, n-propylnitrate (22.65 g, 215 mmol) was added in one portion under frothing and the color changed to orange, maintaining the temperature below -35 °C. The mixture was stirred for five minutes and subsequently the ammonia was replaced by 150 ml diethyl ether over a period of five hours, while the mixture slowly warmed to room temperature. The obtained solid sodium nitronate was filtered washed with diethyl ether and dried in vacuo. The product was obtained by cautiously solving sodium nitronate in 30 ml of ice cold water, acidifying with 10 g of glacial acetic acid until ph = 6 and extraction with chloroform. The organic phase was dried over sodium sulfate and the solvent was removed in vacuo yielding a brownish oil. The product **26** was purified by bulb to bulb distillation (105 °C, 1 mbar) affording a yellow oil. Product **26** slowly turned brown under atmospheric conditions and was stored at -20 °C. Yield: 31 %. b.p. 105 °C (1 mbar). <sup>1</sup>H NMR (CD<sub>2</sub>Cl<sub>2</sub>): δ = 8.64 (d, J = 4.8 Hz, 1H, Pyr1), 7.81 (ddd, J = 7.4 1.6 Hz, 1H, Pyr3), 7.47 (d, J = 8.0 Hz, 1H, Pyr4), 7.38 (m, 1H, Pyr2), 5.63 (s, 2H, CH<sub>2</sub>). <sup>13</sup>C NMR (CD<sub>2</sub>Cl<sub>2</sub>): δ = 150.0 (q, Pyr5), 150.4 (t, Pyr1), 137.7 (t, Pyr3), 125.02 (t, Pyr4), 124.7 (t, Pyr2), 81.4 (s, CH<sub>2</sub>). MS (DEI): *m/z*(%) = 138 (<1) [M]<sup>+</sup>, 92 (100) [M-NO<sub>2</sub>]<sup>+</sup>, 65 (55), 51 (8), 39 (30).



### Experimental data of several isolated compounds

#### *rac*-2,2,3,3,9,9,10,10-Octamethyl-5,7-di(pyridin-2-yl)-4,8-dioxa-3,9-disilaundecan-6-one hydroxylamin (**11**)

<sup>1</sup>H NMR (C<sub>6</sub>D<sub>6</sub>): δ = 8.31-8.26 (m, 2H, Pyr1, Pyr13), 7.04-6.98 (m, 2H, Pyr3, Pyr11), 7.28 (d, J = 8.0 Hz, 1H, Pyr10), 7.32 (d, J = 8.0 Hz, 1H, Pyr4), 6.55-6.50 (m, 2H, Pyr2, Pyr12), 5.56 (d, J = 1.8 Hz, 1H, H6), 5.50 (d, J = 6.4 Hz, 1H, H8), 4.25-4.21 (m, 1H, H7), 0.90 (s, 9H, *tert*-butyl), 0.95 (s, 9H, *tert*-butyl), -0.18 (s, 3H, SiCH<sub>3</sub>), -0.41

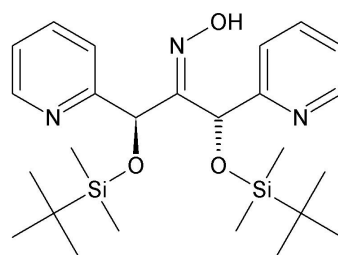


(s, 3H, SiCH<sub>3</sub>), 0.12 (s, 3H, SiCH<sub>3</sub>), 0.14 (s, 3H, SiCH<sub>3</sub>), 6.42 (d, J = 5.6 Hz, 1H, NH), 6.50 (s broad, 1H, OH). <sup>13</sup>C NMR (C<sub>6</sub>D<sub>6</sub>): δ = 162.9 and 161.7 (q, Pyr5 Pyr9), 148.5 and 148.3 (t, Pyr1, Pyr13), 135.9 and 135.6 (t, Pyr3, Pyr11), 122.0 (t, Pyr10), 121.9 (t, Pyr4), 121.5 (t, Pyr2, Pyr12), 75.4 (t, C6), 74.7 (t, C8), 72.7 (t, C7), 26.2 (p, *tert*-butyl), 26.2 (p, *tert*-butyl), 18.5 (q, *tert*-butyl), 18.4 (q, *tert*-butyl), -4.5 (p, SiCH<sub>3</sub>), -4.6 (p, SiCH<sub>3</sub>), -4.7 (p, SiCH<sub>3</sub>), -4.8 (p, SiCH<sub>3</sub>). IR (ATR, cm<sup>-1</sup>):  $\tilde{\nu}$  = 3100 m broad (NH, OH), 2930 m, 2891 m, 2888 m, 1593 m (C=N), 1488 m (C=C), 1435 m, 1401 m, 1359 m, 1253 m, 1216 w, 1100 m, 1074 m, 1000 m, 929 m, 633 st, 773 st, 888 m, 824 m. MS (DEI): *m/z*(%) = 490 (<1) [M+1]<sup>+</sup>, 432 (4) [M-*tert*-butyl]<sup>+</sup>, 412 (3), 300 (1), 267 (5), 223 (100), 191 (3), 166 (20), 152 (8), 135 (15), 118 (11), 93 (12), 73 (72), 59 (4), 44 (6), 28 (2). C<sub>25</sub>H<sub>43</sub>N<sub>3</sub>O<sub>3</sub>Si<sub>2</sub> (489.80).

***rac*-2,2,3,3,9,9,10,10-Octamethyl-5,7-di(pyridin-2-yl)-**

**4,8-dioxa-3,9-disilaundecan-6-one oxime (12)** <sup>1</sup>H

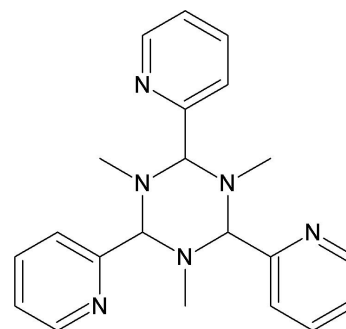
NMR (C<sub>6</sub>D<sub>6</sub>): δ = 8.26-8.24 (m, 2H, Pyr1, Pyr13), 7.11 (ddd, J = 7.6 1.6 Hz, 2H, Pyr3, Pyr11), 7.65 (d, J = 8.0 Hz, 1H, Pyr4), 6.55-6.49 (m, 2H, Pyr2, Pyr12), 7.59 (d, J = 7.6 Hz, 1H, Pyr10), 6.09 (s, 1H, H6), 6.97 (s, 1H, H8), 0.92 (s, 9H, *tert*-butyl), 0.95 (s, 9H, *tert*-butyl), 0.13 (s, 6H, SiCH<sub>3</sub>), 0.09 (s, 3H, SiCH<sub>3</sub>), 0.10 (s, 3H, SiCH<sub>3</sub>),



11.76 (s, 1H, OH). <sup>13</sup>C NMR (C<sub>6</sub>D<sub>6</sub>): δ = 163.1 (q, Pyr5), 162.4 (q, Pyr9), 157.4 (q, C7), 148.5 (t, Pyr1), 148.2 (t, Pyr13), 136.0 (t, Pyr3), 135.9 (t, Pyr11), 122.6 (t, Pyr4), 122.2 (t, Pyr2), 121.8 (t, Pyr12), 121.7 (t, Pyr10), 77.1 (t, C6), 69.4 (t, C8), 26.1 (p, *tert*-butyl), 26.2 (p, *tert*-butyl), 18.7 (q, *tert*-butyl), 18.6 (q, *tert*-butyl), -4.4 (p, SiCH<sub>3</sub>), -4.7 (p, SiCH<sub>3</sub>), -4.9 (p, SiCH<sub>3</sub>), -5.0 (p, SiCH<sub>3</sub>). IR (KBr, cm<sup>-1</sup>):  $\tilde{\nu}$  = 3362 m (OH), 3191 m (OH), 3057 m, 2956 st, 2929 st, 2889 m, 2857 st, 1636 w (C=N exocyc), 1591 st (C=N endocyc), 1572 st (C=C), 1472 st, 1435 st, 1408 m, 1389 m, 1361 m, 1346 m, 1253 st, 1218 w, 1187 w, 1106 st, 1081 st, 1004 st, 939 m, 876 st, 838 st, 779 st, 749 st, 677 m, 644 m, 589 w, 574 w, 520 w. MS (FAB in nba): *m/z*(%) = 488 (100) [M+1]<sup>+</sup>, 470 (70) [M-H<sub>2</sub>O]<sup>+</sup>, 454 (12), 430 (15) [M-*tert*-butyl]<sup>+</sup>, 412 (25), 356 (18), 340 (21), 313 (6), 282 (54), 271 (17), 267 (13), 247 (9), 233 (17), 223 (90), 208 (35). C<sub>25</sub>H<sub>41</sub>N<sub>3</sub>O<sub>3</sub>Si<sub>2</sub> (489.80).

**1,3,5-Trimethyl-2,4,6-tris(2-pyridyl)hexahydro-*s*-tri-**

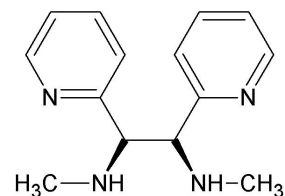
**azine (15a<sub>3</sub>)** <sup>1</sup>H NMR (CDCl<sub>3</sub>): δ = 8.50 (d, J = 4.8 Hz, 3H, Pyr1), 7.70 (ddd, J = 7.6 Hz, j = 2.0 Hz, 3H, Pyr3), 7.90 (t, J = 7.6 Hz, 3H, Pyr4), 7.18-7.20 (m, 3H, Pyr2), 3.85 (s, 3H, CH), 1.64 (s, 9H, CH<sub>3</sub>). <sup>13</sup>C NMR (CDCl<sub>3</sub>): δ = 161.2 (q, Pyr5), 148.0 (t, Pyr1), 136.9 (t, Pyr3), 123.8 (t, Pyr4), 123.2 (t, Pyr2), 90.86 (t, CH), 37.6 (p, CH<sub>3</sub>). IR (KBr, cm<sup>-1</sup>):  $\tilde{\nu}$  = 3068 m, 3052 m, 2995 st, 2967 st, 2899 m, 2860 st, 2750 st, 2761 m, 2740 m, 2696 m, 2645 m, 1593 st, 1568 st, 1472 st, 1456 st, 1426 st, 1371 m, 1361



m, 1333 st, 1281 st, 1233 m, 1139 m, 1086 m, 1044 st, 1081 st, 996 m, 966 st, 938 m, 897 st, 835 w, 785 st, 753 st, 678 m, 621 m, 579 m, 547 m, 509 st. MS (EI):  $m/z(\%) = 360 (<1)$   $[M]^+$ , 282 (34), 162 (33), 119 (100), 105 (18), 92 (67), 78 (46), 65 (12), 51 (30), 42 (40), 29 (28).  $C_{21}H_{24}N_6$  (360.45): calcd. C 69.97, H 6.71, N 23.32; found C 69.75, H 6.76, N 23.28.

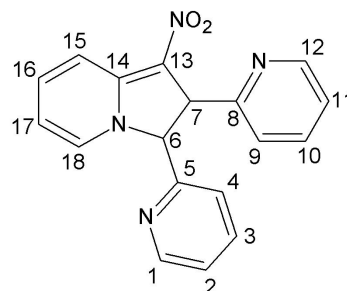
**meso-N,N'-dimethyl-1,2-di(pyridin-2-yl)ethane-1,2-diamine**

(25) The compound was obtained, employing the same procedure as for compound **24** with anhydrous thf instead of acetonitrile.  $^1H$  NMR ( $CD_2Cl_2$ ):  $\delta = 8.51-8.49$  (m, 2H, Pyr1),  $7.56-7.52$  (m, 2H, Pyr3),  $7.00$  (d,  $J = 8.0$  Hz, 2H, Pyr4),  $7.16-7.12$  (m, 2H, Pyr2),  $4.08$  (s, 2H, CH),  $2.22$  (s, 6H,  $CH_3$ ),  $3.06$  (s broad, H, NH).  $^{13}C$  NMR ( $CD_2Cl_2$ ):  $\delta = 160.3$  (q, Pyr5),  $149.5$  (t, Pyr1),  $136.2$  (t, Pyr3),  $123.2$  (t, Pyr4),  $121.7$  (t, Pyr2),  $69.4$  (t, CH),  $34.3$  (p,  $CH_3$ ). MS (DEI):  $m/z(\%) = 258$  (40),  $243$  (84)  $[M+1]^+$ ,  $225$  (15),  $211$  (17),  $184$  (48),  $134$  (26),  $122$  (99),  $107$  (100),  $94$  (82),  $78$  (41),  $65$  (18),  $51$  (24),  $42$  (15),  $39$  (7).



**1-nitro-2,3-di(pyridin-2-yl)-2,3-dihydroindolizine (27)**

$^1H$  NMR ( $CD_2Cl_2$ ):  $\delta = 8.59$  (d,  $J = 4.0$  Hz, 1H, Pyr1),  $8.55$  (d,  $J = 4.0$  Hz, 1H, Pyr12),  $7.73-7.76$  (m, 1H, H16),  $7.77-7.80$  (m, 1H, Pyr3),  $7.58$  (d,  $J = 6.4$  Hz, 1H, H18),  $7.65-7.69$  (m, 1H, Pyr10),  $7.33-7.35$  (m, 1H, Pyr9),  $7.43$  (d,  $J = 7.6$  Hz, 1H, Pyr2),  $7.20-7.23$  (m, 1H, Pyr4),  $7.31-7.33$  (m, 1H, Pyr11),  $8.30$  (d,  $J = 8.8$  Hz, 1H, H15),  $6.71-6.74$  (m, 1H, H17),  $6.08$  (d,  $J = 4.0$  Hz, 1H, H6),  $4.89$  (d,  $J = 4.0$  Hz, 1H, H7).  $^{13}C$  NMR ( $CD_2Cl_2$ ):  $\delta = 159.7$  (q, Pyr8),  $157.5$  (q, Pyr5 and C5),  $150.7$  (t, Pyr1),  $150.4$  (q, C13),  $150.1$  (t, Pyr12),  $142.2$  (t, C16),  $138.0$  (t, Pyr3),  $137.3$  (t, C18),  $136.7$  (t, Pyr10),  $124.4$  (t, Pyr9),  $124.1$  (t, Pyr2),  $122.8$  (t, Pyr4),  $121.8$  (t, Pyr11),  $119.6$  (t, C15),  $114.8$  (t, C17),  $75.3$  (t, C6),  $54.1$  (t, C7).





## References

- [1] W. B. Tolman (Ed.), *Activation of Small Molecules*, Wiley-VCH Verlag GmbH & Co. KGaA, Weinheim, **2006**.
- [2] G. Parkin, *Chem. Rev.* **2004**, *104*, 699–768.
- [3] D. E. Wilcox, *Chem. Rev.* **1996**, *96*, 2435–2458.
- [4] H.-B. Kraatz, N. Metzler-Nolte (Eds.), *Concepts and Models in Bioinorganic Chemistry*, Wiley-VCH Verlag GmbH & Co. KGaA, Weinheim, **2006**.
- [5] A. Erxleben, J. Hermann, *J. Chem. Soc. Dalton Trans.* **2000**, 569–575.
- [6] C. Belle, I. Gautier-Luneau, L. Karmazin, J.-L. Pierre, S. Albedyhl, B. Krebs, M. Bonin, *Eur. J. Inorg. Chem.* **2002**, *2002*, 3087–3090.
- [7] T. Koike, M. Inoue, E. Kimura, M. Shiro, *J. Am. Chem. Soc.* **1996**, *118*, 3091–3099.
- [8] F. Meyer, P. Rutsch, *Chem. Commun.* **1998**, 1037–1038.
- [9] D. R. Moore, M. Cheng, E. B. Lobkovsky, G. W. Coates, *Angew. Chem., Int. Ed.* **2002**, *41*, 2599–2602.
- [10] K. Nakano, T. Hiyama, K. Nozaki, *Chem. Commun.* **2005**, 1871–1873.
- [11] C. Puchot, O. Samuel, E. Dunach, S. Zhao, C. Agami, H. B. Kagan, *J. Am. Chem. Soc.* **1986**, *108*, 2353–2357.
- [12] E. N. Jacobsen, *Acc. Chem. Res.* **2000**, *33*, 421–431.
- [13] J. M. Ready, E. N. Jacobsen, *J. Am. Chem. Soc.* **2001**, *123*, 2687–2688.
- [14] J. T. B. H. Jastrzebski, J. M. Klerks, G. van Koten, K. Vrieze, *J. Organomet. Chem.* **1981**, *210*, C49–C53.
- [15] E. Wissing, S. Vanderlinden, E. Rijnberg, J. Boersma, W. J. J. Smeets, A. L. Spek, G. Vankoten, *Organometallics* **1994**, *13*, 2602–2608.
- [16] E. Wissing, E. Rijnberg, P. A. Vanderschaaf, K. Vangrop, J. Boersma, G. Vankoten, *Organometallics* **1994**, *13*, 2609–2615.
- [17] A. L. Spek, J. T. B. H. Jastrzebski, G. van Koten, *Acta Crystallogr., Sect. C: Cryst. Struct. Commun.* **1987**, *43*, 2006–2007.
- [18] M. Westerhausen, T. Bollwein, N. Makropoulos, T. M. Rotter, T. Habereeder, M. Suter, H. Noth, *Eur. J. Inorg. Chem.* **2001**, 851–857.
- [19] M. Westerhausen, T. Bollwein, N. Makropoulos, S. Schneiderbauer, M. Suter, H. Noth, P. Mayer, H. Piotrowski, K. Polborn, A. Pfitzner, *Eur. J. Inorg. Chem.* **2002**, 389–404.
- [20] M. Westerhausen, T. Bollwein, P. Mayer, H. Piotrowski, A. Pfitzner, *Z. Anorg. Allg. Chem.* **2002**, *628*, 1425–1432.
- [21] M. Westerhausen, T. Bollwein, M. Warchhold, H. Noth, *Z. Anorg. Allg. Chem.* **2001**, *627*, 1141–1145.
- [22] M. Westerhausen, T. Bollwein, K. Karaghiosoff, S. Schneiderbauer, M. Vogt, H. Noth, *Organometallics* **2002**, *21*, 906–911.
- [23] A. Alexakis, I. Aujard, P. Mangeney, *Synlett* **1998**, 873.
- [24] P. Mangeney, T. Tejero, A. Alexakis, F. Grosjean, J. Normant, *Synthesis* **1988**, 255–257.

- [25] A. Alexakis, I. Aujard, P. Mangeney, *Synlett* **1998**, 875.
- [26] A. Alexakis, I. Aujard, T. Kanger, P. Mangeney, *Org. Synth.* **2004**, *Coll. Vol. 10*, 312.
- [27] R. Annunziata, M. Benaglia, M. Caporale, L. Raimondi, *Tetrahedron: Asymmetry* **2002**, *13*, 2727–2734.
- [28] B. Baruah, D. Prajapati, J. S. Sandhu, *Tetrahedron Lett.* **1995**, *36*, 6747–6750.
- [29] M. Westerhausen, A. N. Kneifel, N. Makropoulos, *Inorg. Chem. Commun.* **2004**, *7*, 990–993.
- [30] C. Koch, A. Malassa, C. Agthe, H. Görls, R. Biedermann, H. Krautscheid, M. Westerhausen, *Z. Anorg. Allg. Chem.* **2007**, *633*, 375–382.
- [31] C. Koch, H. Görls, M. Westerhausen, *Z. Anorg. Allg. Chem.* **2008**, *634*, 1365–1372.
- [32] C. Koch, H. Görls, M. Westerhausen, *Acta Crystallogr., Sect. E: Struct. Rep. Online* **2007**, *63*, M2732–U933.
- [33] C. Koch, Ph.D. thesis, Universität Jena, **2008**.
- [34] D. Olbert, A. Kalisch, N. Herzer, H. Görls, P. Mayer, L. Yu, M. Reiher, M. Westerhausen, *Z. Anorg. Allg. Chem.* **2007**, *633*, 893–902.
- [35] A. Malassa, C. Koch, B. Stein-Schaller, H. Görls, M. Friedrich, M. Westerhausen, *Inorg. Chim. Acta* **2008**, *361*, 1405–1414.
- [36] M. Westerhausen, A. N. Kneifel, I. Lindner, J. Grcic, H. Noth, *Z. Naturforsch., B: Chem. Sci.* **2004**, *59*, 161–166.
- [37] E. Jaime, A. N. Kneifel, M. Westerhausen, J. Weston, *J. Organomet. Chem.* **2008**, *693*, 1027–1037.
- [38] G. Anantharaman, K. Elango, *Organometallics* **2007**, *26*, 1089–1092.
- [39] M. Kahnes, J. Richthof, H. Görls, D. Escudero, L. González, M. Westerhausen, *J. Organomet. Chem., In Press, Accepted Manuscript*.
- [40] A. Roth, E. T. Spielberg, W. Plass, *Inorg. Chem.* **2007**, *46*, 4362–4364.
- [41] A. Roth, A. Buchholz, M. Rudolph, E. Schütze, E. Kothe, W. Plass, *Chem.–Eur. J.* **2008**, *14*, 1571–1583.
- [42] A. Roth, W. Plass, *Angew. Chem., Int. Ed.* **2008**, *47*, 7588–7591.
- [43] G. Rosini, R. Ballini, *Synthesis* **1988**, *1988*, 833–847.
- [44] L. Henry, *Compt. Rend. Hebd. Séances Acad. Sci.* **1895**, *120*, 1265–1268.
- [45] G. Rosini, *Comprehensive Organic Synthesis*, B. M. Trost, I. Fleming (Eds.), Pergamon, New York, **1991**, chapter The Henry (Nitroaldol) Reaction, pp. 321–340.
- [46] N. Ono, *The Nitro Group in Organic Synthesis*, Wiley-VCH Verlag GmbH & Co. KGaA, Weinheim, **2001**.
- [47] M. Gruber-Khadjawi, T. Purkarthofer, W. Skranc, H. Griengl, *Adv. Synth. Catal.* **2007**, *349*, 1445–1450.
- [48] N. Ono, T. Hashimoto, T. X. Jun, A. Kaji, *Tetrahedron Lett.* **1987**, *28*, 2277–2280.
- [49] H. Adams, J. Anderson, S. Peace, A. Pennell, *J. Org. Chem.* **1998**, *63*, 9932–9934.
- [50] B. Westermann, *Angew. Chem., Int. Ed.* **2003**, *42*, 151–153.

## REFERENCES

---

- [51] K. R. Knudsen, T. Risgaard, N. Nishiwaki, K. V. Gothelf, K. A. Jorgensen, *J. Am. Chem. Soc.* **2001**, *123*, 5843–5844.
- [52] S. Y. Tosaki, K. Hara, V. Gnanadesikan, H. Morimoto, S. Harada, M. Sugita, N. Yamagiwa, S. Matsunaga, M. Shibasaki, *J. Am. Chem. Soc.* **2006**, *128*, JA064858L.
- [53] J. Boruwa, N. Gogoi, P. P. Saikia, N. C. Barua, *Tetrahedron-Asymmetry* **2006**, *17*, 3315–3326.
- [54] C. Palomo, M. Oiarbide, A. Mielgo, *Angew. Chem., Int. Ed.* **2004**, *43*, 5442–5444.
- [55] F. A. Luzzio, *Tetrahedron* **2001**, *57*, 915–945.
- [56] A. Cwik, A. Fuchs, Z. Hell, J. M. Clacens, *Tetrahedron* **2005**, *61*, 4015–4021.
- [57] M. Bellotto, B. Rebours, O. Clause, J. Lynch, D. Bazin, E. Elkaim, *J. Phys. Chem.* **1996**, *100*, 8527–8534.
- [58] V. J. Bulbule, V. H. Deshpande, S. Velu, A. Sudalai, S. Sivasankar, V. T. Sathe, *Tetrahedron* **1999**, *55*, 9325–9332.
- [59] M. J. Climent, A. Corma, S. Iborra, J. Primo, *J. Catal.* **1995**, *151*, 60–66.
- [60] S. M. Auer, R. Wandeler, U. Göbel, A. Baiker, *J. Catal.* **1997**, *169*, 1–12.
- [61] L. S. Li, S. J. Ma, X. S. Liu, Y. Yue, J. B. Hui, R. Xu, Y. M. Bao, J. Rocha, *Chem. Mater.* **1996**, *8*, 204–208.
- [62] R. Ballini, G. Bosica, *J. Org. Chem.* **1994**, *59*, 5466–5467.
- [63] K. W. Merz, H. J. Janssen, *Arch. Pharm.* **1964**, *297*, 10.
- [64] F. Zymalkowski, *Arch. Pharm.* **1955**, 52–54.
- [65] B. M. Choudary, M. L. Kantam, B. Kavita, *J. Mol. Catal. A: Chem.* **2001**, *169*, 193–197.
- [66] F. H. Allen, O. Kennard, D. G. Watson, L. Brammer, A. G. Orpen, R. Taylor, *J. Chem. Soc. Perkin Trans. 2* **1987**, S1–S19.
- [67] L. M. Jackman, S. Sternhell, *Applications of Nuclear Magnetic Resonance in Organic Chemistry 2nd ed.*, Pergamon Press: Oxford, U.K., **1969**.
- [68] W. R. Roush, T. D. Bannister, M. D. Wendt, M. S. VanNieuwenhze, D. J. Gustin, G. J. Dilley, G. C. Lane, K. A. Scheidt, W. J. Smith, *J. Org. Chem.* **2002**, *67*, 4284–4289.
- [69] IUPAC. *Compendium of Chemical Terminology, 2nd ed. (the "Gold Book")*. Compiled by A. D. McNaught and A. Wilkinson. Blackwell Scientific Publications, Oxford **1997**. XML on-line corrected version: <http://goldbook.iupac.org> (2006-) created by M. Nic, J. Jirat, B. Kosata; updates compiled by A. Jenkins. ISBN 0-9678550-9-8.
- [70] R. Bishop, M. L. Scudder, *Cryst. Growth Des.* **2009**, *9*, 2890–2894.
- [71] C. P. Brock, L. L. Duncan, *Chem. Mater.* **1994**, *6*, 1307–1312.
- [72] A. G. Orpen, L. Brammer, F. H. Allen, O. Kennard, D. G. Watson, R. Taylor, *J. Chem. Soc Dalton Trans.* **1989**, S1–S83.
- [73] M. Westerhausen, B. Rademacher, W. Schwarz, *J. Organomet. Chem.* **1992**, *427*, 275–287.
- [74] M. Westerhausen, M. Wieneke, W. Schwarz, *J. Organomet. Chem.* **1996**, *522*, 137–146.
- [75] M. Westerhausen, T. Bollwein, K. Polborn, *Z. Naturforsch., B: Chem. Sci.* **2000**, *55b*, 51–59.

- [76] M. A. Khan, D. G. Tuck, *Acta Crystallogr., Sect. C: Cryst Struct Commun* **1984**, *40*, 60–62.
- [77] W. L. Steffen, G. J. Palenik, *Inorg. Chem.* **1977**, *16*, 1119–1127.
- [78] D.-M. Chen, X.-J. Ma, B. Tu, W.-J. Feng, Z.-M. Jin, *Acta Crystallogr., Sect. E: Struct. Rep. Online* **2006**, *62*, m3174–m3175.
- [79] C. A. G. Haasnoot, F. A. A. M. de Leeuw, C. Altona, *Tetrahedron* **1980**, *36*, 2783–2792.
- [80] M. Bandini, F. Piccinelli, S. Tommasi, A. Umani-Ronchi, C. Ventrici, *Chem. Commun.* **2007**, 616–618.
- [81] B. Sellergren, R. N. Karmalkar, K. J. Shea, *J. Org. Chem.* **2000**, *65*, 4009–4027.
- [82] B. Sellergren, *J. Chromatogr., A* **2001**, *906*, 227–252.
- [83] G. J. Mohr, *Sens. Actuators, B* **2005**, *107*, 2–13.
- [84] A. Gräfe, K. Haupt, G. J. Mohr, *Anal. Chim. Acta* **2006**, *565*, 42 – 47.
- [85] K. Hamase, K. Iwashita, K. Zaitso, *Anal. Sci.* **1999**, *15*, 411–412.
- [86] M. A. Markowitz, P. R. Kust, G. Deng, P. E. Schoen, J. S. Dordick, D. S. Clark, B. P. Gaber, *Langmuir* **2000**, *16*, 1759–1765.
- [87] M. Comes, M. D. Marcos, R. Martinez-Manez, F. Sancenon, L. A. Villaescusa, A. Graefe, G. J. Mohr, *J. Mater. Chem.* **2008**, *18*, 5815–5823.
- [88] G. Wulff, *Angew. Chem., Int. Ed.* **1995**, *34*, 1812–1832.
- [89] C. Alexander, H. S. Andersson, L. I. Andersson, R. J. Ansell, N. Kirsch, I. A. Nicholls, J. O'Mahony, M. J. Whitcombe, *J. Mol. Recognit.* **2006**, *19*, 106–180.
- [90] P. G. M. Wuts, T. W. Green, *Green's Protective Groups in Organic Synthesis 4th ed.*, John Wiley & Sons, Inc., Hoboken, New Jersey, **2007**.
- [91] C. Rosini, S. Scamuzzi, G. Uccello-Barretta, P. Salvadori, *J. Org. Chem.* **1994**, *59*, 7395–7400.
- [92] E. J. Corey, A. Venkateswarlu, *J. Am. Chem. Soc.* **1972**, *94*, 6190–6191.
- [93] R. C. Larock, *Comprehensive Organic Transformations A Guide to Functional Group Preparations 2nd ed.*, John Wiley & Sons, Ltd., **1999**.
- [94] S. Ram, R. E. Ehrenkauf, *Tetrahedron Lett.* **1984**, *25*, 3415–3418.
- [95] S. Ram, R. E. Ehrenkauf, *Synthesis* **1988**, 91–95.
- [96] A. G. M. Barrett, C. D. Spilling, *Tetrahedron Lett.* **1988**, *29*, 5735–5736.
- [97] A. W. Ingersoll, *Org. Synth.* **1943**, *Coll. Vol. 2*, 503–506.
- [98] J. O. Osby, B. Ganem, *Tetrahedron Lett.* **1985**, *26*, 6413–6416.
- [99] D. H. Lloyd, D. E. Nichols, *J. Org. Chem.* **1986**, *51*, 4294–4295.
- [100] H. H. Seltzman, B. D. Berrang, *Tetrahedron Lett.* **1993**, *34*, 3083–3086.
- [101] G. Heller, F. Horbat, *Z. Naturforsch., B: Chem. Sci.* **1977**, *32*, 989–991.
- [102] S. Horiyama, K. Suwa, M. Yamaki, H. Kataoka, T. Katagi, M. Takayama, T. Takeuchi, *Chem. Pharm. Bull.* **2002**, *50*, 996–1000.
- [103] R. C. Mehrotra, A. K. Rai, A. Singh, R. Bohra, *Inorg. Chim. Acta* **1975**, *13*, 91–103.

## REFERENCES

---

- [104] Z. Rappoport, J. F. Liebman (Eds.), *The chemistry of Hydroxylamines, Oximes and Hydroxamic Acids*, of *The Chemistry of Functional Groups*, John Wiley & Sons Ltd., **2009**.
- [105] R. Ballini, M. Petrini, *Tetrahedron* **2004**, *60*, 1017–1047.
- [106] K.-H. v. Pée, S. Keller, T. Wage, I. Wynands, H. Schnerr, S. Zehner, *Biol. Chem.* **2000**, *381*, 1–5.
- [107] H. Vilter in *Metal Ions In Biological Systems, Vol. 31*, H. Sigel, A. Sigel (Eds.), Marcel Dekker, **1995**, pp. 325–362.
- [108] H. Vilter, *Phytochemistry* **1984**, *23*, 1387–1390.
- [109] W. Plass, *Angew. Chem., Int. Ed.* **1999**, *38*, 909–912.
- [110] D. Rehder, *Inorg. Chem. Commun.* **2003**, *6*, 604–617.
- [111] A. Messerschmidt, L. Prade, R. Wever, *Biol. Chem.* **1997**, *378*, 309–315.
- [112] A. del Campillo-Campbell, A. Campbell, *J. Bacteriol.* **1982**, *149*, 469–478.
- [113] I. Fernandez, N. Khair, *Chem. Rev.* **2003**, *103*, 3651–3706.
- [114] M. Andersson, A. Willetts, S. Allenmark, *J. Org. Chem.* **1997**, *62*, 8455–8458.
- [115] B. R. James, R. S. McMillan, *Can. J. Chem.* **1977**, *55*, 3927–3932.
- [116] C. Bolm, F. Bienewald, *Angew. Chem., Int. Ed.* **1996**, *34*, 2640–2642.
- [117] I. Lippold, H. Görls, W. Plass, *Eur. J. Inorg. Chem.* **2007**, *2007*, 1487–1491.
- [118] W. Plass, *J. Inorg. Biochem.* **1995**, *59*, 587–587.
- [119] I. Lippold, K. Vlay, H. Görls, W. Plass, *J. Inorg. Biochem.* **2009**, *103*, 480–486.
- [120] I. Lippold, J. Becher, D. Klemm, W. Plass, *J. Mol. Catal. A: Chem.* **2009**, *299*, 12–17.
- [121] R. Debel, A. Buchholz, W. Plass, *Z. Anorg. Allg. Chem.* **2008**, *634*, 2291–2298.
- [122] W. Plass, *Z. Anorg. Allg. Chem.* **1994**, *620*, 1635–1644.
- [123] K. M. Anderson, A. G. Orpen, *Chem. Commun.* **2001**, 2682–2683.
- [124] S. Nica, A. Buchholz, H. Görls, W. Plass, *Acta Crystallogr., Sect. E: Struct. Rep. Online* **2007**, *63*, m1450–m1452.
- [125] Z. Guo, L. Li, C. Wang, T. Xu, J. Li, *Acta Crystallogr., Sect. E: Struct. Rep. Online* **2009**, *65*, m1075.
- [126] D. Rehder, *Bioinorganic Vanadium Chemistry*, John Wiley & Sons, Ltd, **2008**.
- [127] P. S. Pregosin (Ed.), *Transition Metal Nuclear Magnetic Resonance*, Vol. 13 of *Studies in Inorganic Chemistry*, Elsevier, Amsterdam-Oxford-New York-Tokyo, **1991**.
- [128] G. Bähr, H.-G. Döge, *Z. Anorg. Allg. Chem.* **1957**, *292*, 119–138.
- [129] C. M. Vogels, P. E. O'Connor, T. E. Phillips, K. J. Watson, M. P. Shaver, P. G. Hayes, S. A. Westcott, *Can. J. Chem.* **2001**, *79*, 1898–1905.
- [130] A. V. Vasylyev, L. W. Castle, D. P. Strommen, *Vib. Spectrosc.* **1999**, *20*, 173–177.
- [131] G. Van Koten, J. T. B. H. Jastrzebski, K. Vrieze, *J. Organomet. Chem.* **1983**, *250*, 49–61.

## REFERENCES

- [132] F. Capitan, A. LaIglesia, F. Salinas, L. F. Capitanvallvey, *An. Quim.* **1977**, *73*, 226–232.
- [133] J.-L. Huang, Y.-L. Feng, *Acta Crystallogr., Sect. E: Struct. Rep. Online* **2007**, *63*, m1395.
- [134] C. Koch, M. Kahnes, M. Schulz, H. Goerls, M. Westerhausen, *Eur. J. Inorg. Chem.* **2008**, 1067–1077.
- [135] S. Das, A. Nag, D. Goswami, P. K. Bharadwaj, *J. Am. Chem. Soc.* **2006**, *128*, 402–403.
- [136] Hong, Zhe, *Acta Crystallogr., Sect. E: Struct. Rep. Online* **2007**, *63*, m132–m134.
- [137] F. Vögtle, E. Goldschmitt, *Angew. Chem., Int. Ed.* **1973**, *12*, 767–768.
- [138] F. Vögtle, E. Goldschmitt, *Chem. Ber.* **1976**, *109*, 1–40.
- [139] P. J. Campos, J. Arranz, M. A. Rodríguez, *Tetrahedron* **2000**, *56*, 7285–7289.
- [140] G. Alvaro, D. Savoia, M. R. Valentinetti, *Tetrahedron* **1996**, *52*, 12571–12586.
- [141] R. J. Baker, C. Jones, M. Kloth, D. P. Mills, *New J. Chem.* **2004**, *28*, 207–213.
- [142] L. H. Polm, G. van Koten, C. J. Elsevier, K. Vrieze, B. F. K. Van Santen, C. H. Stam, *J. Organomet. Chem.* **1986**, *304*, 353–370.
- [143] L. H. Polm, C. J. Elsevier, G. Van Koten, J. M. Ernsting, D. J. Stufkens, K. Vrieze, R. R. Andrea, C. H. Stam, *Organometallics* **1987**, *6*, 1096–1104.
- [144] M. Westerhausen, A. N. Kneifel, P. Mayer, *Z. Anorg. Allg. Chem.* **2006**, *632*, 634–638.
- [145] M. Westerhausen, A. N. Kneifel, H. Noth, *Z. Anorg. Allg. Chem.* **2006**, *632*, 2363–2366.
- [146] D. H. Busch, J. C. Bailar, *J. Am. Chem. Soc.* **1956**, *78*, 1137–1142.
- [147] E. W. Lund, *Acta Chem. Scand.* **1951**, *5*, 678–680.
- [148] M. L. Larter, M. Phillips, F. Ortega, G. Aguirre, R. Somanathan, P. J. Walsh, *Tetrahedron Lett.* **1998**, *39*, 4785–4788.
- [149] D. A. Durham, F. A. Hart, D. Shaw, *J. Inorg. Nucl. Chem.* **1967**, *29*, 509–516.
- [150] A. Furst, R. C. Berlo, S. Hooton, *Chem. Rev.* **1965**, *65*, 51–68.
- [151] E. Uhlig, M. Maaser, *Z. Anorg. Allg. Chem.* **1963**, *322*, 25–33.
- [152] E. Uhlig, B. Borek, *Z. Anorg. Allg. Chem.* **1976**, *425*, 217–226.
- [153] D. P. Madden, S. M. Nelson, *J. Chem. Soc. A* **1968**, 2342–2348.
- [154] X. ming Liu, X. yue Mu, H. Xia, L. Ye, W. Gao, H. yu Wang, Y. Mu, *Eur. J. Inorg. Chem.* **2006**, *2006*, 4317–4323.
- [155] S. Htoon, M. F. C. Ladd, *J. Chem. Crystallogr.* **1973**, *3*, 95–102.
- [156] W. H. Pearson, P. Stoy, *Synlett* **2003**, *2003*, 0903–0921.
- [157] R. Grigg, *Chem. Soc. Rev.* **1987**, *16*, 89–121.
- [158] S. J. Trepanier, S. N. Wang, *Can. J. Chem.* **1996**, *74*, 2032–2040.
- [159] M. Westerhausen, A. N. Kneifel, A. Kalisch, *Angew. Chem., Int. Ed.* **2005**, *44*, 96–98.
- [160] R. Cariou, V. C. Gibson, A. K. Tomov, A. J. White, *J. Organomet. Chem.* **2009**, *694*, 703–716.

## REFERENCES

---

- [161] M. Westerhausen, A. N. Kneifel, *Inorg. Chem. Commun.* **2004**, *7*, 763–766.
- [162] T. Konakahara, M. Matsuki, S. Sugimoto, K. Sato, *J. Chem. Soc. Perkin Trans. 1* **1987**, 1489–1493.
- [163] H. Feuer, J. P. Lawrence, *J. Org. Chem.* **1972**, *37*, 3662–3670.
- [164] H. Feuer, R. P. Monter, *J. Org. Chem.* **1969**, *34*, 991–&.
- [165] O. Wallach, E. Schulze, *Ber.* **1881**, *14*, 421.
- [166] W. Kaim, B. Schwederski, *Bioinorganic Chemistry: Inorganic Elements in the Chemistry of Life*, John Wiley & Sons, **1996**.
- [167] J. Cloete, S. F. Mapolie, *J. Mol. Catal. A: Chem.* **2006**, *243*, 221–225.
- [168] C. A. Brown, *J. Org. Chem.* **1970**, *35*, 1900–1904.
- [169] Z. Otwinowski, W. Minor, *Methods in Enzymology, Macromolecular Crystallography, Part A, Vol. 276*, C. Carter Jr, R. Sweet (Eds.), Academic Press, New York, **1997**.
- [170] *Collect*, Tech. Rep., Delft (The Netherlands), **1998**.
- [171] G. M. Sheldrick, *Acta Crystallogr., Sect. A: Found. Crystallogr.* **1990**, *46*, 467–473.
- [172] G. M. Sheldrick, *SHELXL-97 (Release 97-2)*, Tech. Rep., University of Göttingen, Germany, **1997**.

## A Crystallographic Data

The intensity data for the compounds were collected on a Nonius KappaCCD diffractometer using graphite-monochromatized Mo-K $_{\alpha}$  radiation. Data were corrected for Lorentz and polarization effects but not for absorption.<sup>169,170</sup> The structures were solved by Direct Methods (SHELXS)<sup>171</sup> and refined by full-matrix least-squares techniques against  $F_o^2$  (SHELXL-97).<sup>172</sup> All nonhydrogen atoms were refined anisotropically.<sup>172</sup> Structure representations: XP (Siemens Analytical X-ray Instruments, Inc.).



**Table 16:** The hydrogen atoms for compound **3a**, H1-H4, H6 and H8 of **3bHCl** and H6-H8 of **5** were located in difference Fourier syntheses and refined isotropically. All other hydrogen atoms were included at calculated positions with fixed displacement parameters.

Compound	<b>3a</b>	<b>3bHCl</b>	<b>4a</b>	<b>4b</b>	<b>5</b>
Formula	C <sub>7</sub> H <sub>8</sub> N <sub>2</sub> O <sub>3</sub>	C <sub>8</sub> H <sub>11</sub> ClN <sub>2</sub> O <sub>3</sub>	C <sub>14</sub> H <sub>19.5</sub> N <sub>3</sub> O <sub>4.25</sub>	C <sub>14</sub> H <sub>15</sub> N <sub>3</sub> O <sub>4</sub>	C <sub>21</sub> H <sub>29</sub> Cl <sub>2</sub> N <sub>3</sub> O <sub>6</sub> Zn
M <sub>r</sub> , gmol <sup>-1</sup>	168.15	218.64	297.83	289.29	555.74
T, °C	-90(2)	-90(2)	-90(2)	-90(2)	-90(2)
Crystal system	orthorhombic	monoclinic	triclinic	monoclinic	monoclinic
Space group	P2 <sub>1</sub> 2 <sub>1</sub> 2 <sub>1</sub>	P2 <sub>1</sub> /n	P $\bar{1}$	P2 <sub>1</sub> /c	P2 <sub>1</sub> /c
a, pm	714.50(5)	1268.99(5)	1170.30(12)	1182.18(4)	940.90(2)
b, pm	971.28(7)	890.25(4)	1222.93(15)	2197.76(9)	2104.72(3)
c, pm	1144.61(6)	1842.18(8)	1229.90(16)	1170.01(5)	1312.68(2)
$\alpha$ , deg	90	90	74.350(4)	90	90
$\beta$ , deg	90	101.768(3)	75.045(7)	114.201(2)	107.327(1)
$\gamma$ , deg	90	90	80.880(8)	90	90
V, Å <sup>3</sup>	794.34(9)	2037.40(15)	1630.1(3)	2772.69(19)	2481.57(7)
Z	4	8	4	8	4
D <sub>x</sub> , g cm <sup>-3</sup>	1.406	1.426	1.214	1.386	1.487
$\mu$ (MoK $\alpha$ ), cm <sup>-1</sup>	1.12	3.59	0.91	1.04	12.46
Measured data	5344	13905	10604	19614	18099
Unique data/R <sub>int</sub>	1830/0.0372	4651/0.0600	7168/0.0359	6345/0.0754	5668/0.0291
Data with I $\geq$ 2 $\sigma$ (I)	1397	3092	3800	3532	4811
R <sub>1</sub> [I $\geq$ 2 $\sigma$ (I)] <sup>a</sup>	0.0391	0.0638	0.1141	0.0745	0.0313
wR <sub>2</sub> (all data, on F <sup>2</sup> ) <sup>a</sup>	0.1010	0.1778	0.3553	0.2375	0.0788
GoF (S) <sup>b</sup>	1.018	1.070	1.020	1.039	1.003
$\Delta\rho_{fin}$ (max/min), eÅ <sup>3</sup>	0.143/-0.156	0.950/-0.425	0.887/-0.546	1.370/-0.410	0.779/-0.394
CCDC no.					

<sup>a</sup>  $R_1 = \frac{\sum |F_o| - |F_c|}{\sum |F_o|}$ ,  $wR_2 = \frac{[\sum w(F_o^2 - F_c^2)^2 / \sum w(F_o^2)^2]^{1/2}}{w}$ ,  $w = [\sigma^2(F_o^2) + (aP)^2 + bP]^{-1}$ , where  $P = \frac{(\text{Max}(F_o^2, 0) + 2F_c^2)}{3}$ ;

<sup>b</sup>  $GoF = \frac{[\sum w(F_o^2 - F_c^2)^2 / (n_{obs} - n_{param})]^{1/2}}$ .

**Table 17:** The hydrogen atoms for compound **8** were located in difference Fourier syntheses and refined isotropically. All other hydrogen atoms were included at calculated positions with fixed displacement parameters.

Compound	<b>7</b>	<b>8</b>	<b>14</b>	<b>21</b>	<b>25</b>	<b>27</b>
Formula	C <sub>25</sub> H <sub>41</sub> N <sub>3</sub> O <sub>4</sub> Si <sub>2</sub>	C <sub>20</sub> H <sub>29</sub> N <sub>3</sub> O <sub>4</sub> Si	C <sub>27</sub> H <sub>34</sub> N <sub>3</sub> O <sub>5</sub> SiV	C <sub>34</sub> H <sub>40</sub> Cl <sub>4</sub> N <sub>4</sub> O <sub>2</sub> Zn <sub>2</sub>	C <sub>14</sub> H <sub>18</sub> N <sub>4</sub>	C <sub>18</sub> H <sub>24</sub> N <sub>4</sub> O <sub>2</sub>
M <sub>r</sub> , gmol <sup>-1</sup>	503.79	403.55	559.6	809.24	242.32	318.33
T, °C	-90(2)	-140(2)	-90(2)	-90(2)	-90(2)	-90(2)
Crystal system	triclinic	monoclinic	monoclinic	monoclinic	monoclinic	monoclinic
Space group	P $\bar{1}$	C2/c	P2 <sub>1</sub> /n	P2 <sub>1</sub>	P2 <sub>1</sub> /c	C2/c
a, pm	740.37(4)	2144.97(9)	683.480(10)	1103.53(9)	560.56(3)	2806.88(19)
b, pm	1327.86(11)	1925.24(8)	2311.65(4)	1475.20(12)	1556.04(8)	796.72(6)
c, pm	1587.10(14)	1193.83(6)	1740.92(4)	1211.47(7)	785.03(5)	2118.59(15)
$\alpha$ , deg	70.372(3)	90	90	90	90	90
$\beta$ , deg	84.549(5)	116.901(3)	100.9280(10)	115.481(5)	96.890(3)	131.408(4)
$\gamma$ , deg	84.682(5)	90	90	90	90	90
V, Å <sup>3</sup>	1459.91(19)	4396.5(3)	2700.72(9)	1823.9(2)	679.80(7)	3553.4(4)
Z	2	8	4	2	2	8
D <sub>x</sub> , g cm <sup>-3</sup>	1.146	1.219	1.376	1.474	1.184	1.190
$\mu$ (MoK $\alpha$ ), cm <sup>-1</sup>	1.54	1.36	4.54	16.44	0.74	0.80
Measured data	10124	14988	18952	12325	4509	10925
Unique data/R <sub>int</sub>	6631/0.0437	5028/0.0963	6168/0.0389	7322/0.0540	1564/0.0262	4021/0.057
Data with I $\geq$ 2 $\sigma$ (I)	3707	2937		5461	1239	2564
R <sub>1</sub> [I $\geq$ 2 $\sigma$ (I)] <sup>a</sup>	0.0546	0.0518	0.0408	0.0468	0.0421	0.065
wR <sub>2</sub> (all data, on F <sup>2</sup> ) <sup>a</sup>	0.1323	0.1109	0.1060	0.1044	0.1169	0.216
GoF (S) <sup>b</sup>	0.980	0.993	1.080	1.020	1.045	0.735
$\Delta\rho_{fin}$ (max/min), eÅ <sup>3</sup>	0.249/-0.302	0.294/-0.312	0.340/-0.480	0.405/-0.554	0.217/-0.180	0.28/-0.26
CCDC no.						

<sup>a</sup>  $R_1 = \frac{\sum |F_o| - |F_c|}{\sum |F_o|}$ ,  $wR_2 = \frac{[\sum w(F_o^2 - F_c^2)^2 / \sum w(F_o^2)^2]^{1/2}}{[\sigma^2(F_o^2) + (aP)^2 + bP]^{-1}}$ , where  $P = (Max(F_o^2, 0) + 2F_c^2)/3$ ;

<sup>b</sup>  $GoF = \frac{[\sum w(F_o^2 - F_c^2)^2 / (n_{obs} - n_{param})]^{1/2}}{}$ .

**Table 18:** For the amino group at N2 of **20**, and the whole compound of **19**, the hydrogen atoms were located in difference Fourier syntheses and refined isotropically. All other hydrogen atoms were included at calculated positions with fixed displacement parameters.

Compound	<b>17<sub>3</sub></b>	<i>meso</i> - <b>18</b>	( <i>R,R</i> )/ ( <i>S,S</i> ) <b>18</b>	<i>meso</i> - <b>19</b>	<b>20</b>
Formula	C <sub>21</sub> H <sub>24</sub> N <sub>6</sub>	C <sub>14</sub> H <sub>14</sub> N <sub>4</sub> O <sub>4</sub>	C <sub>14</sub> H <sub>14</sub> N <sub>4</sub> O <sub>4</sub>	C <sub>14</sub> H <sub>18</sub> N <sub>4</sub> · 2H <sub>2</sub> O	C <sub>14</sub> H <sub>18</sub> Cl <sub>4</sub> N <sub>4</sub> Zn <sub>2</sub>
M <sub>r</sub> , gmol <sup>-1</sup>	360.46	302.29	302.29	278.36	514.86
T, °C	-90(2)	-90(2)	-90(2)	-90(2)	-90(2)
Crystal system	triclinic	monoclinic	monoclinic	monoclinic	triclinic
Space group	P $\bar{1}$	P2 <sub>1</sub> /n	P2 <sub>1</sub> /c	P2 <sub>1</sub> /c	P $\bar{1}$
a, pm	1029.18(15)	692.76(8)	948.11(7)	961.60(19)	641.74(6)
b, pm	1036.38(15)	555.43(7)	1059.70(5)	1478.4(3)	913.20(9)
c, pm	1121.31(15)	1817.82(12)	1460.23(9)	520.63(10)	934.39(9)
$\alpha$ , deg	93.352(7)	90	90	90	66.501(5)
$\beta$ , deg	111.797(7)	100.519(7)	104.094(3)	96.74(3)	78.692(7)
$\gamma$ , deg	117.066(6)	90	90	90	71.013(5)
V, Å <sup>3</sup>	950.7(2)	687.71(13)	1422.95(15)	735.0(3)	473.46(8)
Z	2	2	4	2	1
D <sub>x</sub> , g cm <sup>-3</sup>	1.259	1.460	1.411	1.258	1.806
$\mu$ (MoK $\alpha$ ), cm <sup>-1</sup>	0.79	1.1	1.06	0.87	31.01
Measured data	6681	4245	9784	5140	3316
Unique data/R <sub>int</sub>	4209/0.1057	1563/0.0595	3250/0.0417	1690/0.0454	2139/0.0341
Data with I $\geq$ 2 $\sigma$ (I)	1501	942	2325	1228	1641
R <sub>1</sub> [I $\geq$ 2 $\sigma$ (I)] <sup>a</sup>	0.0837	0.0606	0.0476	0.0422	0.0412
wR <sub>2</sub> (all data, on F <sup>2</sup> ) <sup>a</sup>	0.2043	0.1547	0.1360	0.1098	0.1015
Weighting scheme a/b <sup>a</sup>	0.0633/0.0000	0.0643/0.3072	0.0678/0.3257	0.0512/0.1399	0.0435/0.4300
GoF (S) <sup>b</sup>	0.976	1.029	1.031	1.019	1.032
$\Delta\rho_{fin}$ (max/min), Å <sup>3</sup>	0.28/-0.25	0.21/-0.22	0.20/-0.30	0.22/-0.23	0.64/-0.83
CCDC no.	720858	720859	720860	720861	720862

<sup>a</sup>  $R_1 = \sum |F_o| - |F_c| / \sum |F_o|$ ,  $wR_2 = [\sum w(F_o^2 - F_c^2)^2 / \sum w(F_o^2)^2]^{1/2}$ ,  $w = [\sigma^2(F_o^2) + (aP)^2 + bP]^{-1}$ , where  $P = (Max(F_o^2, 0) + 2F_c^2)/3$ ;

<sup>b</sup>  $GoF = [\sum w(F_o^2 - F_c^2)^2 / (n_{obs} - n_{param})]^{1/2}$ .

**Table 19:** For the propene group of **16d** the hydrogen atoms were located by difference Fourier synthesis and refined isotropically. All other hydrogen atoms were included at calculated positions with fixed thermal parameters.

Compound	<b>16a</b>	<b>16b</b>	<b>16c</b>	<b>16d</b>
Formula	C <sub>7</sub> H <sub>8</sub> Cl <sub>2</sub> N <sub>2</sub> Zn	C <sub>12</sub> H <sub>10</sub> Cl <sub>2</sub> N <sub>2</sub> Zn	[C <sub>39</sub> H <sub>36</sub> N <sub>6</sub> Zn][Cl <sub>4</sub> Zn]·CH <sub>4</sub> O	C <sub>9</sub> H <sub>10</sub> Cl <sub>2</sub> N <sub>2</sub> Zn
M <sub>r</sub> , gmol <sup>-1</sup>	256.42	318.49	893.32	282.46
T, °C	-90(2)	-90(2)	-90(2)	-90(2)
Crystal system	triclinic	triclinic	monoclinic	monoclinic
Space group	P $\bar{1}$	P $\bar{1}$	P2 <sub>1</sub> /n	P2 <sub>1</sub> /c
a, pm	775.48(4)	777.17(10)	1182.90(3)	886.58(3)
b, pm	865.95(5)	867.04(11)	1542.36(4)	1688.06(6)
c, pm	1465.03(5)	982.13(11)	2164.08(5)	789.29(2)
$\alpha$ , deg	77.422(3)	100.901(7)	90	90
$\beta$ , deg	83.897(3)	101.139(7)	94.651(2)	102.171(2)
$\gamma$ , deg	79.259(3)	97.063(7)	90	90
V, Å <sup>3</sup>	941.15(8)	628.81(13)	3935.27(17)	1154.70(6)
Z	4	2	4	4
D <sub>x</sub> , g cm <sup>-3</sup>	1.810	1.682	1.508	1.625
$\mu$ (MoK $\alpha$ ), cm <sup>-1</sup>	31.2	23.53	15.31	25.51
Measured data	6681	4198	27832	7719
Unique data/R <sub>int</sub>	4273/0.0289	2761/0.0541	9017/0.0694	2619/0.0279
Data with I $\geq$ 2 $\sigma$ (I)	3235	1801	5809	2316
R <sub>1</sub> [I $\geq$ 2 $\sigma$ (I)] <sup>a</sup>	0.0343	0.0934	0.0446	0.0256
wR <sub>2</sub> (all data, on F <sup>2</sup> ) <sup>a</sup>	0.0799	0.2576	0.1105	0.0673
GoF (S) <sup>b</sup>	0.954	1.082	0.993	1.029
$\Delta\rho_{fin}$ (max/min), eÅ <sup>3</sup>	0.386/-0.563	1.129/-0.805	0.695/-0.696	0.265/-0.499
CCDC no.	717944	717945	717946	717947

<sup>a</sup>  $R_1 = \frac{\sum (|F_o| - |F_c|)}{\sum |F_o|}$ ,  $wR_2 = \frac{[\sum w(F_o^2 - F_c^2)^2 / \sum w(F_o^2)^2]^{1/2}}{w}$ ,  $w = [\sigma^2(F_o^2) + (aP)^2 + bP]^{-1}$ , where  $P = \frac{(\text{Max}(F_o^2, 0) + 2F_c^2)}{3}$ ;

<sup>b</sup>  $GoF = \frac{[\sum w(F_o^2 - F_c^2)^2 / (n_{obs} - n_{param})]^{1/2}}$ .

## Acknowledgment

The presented work would not have been completed with the help and assistance of several people. Firstly, I want to thank Prof. Dr. Matthias Westerhausen for his assistance during the last four years, the granted scientific freedom and an open door and ear for questions and discussions. The unstressed atmosphere, he created by his interaction with the group, impressed me very much. Furthermore, Prof. Dr. Rainer Beckert's expert opinion is gratefully acknowledged.

The numerous NMR experiments as well as EPR investigations were carried out by Dr. Manfred Friedrich, Annerose Blayer, Bärbel Rambach and Gabriele Sentis, to whom I'm very grateful. Also the useful discussions are gratefully acknowledged. Single crystal X-ray diffraction experiments and solution of the crystal structures were done by Dr. Helmar Görls, to whom I want to express many thanks also for discussions and a great sense of humor. Mass spectra and IR spectra under inert conditions were conducted by Dr. Wolfgang Poppitz, Sigrid Schönau and Monika Heineck, to whom I'm very thankful. Elemental analysis was performed by Beate Lentvogt, her work is gratefully acknowledged. X-ray powder diffraction was done by Christina Apfel, to whom I want to express my gratitude. UV-Vis spectroscopies were conducted by Erika Kielmann and Dr. Eckhard Birckner, to whom I express my thanks. AAS analysis was carried out by Kristin Schäfer and Susanne Spangenberg, to whom I'm very thankful. Reparation of glassware was carried out by Anke Jakob and Ulrich Hempel, who's work is gratefully acknowledged.

Besides, I want to express my thanks for fruitful discussions to Dr. Uwe Köhn, Dr. Johannes Notni, Dr. Stephan Schenk, Dr. Stefan Bartram (also for elemental analysis) and Dr. Wolfgang Günther. I'm also indebted to Robert Debel, Dr. Swen Körsten and Dr. Anja Schulz for the good cooperation and their openness to new ideas.

The staff of Haus 1 took care for the daily workflow, such as mail orders, the dispense of chemicals and glassware, dealing with applications, reparations, waste disposal, a welcome atmosphere and many more. Thus, I want to thank Heike Müller, Christine Agthe, Martina Gase, Veronika Lenzner, Karin Landrock, Renate Grunert, Jens Rückoldt, Alexander Müller and Gerhard Wilke. For good cooperation and conditions of give and take the following groups owe a debt of gratitude: The group of Prof. Weigand, the group of Prof. Plass, the group of Prof. Imhof, the group of Prof. Rau and the group of Prof. Kreisel.

A pleasant atmosphere is made by people. For discussions, help, advice, fun I sincerely want to thank my dear colleagues Julia Richthof, Gritt Volland, Dr. Christian Koch, Marcel Kahnes, Dirk Olbert, Astrid Malassa, Maurice Klopffleisch, Carsten Glock, Tobias Kloubert, Tareq Al-Shboul, Taghreed Jazzazi, Katja Wimmer, Dr. Jens Langer, Sven Krieck and Dr. Heike Schreer.

Also I want to thank my former student apprentices Michael Bessel, Kevin Stippich, Steve Landsmann, Marcel Kahnes, Maurice Klopffleisch, Tobias Kloubert, Marc Dittmer, Carmen Bohlender, Velina Sarbova, Katja Wimmer and Dirk Ziegenbalg (for IT solutions) for contributions to the experimental work.

Sincere thanks are given to Dr. Reinald Fischer, Dr. Helmar Görls, Tobias Niksch, Sven Harms, Elke Wenske, Rita Schadewald, Regina Suxdorf, Andreas Geber, Sven

Kriek, Dr. Jens Langer, Carsten Glock, Thomas Weisheit for their assistance and friendliness during the practical courses.

Julia Richthof's, Dr. Anja Schulz' and Dr. Daniel Tietze's comments on the manuscript are gratefully acknowledged.

Encouragement, backing, inspiration and also financial support were provided throughout my studies by my friends, my parents, my brother and my wife. Sincere thanks are given to them all.

## Declaration of Originality

I certify that the work presented here is, to the best of my knowledge and belief, original and the result of my own investigations, except as acknowledged, and has not been submitted, either in part or whole, for a degree at this or any other university.

Ich erkläre, dass ich die vorliegende Arbeit selbstständig und nur unter Verwendung der angegebenen Hilfsmittel, persönlichen Mitteilungen und Quellen angefertigt habe und dass ich nicht die gleiche, eine in wesentlichen Teilen ähnliche oder eine andere Abhandlung bei einer anderen Hochschule als Dissertation eingereicht habe.

Martin Schulz

Jena, den 12.11.2009